UNIVERSITY OF CALGARY

Asphaltene and Solids-Stabilized Water-in-Oil Emulsions

by

Danuta M. Sztukowski

A THESIS

SUBMITTED TO THE FACULTY OF GRADUATE STUDIES

IN PARTIAL FULFILMENT OF THE REQUIREMENTS FOR THE

DEGREE OF DOCTOR OF PHILOSOPHY

DEPARTMENT OF CHEMICAL AND PETROLEUM ENGINEERING

CALGARY, ALBERTA

FEBRUARY, 2005

© Danuta M. Sztukowski 2005

UNIVERSITY OF CALGARY

FACULTY OF GRADUATE STUDIES

The undersigned certify that they have read, and recommended to the Faculty of Graduate Studies for acceptance, a thesis entitled “Asphaltene and Solids-Stabilized Water-in-Oil Emulsions” submitted by Danuta M. Sztukowski in partial fulfilment of the requirements for the degree of Doctor of Philosophy.

_____
Supervisor, Dr. H. W. Yarranton
Department of Chemical and Petroleum Engineering

_____
Dr. W. Y. Svrcek
Department of Chemical and Petroleum Engineering

_____
Dr. A. Kantzas
Department of Chemical and Petroleum Engineering

_____
Dr. B. Maini
Department of Chemical and Petroleum Engineering

_____
Dr. L. Bentley
Department of Geology and Geophysics

_____
External Examiner, Dr. Z. Xu
University of Alberta

_____
Date

ABSTRACT

Water-in-crude oil emulsions are a problem in crude oil production, transportation, and processing. Many of these emulsions are stabilized by asphaltenes and native oilfield solids adsorbed at the oil-water interface. Design of effective emulsion treatments is hampered because there is a lack of understanding of the role asphaltenes and solids play in stabilizing these emulsions. In this work, the structural, compositional and rheological properties of water/hydrocarbon interfaces were determined for model emulsions consisting of water, toluene, heptane, asphaltenes and native oilfield solids. The characteristics of the interface were related to the properties of asphaltenes and native solids. Emulsion stability was correlated to interfacial rheology.

A combination of vapour pressure osmometry, interfacial tension and emulsion gravimetric studies indicated that asphaltenes *initially* adsorb at the interface as a monolayer of self-associated molecular aggregates. It was demonstrated why it is necessary to account for asphaltene self-association when interpreting interfacial measurements. The interfacial area of Athabasca asphaltenes was found to be approximately 1.5 nm^2 and did not vary with concentration or asphaltene self-association. Hence, more self-associated asphaltenes simply formed a thicker monolayer. The interfacial monolayer observed in this work varied from 2 to 9 nm in thickness.

The asphaltene monolayer was shown to adsorb reversibly only at short interface aging times. The film gradually reorganizes at the interface to form a rigid, irreversibly adsorbed network. The elastic and viscous moduli can be modeled using the Lucassen-van den Tempel (LVDT) model when the aging time is less than 10 minutes. An increase in film rigidity can be detected with an increase in the total elastic modulus.

Increased film rigidity was shown to reduce the rate of coalescence in an emulsion and increase overall emulsion stability (reduce free water resolution). The rate of coalescence

and the free water resolution of emulsions decreased when the interface aging time increased, the heptane fraction in heptol increased, and the asphaltene concentration decreased. For systems in which asphaltenes do not leave the interface during coalescence, the rate of coalescence correlated to the measured total modulus over a range of asphaltene concentrations, solvent qualities, and interface aging times. For systems in which asphaltenes leave the interface during coalescence, the correlation under-predicted the coalescence rate because the total modulus increases as material leaves the interface. The total modulus is believed to increase during coalescence because the most weakly bound asphaltenes are expelled from the interface, while the asphaltenes that remain on the interface are those that cross-link more readily and form the most rigid interfacial film. For any given solvent, emulsion stability correlated to the total modulus; however, the correlation was different for each solvent system considered. It is likely that other factors such as rigid film formation during coalescence also influence emulsion stability.

Native solids were clay platelets and fell into two size categories: 1) fine solids 50 to 500 nanometers in diameter; 2) coarse solids 1 to 10 microns in diameter. Emulsions stabilized by fine solids and asphaltenes were most stable at a 2:1 fractional area ratio of asphaltenes to solids. It appears that when the asphaltene surface coverage is high, insufficient solids remain to make an effective barrier. When the solids coverage is high, insufficient asphaltenes remain on the interface to immobilize the solids. Treatments that weaken the interface, such as toluene dilution, are recommended for emulsions stabilized by fine solids. Emulsions stabilized by coarse solids were unstable at low solids concentrations but became very stable at solids concentrations greater than 10 kg/m^3. At low concentrations, these solids may act as bridges between water droplets and promote coalescence. At high concentrations, layers of coarse solids may become trapped between water droplets and prevent coalescence. Treatments that flocculate the solids, such as heptane dilution, are recommended for emulsions stabilized by high concentrations of coarse solids.

ACKNOWLEDGEMENTS

I would like to express my deepest gratitude to my supervisor, Dr. Harvey W. Yarranton, for his superb supervision and guidance throughout my studies. His encouragement, unfailing support, and the many thought-provoking discussions during my studies were exceptional and are sincerely appreciated.

I wish to thank all members, past and present, of the Asphaltene Research Group for their support and assistance. I would especially like to thank Olga Gafonova, Dr. Kamran Akbarzadeh and Dr. Hussein Alboudwarej for teaching me many of the experimental techniques.

I would like to thank many others who have also contributed to this work. I thank Louise Klatzel-Mudry for assistance with the X-Ray diffraction work, Brenda Mottle for the particle size analyses, and Richard Humphries for the SEM and TEM analyses. I would also like to acknowledge Dr. Alain Cagna and Dr. Lee Gilman for their exceptional support and valued discussions of the asphaltene elasticity work. I also thank Dr. Anthony Yeung for his helpful discussions.

I thank the administrative and technical staff of the Department of Chemical and Petroleum Engineering for their support throughout the duration of my studies.

The financial support from the Department of Chemical and Petroleum Engineering at the University of Calgary, the Natural Sciences and Engineering Research Council (NSERC), the Alberta Ingenuity Fund (AIF), the Alberta Energy Research Institute (AERI), and Imperial Oil, Ltd., is greatly appreciated. I also thank Imperial Oil, Ltd., Syncrude Canada, and the EnCana Corporation (formerly the Alberta Energy Company, AEC) for bitumen and emulsion samples.

The support of friends and fellow graduate students is also highly appreciated. Finally, I would like to extend my deep gratitude to my family for their patience and support.

DEDICATION

To my parents,
Teresa and Stanisław Sztukowski

TABLE OF CONTENTS

LIST OF TABLES

LIST OF FIGURES

LIST OF SYMBOLS

a	fitting parameter
a	fitting parameter for diffusion coefficient (m^2/s)
a	interfacial area of molecule (m^2/mol)
A	area of molecule (m^2/molecule)
A	interfacial area during oscillation (m^2)
A	total emulsion interfacial area (m^2)
A_o	interfacial area prior to oscillation (m^2)
b	fitting parameter
b	amplitude of oscillation (m^2)
b	fitting parameter for diffusion coefficient (-)
c	fitting parameter
C	concentration (kg/m^3 or mol/m^3)
d	fitting parameter
d	diameter of capillary (m)
d_{32}	Sauter mean diameter (m^2)
d_i	water droplet diameter (m^2)
d_i	diameter of solid particle
D	diffusion coefficient (m^2/s)
f	frequency of oscillation (1/s)
f_i	frequency (-)
f_{ni}	number frequency (-)
f_t	fraction of trapped solids (-)
f_{vi}^{disc}	volume frequency (-)
g	acceleration due to gravity (9.81 m/s^2)
H	enthalpy of mixing (J/mol)
ΔH_v	enthalpy of vaporization (J/mol)
K	VPO calibration constant (V·kg/kmol)
K_1	VPO calibration constant (kg·K/kmol)

K_2	VPO calibration constant (V/K)
m	mass (kg)
M	molar mass (g/mol)
n	number of molecules in interfacial layer
N_A	Avogadro's number (6.022×10^{-23})
Q	flowrate (m^3/s)
R	universal gas constant (8.314 J/molK)
S	shape factor (-)
t	time (s)
t	thickness (m)
T	absolute temperature (K)
T	period of oscillation (s)
V	volume (m^3)
V	voltage (V)

Greek symbols

α	initial shift factor (rad)
γ	interfacial tension (N/m)
Γ	molecular surface coverage (mol/m^2)
Γ_A	mass surface coverage (kg/m^2)
Γ_A^m	monolayer mass surface coverage (kg/m^2)
ε	total elastic modulus (N/m)
ε'	elastic modulus (N/m)
ε''	viscous modulus (N/m)
ε_o	instantaneous elasticity (N/m)
ε_d	interfacial dilational elasticity (N/m)
ζ	diffusional parameter (-)
η_d	interfacial viscosity (Pa·s)
θ	fractional surface coverage (-)

θ	three phase contact angle (^{o})
θ	fractional area occupied on interface (-)
Π	surface pressure (N/m)
ρ	density (kg/m^3)
τ_D	characteristic time of diffusion (s)
ϕ	phase angle (rad)
ω	frequency of oscillation (rad/s)

Subscripts

'1'	solvent
'2'	solute/surfactant
'A'	Asphaltene
'c'	continuous phase
'cp'	continuous phase
'd'	dispersed phase
'drop'	drop in DVT
'eq'	equilibrium
'I'	interface
'o'	bulk or initial
'S'	Solid
'T'	total emulsion
'w'	water

Abbreviations

'AS'	Asphaltenes-Solids
'DSA'	Drop Shape Analyzer
'DVT'	Drop Volume Tensiometer
'heptol'	mixture of heptane and toluene
'LVDT'	Lucassen – van den Tempel
'SEOS'	Surface Equation of State

CHAPTER 1
INTRODUCTION

1.1 GENERAL DESCRIPTION

Water-in-crude oil emulsions are a recurring problem faced by oil producers during the recovery, treatment, and transportation of crude oil. Oil field emulsions can be formed during waterfloods or steamfloods when oil and water mix in the reservoir, at the wellbore, and in various uphole surface facilities. They are also formed when recovering bitumen from oil sands in a hot water extraction process. Emulsions are deliberately created in refineries in an effort to prevent corrosion of equipment and piping by washing chlorides and other contaminants out of the crude oil (Grace, 1992). Whether they are created unintentionally or deliberately, emulsions must be eventually broken so as to obtain separate oil and water phases.

Heavy crude oils and bitumen usually contain large proportions of emulsion stabilizing components, and gravity settling alone will not result in timely separation of oil and water. Hence, oil producers are forced to employ a variety of heating and chemical demulsifying techniques in order to increase the speed and efficiency of water/oil separation. Emulsion treatment can be costly, and it is desirable to develop new and less expensive techniques for emulsion destabilization. To do so, it is useful to have an understanding of the factors that contribute to emulsion stability.

The asphaltene and non-asphaltenic solids (such as clays) components of crude oil/bitumen have been identified as the primary stabilizers of water-in-crude oil emulsions (Yarranton *et al.*, 2000a; McLean and Kilpatrick, 1997b). It is generally believed that these components adsorb as surfactants or as particles at the oil/water interface, resulting in rigid films that encapsulate water droplets and prevent their

coalescence (Yarranton *et al.*, 2000a, McLean and Kilpatrick, 1997a and 1997b, Singh *et al.*, 1999). Aggregated droplets form a viscous, voluminous "rag" layer that often must be removed mechanically during periodic shut downs of desalters and demulsifiers. Heat and chemical treatment techniques may fail to break these emulsions.

Asphaltenes are a solubility class of crude oil, meaning that they precipitate in the presence of aliphatic solvents such as pentane or heptane, but remain solubilized in aromatic solvents such as toluene. Since they are a solubility class, asphaltenes cannot be considered a pure component; however, it is known that asphaltenes are large, polar, polynuclear molecules consisting of condensed aromatic rings, aliphatic side chains, and various heteroatom groups (Strausz *et al.*, 1992). Asphaltenes are amphiphilic, meaning they have both lyophilic and hydrophilic parts and therefore exhibit surface-activity (McLean and Kilpatrick, 1997a and 1997b, Sheu *et al.*, 1995). They tend to adsorb at water/oil interfaces where they hinder coalescence and act to stabilize an emulsion. As well, asphaltene molecules can self-associate and form increasingly large macromolecules as their concentration in the bulk solution increases. Self-association must be accounted for when interpreting asphaltene interfacial behaviour.

Non-asphaltenic solids can also adsorb at the water/oil interface, creating a steric barrier to coalescence. This type of adsorption leads to a stabilized water droplet only if the adsorbed particle is small relative to the water droplet. Hence, the solids that potentially lead to stable films are in the 100 nm to 1 μm size range (Yan *et al.*, 1999). It is believed that the finest solids lead to the most stable and difficult-to-break emulsions. Solids may also become trapped between water droplets preventing both aggregation and coalescence.

The non-asphaltenic solids are typically fine clays, silicates or ash present in the crude oil/bitumen (native solids), or corrosion products and/or precipitated material that has

become insoluble (non-native solids) (Kotlyar *et al.*, 1993 and 1998, Bensebaa *et al.*, 2000). The effectiveness of solids in stabilizing emulsions depends on several factors, including their concentration, density, size distribution, and surface properties. The interaction of asphaltenes with solids (i.e., the possible adsorption or desorption of asphaltenes on solid surfaces) also contributes to their effectiveness in stabilizing emulsions.

This thesis attempts to relate water-in-oil emulsion stability to interfacial properties and the characteristics of asphaltenes and solids. In this work, emulsion stability is defined in terms of the free water resolution from the emulsion over time when it is subjected to a given destabilization treatment. High free water indicates low emulsion stability; low free water indicates high emulsion stability. Despite numerous studies in this area of research, a clear understanding of the relationship between crude oil properties, the water/oil interface and emulsion stability is still lacking. In fact, experimental results from one study to the next are sometimes contradictory despite seemingly similar emulsion systems. The variability and complexity of crude oil can contribute to the apparent inconsistencies in the literature. Nonetheless, there is agreement that the key to understanding emulsion stability, and subsequently designing more effective emulsion treatments, lies in identifying the interfacial components and determining film properties.

As noted, asphaltenes have been identified as one of the primary stabilizers of oilfield emulsions. However, their role in the formation of interfacial films is not clearly understood. For example, the state in which asphaltenes adsorb (molecules, colloids, micelles) and their structure at the interface is not fully understood. Their effect on the strength of the interface with time is also not fully known. Several groups have hypothesized that once asphaltenes adsorb at the interface, they rearrange and form a rigid, three-dimensional network. A viscous film is believed to hinder drainage from between drops and reduce coalescence. Despite these speculations, few rheological assessments of the interface have been made quantifying film rigidity. By studying model

asphaltene/heptane/toluene and water interfaces and emulsions, this study attempts to better understand the nature of asphaltene interfacial adsorption, the properties of the interface as the film ages, and their relation to emulsion stability.

Generally, it has been observed that solids less than one micrometer can greatly enhance the stability of oilfield emulsions. However, the stabilization mechanisms involved (for example, steric stabilization or trapping) have not been examined in a consistent study. Further, many experiments have been performed with model solids (for example, silica or latex particles) rather than actual solids found in the real emulsions. The difficulty in using actual solids is that their surface properties may change upon extraction from the crude oil or bitumen. When the solids are re-dispersed in a model emulsion system, they may behave differently and original emulsion stability may not be reproduced. This thesis addresses this issue and then attempts to elucidate the stabilization mechanisms relevant for solids and asphaltene-stabilized emulsions.

1.2 OBJECTIVES

The primary objective of this study is to relate the compositional, structural and rheological properties of the water/oil interface to emulsion stability. Ultimately, this may lead to a greater understanding of water-in-oil emulsions and the development of more effective emulsion treatment techniques. As already mentioned, the unusual stability of the emulsions encountered in the production, processing and transportation of crude oil is often related to the asphaltene and native solid materials. This thesis examines the nature of the interface when asphaltenes and solids are the stabilizing particles. Model systems are employed in the majority of experiments in order to eliminate the complexity of a real emulsion and also to isolate the effects of asphaltenes and native solids. The thesis is divided into two main sections with the following objectives:

Effect of Asphaltenes

1. Determine the structure of model water/oil interfaces.
2. Determine the rheology of the water/oil interfaces by measuring the elastic and viscous moduli at various interface aging times.
3. Attempt to apply a Surface Equation of State (SEOS) and diffusional relaxation model describing the rheology of model water/oil interfaces.
4. Relate the structure, composition and rheology of the water/oil interfaces to emulsion stability.

Effect of Native Solids

5. Determine the effect of “fine” and “coarse” native solids on the structure and composition of the water/oil interface.
6. Measure the bulk and surface properties of the native solids.
7. Relate solids properties, and the composition and structure of the water/oil interface, to emulsion stability.

1.3 THESIS STRUCTURE

This thesis is separated into eight chapters. Chapter 2 serves as an introduction to the subject of water-in-crude oil emulsions. First, basic emulsion principles, emulsifiers, emulsions stabilization mechanisms, and the methods used to commercially treat oilfield emulsions are introduced. Second, crude oil composition, with focus on asphaltenes and native oilfield solids, is discussed. Finally, the work on the role of asphaltenes and solids in emulsion stability is reviewed. The role of interfacial film formation is emphasized.

Chapter 3 describes the experimental techniques used in this thesis including: asphaltene molar mass, interfacial tension and elasticity measurements; the techniques used to characterize the size, shape, and mineralogy of native oilfield solids; the experimental

techniques used for the preparation and analysis of model water-in-oil emulsions (gravimetric and drop size measurements) and the assessment of relative emulsion stability.

Chapter 4 summarizes the compositional and structural properties of asphaltene stabilized films and model emulsions. Specifically, a methodology is developed to determine how asphaltenes adsorb at the water/oil interface using a combination of molar mass, interfacial tension, gravimetric and drop size experiments. The results are used to determine if asphaltenes adsorb as a monolayer or in multilayers.

Chapter 5 presents the rheological assessments of the interface; that is, the elastic and viscous moduli of model asphaltene/heptane-toluene/water films are shown at various interface aging times. The early time, asphaltene/toluene/water elastic and viscous moduli are modeled with the Butler Equation of State and the Lucassen-van den Tempel model. The results are used in part to assess the structure of aged interfaces.

Chapter 6 relates the rheology of the interface to the coalescence rate of droplets and the stability of the model water-in-oil emulsions. The effect of asphaltene concentration, solvent quality and interface aging time are examined.

Chapter 7 shows how native solid particles affect the composition and structure of the water/oil interface and their role in emulsion stability. Specifically, the roles of “fine” and “coarse” solids are examined and their stabilization mechanisms elucidated. Treatments geared towards each type of emulsion are proposed and tested on existing wellhead and refinery emulsions.

Chapter 8 summarizes the conclusions of this study and suggests recommendations for further research.

CHAPTER 2
LITERATURE REVIEW

The objective of the current study is to relate the structural, compositional and rheological properties of the water/oil interface to emulsion stability. In order to reduce the complexity of the system, only asphaltenes and native solids have been utilized as emulsion stabilizers. This chapter describes asphaltenes, solids, interfacial properties, and their relation to emulsion stability. Section 2.1 describes basic emulsion principles, emulsifying agents, mechanisms of emulsion stabilization and destabilization, and industry methods used to treat oilfield emulsions. Section 2.2 describes the composition of crude oil with particular focus on asphaltenes and native solids. The concepts of asphaltenes as surface-active and self-associating materials are also discussed. Section 2.3 describes the role of asphaltenes and solids in the formation of interfacial films and their effects on emulsion stability. Section 2.4 summarizes the points most relevant for this thesis.

2.1 EMULSION CHARACTERISTICS

2.1.1 Basic Principles

Two conditions must be satisfied for an emulsion to form:

1) The presence of two immiscible liquids
2) The presence of agitation

An additional condition is required for an emulsion to be stable:

3) The presence of emulsifying agents

An emulsion is defined as a mixture of two immiscible liquids in which one liquid is dispersed in the other in the form of droplets. The droplet phase, or dispersed phase, is often referred to as the internal phase, whereas the continuous phase is called the external

phase. When water is dispersed in oil, a water-in-oil (W/O), or regular, emulsion is formed. When oil is the dispersed phase, an oil-in-water (O/W), or reverse, emulsion is formed. The nature of the emulsion (i.e., W/O or O/W) can usually be identified by analyzing the following (Schramm, 1992):

- texture: an emulsion has the same "feel" as the continuous phase ("watery" for O/W, "oily" for W/O)
- mixing ability and inversion: an emulsion mixes easily with a liquid of the same miscibility as the continuous phase; if the emulsion is very concentrated it will invert when diluted with the dispersed phase
- dyeing capacity: an emulsion is colored by dyes soluble in the continuous phase
- conductance: an emulsion has the same conductance as the continuous phase (high for O/W, low for W/O)
- fluorescence: if an emulsion fluoresces and the droplets are larger than the resolution of the microscope the emulsion type can be identified.

For oilfield applications, the two immiscible liquids are usually water (or brine) and oil (or light hydrocarbons). In the petroleum industry, both regular (W/O) and reverse (O/W) emulsions can occur, as indicated in Table 2.1.

Table 2.1: Examples of emulsions in the petroleum industry (Schramm, 1992)

Occurrence	Usual Type
Undesirable Emulsions	
Well-head emulsions	W/O
Oil sand flotation process, froth	W/O or O/W
Oil spill emulsions	W/O
Desirable Emulsions	
Heavy oil pipeline emulsions	O/W
Oil sand flotation process, slurry	O/W
Emulsion drilling fluid	
Oil-emulsion mud	O/W
Oil-base mud	W/O
Asphalt emulsion	O/W
Enhanced oil recovery in situ emulsions	O/W

To form an emulsion that has at least short term stability, the liquids must be thoroughly mixed such that sufficiently small drops are created. However, the formation of small drops results in an increase in the surface area between the two liquids and in turn results in an increase in excess free energy. The excess energy results because oil and water molecules are in contact with unlike molecules at the interface. When the interfacial area decreases, the free energy also decreases. In emulsion systems, the interfacial area tends to be minimized because the drops assume a spherical shape and because they coalesce into larger drops as time progresses. Consequently, immiscible mixtures have a propensity to separate into the respective liquids.

The current work is devoted solely to model and oilfield water-in-oil emulsions. Some of these emulsions exhibit remarkable long term stability, that is, water droplets remain dispersed in the continuous oil phase for long periods of time and the resolution of separate, clean oil and water phases may occur only upon addition of heating and centrifugation. Although mixtures of oil and water naturally separate into two phases, these oilfield emulsions often resolve only marginally. Other emulsions, such as those encountered in the food and cosmetic industries, never resolve unless subjected to improper use (e.g., addition of heat). The reason these types of oil/water mixtures remain emulsified for long periods of time is because emulsifying agents adsorb at the interface and therefore prevent or retard drop aggregation and/or coalescence.

2.1.2 Emulsifying Agents

Emulsion stability is possible due to adsorption of molecules at the water/oil interface and the formation of strong interfacial films. These molecules are known as emulsifying agents and include surfactants, which lower the interfacial tension at the interface, and solid particles, which create a mechanical barrier at the interface.

2.1.2.1 Surfactants

Surfactants are the most common emulsion stabilizers. Generally, they are composed of polar hydrophilic “heads” and non-polar hydrophobic “tails” that consist of several carbon atoms. Surfactants are classified according to the nature of the polar head group. The most common species are nonionic surfactants of polyoxyethylene moieties, -(OCH_2CH_2)-$_m$, such as polyoxyethylene alcohol or alkylphenol ethoxylate. Other nonionic surfactants include sorbitan esters of oleic or lauric acids, ethocylated sorbitan esters of oleic or lauric acids, as well as polyethylene glycol esters of oleic acids. The ionic surfactants include anionic structures such as sodium stearate (-COO^-), sodium dodecyl sulfate (-SO_4^-) and sodium dodecyl benzene sulfonate (-SO_3^-), and cationic structures such as laurylamine hydrochloride (-NH_3^+) and cetyl trimethylammonium bromide (-N^+). When both negatively and positively charged groups are present in the head, the surfactant is classified as zwitterionic. For example, lauramidopropyl betaine contains a positive group, -N^+, and a negative group, -COO^- (Schramm, 1992).

The behaviour of surfactants is determined by the Hydrophilic-Lipophilic Balance, or HLB value. The HLB scale, defined by Griffin in the mid 1950s, ranges in value from 1 to 20 (NRC, 1989) and is related to the solubility of the surfactant in oleic and aqueous phases. A value of 1 represents a strongly hydrophobic surfactant, i.e., one which is oil soluble. Conversely, a value of 20 indicates a strongly hydrophilic surfactant, i.e., one which is water soluble. Because they have an affinity for oil and water, surfactant molecules orient in such a way that the head is located in the water phase, while the tail is located in the oil phase. A surfactant with an HLB of 3-6 will generally stabilize a water-in-oil emulsion, while an oil-in-water emulsion will be stabilized by a surfactant of HLB 8-18 (NRC, 1989). Other researchers report these values at 1 to 8 and 12 to 20, respectively (Fingas *et al.*, 1995).

The HLB value of the surfactant influences not only solubility and emulsion formation, but also the likelihood of micelle formation. When present in low concentrations,

surfactants behave as normal electrolytes. However, at higher concentrations, they are able to organize into structures known as micelles or reverse micelles. For surfactants with high HLB, i.e., those easily dissolved in aqueous media, the hydrophilic heads face outwards whereas the hydrophobic tails face inwards. The opposite is true for low HLB surfactants in an organic media: the heads face inwards whereas the tails face outwards and reverse micelles are formed. In each case, the contact between unlike molecules is minimized. The concentration at which micellization begins is called the Critical Micelle Concentration (CMC). For pure surfactants, the CMC is most commonly observed by a sharp break in the interfacial tension (or surface pressure) versus concentration curve, as shown in Figure 2.1. At concentrations below the CMC, surfactants exist in solution as individual molecules. At concentrations exceeding the CMC, excess surfactants remaining in solution can aggregate into micellar structures. The break in the plot reflects the change in apparent molar mass of the solute (i.e., surfactants grouped as micelles) in solution (Lyklema, 1994). Note that for mixtures of surfactants, the break in the curve may not be sharp; rather, a more gradual decline in the interfacial tension (IFT) may be observed. Also note that, although interfacial tension is the most common property for determining the CMC, other solution properties such as turbidity and conductivity may also be used to assess micellization and the CMC.

The adsorption of surfactants at the interface provides an expanding force against the normal tension between the oil and water, thus resulting in a reduction in the interfacial tension. A reduction in the interfacial tension reduces the free energy associated with the interface and increases the likelihood that oil and water will remain emulsified. However, besides lowering IFT at the interface, surfactants can also increase the interfacial viscosity, resulting in a mechanical resistance to coalescence. Further, they can create an electrostatic repulsion amongst drops and reduce the chances of flocculation. The combination of reduced IFT, increased film viscosity, and/or electrostatic repulsion can result in stable emulsions.

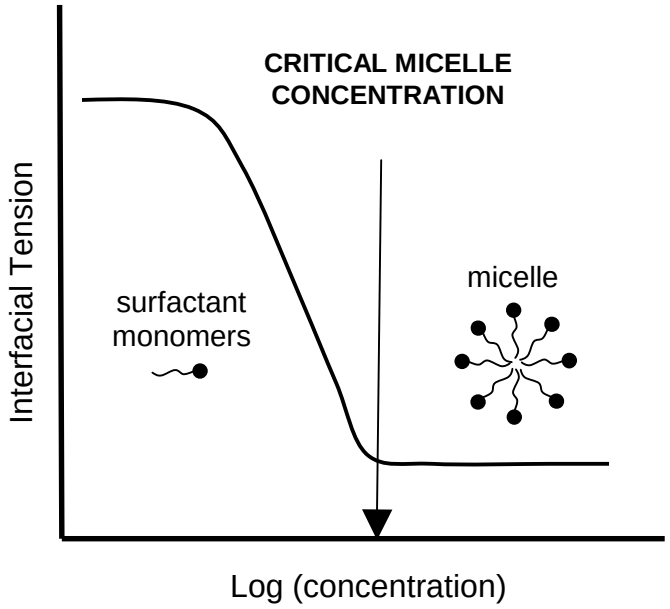

Figure 2.1: Micellization of pure surfactant molecules

2.1.2.2 Solid Particles

Solids can potentially stabilize an emulsion by adsorbing at the water/oil interface directly or by adsorbing on an existing surfactant film. The solids adsorbed on the interface or existing emulsion film can create a steric barrier between adjacent water drops, hindering droplet collisions, film drainage, and coalescence (Tambe and Sharma, 1993; Tadros and Vincent, 1983). They can also contribute to the mechanical rigidity and viscosity of the film if a tightly packed network structure is created and there are strong particle-particle interactions (Tambe and Sharma, 1993; Menon and Wasan, 1984; Tambe and Sharma, 1994; Abend *et al.*, 1998; Binks and Kirkland, 2002; Aveyard *et al.*, 2003). There is also evidence that partial surface coverage by solids can be sufficient to stabilize emulsions (Binks and Kirkland, 2002; Vignati *et al.*, 2003). If solids are trapped between drops, they may reduce aggregation and creaming/sedimentation of an emulsion phase

and further decrease the chances of coalescence (Yan *et al.*, 2001). They may also increase the overall emulsion viscosity (Aveyard *et al.*, 2003; Yan and Masliyah, 1993; Yaghi *et al.*, 2001; Houache and Yaghi, 2003) and reduce the chances of segregation of water and oil.

The mechanisms associated with solids-stabilized emulsions and the degree to which solids increase emulsion stability depends on several factors such as particle size, shape and morphology, density, concentration and surface coverage, and wettability. These issues will be addressed specifically for particles encountered in oilfield water-in-oil emulsions in Section 2.2.7, but generally, it can be said that emulsion stability increases with decreasing particle size and density and increasing particle concentration. In fact, to be effective emulsion stabilizers, solid particles must be at least ten times smaller than the droplet (Aveyard *et al.*, 2002; Binks and Kirkland, 2002). They should also be locally biwettable; that is, they should contain some surfaces preferably wetted by water and some by oil. As the names imply, a "water-wet" solid refers to one preferentially wetted by water whereas an "oil-wet" solid is more easily wetted by oil. A water-wet solid is one in which the apparent contact angle, θ, as measured through the water phase, is smaller than 90º and an oil-wet solid is one in which the apparent contact angle is larger than 90º. This is illustrated in Figure 2.2 (a).

For solids to form a sufficiently thick and strong mechanical barrier between drops, the majority of the solid should protrude into the continuous phase. Note that the measured contact angle does not take into account the molecular orientation of water-wet and oil-wet regions on the solid; rather, an apparent contact angle is measured. Therefore, the potential arrangement of solids at the interface is such that oil-in-water emulsions are stabilized by water-wet solids, whereas water-in-oil emulsions are stabilized by oil-wet solids, as illustrated in Figure 2.2 (b). As will be shown in Section 2.3.3.3, some of the most stable emulsions are those stabilized with biwettable solids, in which the apparent contact angle between the oil, water and solid does not deviate far from 90º.

Adsorbed solids do not generally cause a decrease in interfacial tension, although the contrary has been observed by Nushtaeva and Kruglyakov (2004). Usually, solids pose a mechanical barrier at the interface.

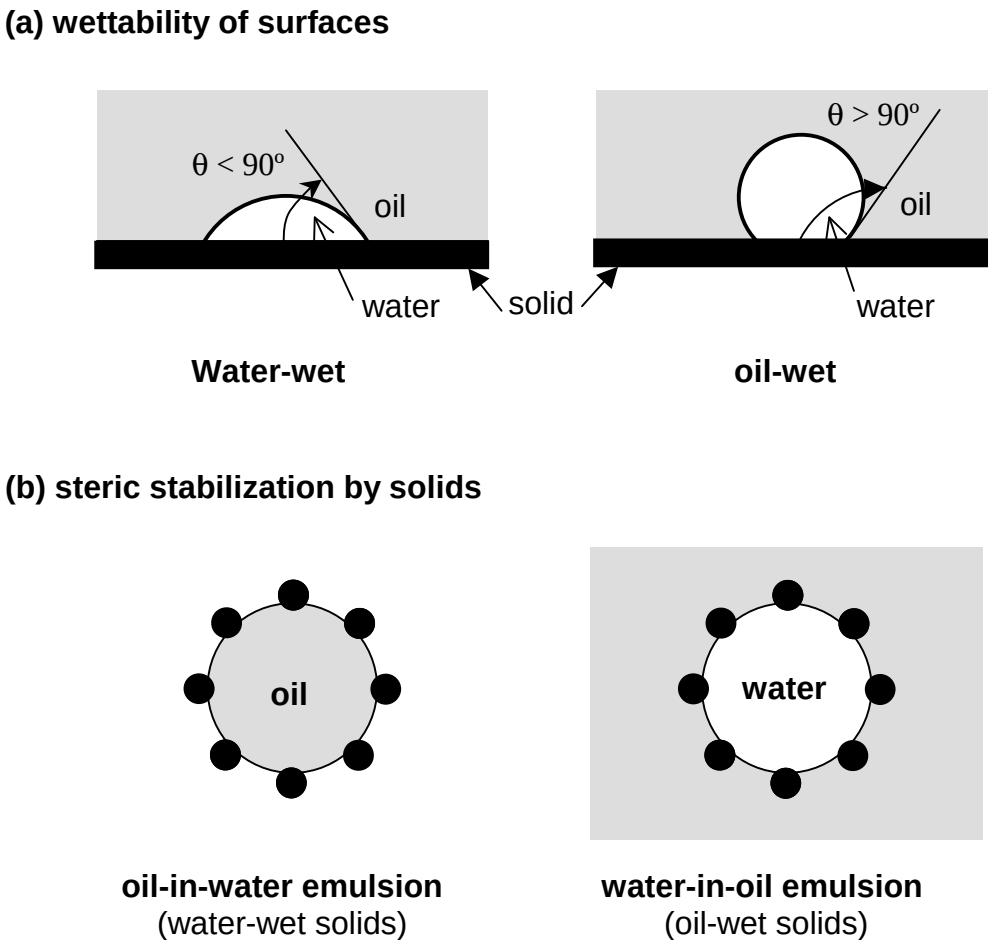

Figure 2.2: Steric stabilization by solid particles

2.1.3 Emulsion Stabilization and Destabilization

Emulsion stability depends on several factors including the characteristics of the continuous and dispersed phases, the drop size distribution, the properties of the emulsifier and its concentration, the agitation energy present at the time of emulsification, the temperature and pH, as well as the elapsed time since emulsification (i.e., the age of the emulsion). Most emulsions are not thermodynamically stable and tend to "break" into separate liquid phases. Emulsion destabilization processes include: creaming/ sedimentation, flocculation/aggregation, coalescence and Ostwald ripening. The first two processes result in a change in the spatial location of the drops but no change in the drop size distribution, whereas the last two processes result in a change in the drop size distribution and may or may not result in spatial rearrangement. The processes are summarized in Figure 2.3.

Creaming/Sedimentation

Creaming and sedimentation are processes in which droplets rise and fall, respectively, because of the density difference between the continuous and dispersed phases. Hence, oil-in-water emulsions undergo creaming whereas water-in-oil emulsions undergo sedimentation. Most emulsions undergo creaming/sedimentation unless the density difference between the phases is very small or the viscosity of the continuous phase is very high. High viscosity can be a problem for water-in-oil emulsions, specifically those encountered in the petroleum industry.

Aggregation

Aggregation occurs when droplets are brought together without rupture of the interface. The formation of flocs results in increased creaming (or settling) since the effective size of the drop increases. Larger drops rise/fall more rapidly than smaller drops.

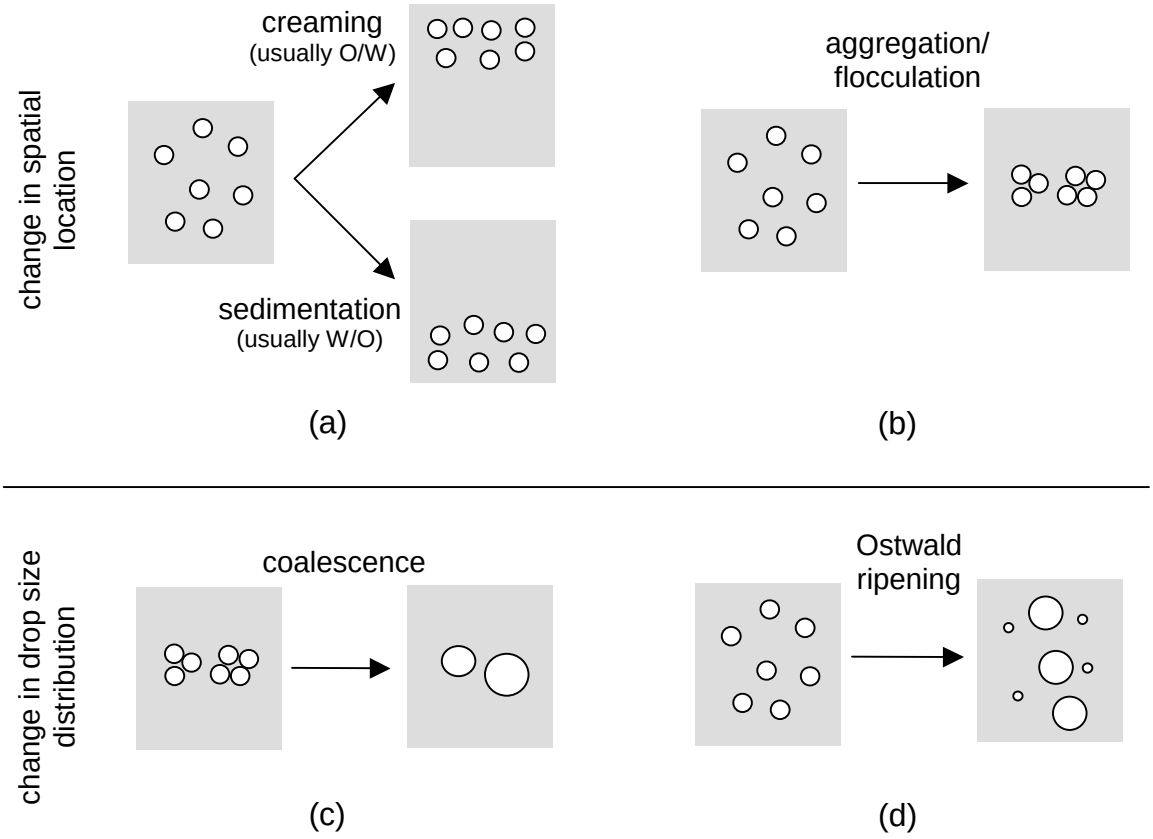

Figure 2.3: Natural emulsion destabilization processes

Water-in-oil emulsions are usually sterically stabilized; that is, a structural barrier is present at the interface. A steric barrier can be the result of adsorbed solid particles or the mechanical barrier formed as a result of tail groups of an adsorbed surfactant protruding out of the water droplet. Steric stabilization also occurs for oil-in-water emulsions. However, for oil-in-water emulsions, the presence of electrical barriers offers additional resistance to aggregation and subsequent coalescence of drops. Oil droplets have a net charge because the head groups of ionic surfactants surround the drop and protrude into the water phase. The net charge on the drop is equivalent to the charge of the head group of the surfactant. The effect is to influence the position of nearby ions in the continuous water phase, giving rise to an “ionic atmosphere” that surrounds the charged droplets. The charged atmosphere, known as the double layer, can prevent close contact among drops and therefore reduce the chances of aggregation.

The extent of creaming and flocculation/aggregation depends on the shape of the energy potential curve shown in Figure 2.4. For oil-in-water emulsions, the electrostatic repulsive forces arising from the double layer are countered by van der Waals attractive forces resulting from intermolecular attractions in the form of permanent dipole-dipole interactions, dipole-induced dipole interactions and dispersion forces (i.e., London dispersion forces). The sum of attractive and repulsive forces at short distances is described by DLVO theory which relates the total energy potential to the distance between the surfaces of charged particles. The curve is characterized by a primary minimum which is related to the flocculation capacity of the particles. Depending on the magnitude of the attractive and repulsive forces, the curve may also contain a maximum and a secondary minimum which represent the capacity for coalescence and flocculation, respectively.

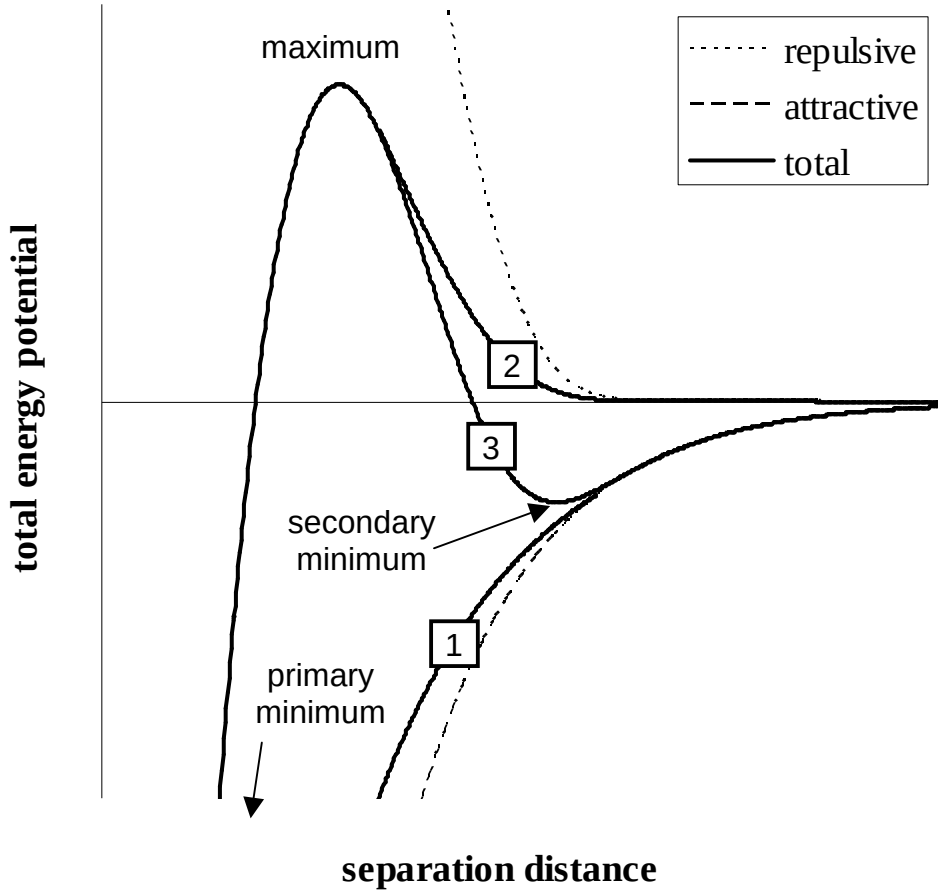

Figure 2.4: Interaction energy between particles

(1) high ionic strength

(2) low ionic strength

(3) intermediate ionic strength

The presence of the maximum and the secondary minimum depends on the ionic strength of the aqueous phase. Curve (1) in Figure 2.4 represents a system of high ionic strength, meaning that repulsive forces are small and attractive van der Waals forces dominate at all separation distances. Particle aggregation would occur only in the primary minimum and a very large energy would be required to separate particles. Conversely, curve (2) represents a system of low ionic strength. Here, electric double layer repulsion is strong, and an energy barrier appears at intermediate separation distances. Only if the energy barrier is overcome can drops coalesce. Coalescence occurs when there are strong droplet-droplet attractions and when radial hydrodynamic forces at the front ends of the droplets are large enough to overcome this energy barrier. Curve (3) represents a system of intermediate ionic strength. In this case, repulsive and attractive forces are comparable. At low droplet velocity (i.e., poor sedimentation or creaming), droplets cannot climb over the energy barrier presented by the primary maximum, so weak attraction amongst droplets at intermediate distances will occur in the secondary minimum. If hydrodynamic forces increase, droplets may be able to exceed the energy required to surmount the maximum, either coalescing, or aggregating with very strong attractive forces in the primary minimum (Masliyah, 1994).

Coalescence

Aggregation may lead to droplet coalescence depending on the characteristics of the continuous phase and the stabilizing film. Coalescence is summarized in Figure 2.5. During coalescence, two droplets approach each other to within molecular separation distances (2.5 a). As they are drawn or forced together, their surfaces begin to dimple creating a planar interface between the droplets. Simultaneously, the continuous phase drains from between the droplets (2.5 b). As the surface dimples and stretches, any surface-active materials adsorbed on the interface are spread apart and surfactant-free pockets may develop on the interface. As the fluid trapped between droplets continues to drain, the droplets approach each other to within nanometers and the dispersed phase fluid can bridge the gap between the interfaces and trigger coalescence (2.5 c and d). The

probability of coalescence decreases if the droplets do not come into close contact, drainage is hindered, there is a strong resistance to dimpling, and the surfactant diffuses rapidly into the dimpled area (relaxation). High continuous phase viscosity and the presence of large particles dispersed throughout the continuous phase may impede film drainage and prevent close contact among droplets. High concentrations of surfactant may impede dimpling and the formation of surfactant-free pockets.

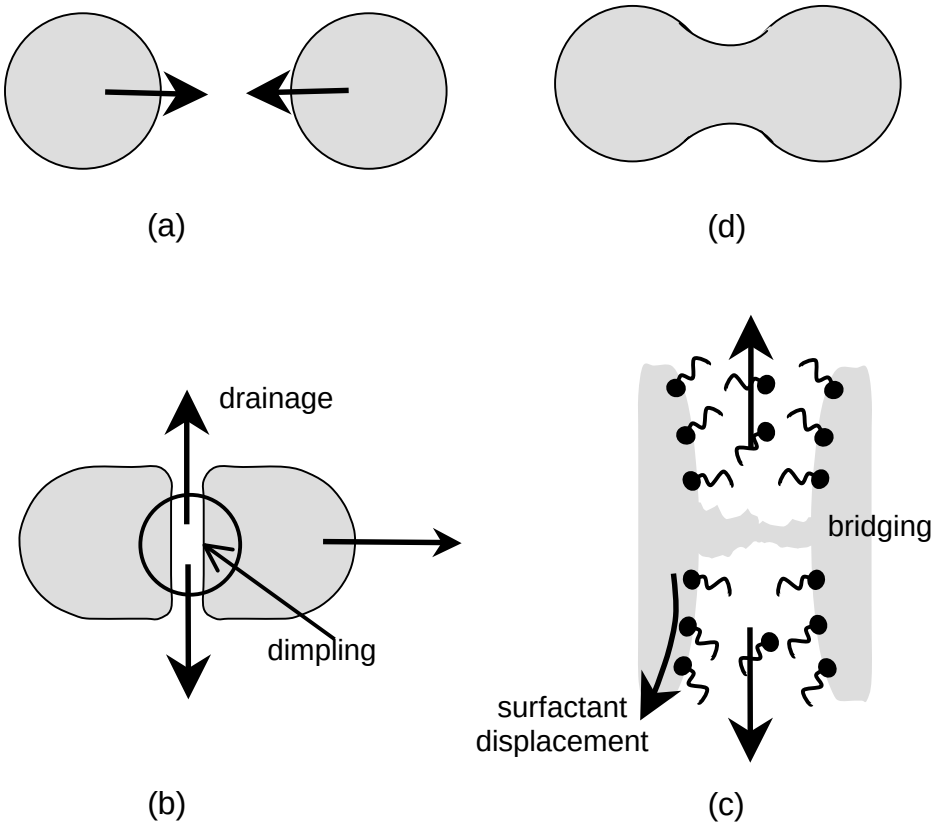

Figure 2.5: Steps in coalescence

Ostwald Ripening

Ostwald ripening involves mass transfer through the continuous phase between droplets of disparate size. The concentration of the dispersed phase at the surface of a drop is inversely proportional to its radius of curvature (Kabalnov and Shchukin, 1992). Hence, there is a higher dispersed phase concentration near small drops and a lower concentration near large drops. Mass transfer occurs from small drops to large drops, resulting in shrinkage of the small drops and growth in the large drops. Eventually, the smaller drops disappear. Although these changes are relatively slow, they do result in a change in the drop size distribution.

2.1.4 Treatment of Emulsions

Oilfield emulsions are usually treated with a combination of physical and chemical methods and are designed to improve creaming/sedimentation, aggregation, and coalescence. The oldest and simplest treatment is gravity settling. However, additional treatments are usually employed because gravity settling can be very slow, especially when the continuous phase viscosity is high, the density difference between the oil and water is small, and the dispersed droplets are very small. In fact, as stated by Smith and Arnold (1987), gravity settling is only used to treat relatively loose, unstable emulsions. In the oilfield, gravity settling is usually supplemented with heating, electrostatic coalescers, and/or chemical treatments.

Heating reduces the bulk emulsion viscosity, which facilitates drainage of the continuous phase from between drops and may also reduce the rigidity of the interface. For example, asphaltenes adsorbed at the interface may form a looser, less viscous network and therefore may be more easily removed from the interface when droplets collide. For waxy oils, adsorbed solid wax particles may become dissolved upon heating and the emulsion film broken. Heating also promotes movement of drops and hence increases the likelihood of collision amongst drops. However, heating may lead to loss of light end hydrocarbons, leaving oil that is more dense and viscous upon cooling. The total volume

of oil is also reduced. Further, the cost of fuel necessary to heat the emulsion may also reduce the cost-efficiency of the heating process (Smith and Arnold, 1987).

In addition to heat, electrostatic coalescers may also be used to increase the resolution of water and oil. In an electrostatic coalescer, a high-voltage electric field is applied to water-in-crude oil emulsions. Water droplets dispersed throughout the oil become polarized and align with the lines of the electric force (Smith and Arnold, 1987). As a result, the positive and negative poles of the droplets align and when in close contact, the droplets coalesce. The electric field also causes distortion of the stabilizing film which may promote rupture and subsequent coalescence. Electrostatic methods are only applicable for water-in-oil emulsions because the dispersed phase (water) must be conductive in order to induce a dipole in the droplets. Additionally, the continuous phase should not be conductive in order to prevent large power losses.

Chemical demulsifiers are usually used in addition to heating. Most commercial demulsifiers are flocculants aimed at promoting rapid settling. However, chemical demulsifiers may also replace emulsion stabilizers at the interface. In order to be effective, they must first mix closely with the emulsion, reach all water/oil interfaces, and finally replace existing stabilizers on the interface. For adsorbed solids, demulsifiers may alter the wettability and promote desorption of the particles. In both cases, a weaker film is created and the chances of coalescence increased. Most chemical demulsifiers are surface-active species with complex organic compounds. Smith and Arnold (1987) list several types of demulsifiers: polyglycol esters, low-molecular weight resin derivates, sulfonates, polymerized oils and esters, alkanolamine condensates, oxyalkylated phenols and polyamine derivatives. They may be used alone or in combination depending on the desired HLB and on the stability problems of the particular emulsion to be treated. Often, the optimal composition and combination of demulsifiers is determined by performing extensive bottle tests on small emulsion samples. The effects of concentration, operating

temperature, settling time, and cost must be taken into account. A good understanding of the factors contributing to emulsion stability is beneficial for proper demulsifier selection.

2.2 CRUDE OIL COMPOSITION

Crude oil, or equivalently petroleum, is a complex mixture of thousands of organic chemical species. It is primarily composed of hydrocarbon compounds but also includes heteroatom groups that contain nitrogen, oxygen and sulfur and species which incorporate metals such as vanadium, nickel and iron. The origin of the crude oil can have a significant effect on its composition, resulting in oils varying widely in volatility, density, viscosity, and colour.

“Conventional crude oil” refers to oil that can be produced at least initially through primary recovery without the addition of heat, chemicals or solvents. Because these oils have relatively low viscosity and density, they can be produced through pumping operations as free-flowing oil. Oil that is significantly more viscous and has a lower API gravity (higher density) is called “heavy crude oil”. These oils are more difficult to produce by primary recovery and require some thermal stimulation or the addition of solvents to reduce viscosity. Although the distinction between light oil and heavy oil is somewhat arbitrary, it is generally accepted that heavy oil has an API gravity less than 20^{o} (density greater than 934 kg/m^{3}) and contains more than 2 wt% sulfur (Speight, 1981).

“Bitumens” or “extra heavy crude oils” are solid or near-solid materials that do not flow freely under ambient conditions. They are extremely viscous and are usually produced through mining of oil sand deposits or through secondary and enhanced recovery techniques. Bitumen is denser than heavy oil and usually contains significantly higher quantities of heteroatoms and metallic groups.

Petroleum is primarily composed of hydrocarbons including paraffins, cycloparaffins and aromatics. Paraffins are saturated hydrocarbons with straight or branched chains. The cycloparaffins, also called naphthenes, contain saturated hydrocarbon of one or more rings with paraffinic side-chains. The aromatics contain ring structures of benzene, naphthalene and phenanthrene and may be linked with substituted naphthalene rings, paraffinic side chains, or a combination of both (Speight, 1999).

Nitrogen, oxygen and sulfur may be incorporated in various hydrocarbon organic groups. In petroleum, nitrogen occurs either in basic or non-basic form. The basic compounds are primarily pyridine homologues, including quinoline, indoline and benzoquinoline and various porphyrins. Potentially, they can be problematic in acid-catalyzed processes (catalyst fouling, increased amounts of acids required) and in petroleum refining. The non-basic compounds include pyrroles, indoles and carbazoles (Speight, 1999). Oxygen occurs in numerous forms such as alcohols, ethers (chain and cyclic), carboxylic acids, acid anhydrides and esters, ketones and furans (Speight, 1999). In petroleum, the majority of oxygen compounds occur as phenols, naphthenic acids, and esters. Sulfur occurs as mercaptans (thiols), sulfides (chain and cyclic) and disulfides (Speight, 1999) and other sulfur compounds such as thiophene which is aromatic.

2.2.1 Classification of Petroleum

Petroleum can be classified in a number of ways including by chemical composition, density, viscosity, boiling cut, H/C ratio, carbon distribution, heteroatom content, and solubility class. In the current work, the most relevant and easily implemented method is solubility class. The four solubility classes are saturates, aromatics, resins (collectively called maltenes) and asphaltenes. Their method of separation, shown in Figure 2.6, is called SARA fractionation (the abbreviation is made up of the first letter of each solubility class). There are several variations of SARA, but the most commonly used methods are any of the ASTM methods.

The first step of SARA fractionation is the separation of asphaltenes from bitumen. Asphaltenes are precipitated by adding 40 volumes of pentane to one volume of bitumen. The mixture is usually stirred, allowed to settle, and filtered. The dark brown/black powder remaining in the filter paper comprises the asphaltenes. The maltenes passing through the filter paper are concentrated by evaporating the associated pentane and then separated into saturates, aromatics and resins through clay-gel adsorption chromatography. Resins adsorb on Attapulgus clay, aromatics adsorb on silica gel, and saturates elute directly. The resins are separated from the clay with a 50/50 mixture of toluene and pentane. The aromatics are separated with a mixture of 50/50 toluene and acetone. The solvents are evaporated to concentrate each.

A typical SARA analysis of Alberta and international bitumens and heavy oils is given in Table 2.2 (Peramanu *et al.*, 1999; Akbarzadeh *et al.*, 2004). Note that other solvents may be used for deasphalting oil. Pentane is used if one requires all four solubility classes for use; however, asphaltenes are often precipitated with hexane or heptane if their recovery alone is desired. In fact, asphaltene yields reported in the literature more commonly refer to the yield with heptane rather than pentane. The asphaltene yield decreases with increasing carbon number up to approximately C_{10} (Speight, 1999). It also decreases as the temperature and pressure increase and as the contact time between the solvent and bitumen decreases.

Table 2.2: SARA fractionation of Alberta and international bitumen and heavy oil (Peramanu[(a)] *et al.*, 1999; Akbarzadeh[(b)] *et al.*, 2004)

Source	Saturates (wt%)	Aromatics (wt%)	Resins (wt%)	Asphaltenes (wt%)
Western Canadian				
Athabasca	17.3[(a)], 16.3[(b)]	39.7[(a)], 39.8[(b)]	25.8[(a)], 28.5[(b)]	17.3[(a)], 14.7[(b)]
Cold Lake	20.7[(a)],19.4[(b)]	39.2[(a)],38.1[(b)]	24.8[(a)],26.7[(b)]	15.3[(a)], 15.5[(b)]
Lloydminster[(b)]	23.1	41.7	19.5	15.3
International				
Venezuela[(b)]	15.4	44.4	25.0	15.2
Russia[(b)]	25.0	31.1	37.1	6.8
Indonesia[(b)]	23.2	33.9	38.2	4.7

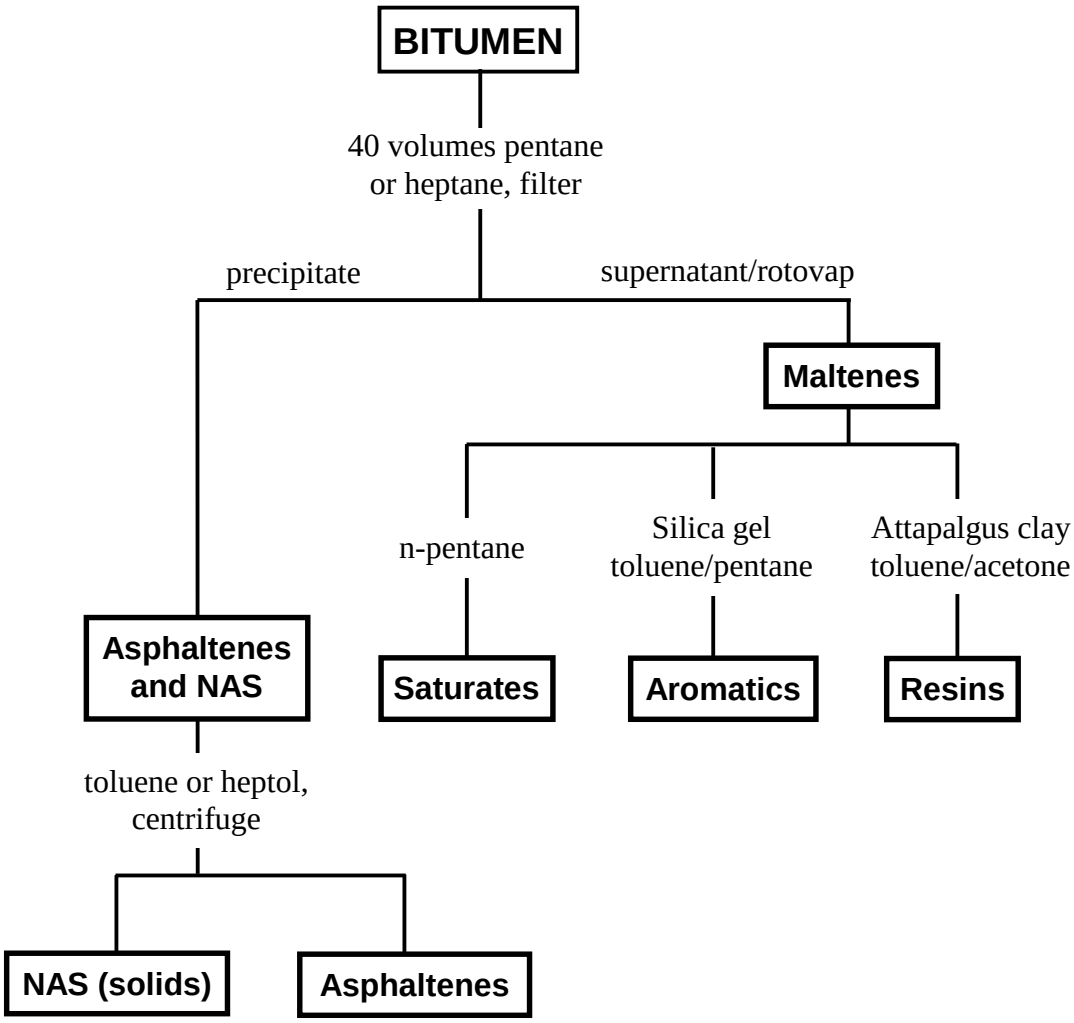

Figure 2.6: SARA fractionation of bitumen

As suggested by Figure 2.6, the material commonly called “asphaltenes” is actually a mixture of asphaltenes and Non-Asphaltenic-Solids (NAS). Most heavy crude oils and bitumens contain at least some fraction of solids, usually less than 1% weight of the bitumen. The solids are a mixture of clays, sand, ash and other materials. They can be separated from the asphaltenes by redissolving the asphaltene-solids in heptol (a mixture of heptane and toluene) or toluene and then centrifuging the solution. During centrifugation, the asphaltenes remain solubilized in the toluene (or heptol if the heptane content is less than the onset of precipitation) whereas the solids are concentrated at the bottom of centrifuge tubes. The methodologies used for their recovery are given in detail in Chapter 3.

Since SARA fractions are separated according to solubility rather than chemical nature, each class contains thousands of individual molecular species. In fact, aromatics, resins and asphaltenes form a continuum of molecules of increasing molecular weight, density, polarity and heteroatom content. While there is no single representative molecule for each class, the molecules within each class do have common characteristics.

2.2.2 Saturates and Aromatics

The saturate and aromatic classes are more precisely defined than resins and asphaltenes because they contain significantly fewer and simpler types of molecules. The saturate fraction is composed of paraffins and naphthenes (cycloparaffins). The most prevalent single ring naphthenes are methyl, ethyl or propyl-substituted cyclopentanes and cyclohexanes. Saturates are sometimes referred to as “white oils” due to their pearly colour. The molar mass and density of saturates extracted from several Alberta and international bitumens and heavy oils was found to vary from approximately 360 to 545 g/mol and 853 to 900 kg/m^3, respectively (Akbarzadeh *et al.*, 2004).

As the name suggests, aromatics are composed of structures containing aromatic rings. They include monoaromatics, substituted naphthalenes and phenanthrenes (one, two and

three ring aromatic structures, respectively). The molar mass and density of aromatics is slightly more than saturates: values varying from 450 to 550 g/mol and 960 to 1003 kg/m³, respectively, have been reported in the literature (Akbarzadeh *et al.*, 2004).

2.2.3 Asphaltenes

Asphaltenes are large, polar, polynuclear molecules consisting of condensed aromatic rings, aliphatic side chains, and various heteroatom groups (Strausz *et al.*, 1992; Watson and Barteau, 1994). They are the highest molecular weight, most polar and aromatic fraction, and are responsible for the high density and viscosity of some heavy crudes and bitumens. The density of asphaltenes has been reported as 1132 to 1193 kg/m³ (Akbarzadeh *et al.*, 2004). The chemical characteristics of asphaltenes cause them to be amphiphilic and therefore exhibit surface activity (Taylor, 1992; McLean and Kilpatrick, 1997a and 1997b; Siffert *et al.*, 1984; Sheu *et al.*, 1995; Schildberg *et al.*, 1995; Rogacheva *et al.*, 1980). The chemical nature, structure and surface activity of asphaltenes are discussed in detail in the following sections.

2.2.3.1 Asphaltene Elemental Composition

Although the literature alludes to the complexity of the asphaltene solubility class, the elemental composition is well known with relatively few differences between asphaltene samples. Table 2.3, summarized from the extensive data given by Speight (1999), shows the elemental composition and atomic ratios of pentane extracted asphaltenes from oils originating in Canada, Iran, Kuwait, and Venezuela. The data indicates similarity in the carbon and hydrogen content between sources. In fact, as stated by Moschopedis *et al.* (1976), the H/C ratio is usually 1.15 ±0.5%, suggesting that asphaltenes have a specific composition and molecular structure and can therefore be described as more than just a solubility class. The nitrogen content is also fairly constant (0.2 to 3.3%), whereas the oxygen and sulfur contents are more variable (0.3 to 4.9% and 0.3 to 10.3%, respectively). Note these limits include oils not listed in Table 2.3. Heptane precipitated asphaltenes have a slightly smaller H/C ratio and larger N/C, O/C and S/C ratios.

Although the differences are not marked, they do reveal that heptane precipitated asphaltenes have a higher degree of aromaticity and larger proportion of hetero elements.

Table 2.3: Elemental composition of asphaltenes from world sources (Speight, 1999)

	Canada	**Iran**	**Kuwait**	**Venezuela**
Carbon (wt%)	79.0 – 88.7	83.7	81.6 – 82.4	81.1 – 84.7
Hydrogen (wt%)	6.9 – 11.1	7.8	7.8 – 8.1	7.8 – 8.3
Nitrogen (wt%)	0.7 – 2.8	1.7	0.6 – 1.7	0.2 – 2.0
Oxygen (wt%)	0.4 – 3.9	1.0	0.6 – 1.8	1.0 – 4.2
Sulfur (wt%)	0.3 – 8.1	5.8	7.4 – 8.0	2.7 – 6.9
H/C Ratio	0.98 – 1.56	1.19	1.14 – 1.19	1.13 – 1.19
N/C Ratio	0.007 – 0.029	0.017	0.008 – 0.017	0.002 – 0.02
O/C Ratio	0.004 – 0.037	0.009	0.005 – 0.017	0.013 – 0.039
S/C Ratio	0.001 – 0.038	0.026	0.034 – 0.039	0.012 – 0.032

Asphaltenes also contain metal elements, most notably vanadium, nickel and iron (Nalwaya *et al.*, 1999). The nickel and vanadium can occur in porphyrins (Speight, 1999); however, they are also believed to be chelated with ligands that are not porphyrins (Crouch *et al.*, 1983). Further, some of these elements may actually be associated with the native solids. Kotlyar *et al.* (1999) emphasize the importance of analyzing metal content of asphaltenes on a solids-free basis.

2.2.3.2 Asphaltene Molecular Structure

Although the elemental composition of asphaltenes is well established, the structure is still debated. No single asphaltene molecule has ever been identified; however, various studies of the fraction have led to agreement on some general characteristics.

Asphaltenes are believed to be large, polynuclear structures containing condensed aromatic rings with aliphatic side chains and dispersed heteroatom groups. Infrared and nuclear magnetic resonance spectroscopic techniques reveal that the aromatic ring systems are composed of six to 15-20 rings. It has been suggested that repeating units of these condensed structures, linked by alkyl side chains and rings, accounts for the high

molar mass of asphaltenes (Speight, 1999; Calemma *et al.*, 1998). The degree of condensation may affect ultimate emulsion stability. Khadim and Sarbar (1999) have suggested that increased aromaticity, decreased side chain length and reduced chain branching may lead to the formation of more stable emulsions. However, Papirer *et al.* (1982) noted that asphaltenes of intermediate aromaticity resulted in the highest emulsion forming ability.

The polarity of asphaltenes arises from the nitrogen, oxygen and sulfur heteroatom groups located throughout the molecule. Watson and Barteau (1994) suggest that the heteroatoms are most likely incorporated into the aromatic sheets. Various heterocyclic and four-ring aromatic nitrogen species have been identified in the asphaltene structure. Mitra-Kirtley *et al.* (1993) suggest most of the nitrogen found in asphaltenes is aromatic and occurs primarily in the pyrrolic rather than pyridinic form. However, Strausz *et al.* (1992) identify n-alkyl pyridine as a possible group in their formulation of a hypothetical asphaltene molecule. They also suggest the presence of porphyrins, consistent with the work of Yen (1974) and Strausz (1989). Interestingly, the more conventional primary, secondary and tertiary aromatic amines have not been identified in the asphaltene structure. Carbazoles and amides were identified by Moschopedis and Speight (1979). Oxygen usually occurs in carboxylic, phenolic and ketonic groups (Ritchie *et al.*, 1979; Nicksic and Jeffries-Harris, 1968; Moschopedis and Speight, 1976; Bestougeff and Byramjee, 1994), but is not usually found in the aromatic ring structures. Sulfur can occur as benzothiophenes, di- and naphthene-benzothiophenes (Speight, 1999; Nicksic and Jeffries-Harris, 1968; Ritchie *et al.*, 1979), as well as alkyl-alkyl, alkyl-aryl, and aryl-aryl sulfides (Speight, 1999).

Several researchers have proposed hypothetical “average” asphaltene molecules (Strausz *et al.*, 1992; Yen, 1974; Murgich and Strausz, 2001). One such example is the molecule proposed by Strausz *et al.* (1992), here shown in Figure 2.7.

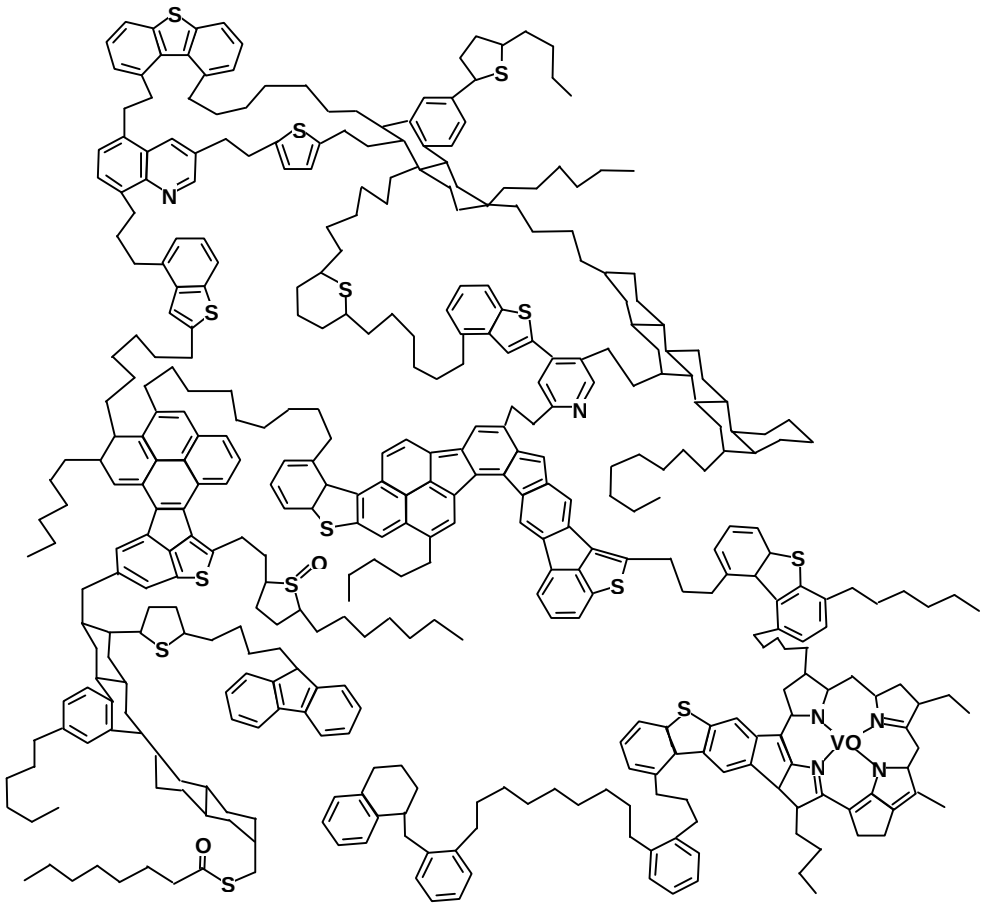

Figure 2.7: Hypothetical asphaltene molecule (Strausz *et al.*, 1992)

This molecule has an elemental formula of $C_{420}H_{496}N_6S_{14}O_4V$, an H/C ratio of 1.18, N/C 0.014, O/C 0.010, S/C 0.033, and a molecular weight of 6191 g/mol. The composition is 81% C, 8% H, 7.3% S, 1.4% N, 1.0% O and 0.8% V. These values compare well with those summarized previously in Table 2.3.

Although this structure appears to satisfy the chemical and compositional requirements, it can be potentially misleading, especially where molar mass is concerned. As will be seen shortly, the molar mass of the hypothetical molecule given by Strausz suggests it is one that has self-associated, since the molar mass of asphaltene monomers is believed to be significantly less. In fact, the structure of asphaltenes in petroleum is still debated: some evidence supports the existence of small molecules (less than 1000 g/mol) whereas other studies support large, macromolecular structures with high molecular weights (up to 30,000 g/mol).

2.2.3.3 Asphaltene Molar Mass

The molar mass of asphaltenes is an extensively studied and debated topic. Table 2.4 summarizes the molar mass of asphaltenes as determined with several techniques on various crude oils. Although source oil and experimental conditions do influence the apparent molecular weight, the extremely wide variation observed in Table 2.4 strongly suggests that asphaltenes self-associate; that is, they form aggregates and in most cases the measured molar mass is that of a macromolecule and not an individual asphaltene molecule. The concept of asphaltene self-association and its consequence on the structure of asphaltenes in petroleum and at the interface will be discussed in more detail in Section 2.2.5.

The most common methods used today for measuring molar mass are gel permeation chromatography (GPC) and vapour pressure osmometry (VPO). For a solution technique such as VPO, the measured molar mass can depend significantly on the solvent, temperature and concentration. Moschopedis *et al.* (1976) found that asphaltene molar

mass increases as the temperature and aromaticity of the solvent decrease and as the concentration increases. Agrawala and Yarranton (2001) observed the same trends with the molar mass from VPO usually varying between 1000 and 10,000 g/mol (Table 2.4). The lower limit is usually taken as the monomer molar mass, whereas the upper limit corresponds to an aggregate composed of several monomers. Yarranton and coworkers (Agrawala and Yarranton, 2001; Akbarzadeh *et al.,* 2004) deduced the monomer molar mass from VPO and found that it varies between 1500 to 2000 g/mol. Fluorescence depolarization measurements made by Groenzin and Mullins (2001) place the value at 500 to 1000 g/mol.

Table 2.4: Asphaltene molar mass determined with various techniques

Technique	**Molar Mass (g/mol)**
Ultracentrifugation[a]	Up to 300,000
Osmotic Pressure[a]	80,000
Monomolecular Film[a]	80,000 – 140,000
Gel Permeation Chromatography[b]	20,000 – 65,000
Dynamic Light Scattering[b]	20,000 – 100,000
Ebullioscopic[a]	2500 – 4000
Cryoscopic[a]	600 – 6000
Viscosity[a]	900 – 7000
Vapour Pressure Osmometry[a, c]	1000 – 5000
	1000 – 27000

a Moschopedis *et al.,* 1976
b Yen, T.F., 1994
c Alboudwarej *et al.,* 2002

Although generally accepted as an accurate method for the determination of asphaltene molar mass, VPO has one major drawback: it cannot measure the apparent molar mass of asphaltenes in the crude oil and bitumen. Rather, VPO measures the molar mass of an extracted sample in a pure solvent since the method relies on the differences in vapour pressure between pure solvents and solvents containing solutes (here, asphaltenes). Therefore, VPO measurements cannot be used directly in modeling studies of asphaltenes in crude oils and bitumens. It is expected that the molar mass of asphaltenes at any given concentration is smaller in bitumen than in a solvent such as toluene because bitumen

contains resins which tend to reduce asphaltene association. For example, Akbarzadeh *et al.* (2004) found that for successful modeling of asphaltene precipitation in bitumen, molar masses smaller than that measured with VPO had to be utilized. VPO is best used for relative comparisons assessing the effects of asphaltene source, degree of washing, and concentration.

2.2.4 Resins

Aromatics, resins and asphaltenes form a continuum of molecular species that increase in polarity, heteroatom content, and molar mass. Hence, resins contain molecules similar to those found in the aromatic class except they are generally larger and contain more sulfur, oxygen and nitrogen. During SARA fractionation, resins are removed from Attapulgus clay with a toluene/acetone mixture. The solvent is evaporated leaving a sticky, brown-black semi-solid. The density of resins has been reported as 1007 to 1066 kg/m^3 for Alberta and international crude oils and bitumen (Akbarzadeh *et al.*, 2004).

2.2.4.1 Resin Elemental Composition

Although smaller, less aromatic and less polar, resins are chemically similar to asphaltenes. Table 2.5 summarizes the elemental composition of resins extracted from oils originating in Canada, Iran, Kuwait and Venezuela. The H/C ratio is higher for resins than asphaltenes, whereas the heteroatom elements occur in smaller amounts (Koots and Speight, 1975). As for the asphaltenes, there is substantial variation in the sulfur content. Resins are thought to be the precursor to asphaltenes (Speight, 1999). During the maturation process, the cyclic portion of the resins undergoes aromatization. This explains the lower H/C ratio and higher heteroatom content of the asphaltenes.

Table 2.5: Elemental composition of resins from world sources (Speight, 1999)

	Canada	**Iran**	**Kuwait**	**Venezuela**
Carbon (wt%)	81.9 – 87.8	77.5	83.1	79.6
Hydrogen (wt%)	9.7 – 11.9	9.0	10.2	9.6
Nitrogen (wt%)	0.3 – 1.5	3.1	0.6	
Oxygen (wt%)	0.2 – 0.8	0.3	0.5	
Sulfur (wt%)	0.4 – 5.1	10.1	5.6	6.3
H/C Ratio	1.36 – 1.69	1.39	1.47	1.45
N/C Ratio	0.002 – 0.013	0.03	0.005	
O/C Ratio	0.002 – 0.008	0.003	0.005	
S/C Ratio	0.002 – 0.023	0.048	0.025	0.03

2.2.4.2 Resin Molecular Structure and Molar Mass

Nuclear magnetic resonance studies show that resin molecules, although smaller, are similar to asphaltenes extracted from the same oil (Speight, 1999). Initially, Speight suggested that resins were composed of long aliphatic chains with naphthenic rings in the center. It was also suggested that heteroatoms were dispersed throughout condensed aromatic and naphthenic ring structures. The more recent work of Hammami *et al.* (1998) suggests resins are composed of a polar end group and a long non-polar paraffinic group. Infrared spectroscopic studies reveal hydrogen-bonded hydroxyl groups, pyrroles and indoles. Ester functions, acid functions, as well as ketone and quinine functions have also been identified (Speight, 1999).

The molar mass of resins appears to vary little with method and experimental conditions. Speight observed that the molar mass of the resins listed in Table 2.5 varied from 731 to 1019 g/mol. Peramanu *et al.* (1999) observed similar results (825 and 947 g/mol for Cold Lake and Athabasca resins, respectively). Akbarzadeh *et al.* (2004) measured the molar mass of resins in toluene at 50ºC for several Alberta and international oils and found values to fall in the range of 859 to 1240 g/mol.

2.2.5 Self-Association of Asphaltenes and Resins

The molar mass measurements obtained with vapour pressure osmometry (and the other techniques that yield values greater than the monomer molar mass) have lead to the general conclusion that asphaltenes self-associate. Although this is widely accepted in the literature, debate still exists as to the nature of self-association. There are two competing models: the colloidal model and the thermodynamic model. Not only does each model explain self-association differently, but each has major consequences on the interpretation of interfacial film structure.

2.2.5.1 Colloidal Models

The colloidal model was first proposed by Nellensteyn (1938) and Pfeiffer and Saal (1940). This model, illustrated in Figure 2.8, suggests that asphaltenes are solvated in crude oil by non-asphaltenic molecules, primarily resins, and associate into colloid structures. It was postulated that resins maintain asphaltene molecules in the crude oil as a colloidal dispersion and are necessary to stabilize the asphaltenes from redissolution in the crude oil (Koots and Speight, 1975; Hammami *et al.*, 1998; Carnahan *et al.*, 1999).

The model of Dickie and Yen (1967) is similar to the Pfeiffer and Saal model except it assumes that asphaltenes form the centers of micelles as clusters rather than individual molecules. From X-ray diffraction of solid asphaltenes, they postulated that asphaltene colloids are composed of aggregated stacks of pylycyclic aromatic compounds, as illustrated in Figure 2.9. Each stack contains a flat, disc-shaped fused aromatic ring center and a periphery of naphthenic rings and aliphatic side chains. The stacks contain up to five particles and are held together by π–π bonding. The spacing between the stacks varies from 3.5 to 5 Å (Erdman *et al.*, 1961), a range later confirmed by Siffert *et al.* (1984).

Numerous small angle X-ray scattering (SAXS) (Herzog *et al.*, 1988; Kim and Long, 1979; Sirota, 1998; Espinat and Ravey, 1993) and small angle neutron scattering (SANS)

(Sheu and Shields, 1995; Sheu, 1996; Overfield *et al.*, 1989, Ravey *et al.*, 1988; Roux *et al.*, 2001; Fenistein *et al.*, 1998) studies have examined the size and shape of the asphaltene clusters. Evidence of disc-like particles, varying from 0.3 to 0.8 nm thick with radii between 0.6 and 80 nm, was found by Herzog *et al.* (1988), Acevedo *et al.* (1994), Ravey *et al.* (1988), Espinat and Ravey (1994), and Fenistein *et al.* (1998). Other shapes, such as flat ellipsoids (Reerink, 1973) and rods (Overfield, 1989) have also been proposed. Unfortunately, the small angle scattering techniques are very sensitive to the choice of model used to interpret the data (Shaw, 2004). The results are open to interpretation.

Some evidence from interfacial tension studies suggests that asphaltenes can form “true” surfactant micelles. Sheu and Shields (1995) observed a change in the slope of the interfacial tension versus asphaltene concentration curve, suggesting micellization. This also suggests that asphaltenes exist as individual asphaltene molecules in the crude oil, surrounded by resins, rather than as aggregated colloidal stacks. Evidence of reverse micellization was also observed by Andersen and Birdi (1991), although some of their more recent studies do not support their previous findings. These differences can partly be attributed to asphaltene source, solvent, and the concentration range tested. Further, as will be shown in Chapter 4, it is necessary to account for asphaltene self-association when interpreting interfacial tension plots. Using a mass concentration IFT plot, which does not account for self-association, as opposed to a molar concentration plot (which does) can significantly alter the interpretation of the average area of adsorbed molecules. It may also erroneously identify micellization.

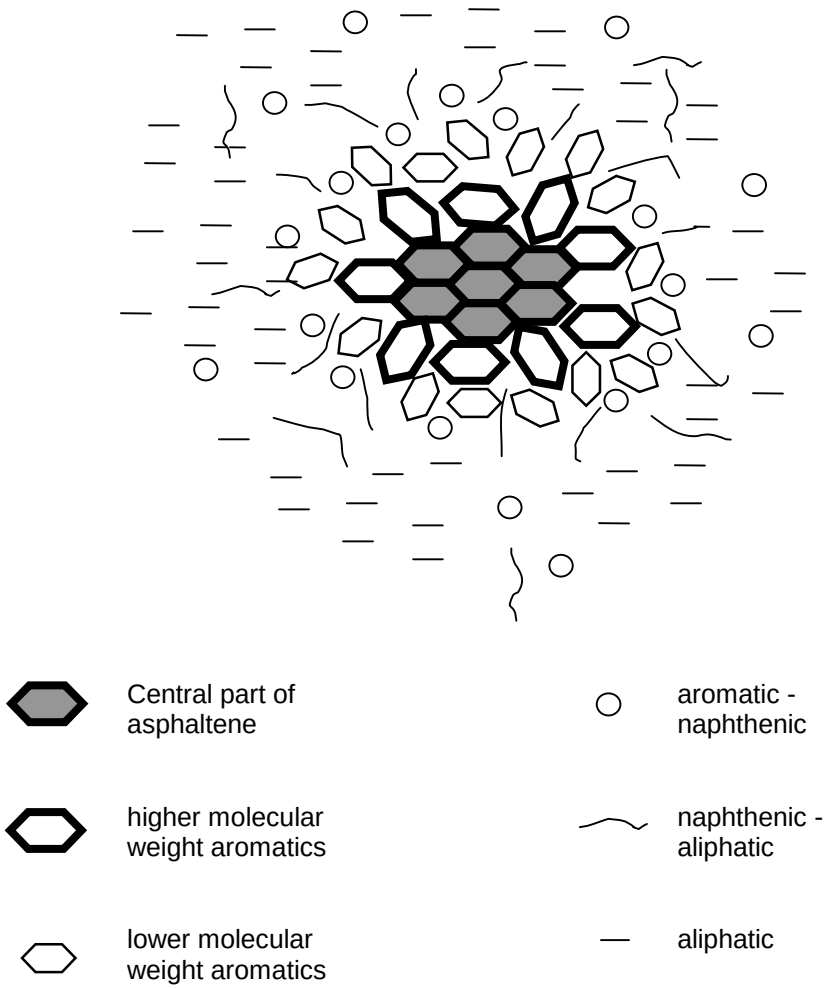

Figure 2.8: Pfeiffer – Saal model of asphaltene-resin complex (Pfeiffer and Saal, 1940).

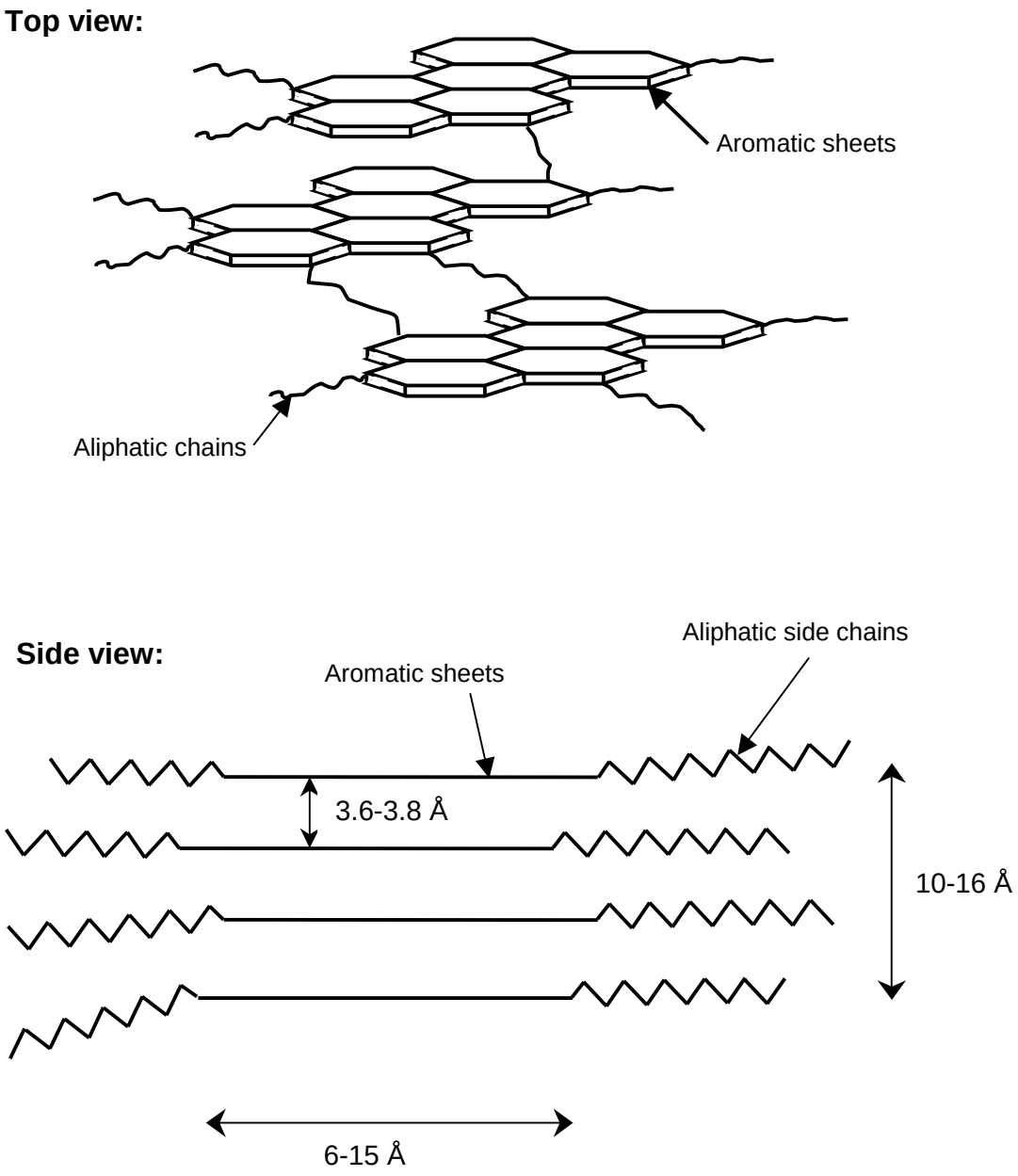

Figure 2.9: Dickie-Yen colloidal cluster model (Dickie and Yen, 1967)

2.2.5.2 Thermodynamic Models

The model proposed by Hirschberg *et al.* (1984) assumes that asphaltenes are a fraction of the oil in the same way as are saturates, aromatics and resins. Here, the asphaltene unit, or monomer, is equivalent to a single sheet in the Dickie-Yen model. Asphaltene self-association occurs through a linear polymerization process. Mitchell and Speight (1973) suggested that higher molecular weight asphaltenes were polymeric analogues of resins and lower molecular weight asphaltenes. A polymerization analogy was utilized by Agrawala and Yarranton (2001) to model the observed increase in asphaltene molar mass with concentration. They assumed that asphaltenes behaved as "propagator" molecules capable of forming chains of associated molecules. Resins reduce this polymerization because they behave as "terminator" molecules and cease the lengthening of asphaltene chains.

Although numerous studies appear to support either the colloidal or thermodynamic models, there is as yet no consensus on the nature of asphaltene self-association. It is also possible that a combination of the two models may be correct, as suggested by Kawanaka *et al.* (1989).

2.2.6 Surface-Activity of Asphaltenes and Resins

Although dispute remains regarding the structure of asphaltenes and the manner in which they self-associate, there is agreement that asphaltenes and resins are some of the most surface-active molecules in petroleum. The surface activity arises from hydrophilic functional groups embedded in a hydrophobic hydrocarbon structure. For example, acidic and basic heteroatom groups containing oxygen, nitrogen and sulfur are hydrophilic. Hence, asphaltenes behave as surfactants and can adsorb at the water/oil interface. Resins are also thought to be surface active (Murzakow *et al.*, 1980) due to the presence of acidic heteroatom groups (Strassner, 1968).

The most commonly cited evidence of asphaltene and resin surface activity is the fact that the interfacial tension between liquids is reduced in the presence of these molecules. Numerous studies show that as the asphaltene (or resin) concentration increases in solution, the interfacial tension decreases (Schildberg *et al.*, 1995; Mohamed *et al.*, 1999; Yarranton *et al.*, 2000b). Some of these studies support micellization (Leon *et al.*, 2000; Mohamed *et al.*, 1999; da Silva Ramos *et al.*, 2001; Sheu *et al.*, 1992, 1995; Rogacheva *et al.*, 1980); others do not (Bhardwaj and Hartland, 1994; Yarranton *et al.*, 2000b). The reduction in IFT was noted to be highest at the limits of pH; that is, in highly acidic or basic media (Acevedo *et al.*, 1992; Sheu *et al.*, 1995; Strassner, 1968; Jones *et al.*, 1978), suggesting that both acidic and basic groups interact at the interface.

Although asphaltenes and resins both lower the interfacial tension of water/oil interfaces, their effects on emulsion stability are not always similar. Some evidence shows that resins adsorb readily at the interface and in fact lower the IFT more than asphaltenes at any given concentration. Gafonova and Yarranton (2001) showed that emulsions prepared with resins are relatively unstable. Other studies indicate that the most stable interfacial films and emulsions are created by a combination of asphaltenes and resins (Mohammed *et al.*, 1993, Khristov *et al.*, 2000). The effects of asphaltenes and resins on emulsion stability will be discussed in detail in Section 2.3.2.1.

Asphaltene and resin adsorption at the water/oil interface has major consequences on the fluidity or rigidity of the interface and the stability of the film. “Skin” formation has been observed since the 1950’s and is believed to be intimately linked to emulsion stability (Reisberg and Droscher, 1956). The effect of asphaltenes on the rheological properties of oil/water interfaces will be discussed in detail in Section 2.3.1.2.

2.2.7 Solids

Some of the most stable and difficult to break oilfield emulsions have been noted to contain a relatively large proportion of small, usually less than 1 micron, non-asphaltenic

solids (NAS). Solids may be clays or silicates present in the crude oils (native solids), corrosion products, or precipitated material such as chemical additives that have become insoluble (introduced solids).

Solid particles have been known to adsorb at water/oil interfaces and stabilize dispersions and emulsions since the beginning of the last century (Ramsden, 1903; Pickering, 1907). The effectiveness of solids in stabilizing emulsions depends on a variety of factors including the solids concentration, density, surface properties, size distribution and interaction with asphaltenes. These properties are discussed in detail in the following three sections. Solids relation and importance to emulsion stability will be discussed in Section 2.3.3.

2.2.7.1 Solids Composition and Structure

Bi-wettable solids in oilfield applications may be natural reservoir solids or material introduced during production and processing. Reservoir solids include silicates, clays, quartz, calcite, feldspar and pyrite (Grim, 1968). The most common clay mineral found in oilsands reservoirs is kaolinite (Gunter, 1992). Other particles may include crystallized paraffins, iron, zinc, calcium carbonate, and iron sulphide (Smith and Arnold, 1987). Introduced solids include precipitated chemical additives and insoluble corrosion products. Only reservoir solids are considered in this work.

Numerous studies identify finely divided clays (i.e., less than one or two micrometers in diameter) as stabilizers of water-in-crude oil emulsions (Yan *et al.*, 2001; Bensebaa *et al.*, 2000; Kotlyar *et al.*, 1998). As stated by Grim (1968), clays are the products of weathering and deposited as sediment. Their properties depend on the composition, (both “clay” and a certain amount of “non-clay” minerals), texture, the presence of adsorbed organic materials, and the presence of exchangeable ions and soluble salts.

Most clay is crystalline in nature and composed of two structural units as illustrated in Figure 2.10. The first unit (2.10 a) consists of aluminum, iron or magnesium atoms surrounded by six oxygen atoms or hydroxyl units in an octahedral formation. When aluminum is present, only two-thirds of the possible positions are filled to balance the structure, giving the formula $Al_2(OH)_6$. When magnesium is present, all positions are filled and the formula is $Mg_3(OH)_6$. The second unit (2.10 b) contains silicon atoms surrounded by four oxygen atoms (or hydroxyl groups) in tetrahedral formation. The tetrahedrons form a repeating hexagonal network with an elemental composition of $Si_4O_6(OH)_4$. Alternating sheets of the octahedral and tetrahedral units combine to form the various clay minerals. The “two layer” types in which alternating sheets of tetrahedral and octahedral structures touch to form common layers include the kaolin clays (such as kaolinite, nacrite) and the halloysite clays. “Three layer” types in which two layers of the silica tetrahedral units alternate with a single central dioctahedral or trioctahedral layer include the montmorillonitic and vermiculitic minerals. Other types of clays include the chlorite group and the chain-structured clays. The former is composed of ordered stacks of alternating layers of different octahedral sheets (i.e., some containing aluminum, some magnesium) and tetrahedral sheets. The latter is a “fibrous” structure composed of silica tetrahedrons linked by octahedral groups (Grim, 1968). The individual structures and composition of clay minerals are numerous and it is not the intent here to describe each variation. Rather, the preceding shows that clays are hydrous aluminum silicates with magnesium or iron sometimes replacing the aluminum.

Compositional studies of oilsands solids support the presence of aluminosilicate clays and other solids such as quartz. Bowman (1967) detected the presence of magnesium, calcium, iron, titanium, and zirconium as well as carbon, hydrogen, nitrogen and sulfur in tar sands solids. Kotlyar *et al.* (1999) identified similar elements using Energy Dispersive X-Ray analysis (EDX) and also observed the presence of iron, manganese, vanadium, nickel and aluminum. In that study, they identify pyrite as the source of sulfur and

titanium oxide as the source of titanium in toluene-insoluble solids associated with Athabasca bitumen.

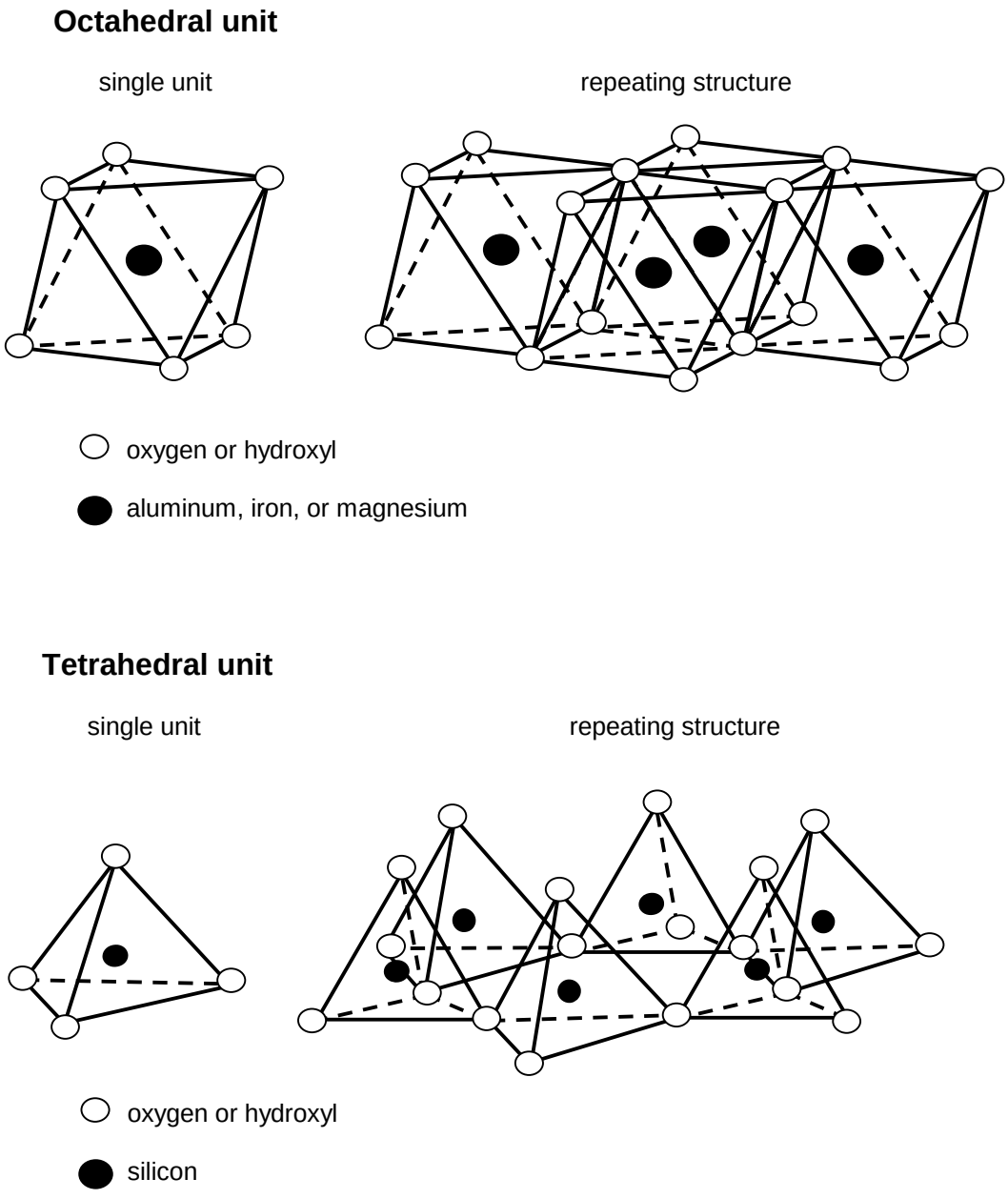

Figure 2.10: Structural units of crystalline clays (Grim, 1968)

Kotlyar *et al.* (Kotlyar *et al.*, 1998 and 1999) also found a large portion of toluene insoluble organic matter associated with the solids, consistent with the previous work of Bowman. Bulk elemental analysis of the solids showed that carbon represents more than 18 wt/wt% of the solids and that carbon represents more than 37% of those atoms exposed. Solid state ^{13}C NMR measurements on the solids showed that the amount of carbon present in aromatic rings (38%) is close to that of typical Athabasca asphaltenes (46%). This suggests that "asphaltene-like" materials are tightly bound to the bitumen solids. They concluded that the surfaces of bitumen solids were highly active and readily adsorbed polar, aromatic, toluene-insoluble organic compounds, similar to asphaltenes. The ability of asphaltenes to adsorb on various surfaces has been demonstrated by several authors (Kokal *et al.*, 1995; Bantignies *et al.*, 1998; da Silva Ramos *et al.*, 2001; Alboudwarej, 2004, Acevedo *et al.*, 1995; Castillo *et al.*, 1998). Asphaltene adsorption can have a significant impact on the wettability of solids, as discussed in Section 2.2.7.3.

Kotlyar and coworkers (1998 and 1999) concluded that bitumen solids were aluminosilicate clay crystallites. X-ray diffraction revealed the clays were primarily kaolinite and mica minerals although traces of smectite and vermiculitic minerals were also found (Kotlyar *et al.*, 1993).

2.2.7.2 Solids Size and Shape

Usually, solids capable of stabilizing emulsions are in the submicrometer to micrometer range (Tambe and Sharma, 1993; Binks and Lumsdon, 2000; Zaki *et al.*, 2000). Yan *et al.* (2001) stated that the solids associated with oilfield emulsions are generally less than one micron in diameter. Bensebaa *et al.* (2000) and Kotlyar *et al.* (1998 and 1999) have identified these oilfield emulsion solids to be aluminosilicate clays with diameters of 100 to 200 nm and thicknesses of approximately 10 nm. In another study, they found that mature fine tailings varied from 50 to 400 nm, and that the particles were plate-like with an irregular morphology (Kotlyar *et al.*, 1993). Elemental and structural analyses lead them to propose a conceptual model of the solids as illustrated in Figure 2.11. In this

model, aluminosilicate clays are covered with adsorbed humic and petroleum matter and larger heavy bitumen molecules resembling asphaltenes. The particles have a predominantly hexagonal/platelet shape, consistent with the shape of kaolinite and mica.

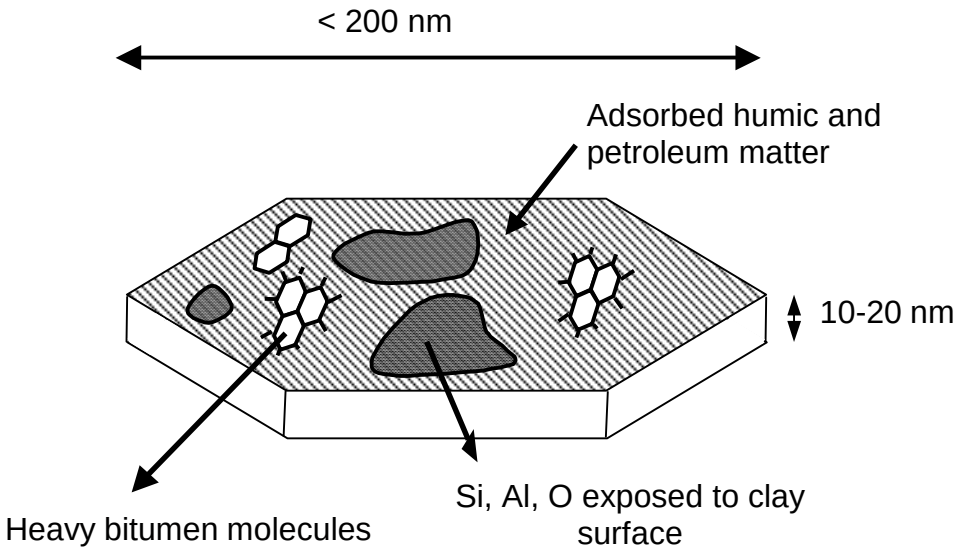

Figure 2.11: Conceptual model of bitumen solids (Bensebaa *et al.*, 2000)

2.2.7.3 Solids Wettability

Wettability relates the affinity a given material has for oil and water. It is quantified by measuring the three phase contact angle formed between a solid and two liquids (or a liquid and vapour) as previously illustrated in Figure 2.2. It is speculated that the most stable emulsions are formed with very fine particles with biwettable surfaces. For native solids encountered in oilfield emulsions, the particles possess hydrophilic characteristics in the form of exposed aluminosilicate surfaces and hydrophobic characteristics in the form of adsorbed humic and petroleum, i.e., “asphaltene-like”, materials. The effect of

adsorbed hydrocarbons can be important to wettability. In their study of heptane-washed native solids extracted from Athabasca Bitumen, Chen *et al.* (1999) observed that the three-phase contact angle of dried solids decreased from 150º (i.e., very oil-wet) to between 20 and 80º when the solids were washed with toluene. Washing with heptane decreased the contact angle to only 130º. They concluded that further washing of heptane-washed solids with toluene removed a significant portion of adsorbed asphaltenes. While clays are water-wet, asphaltene adsorption leads to biwettable or oil-wettable particles.

2.3 CRUDE OIL EMULSION STUDIES

2.3.1 Effect of Asphaltenes and Resins on Film Formation

Numerous studies indicate that asphaltenes are emulsion stabilizers when adsorbed at the interface and generally reduce the resolution of water and oil into separate phases. The role of resins is disputed. Although factors such as increased continuous phase viscosity and density are known to reduce the efficiency of water/oil segregation, most current work is aimed at understanding the composition, characteristics and rheological properties of the water/oil interface.

Asphaltenes and resins are both surface-active species capable of adsorption at water/oil interfaces. The interfacial properties of the resultant films are believed to have a significant effect on emulsion stability. In particular, the rigidity/elasticity of the films and the formation of “skins” appear to be important (Taylor, 1992). These phenomena have received considerable attention because it is believed that formation of viscous interfacial films will retard the rate of film drainage during coalescence. Decreased coalescence may result in slow or no demulsification of oilfield water-in-oil emulsions (Jones *et al.*, 1978). The formation of interfacial films, their properties and relation to emulsion stability depends on several factors including the nature of the materials at the interface, the pH and temperature.

2.3.1.1 Visual Observations

Visual observations of interfacial “skins” have been made by several researchers. Examples using the pendant-drop method, micropipette method, and thin-liquid film apparatus are illustrated in Figures 2.12 through 2.16. A brief description of each is given below.

The pendant-drop method is a technique in which an oil drop surrounded by water (or brine) is retracted into a capillary and its shape observed for irregularity. An example of such an experiment is illustrated in Figure 2.12. Here, Reisberg and Doscher (1956) observed the formation of a “membrane” around an oil drop surrounded by brine at 30ºC. Upon retraction into the capillary, the oil drop folded and wrinkled and re-expansion into the brine occurred in angular, irregular forms. They noted that when the volume of the drop was increased significantly, a regular drop did form but had remnants of the membranous material suspended within.

Strassner (1968) made similar observations of compressed films using the pendant drop method. His experiments revealed three types of interfaces: 1) solid (or rigid) films with relatively insoluble skins, 2) highly mobile (liquid) films that packed under compression and momentarily distorted the drop, and 3) transition or non-measurable films that showed no distortion under compression and were deduced only by a lowering in IFT. Taylor (1992) suggested that rigid skins (illustrated in Figure 2.13) should be the target of chemical demulsifiers.

Jeribi *et al.* (2002) also used the pendant drop method to observe the shapes formed during expansion/compression cycles of asphaltene solutions in toluene, as illustrated in Figure 2.14. Their results also indicate the presence of rigid skins. They concluded the formation of skins was irreversible because the distortion in shape remained upon drop re-expansion. The worst distortions occurred during rapid compression. Skin formation was accelerated as the concentration of asphaltenes increased.

The micropipette technique used by Yeung *et al.* (1999) is similar to the pendant-drop method because it involves retraction of the drop into a capillary. However, the length scale is in the micron rather than millimeter range. The vast majority of oilfield emulsions are composed of drops that are less than 10 microns in diameter (Wu, 2002). Therefore, it is possible that this method is more representative of the crumpling phenomena in an emulsion system than that observed with the pendant-drop technique. As illustrated in Figure 2.15, Yeung *et al.* (1999) observed that a ~20 micrometer water droplet crumpled upon retraction into the micropipette. The crumpling was attributed to the formation of a rigid interface. When two such drops were brought together, they resisted coalescence. Interestingly, Yeung *et al.* also observed that as the concentration of surface-active components increased (i.e., as oil concentration increased), the adsorbed layer actually transformed from a rigid to fluid interface. However, coalescence of two such drops still did not occur (Yeung, 2004).

Taylor *et al.* (2002) observed rigid skins with a thin liquid film-presure balance apparatus, as illustrated in Figure 2.16. They noted that toluene-diluted asphaltene films formed protective coatings and concluded that film stability was due to strong, short-range steric repulsion created by surfactant bilayers. Similar thin-film studies were conducted earlier by Khristov *et al.* (2000) who observed “dimpling” of the interface during film drainage. The dimpling was caused by irregularities in the films and attributed to the formation of skins.

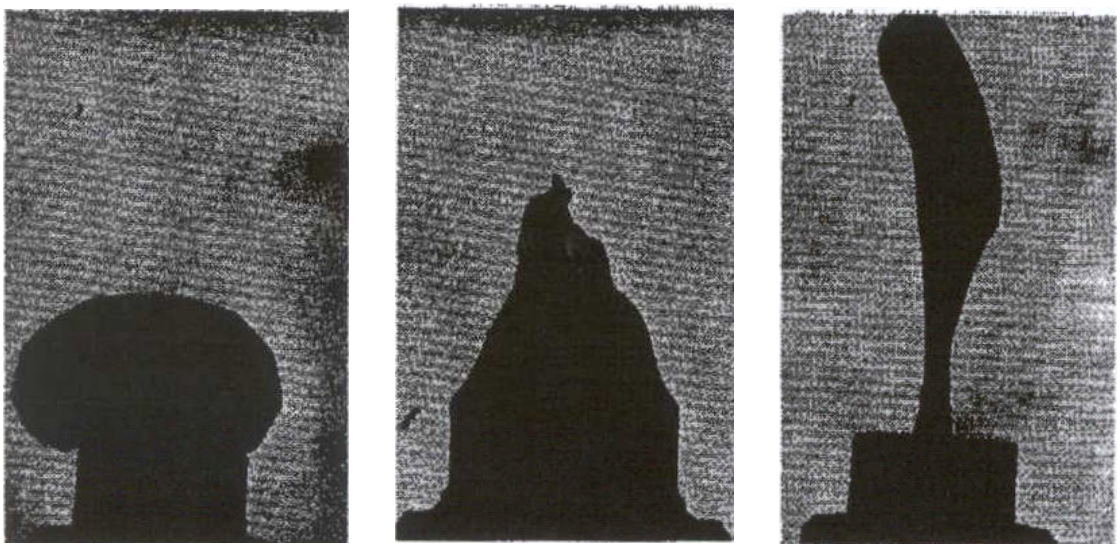

compressed expanded expanded

Figure 2.12: Rigid film formation of pendant drops of anaerobically sampled crude oil (Reisberg and Droscher, 1956)

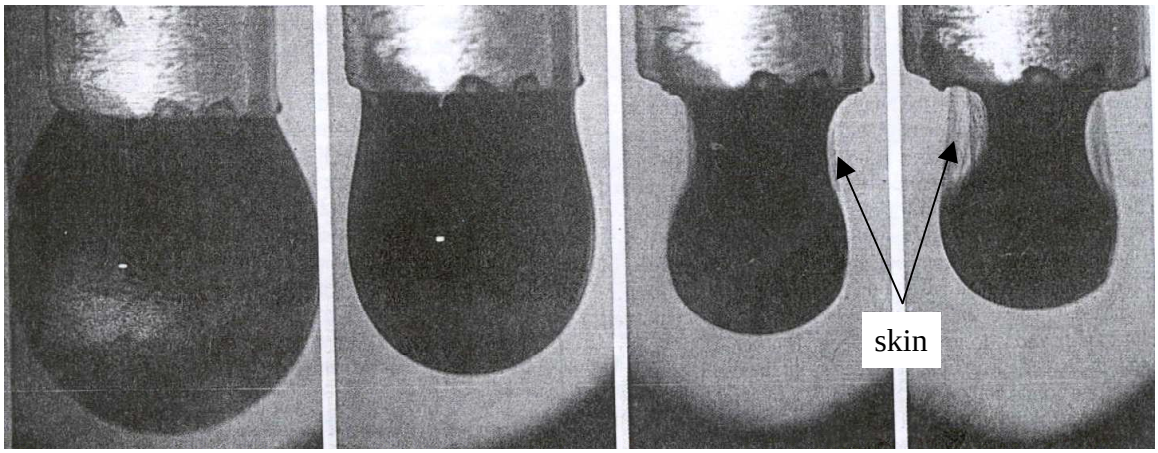

Figure 2.13: Rigid film formation of pendant drops (Taylor, 1992)

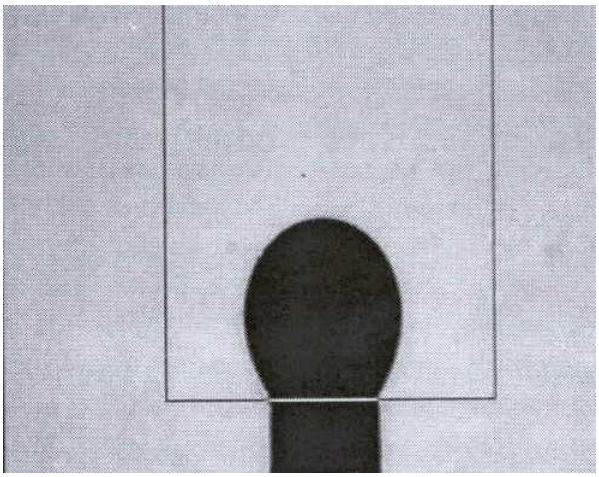

regular shape

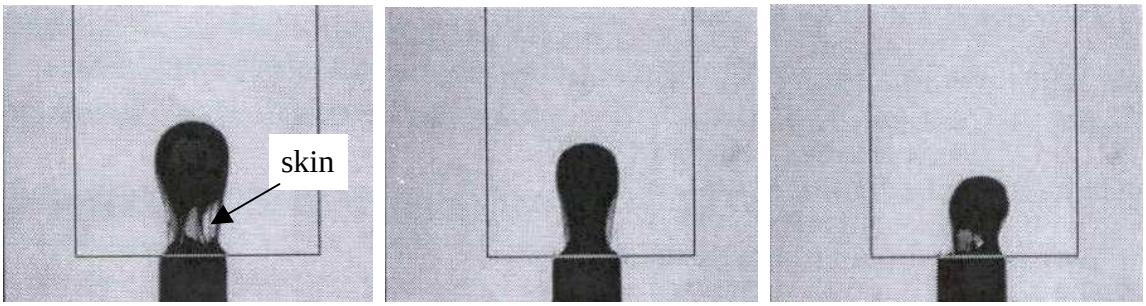

examples of shapes obtained at long times and large asphaltene concentration

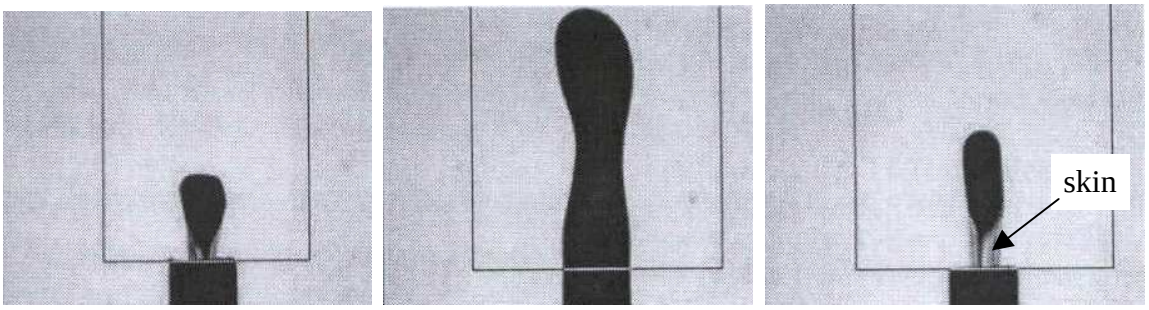

shapes obtained during expansion/contraction cycles

Figure 2.14: Drops of asphaltene solution in toluene using pendant drop method (Jeribi *et al.*, 2002)

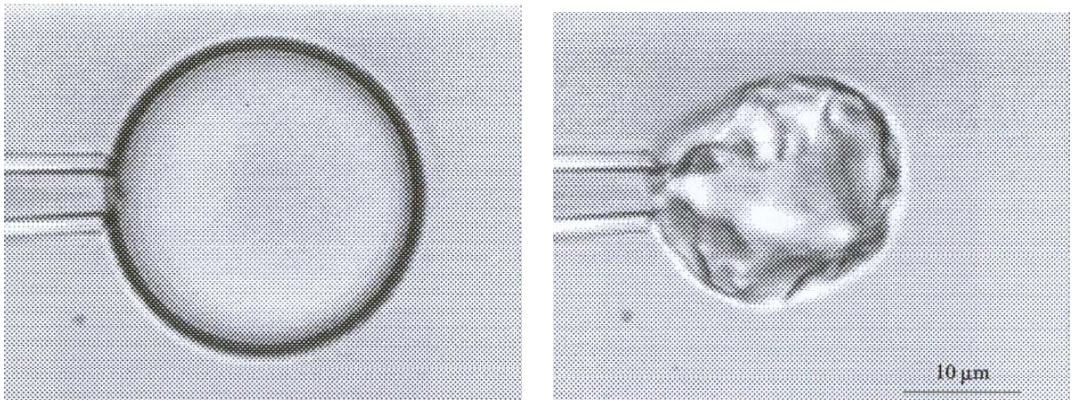

Figure 2.15: Protective layer around water drop surrounded by oil phase (Yeung *et al.*, 1999)

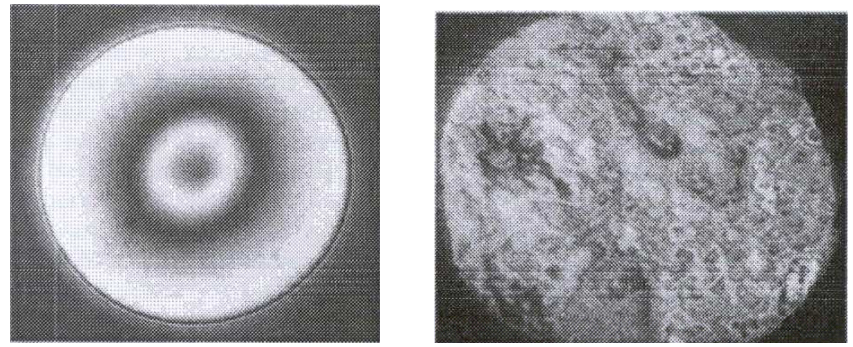

fluid interface — protective skin on interface

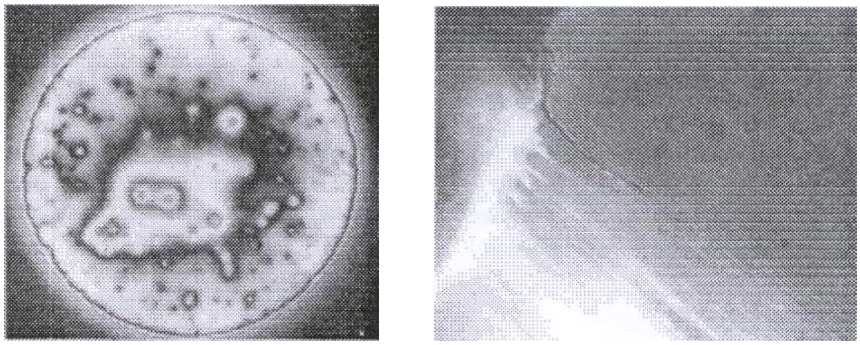

rigid interface — protective skin remains after film rupture

Figure 2.16: Effect of fluid and rigid interfaces on water/toluene-diluted asphaltene films (Taylor *et al.*, 2002)

2.3.1.2 Interfacial Components and Film Structure

It is generally believed that the water/oil interface of oilfield emulsions consists primarily of asphaltenes, resins and biwettable solids. In the study performed by Reisberg and Droscher (1956), an analysis of the material at the interface showed that the H/C ratio and molar mass resembled that of asphaltenes and resins, suggesting these materials are responsible for the skin formed at the interface. Strassner (1968) concluded that rigid films were formed by asphaltenes whereas mobile films were formed by resins. He concluded that the film lifetime was directly proportional to the concentration of film-forming materials at the interface. Wu (2003) noted "flexible" interfacial films were composed of asphaltenes and carboxylic salts, whereas rigid films were composed of asphaltenes alone.

Using the thin liquid film-pressure balance apparatus, Taylor *et al.* (2002) observed that toluene-asphaltene films and toluene-bitumen films could be compressed to the same thickness (8.5 nm bilayer). Therefore, they concluded that the surface active materials at the bitumen-water interface were mainly asphaltenes. They also noted that upon removal of high molecular weight asphaltenes, the bilayer decreased from 8.5 nm down to 5.1 – 7.3 nm and the film stability was reduced.

The visual observations of interfacial skin have lead many researchers to speculate about the structure of the film. A commonly accepted view is that asphaltenes adsorbed at the interface form a three-dimensional network of interlinked molecules or colloid structures (Ese *et al.*, 1998; Freer *et al.*, 2003; Freer and Radke, 2004; McLean and Kilpatrick, 1997a; Mohammed *et al.*, 1993). The irregularity of this network causes the crumpling phenomena during droplet retraction or film drainage. Rigidity and the degree of deformation also appear to increase as the interface ages (Mohammed *et al.*, 1993; Bouriat *et al.*, 2004).

2.3.1.3 Measurement of Rheological Properties

In addition to visual observations, measurements of interfacial rheological properties also support the hypothesis that asphaltenes form a network structure at the interface. Attempts to quantify interfacial film compressibility and elasticity have been made via Langmuir film balance techniques, shear viscometric measurements, and oscillatory drop measurements. Other properties such as crumpling ratios and film lifetimes have also been used to deduce the relative rigidity of interfacial films (Bauget *et al.*, 2001; Jafari, 2005).

In the Langmuir film balance experiments, the surface pressure (i.e., the difference in the tension between the pure solvent and the solvent in the presence of surfactant) is measured as a function of film area. Alternately, the film is compressed to a predetermined area and the change in surface pressure measured. The shape of the curve, as well as the extent to which a monolayer can be compressed, can be used to deduce the relative rigidity of the interface and the size of adsorbed molecules. This technique has been utilized by several researchers. In one extensive study, Jones *et al.* (1978) examined various effects including the role of crude oil type and interface age. Marked differences in the shapes of the isotherms were seen for various crude oils, but the final compression ratio (i.e., final to initial area) varied from about 0.2 to 0.3 for all crude oil monolayers adsorbed at water/air interfaces. In a similar study, Mohammed *et al.* (1993) noted that asphaltene monolayers at air/water interfaces could be compressed to 30% of the original area.

Others have performed similar experiments and used the surface-pressure isotherm to show that at the highest attainable surface pressure, the area per adsorbed asphaltene molecule could be reduced to less than 1 nm^2. Ese *et al.* (1998) found that this area was 0.65 nm^2 for asphaltenes and approximately 0.35 nm^2 for resins (Ese *et al.*, 1999). The recent work of Zhang *et al.* (2003a) is consistent with these results: they showed that the area of high-molecular weight asphaltenes was about 1 nm^2. They also observed that high

molecular weight asphaltenes formed more expanded films than low-molecular weight asphaltenes. They did not observe an abrupt collapse of the monolayer and concluded that asphaltenes entangled at the interface formed an elastic skin. They were able to identify 2D gaseous, liquid expanded and liquid condensed regimes, consistent with the earlier work of Ese *et al.* (1998) and Strassner (1968). In another study, a solid regime was indirectly observed for asphaltene monolayers at heptol/water interfaces when the interface buckled (an abrupt kink occurred in the surface-pressure area isotherm at high surface pressures). Because the regimes were less obvious than for the air/water interfaces, Zhang *et al.* (2003b) concluded these interfaces were more fluid and asphaltenes occupied smaller molecular areas. The area per molecule at maximum interfacial pressure was ~0.45 nm^2, less than that at the air/water interface.

The observations of the Langmuir balance studies show that asphaltene monolayers can exhibit rigidity. Unfortunately, they give relative comparisons through the shape of the surface pressure isotherm, but do not necessarily elucidate the rheology of the interface. Nonetheless, they do suggest that asphaltene molecules, not colloids, have adsorbed on the interface because the areas are more representative of individual asphaltene molecules rather than colloids. This view is confirmed by the work of Khristov *et al.* (2000). In their study of bilayers of thin liquid films, the film thicknesses could be reduced to 7.5 nm per asphaltene layer, a value more representative of molecular rather than colloidal asphaltenes.

In recent years, two main methods have been used to measure the total elastic modulus of asphaltene or crude oil films: oscillating pendant-drop experiments and shear viscometric experiments. The objective of each is to measure the elastic and viscous moduli of an interface.

In the shear viscometric method, the oil/water interface is subjected to shear. A bob is placed on the water/oil interface and a shear stress applied by means of a motor,

through a torsion wire. The deflection of the bob can be measured with time and related to the viscosity of the interface. Several researchers have used this technique to measure the rheological properties of the water/oil interface. Eley and coworkers (1987) observed a “stick-slip” phenomenon occurred during the experiments at relatively high asphaltene concentrations. They attributed this to the formation of thick asphaltene films. Mohammed *et al.* (1993b) used this method to show that interfacial films composed of water and North Sea Buchanan crude oil become more viscous and rigid with time. They speculated that the build-up of interfacial films occurred due to adsorption of higher molecular weight materials. Over time, these materials rearranged to form a viscous network on the interface. Acevedo *et al.* (1993) performed similar experiments and noted that when films were subjected to shear, they always displayed either viscous or solid behaviour. They also speculated that a three-dimensional cross-linked network structure developed as natural surfactants such as resins and asphaltenes adsorbed onto the interface from the bulk oil. The network structure was believed to consist of multilayers of adsorbed surfactants. The formation of such multilayers was believed to occur more rapidly in the absence of resins. Recently, Li *et al.* (2002) used a similar method to show that shear viscosity increased sharply with time, indicating a change in the interfacial structure. They also speculated that at low interfacial asphaltene concentrations, the space between asphaltene molecules was high and the films were of the liquid expanded type. As the concentration increased, asphaltenes become more packed and therefore formed liquid condensed films. The condensation continued until a three-dimensional network was formed. Recently, Spiecker and Kilpatrick (2004) measured the elastic and viscous moduli of heptane/toluene-water interfaces using the shear viscometric method. They examined the effects of solvent quality and interface aging time. They observed an increase in the elastic modulus as the fraction of heptane in the solvent increased (up to the point of precipitation). The elastic modulus also increased as the interfaces were aged.

In the oscillating pendant-drop method, the area of an oil drop surrounded by water/brine is perturbed repeatedly and the corresponding change in interfacial tension measured. In

most studies, the changes in area follow a sinusoidal profile, as do the changes in interfacial tension during expansion/compression cycles. For such an oscillating system, the interfacial elasticity, ε, is defined as follows:

$$\varepsilon = \frac{\mathrm{d}\gamma}{\mathrm{d}\ln \mathrm{A}} \tag{2.1}$$

where γ is the interfacial tension and A is the interfacial area. Equation (2.1) reveals that elasticity is a measure of the change in interfacial energy with a change in interfacial area. A high elasticity means that a change in interfacial area significantly increases the interfacial tension and therefore the energy of the system. Elasticity is composed of both a real and imaginary part defined for an oscillating system as follows:

$$\varepsilon = \varepsilon_d + i\omega\eta_d \tag{2.2}$$

where ε_d is the dilational elasticity, η_d the interfacial viscosity and ω the frequency of oscillation. The elastic modulus represents the energy stored in the system, whereas the interfacial viscosity represents the energy dissipated during relaxation. During relaxation, surfactants can diffuse from the bulk phase to the interface or from interfacial regions of higher surfactant concentration (lower interfacial tension) to interfacial regions deficient in surfactant (higher interfacial tension). The latter mechanism is known as the Gibbs-Marangoni effect.

The oscillatory pendant drop method has been used by several researchers to deduce that asphaltenes form a rigid network at the interface. Further, they have quantified the rigidity/elasticity of asphaltene and crude oil/water interfaces by measuring the total elastic modulus. Aske *et al.* (2002) measured the interfacial tension and total modulus as a function of time for 21 different crude oils and condensates originating from the North Sea and West Africa. They observed that the measured moduli depended on the origin of

the crude oil, concentration and solvent. In all cases, the total modulus increased with time and as the heptane in the heptane/toluene solvent increased (from 9 mN/m in pure toluene to 25 mN/m in pure heptane). The effect of concentration was variable: for some crude oils the total modulus exhibited a maximum at intermediate crude oil concentrations, for some it always increased with increasing crude oil concentration, and sometimes no correlation was observed. It was concluded that the source oil and the concentration of surface active species had a significant effect on the measured elasticity.

Freer *et al.* (2003) also observed that source oil had an effect on the elasticity. However, the more asphaltic crude oil exhibited higher elasticity. They speculated that the high elasticity results in film rigidity and the formation of the asphaltene network structure at the interface responsible for the "skins" observed in visual observations. Consistent with the work of Aske *et al.* (2002), the total modulus was observed to increase as the interface was aged indicating that the network strengthens with time. Similarly, Bouriat *et al.* (2004) observed that the total modulus of 100 g/L asphaltene in cyclohexane/water films doubled from about 12 to 24 mN/m over the course of 15 hours. Bauget *et al.* (2001) showed that the increase in total modulus was more rapid and severe for solutions containing higher concentrations of asphaltenes.

The various experimental techniques all seem to suggest the formation of network-type interfacial structures that increase in rigidity as the interface is aged. Although several relative comparisons of the elastic and viscous moduli exist, few attempts have been made to model the rheology. Most notably, Freer and Radke (2004) have used a combination of purely-diffusional and visco-elastic models to describe the interfacial rheology of aged asphaltene toluene-water interfaces. They found that the film could be described by a combination of the Lucassen-van den Tempel model (Lucassen and van den Tempel, 1972; Lucassen-Reynders *et al.*, 2001) and a Maxwell model. A detailed discussion of this type of model will be given in Chapter 5.

2.3.2 Effect of Asphaltenes and Resins on Emulsion Stability

The preceding discussions have shown that the formation of interfacial films is inevitable when oil, water and natural surfactants are present. Many studies show that asphaltenes and resins are the materials adsorbed at the interface and that they are responsible for the formation of three-dimensional, viscous networks. The networks appear to become more rigid with time, and increased film viscosity will likely pose a barrier to effective film drainage and coalescence in an emulsion. It is of interest to see how film strength (and other properties) relate to emulsion stability. Some of the early emulsion studies showed that emulsion stability could be correlated with properties such as the density, viscosity and asphaltic content of crude oils (Dow, 1926). However, many discrepancies still exist.

2.3.2.1 Effect of Resin to Asphaltene Ratio

The previous discussions showed that asphaltenes and resins were the main components adsorbed at the water/oil interface. Some authors have shown that resins lead to unstable, fluid-like films. For example, Ese *et al.* (1998) showed that resin films were more compressible than asphaltene films. In a later study, Ese *et al.* (1999) stated that demulsifiers had the same type of effect on asphaltene films as did resins: they increased the compressibility of films and reduced the rigidity. Bauget *et al.* (2001) confirmed that resins reduced film rigidity by showing that as the resin/asphaltene ratio increased, resins dominated the interface and “skins” did not form. The work of Freer and Radke (2004) was also consistent with these types of observations. They noted that smaller asphaltene or resin molecules that could be solvent-washed from the interface acted as solubilizers to soften the irreversibly adsorbed viscoelastic interfacial film. The removal of resins and small asphaltenes from the interface resulted in more rigid films with higher total moduli. The apparent reduced film rigidity in the presence of resins has been speculated by some to cause the formation of less stable emulsions (Ese *et al.*, 1998; Li *et al.*, 2002; Acevedo *et al.*, 1993). Recently, Gafonova and Yarranton showed that as the resin/asphaltene ratio increased, model emulsions become progressively less stable (Gafonova and Yarranton, 2001).

Although resins alone have not been shown to create emulsions more stable than those stabilized solely from asphaltenes, several authors have demonstrated that the most rigid films and stable emulsions can be created at intermediate resin/asphaltene ratios. For example, Mohammed *et al.* (1993b) noted that asphaltene monolayers at air/water interfaces could be compressed to 30% of the original area. As resins were added, the monolayers were less compressible. The least compression occurred when the asphaltene to resin ratio was 1:1. However, higher resin to asphaltene ratios resulted in more compressible films with a final compressed area 15% of the original. They speculated that a 1:1 ratio of resins to asphaltene resulted in the best packing and most strongly interacting film. They also showed that emulsions stabilized solely by asphaltenes were stable over an 18 month period, whereas emulsions stabilized solely by resins were completely unstable. The work of McLean and Kilpatrick (1997a) indicated that emulsions stabilized by 1/3 resin/asphaltene ratio were the most stable. The thin liquid film studies of Khristov *et al.* (2000) were consistent. However, despite numerous studies, it is apparent that discrepancies in the literature exist.

2.3.2.2 Effect of Temperature

Generally, emulsions become less stable when the temperature increases, which is why elevated temperatures are utilized in commercial emulsion destabilization processes. However, as noted by Jones *et al.* (1978), interfacial films can remain incompressible at high temperatures and film rheology may not necessarily predict emulsion stability. Jones *et al.* speculated that a kinetic barrier to coalescence can exist even at 65ºC. In fact, Reisberg and Droscher (1956) observed rigid skins at temperatures as high as 90ºC, even when the oleic phase was dispersed in 50% solutions of strong solvents such as carbon disulphide, benzene and carbon tetrachloride.

In a Langmuir balance study of North Sea crude oils, Nordli *et al.* (1991) noted that surface pressure area isotherms became more condensed at higher temperatures. A more contracted monolayer was also observed for 49.5ºC interfaces compared to 20ºC

interfaces in the study conducted by Zhang *et al.* (2003a). However, they noted that the film was more compressible at higher temperatures. On the other hand, limited differences in pressure-area isotherms were observed in the study of Mohammed *et al.* (1993b) and it was shown that the limiting area to which asphaltene interfaces could be compressed ranged between 30 to 40% for a temperature range of 30 to 55ºC. Fewer attempts have been made to correlate the elastic modulus with temperature. Recently, Bouriat *et al.* (2004) observed that the elastic modulus of a water/asphaltenated-cyclohexane interfaces aged for 48 hours at ambient temperature decreased when the temperature was increased.

2.3.2.3 Effect of pH

The pH of the aqueous phase is expected to have an effect on the composition and rigidity of the water oil interface and the stability of the resulting emulsion. Because asphaltenes are amphiphilic, a change in pH causes the acidic and basic groups of the asphaltene to undergo ionization. This may affect the type and amount of asphaltenes/resins adsorbed at the interface (Papirer *et al.*, 1982), which in turn may affect the strength of the interfacial film. Reisberg and Droscher (1956) showed that rigid interfacial skins formed by asphaltenes were strongest in acidic pH, intermediate at neutral pH, and mobile at basic pH. Using the Langmuir balance, Nordli *et al.* (1991) showed that the pressure-area isotherm of basic systems was similar to neutral ones but the film become more compressible at higher film pressures. Jones *et al.* (1978) observed that the interfacial elasticity of aged Ninian crude oils increased for acidic and basic conditions, and the lowest elasticity occurred at neutral pH. Correlation was also found between film ratio, interfacial tension and free water resolution for Venezuelan crude oil-distilled water emulsions. Acidic pH of the water resulted in large film ratios, high interfacial tension, and intermediate free water resolution. Here, solid films were formed. As the pH increased, the film ratio and interfacial tension decreased and the free water increased. At still higher pH, i.e., basic conditions, a reversal in trend was observed. Liquid films were formed and the film ratio increased dramatically, the IFT dropped to

near zero values, and the free water resolution decreased. The various studies seem to indicate that films and emulsions are most stable at the limits of pH, although exceptions do exist.

2.3.3 Effect of Solids on Emulsion Stability

As mentioned earlier, solids can adsorb at the water/oil interface, onto an existing surfactant-stabilized film, or become trapped between water droplets. Adsorption or trapping will reduce film drainage, increase film viscosity and potentially increase the bulk viscosity of the emulsion. The extent to which solids increase overall emulsion stability depends strongly on the size and concentration of solids, their shape, morphology and density, and their wettability.

2.3.3.1 Effect of Solids Size and Concentration

Emulsion stability increases with decreasing particle size and increasing particle concentration (Menon and Wasan, 1988; Yan *et al.*, 1999; Tambe and Sharma, 1993; Menon and Wasan, 1984; Abend *et al.*, 1998; Schulman and Leja, 1954; Bowman, 1967; Gelot *et al.*, 1984; Yan and Masliyah, 1995; Binks and Lumsdon, 2001; Sullivan and Kilpatrick, 2002). The dispersed phase droplet diameter decreases both with an increasing solids concentration and a decreasing particle size (Tambe and Sharma, 1993; Aveyard *et al.*, 2003; Gelot *et al.*, 1984). A decrease in the average drop size tends to result in more stable emulsions. Free energy considerations support these observations (Levine and Sanford, 1985).

The size of the solids in relation to water droplets is an important factor in their potential to enhance emulsion stability (Aveyard *et al.*, 2002; Tadros and Vincent, 1983; Schulman and Leja, 1954). Solids that tend to stabilize emulsions vary anywhere from less than a micrometer (Yan *et al.*, 2001; Levine and Sanford, 1985; Kotlyar *et al.*, 1998b) up to a few micrometers (Zaki *et al.*, 2000). Generally, the most stable emulsions also occur when interfaces are stabilized by the smallest particles. For example, Bowman (1967)

found that the emulsion stability increased when the size of model and tar sand solids decreased from 37 to 1 μm, with a pronounced increase in stability for particles smaller than 8 μm. Sullivan and Kilpatrick (2002) observed that the water resolution in a model water-in-crude-oil emulsion decreased from 83 to 63% when the diameter of added iron oxide particles decreased from 0.89 to 0.026 μm. When larger particles such as silica, 1.45 μm sized montmorillonite clay, and 16.65 μm sized $Ca(OH)_2$ particles were added, no stable emulsions could be created. Binks and Lumsdon (2001) observed that as the size of hydrophobic latex particles decreased from 2.7 to 0.21 μm, the stability to sedimentation of a model water-in-cyclohexane emulsion increased and the average water drop diameter decreased. These results all suggest that the most effective stabilizers are small particles.

The effect of the particle size distribution on emulsion stability is less well documented, although Sethumadhaven *et al.* (2002) provide evidence that foams are more stable when stabilized by monodisperse particles and that even a small fraction of larger particles can decrease foaminess. Extending this idea to emulsions, it is possible that a wide particle size distribution may potentially lead to less stable emulsions. Perhaps larger particles occupy interfacial areas but do not contribute to the stability of these regions.

2.3.3.2 Effect of Solids Shape and Density

The particle density and shape can also be important in emulsion stability. Emulsions created with denser particles are expected to be less stable than those created with less dense particles (Schulman and Leja, 1954; Gelot *et al.*, 1984). Tadros and Vincent (1983) suggest that asymmetric particles such as bentonite clays are more effective stabilizers than spherical particles. However, there is also evidence suggesting that irregularities on a surface lessen the emulsifying capability of a particle (Vignati *et al.*, 2003). Sabbagh and Lesser (1998) showed that unstable polyethylene/asphalt emulsions contained teardrop-shaped polymer particles and that stable emulsions contained more spherical particles. Cylindrical particles were also observed in the stable emulsions. Yekeler *et al.*

(2004) showed that particle morphology can alter wettability and that smooth particles tend to be more hydrophobic.

2.3.3.3 Effect of Solids Wettability

Wettability is another important factor when considering the capacity of solids to stabilize emulsions. Hydrophilic particles, i.e., those with a contact angle less than 90º tend to stabilize oil-in-water emulsions, whereas hydrophobic particles, i.e., those with a contact angle greater than 90º, stabilize water-in-oil emulsions (Tambe and Sharma, 1993; Aveyard *et al.*, 2003; Bensebaa *et al.*, 2000b; Schulman and Leja, 1954; Gelot *et al.*, 1984). For example, Gelot *et al.* (1984) showed that Ca-bentonite, a hydrophilic particle, stabilized an oil-in-water emulsion, whereas carbon lampblack, a hydrophobic particle, stabilized a water-in-oil emulsion. Thermodynamic considerations suggest that the most stable emulsions will result when the contact angle is 90º for very finely divided solids (Binks and Kirkland, 2002; Aveyard *et al.*, 2002; Binks and Lumsdon, 2000). Some experimental evidence supports this conclusion (Yan and Masliyah, 1995), although there is also evidence showing maximum stability at angles other than 90º (Yan *et al.*, 2001; Yan and Masliyah, 1995b; Menon and Wasan, 1986). These authors have shown that factors such as particle partitioning, surface coverage, and the phase in which the particle is originally dispersed must be considered in addition to contact angle.

2.4 CHAPTER SUMMARY

Oilfield water-in-crude oil emulsions are often encountered in the petroleum industry. They are formed when oil and water are sufficiently agitated and stabilized, and when emulsifying agents such as surfactants and solid particles adsorb on the interface or an existing stabilizing film. Most oilfield emulsions are treated with gravity settling and heating and supplemented with chemical techniques. In order to optimize or devise new treatments, it is necessary to have a good understanding of the naturally occurring surface-active species found in a crude oil and their relation to emulsion stability.

The literature shows that water-in-crude oil emulsion stability is primarily attributed to the formation of rigid interfacial skins. The interfacial film appears to be composed of surface-active species such as asphaltenes and resins, and small, biwettable particles such as native solids. Generally, asphaltenes and solids are believed to increase emulsion stability, but the role of resins is still disputed.

Asphaltenes contain polynuclear aromatic ring structures with aliphatic side chains and dispersed heteroatom groups. They are known to self-associate. Resins are similar to asphaltenes except they are generally smaller, less polar molecules with fewer heteroatoms. They do not appear to self-associate. Asphaltene and resins are surface-active species and therefore able to adsorb at the water/oil interface. Some authors believe asphaltenes adsorb either as colloids peptized by resins or micelles, and some believe asphaltenes or resins adsorb as individual molecules. Further, it is hypothesized that adsorbed asphaltenes form a viscous, three dimensional network structure at the interface. Generally, resins reduce the rigidity of the network, although there is evidence that the least compressible films (i.e., most rigid) are those composed of combinations of asphaltenes and resins. It is speculated that a rigid network will result in stable emulsions and a weak network in relatively unstable emulsions. The relative strength of the network depends on several factors including the film composition, the pH and the temperature. Factors such as the resin/asphaltene ratio may also affect film rigidity and emulsion stability.

Naturally occurring solid particles such as clays, sand and silica can also enhance film rigidity and emulsion stability. Solid particles must be significantly smaller than water drops and have biwettable surfaces in order to adsorb at a droplet interface. Generally, emulsion stability increases as the solids concentration increases and the solid size decreases. Solid particles adsorbed on a film may increase film viscosity. Solids trapped between drops may increase continuous phase viscosity and reduce drainage.

CHAPTER 3
EXPERIMENTAL METHODS

As stated in Chapter 1, the primary research objective of this project is to investigate the nature of the water/oil emulsion interface by studying the film-stabilizing characteristics of asphaltenes and solids and relating them to emulsion stability. Specifically, the composition, structure, interfacial properties and rheology of the interface are to be assessed for emulsions stabilized by asphaltenes and solids. The properties of asphaltenes and solids are to be related to observed trends in model emulsion stability and to the stability exhibited by existing wellhead and refinery emulsions.

Since the focus of the present work is on asphaltenes and native solids, the separation of these materials from several bitumen and existing emulsions is first described in Section 3.1. Asphaltenes were precipitated from Athabasca bitumen, a coker-feed bitumen that has been treated to remove most of the large solids and all of the water. “Fine” oil-sand solids were also obtained from the Athabasca bitumen. “Coarse” solids were obtained from a wellhead emulsion sample from a heavy oil field, supplied by Alberta Energy Company (AEC) Ltd., now EnCana Corporation. Both fine and coarse solids were recovered from a refinery emulsion supplied by Imperial Oil Ltd. (IOL). For the Athabasca bitumen, the asphaltenes and solids were recovered in two main steps: 1) the precipitation of Asphaltene-Solids from bitumen and, 2) the separation of solids from asphaltenes. For the wellhead and refinery emulsions, solids were extracted directly from the emulsion.

The techniques used to characterize asphaltenes and solids are explained next. The methods used to characterize asphaltenes are described in Section 3.2 and include: 1) the molar mass as measured with vapour pressure osmometry (VPO), 2) the interfacial tension of water and asphaltene solutions as measured using a drop volume tensiometer

(DVT) and a drop shape analyzer (DSA), 3) the elastic and viscous moduli of asphaltene films as measured with a drop shape analyzer (DSA). The methods used to characterize native solids are described in Section 3.3 and include: 1) particle size and size distribution as measured using a particle size analyzer, 2) particle size and shape as discerned from images obtained from transmission and scanning electron microscopy (TEM and SEM), 3) particle composition as measured with X-ray diffraction (XRD).

The composition and structure of the interface has been assessed by studying model emulsions created from asphaltenes, solids, toluene, heptane, and water. Gravimetric measurements and optical microscopy were required to assess interfacial composition and structure and are described in Section 3.4. Finally, stability tests were conducted on model and existing wellhead and refinery emulsions. The stability tests are also described in Section 3.4.

3.1 MATERIALS

3.1.1 Chemicals

Reagant-grade *n*-heptane and toluene were purchased from Van Waters & Rogers Ltd. (VWR), and used in the precipitation of asphaltenes, the extraction of solids, and the preparation of emulsions. 99.99% purity toluene and 99.6% purity heptane, both obtained from VWR, were used for the measurement of interfacial tension, elasticity and asphaltene molar mass. Distilled water was supplied by the University of Calgary water plant.

Note that many of the experiments presented in this thesis involve solutions of heptane and toluene. For convenience, a mixture of X vol% heptane and Y vol% toluene will be described as “X/Y heptol.”

3.1.2 Recovery of Asphaltenes and Solids from Athabasca Bitumen

Asphaltenes were precipitated from Athabasca bitumen, a coker-feed bitumen that has been treated to remove most of the large solids and all of the water. “Fine” oil-sand solids were also obtained from the Athabasca bitumen. Two sources of bitumen were used in order to complete all of the desired experiments.

3.1.2.1 Recovery of Asphaltenes

As outlined in Chapter 2, one way of describing the composition of heavy crude oil and bitumen is in terms of solubility classes which consist of saturates, aromatics, resins, and asphaltenes. Recall that “asphaltenes” are defined as the fraction of bitumen soluble in an aromatic solvent such as toluene, but insoluble in a paraffinic solvent such as pentane or heptane. Native solids are usually associated with the asphaltene fraction and coprecipitate with asphaltenes. Hence, asphaltenes and solids can be recovered from bitumen when excess paraffinic solvent is added. Because the material that precipitates is a mixture of asphaltenes and solids, it is referred to as “Asphaltene-Solids” and abbreviated as “AS” in this work.

To precipitate AS, *n*-heptane was added to Athabasca bitumen at a 40:1 (cm^3/g) ratio. The mixture was sonicated for 45 minutes at room temperature and then left to equilibrate for 24 hours. After settling, the supernatant was filtered through a Whatman #2 filter paper without disturbing the whole solution. At this point approximately 10% of the original mixture remained unfiltered. Additional *n*-heptane was added to this solution at a 4:1 (cm^3/g) ratio of *n*-heptane to the original bitumen mass. The mixture was sonicated for 45 minutes, left overnight and finally filtered using the same filter paper. Table 3.1 summarizes the yield of AS from Athabasca bitumen. The yields in Table 3.1 vary from the reported value on average by ±0.7% for a 95% confidence interval. The details are in Appendix A, Section A.2.

Table 3.1: Yields of Asphaltene-Solids (AS) from Athabasca bitumen

AS sample	Bitumen 1 (wt%)	Bitumen 2 (wt%)
AS*	17.2	15.1
C_5 AS	23.1	-
SW AS	12.3	-

* precipitated from the bitumen with *n*-heptane

The preceding description of AS recovery was given for *n*-heptane as the solvent. The same procedure would apply if other paraffinic solvents were used. In this study, the majority of experiments required asphaltenes and AS precipitated with *n*-heptane; however, a few experiments were also performed with asphaltenes and AS precipitated with *n*-pentane. The AS recovered with *n*-pentane will be called "C_5 AS" in order to distinguish it from *n*-heptane recovered AS. Precipitation with *n*-pentane was only applied to Bitumen 1 and the yield is given in Table 3.1.

Table 3.1 shows that the yield of C_5 AS is approximately 6% higher than the yield of AS. The C_5 AS contains asphaltenes that are more resinous than those found in AS because a larger cut of the bitumen was precipitated. In fact, it is likely that the AS itself also has a significant portion of resinous material. As demonstrated by others (Agrawala and Yarranton, 2001; Alboudwarej *et al.*, 2002), the presence of resinous material in an asphaltene sample results in a measured molar mass and density smaller than for asphaltenes treated to remove the resinous material. Asphaltenes can be "purified", ie., the resinous material can be removed, by washing the asphaltenes with a paraffinic solvent such as heptane. There are different degrees of washing that result in asphaltenes of increasingly higher molar mass. In the current work, although AS and Asphaltenes are utilized in almost all of the experiments, some experiments have been performed with "Soxhlet Washed" AS and Asphaltenes in an attempt to elucidate the importance of the residual resinous material associated with the AS precipitated from bitumen. Soxhlet washing is expected to remove most of the resinous materials.

A Soxhlet apparatus was employed for the purification of AS. To obtain Soxhlet Washed AS, a two to three gram sample of AS was placed in the Soxhlet apparatus for 24 hours of continuous washing with *n*-heptane. The sample was removed from the apparatus, dried, crushed, and replaced in the Soxhlet apparatus for a further 24 hours of washing. This procedure was repeated again for a total of 72 hours of washing. Soxhlet washing was applied only to Athabasca Bitumen 1 and the yield of Soxhlet Washed AS, abbreviated as "SW AS", is given in Table 3.1. The procedure reduces the yield from 17.2 to 12.3 wt%.

3.1.2.2 Recovery of Solids

Two techniques were utilized for the separation of solids from the asphaltenes. The first technique is referred to as the "Centrifugation Technique" and is expected to remove most of the solids from the AS precipitate. The second method is called the "Precipitation Technique" and is expected to remove all of the solids, including any ultrafine materials less than approximately 50 nm.

3.1.2.2.1 Centrifugation Technique

To separate the asphaltenes and solids using this method, an AS mixture was dissolved in toluene at a ratio of 100 cm^3 toluene per gram AS. The mixture was sonicated for 20 to 40 minutes to ensure complete asphaltene dissolution and solids dispersion. The mixture was allowed to stand for one hour, after which it was centrifuged at 4000 rpm (1640 RCF) for six minutes. To recover asphaltenes, the supernatant was decanted and the solvent evaporated until only dry asphaltenes remained.

For XRD, SEM, TEM and particle size analysis, the solids remaining in the centrifuge tubes were allowed to dry until the mass was invariant, then collected and stored in glass vials. It has been assumed that the drying process will not alter mineralogy or the particle size significantly. However, it was found that dried solids were not suitable for emulsion stability experiments. Figure 3.1 compares the free water resolution after eight hours of

treatment (see section 3.4.5) for model emulsions stabilized by Athabasca Bitumen 1 Asphaltenes, AS, and Asphaltenes and dry or wet solids recombined in their original ratios. The stability trends show that, if dry solids are utilized, the original emulsion stability (free water resolution) cannot be restored whether the solids are dispersed in the continuous hydrocarbon phase or in the aqueous phase. In fact, these solids appear to have no effect on the emulsion stability since the free water resolution is the same as when only asphaltenes are used as stabilizers. However, if wet solids are used, the resulting emulsions have the same stability as the original emulsion. Chen *et al.* (1999) observed that drying the solids extracted from bitumen froth leads to a change in the three phase contact angle between solid tablets, water, and mixtures of heptane and toluene. They showed that the three phase contact angle between "wet" solids, heptol, and water varied between 0 to 50º (depending on the heptane content in the heptol). When "dry" solids were used, the contact angle increased to 150º. This means that the solids become highly oil-wet upon drying. Such a change in wettability would change how the solids in an emulsion are distributed between the bulk phases and the interface. It is likely that drying induced changes have affected emulsion stability. Therefore, in this thesis, all emulsion experiments have been performed with freshly extracted wet solids.

The centrifugation technique was applied to Bitumen 1 AS, C_5 AS, and SW AS, and to Bitumen 2 AS. The composition of each sample after application of the Centrifugation Technique is summarized in Table 3.2. The solids fraction in AS, summarized in Table 3.2, vary from the reported value on average by ±0.3% for a 95% confidence interval. The details are in Appendix A, Section A.2.

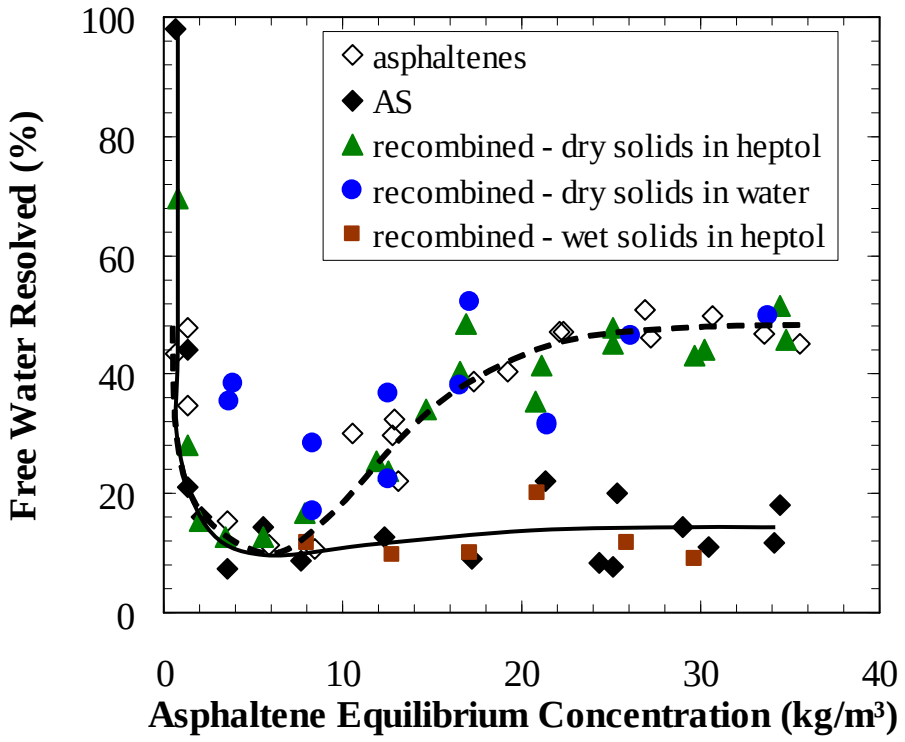

Figure 3.1: Free water resolution after eight hours of treatment for emulsions stabilized by Asphaltenes, AS, recombined Asphaltenes and dry fine solids in heptol, recombined Asphaltenes and dry fine solids in water, recombined Asphaltenes and wet fine solids in heptol. Athabasca Bitumen 1, 25/75 heptol, 40 vol% water, 1.5 hours settling. The lines are visual aides

Table 3.2: Composition of Asphaltene-Solids (AS) from Athabasca bitumen

Component	Fraction of AS (wt%)	Fraction of Bitumen (wt%)
Bitumen 1		
Asphaltenes	95.3	16.4
Solids	4.7	0.81
C_5 Asphaltenes	97.0	16.7
C_5 solids	3.0	0.52
SW Asphaltenes	93.4	16.1
SW Solids	6.6	1.1
Asphaltenes free of Ultrafine Solids	93.3	15.9
Total Precipitated Solids	6.7	1.3
Bitumen 2		
Asphaltenes	96.9	14.6
Solids	3.1	0.47

3.1.2.2.2 Precipitation Technique

The Precipitation technique was applied only to Athabasca Bitumen 1 AS. It is based on the observation that all solids can be removed from the AS if a small portion of asphaltenes are precipitated along with the solids. As described by others (Gafonova and Yarranton, 2001), the solvent used to recover the solids is heptol with a heptane content that corresponds to the onset of asphaltene precipitation. Figure 3.2 shows the fraction of precipitated material from Bitumen 1 AS at various toluene in heptol compositions. The solid content is shown as a solid line. It is apparent that the onset of precipitation occurs at approximately 50/50 heptol. To ensure complete solids removal, the solvent chosen for the precipitation is 55/45 heptol. At this ratio, 2% of the asphaltenes are expected to precipitate, as indicated in the insert in Figure 3.2.

Three grams of AS were dissolved in 135 cm^3 of toluene. The mixture was sonicated for 20 minutes and then 165 cm^3 of heptane was added to achieve an asphaltene concentration of 10 kg/m^3 in a solution of 55/45 heptol. After settling overnight, the mixture was centrifuged at 3500 rpm (1260 RCF) for five minutes and the supernatant decanted. The solids remaining in the centrifuge tubes were recovered and are referred to

as “Total Precipitated Solids”. The solvent was evaporated from the supernatant and the remaining asphaltenes are referred to as “Asphaltenes-free-of-Ultrafine-Solids”. The yield of each material is given in Table 3.2.

The two solids removal techniques were compared in terms of the stability of the emulsions created from asphaltenes and asphaltenes free of ultrafine solids in order to quantify the importance of ultrafine solids. Figure 3.3 compares the free water resolution after eight hours of treatment (see section 3.4.5) for model emulsions stabilized by Athabasca Bitumen 1 Asphaltenes-free-of-Ultrafine-Solids, Asphaltenes, and AS. The results imply that the effect of ultrafine solids is insignificant for asphaltene equilibrium concentrations smaller than 1 kg/m^3 and larger than 15 kg/m^3. For concentrations between 1 and 15 kg/m^3, the free water resolution experienced by the emulsions stabilized by Asphaltene-free-of-Ultrafine-Solids is 10% greater than for emulsions stabilized by Asphaltenes. It appears that the effect of ultrafine solids, or possibly the 2% fraction of asphaltenes precipitated, does not alter the general stability trends and the same conclusions regarding the effect of solids can be made.

Because the Centrifugation technique gives similar results and is less time consuming than the Precipitation technique, it has been employed for all experiments in this thesis.

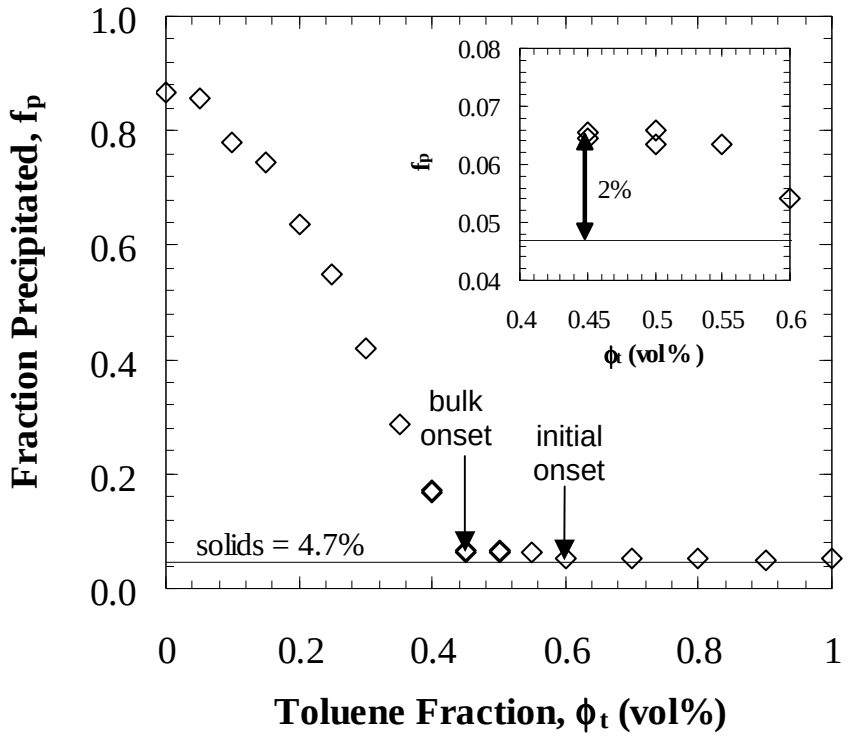

Figure 3.2: Fractional precipitation of AS from Athabasca Bitumen 1. "Initial onset" is the onset of fine solids settling or low solubility asphaltene precipitation. "Bulk onset" is the onset of bulk asphaltene precipitation

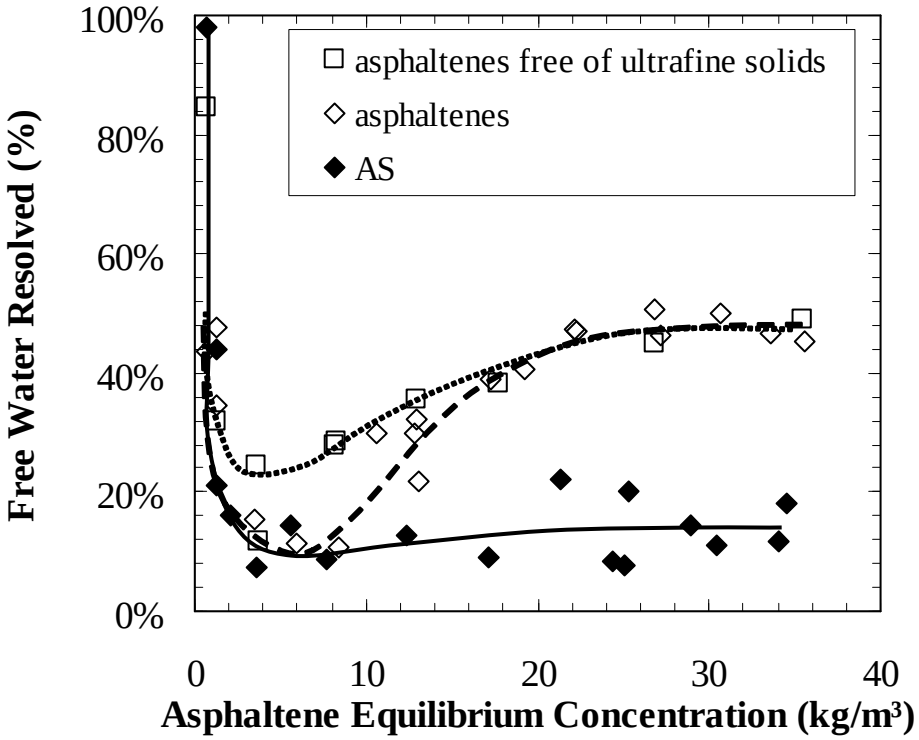

Figure 3.3: Free water resolution after eight hours for Asphaltenes-free-of-Ultrafine Solids, Asphaltenes, and AS. Athabasca Bitumen 1, 25/75 heptol, 40 vol% water, 1.5 hours settling. The lines are visual aides

3.1.3 Recovery of Solids from AEC Wellhead Emulsion

The wellhead sample obtained from AEC contained 35 vol% emulsified water. The water had to be removed prior to the separation of asphaltenes from solids with consistent results. To remove the water, reagent-grade toluene was added to the emulsion in a ratio of 0.6 cm³/g. The mixture was shaken on a shaker table for five minutes, ensuring the dispersion of the emulsion in the toluene. The diluted mixture was poured into several 12 cm³ centrifuge tubes. Each tube was capped with a rubber septum and centrifuged for five minutes at 4000 rpm (1640 RCF, i.e., relative centrifugal force). After five minutes of centrifugation, the mixture separated into a continuous phase and a "rag" layer. The continuous phase contained the bulk of the heavy oil and toluene with only 2.5 vol% water (as measured with Karl Fischer Titration, a standard technique not described here). The rag layer consisted of emulsified water and a small volume of continuous phase fluid.

The continuous phase was decanted and the toluene evaporated in a fume hood until the mass was invariant. AS was precipitated and recovered from the residual bitumen using the technique described previously for Athabasca bitumen. This material is termed "Continuous-Phase AS".

The concentrated rag layer was removed from the centrifuge tubes and placed into a 1 L beaker. *n*-heptane was added to the rag in a 40:1 (cm³/g) ratio. This mixture was sonicated for 45 minutes and left to settle for 24 hours. After settling, the supernatant was filtered through a Whatman #2 filter paper. Additional *n*-heptane was added to this solution at a 4:1 (cm^3/g) ratio of *n*-heptane to the original rag mass. The mixture was sonicated for 45 minutes and left overnight, then filtered using the same filter paper. Note that the water associated with the rag collected in pools on the drying filter cake and evaporated overnight. The dry filter cake is deemed "Rag-Layer AS". The Centrifugation technique was employed for the separation of asphaltenes and solids. The yield of both materials from the continuous phase and rag layer are summarized in Table 3.3.

Table 3.3: Composition of Asphaltene-Solids (AS) from AEC wellhead emulsion

Component	Continuous Phase (wt%)	Rag Layer (wt%)	Total (wt%)
AS (fraction of phase)	16.1	5.1	
AS (fraction of bitumen)	14.4	3.7	18.2
Asphaltenes (fraction of bitumen)	14.3	2.0	16.2
Solids (fraction of bitumen)	0.17	1.8	1.9
Asphaltenes (fraction of AS)	98.8	53	89.3
Solids (fraction of AS)	1.2	47	10.7

3.1.4 Recovery of Solids from IOL Refinery Emulsion

The refinery emulsion contained 43 vol% emulsified water. However, unlike the wellhead emulsion, the IOL sample destabilized after five minutes of centrifugation at 4000 rpm into four distinct phases: 1) a continuous phase free of water; 2) a rag-layer consisting of 51 vol% water; 3) a free water phase; 4) a solids-slurry consisting of 48 vol% water. The rag-layer and solids-slurry made up only 9 and 7 vol%, respectively, of the total emulsion. Note that, on average, approximately 80% of the water was resolved as a free water phase from the IOL emulsion after this initial centrifugation.

Each phase was decanted from the centrifuge tubes. AS were precipitated from the continuous phase in the manner described previously for Athabasca bitumen. Since only small volumes of both the rag layer and solids slurry were recovered from the refinery emulsion, the solids were recovered directly from these samples rather than first precipitating asphaltenes. Toluene was added to either the rag layer or solids slurry in a 25:1 (cm^3/g) ratio. The mixture was sonicated for 20 minutes and then left to stand for one hour. After settling, the mixture was sonicated briefly for 10 minutes and then transferred into centrifuge tubes for six minutes of centrifugation at 4000 rpm. The supernatant was decanted and the solids remaining in the centrifuge tubes were allowed to dry until their mass was invariant. The solids yield from the continuous phase, rag layer and solids slurry are given in Table 3.4. As mentioned previously, the asphaltene

content was not determined because solids were recovered from the rag layer and solids slurry directly. However, the AS yield from the continuous phase was 7.6 wt%. Solids made up 1.7 wt% of the continuous phase AS.

Table 3.4: Solid yield of each phase of the IOL refinery emulsion

Component	Continuous Phase (wt%)	Rag Layer (wt%)	Solids Slurry (wt%)	Total (wt%)
Solids (fraction of phase)	0.11	1.8	11.8	
Solids (fraction of bitumen)	0.09	0.29	1.7	2.1

3.2 TECHNIQUES UTILIZED TO CHARACTERIZE ASPHALTENES

3.2.1 Molar Mass Measurements

The molar mass of asphaltenes was determined with a Jupiter instrument model 833 Vapour Pressure Osmometer (VPO). Vapour pressure osmometry relies on the fact that there is a difference in vapour pressure when a solute is added to a solvent. In the Jupiter 833 instrument, two drops, one containing pure solvent and one containing a solute dissolved in the same solvent, are deposited on separate thermistors. A change in temperature at each thermistor is caused by the difference in vapour pressure of the two drops. For a sufficiently dilute ideal solution, the temperature difference, ΔT, is given by:

$$\Delta T = K_1 \frac{c_2}{M_2} \tag{3.1}$$

where c_2 is the mass wt/wt concentration of the solute, M_2 the molar mass of the solute, and K_1 a constant which is defined as:

$$K_1 = \frac{RT^2 M_1}{\Delta H_v} \tag{3.2}$$

R is the universal gas constant, T the absolute temperature, M_1 the molar mass of the solvent, and ΔH_v the enthalpy of vaporization of the solvent. The temperature change defined in Equation (3.1) is proportional to an observed change in voltage, ΔV:

$$\Delta V = K_2 \Delta T \tag{3.3}$$

where K_2 is another constant. Equation (3.1) and (3.3) are combined such that the molar mass of the solute is related to its concentration through the observed change in voltage:

$$M_2 = K \frac{c_2}{\Delta V} \tag{3.4}$$

where K is a combined constant that can be found for a given solvent and temperature by calibrating with a solute of known molar mass. In the current work, the instrument was calibrated with sucrose octaacetate (molar mass 678.6 g/mol). On average, the value of K was 4879 V·kg/kmol. The calibration was verified with octacosane: the average of five runs performed at concentrations varying from 1 to 5 kg/m³ gave a molar mass of 394.46 g/mol ±3%, which is within 0.2% of the actual value of 394.77 g/mol. Note that the calibration must be performed each time the solvent and temperature conditions are altered. The instrument must also be calibrated after each cleaning.

In the current work, all molar mass measurements were made in toluene at 50°C. The errors in the molar mass over the entire concentration range are ±221 g/mol, ±134 g/mol, and ±520 g/mol for Athabasca Bitumen 1 Asphaltenes, C_5 Asphaltenes and Soxhlet-Washed asphaltenes, respectively. The error in the molar mass for Athabasca Bitumen 2 Asphaltenes is ±200 g/mol. The details of the error analysis are shown in Appendix A, Section A.3.

To prepare the solutions, asphaltenes were added to toluene and the mixture sonicated for 20 minutes until the asphaltenes had dissolved. Asphaltene concentrations from 1 to 60 kg/m^3 were tested. Note that the asphaltenes were treated to remove fine solids with the centrifugation technique. Fine solids can potentially introduce error into the measurements and can also foul the thermistors and needles used for the deposition of the solution.

3.2.2 Interfacial Tension Measurements

3.2.2.1 Drop Volume Tensiometry

Interfacial tension between solvent-asphaltene solutions and water was measured with a Kruss Model DVT10 drop volume tensiometer. In a drop volume tensiometer, a liquid (dispersed phase) is flowed through a capillary into a surrounding continuous phase of higher density. In the DVT10 model, a Harvard Apparatus Model 44 syringe pump, accurate to ±1%, is used to pump the dispersed phase through the capillary at a constant flow rate. A droplet of the dispersed phase forms at the capillary tip and detaches when the buoyancy force acting on that droplet equals the tension holding the droplet to the capillary. A photodiode located above the capillary is used to detect detached drops. After the detachment of a drop, a timer is started and the time, *t*, between successive drops passing the detector is measured. Since the flowrate, *Q*, is constant, the volume of the drop can be found and the interfacial tension, γ, calculated as:

$$\gamma = \frac{(Qt)(\rho_c - \rho_d)g}{\pi d} = \frac{V_{drop}(\rho_c - \rho_d)g}{\pi d} \tag{3.5}$$

V_{drop} is the volume of the drop formed at the capillary, g the acceleration due to gravity, d the diameter of the capillary, and ρ_c and ρ_d the density of the continuous and dispersed phase, respectively.

The time of detachment depends on the flow rate of the dispersed phase; hence, drop volume tensiometers are typically used to measure dynamic interfacial tension. Yarranton *et al.* (2000b) showed that the equilibrium interfacial tension between solutions of asphaltenes and various solvents versus water could be determined with a drop volume tensiometer to within 10% of the equilibrium value when a flow rate smaller than 1.5 cm^3/hr was utilized.

The measurements with the DVT are accurate to ±0.12 mN/m. The details of the error analysis are shown in Appendix A, Section A.4. Before measuring the interfacial tension of asphaltene-solvent and water systems, the tension of pure toluene and heptane over water was determined. Note that a droplet of the aqueous phase was added to the solvent, and vice versa, to saturate the respective liquids. Equilibration for two hours was employed prior to measurement of interfacial tension. Table 3.5 shows the results and indicates good agreement with the literature. Note that experimental values as determined with the Drop Shape Analyzer are also shown; the DSA is described in the next section.

Table 3.5: Interfacial tension of organic solvents versus distilled water

	Interfacial Tension (mN/m)		
Solvent	Drop Volume Method	Drop Shape Method	Literature Values
toluene	35.3	35.0	35.8[a], 35.9[b]
n-heptane	49.8	50.1	50.1[a], 49.5[b]

[a] Li and Fu, 1992
[b] Gafonova, 2000

In the current work, the continuous phase was distilled water. To prepare the dispersed phase, asphaltenes treated to remove solids (using the Centrifugation technique) were added to toluene and the mixture sonicated for 20 minutes until the asphaltenes were completely dissolved. If required, *n*-heptane was added to reach the desired volume ratio of heptane to toluene. As for the pure solvent measurements, each phase was saturated with the other and allowed to equilibriate for two hours. The asphaltene-heptol solutions were pumped into the water phase at a flow rate of 1 cm^3/hr at a temperature of 23°C. Six

drops were passed through the capillary. This procedure was repeated two to three times, and the reported interfacial tension at any given concentration is the average of the measured values. Note that the asphaltene-solvent solution density was utilized in Equation (3.5) to account for non-dilute conditions at higher asphaltene concentrations. The Asphaltene density was taken as 1181 kg/m³ and the Soxhlet-Washed Asphaltene density as 1192 kg/m³ (Alboudwarej *et al.*, 2002).

3.2.2.2 Drop Shape Analysis

Interfacial tension was also measured using a Drop Shape Analyzer (DSA) manufactured by Tracker, IT Concept. A schematic of the instrument is shown in Figure 3.4. A less dense liquid is loaded into a syringe (Item 4, Figure 3.4) and injected through a U-shaped needle into an optical glass cuvette containing a more dense liquid (Item 3). A droplet forms at the tip of the needle and is illuminated by a light source (Item 2). The profile of the droplet is captured using a CCD camera (Item 7) and analyzed using a video image profile digitizer board connected to a personal computer (Item 8). The bench (Item 1) is placed on a wooden platform which in turn sits on a foam mat in order to remove potential vibrations.

The shape of the drop results from the balance between the forces of interfacial tension and gravity. The interfacial tension force acts to minimize the surface area and tends to pull the droplet into a spherical shape. The gravity force acts upwards on the droplet and therefore tends to elongate the droplet since the droplet phase is less dense than the phase in the cuvette. The equations determining the drop profile can be solved from the Young-Laplace equation and hydrostatic calculations. As long as the density of the two phases and the shape of the droplet are known, the equations can be fitted to the measured drop profile and the interfacial tension obtained from the best fit parameters.

The Tracker instrument requires several physical and calculation parameters for the measurement of interfacial tension. The physical parameters required are the light and

heavy liquid densities, the droplet configuration and droplet size. The densities of distilled water, heptane, and toluene at the desired temperature were taken from the CRC handbook. The density of heptol was calculated by assuming ideal mixing. The droplet configuration is either rising or falling. In this work, for liquid/liquid systems the light liquid is always the dispersed phase and hence a rising drop configuration is utilized. The droplet size is important because very small drops do not have a Laplacian shape and therefore too small a drop will invalidate the shape analysis. A Laplacian shape was observed for drops varying from 8 to 30 μL. In the current work, 22 μL droplets were employed for most measurements. However, it was found that for 25/75 and 50/50 heptol-water interfaces aged for very long times (longer than 4 hours), 10 or 15 μL drops were required.

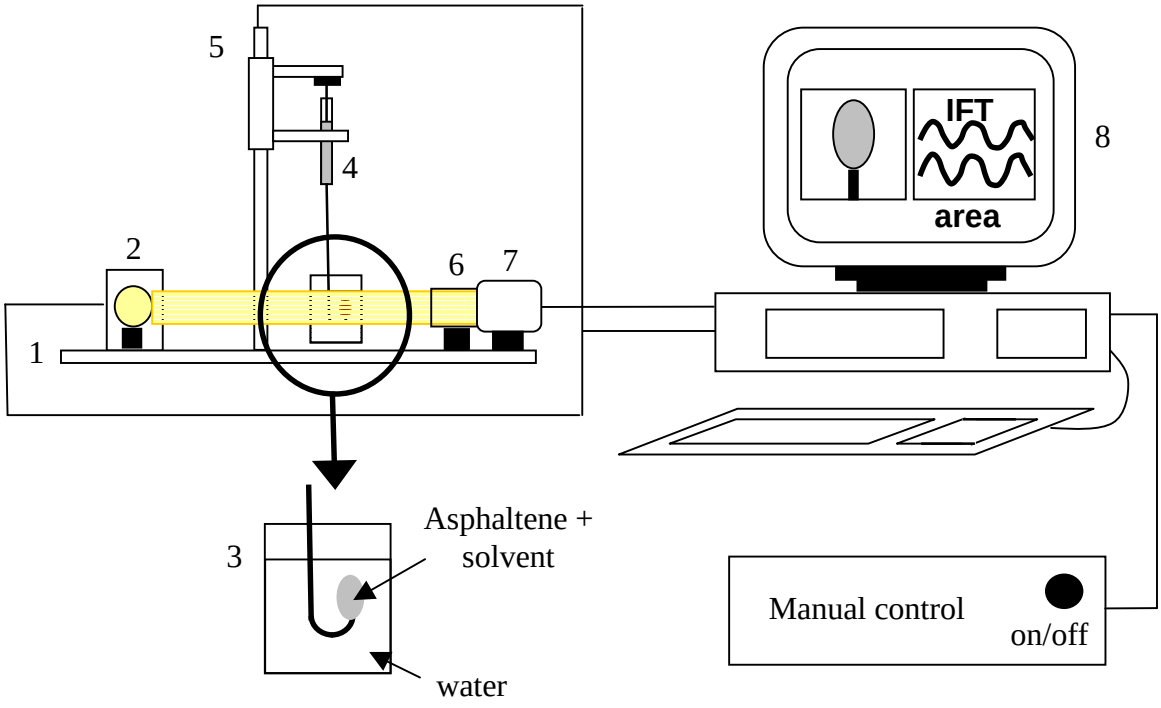

Figure 3.4: Schematic of Drop Shape Analyzer. 1. optical bench, 2. light source, 3. u-shaped needle and cuvette, 4. syringe, 5. dc motor drive, 6. telecentric lens, 7. CCD camera, 8. PC with analysis and control software

The calculation parameters include the precision with which the Laplace equation is solved and the sampling interval. Three modes of evaluation are available: High Precise, Precise, and Normal. The High Precise mode allows for the greatest precision in measuring the interfacial tension (IFT) since more points along the perimeter of the drops are used when fitting the Laplace equation. However, this mode results in fewer measurements per second because the time required to solve the Laplace equation with more precision is longer. Conversely, the Normal mode results in a slightly less precise measurement but more measurements can be made per second. In this study, all IFT measurements were made in the High Precise mode. However, it was observed that the least precise mode, i.e., Normal, still gave IFTs within 0.5% of the High Precise mode values. As will be seen in Section 3.2.3, the Normal mode was applied for elasticity measurements because more measurements per second could be made resulting in smoother sinusoidal profiles for both area and IFT. During collection of IFT with time, measurements were made every second during the first two to three minutes after drop formation and then every 10 seconds. These intervals ensured files of manageable sizes.

The IFT of organic solvents over distilled water was measured with the DSA and the results are given in Table 3.4. The IFT was measured for four hours and since no deviation from the initial value was seen, it was also concluded that there were no surface-active impurities in the needle and syringe. In the current work, the DSA was used to gather the interfacial tension of asphaltene solutions over water. The asphaltene solutions were prepared in the same manner as described in Section 3.2.2.1. Athabasca Bitumen 2 Asphaltenes were utilized for all interfacial tension and elasticity measurements made with the DSA. The solids were removed using the Centrifugation technique.

3.2.3 Elasticity Measurements

Interfacial elasticity, ε, is defined as follows:

$$\varepsilon = \frac{d\gamma}{d\ln A} = A\frac{d\gamma}{dA} \tag{3.6}$$

where γ is the interfacial tension and A the interfacial area. Elasticity is a measure in the change in interfacial energy with a change in interfacial area. In an oscillating system, elasticity is a complex quantity and has both a real and imaginary component defined as follows:

$$\varepsilon = \varepsilon' + i\varepsilon'' \tag{3.7}$$

where ε' is the real component, or elastic modulus and ε'' the imaginary part, or viscous modulus. The total modulus represents a change in the energy of the system with a corresponding change in area. The elastic modulus can be thought of as the energy stored in the system and the viscous modulus as the loss energy. The elastic and viscous moduli can also be expressed in terms of the total modulus, $|\varepsilon|$, and phase angle, ϕ, as follows:

$$\varepsilon' = \varepsilon_d = |\varepsilon|\cos\varphi \tag{3.8}$$

and

$$\varepsilon'' = \omega\eta_d = |\varepsilon|\sin\varphi \tag{3.9}$$

The viscous modulus is the product of the frequency of oscillation, ω, and the interfacial viscosity, η_d.

To measure the elasticity, the area of the droplet must be changed. In this case, the syringe is controlled with a dc motor drive shown in Figure 3.4 as Item 5. A variety of profiles can be imposed on the drop including linear, pulse and sinusoidal profiles, or combinations. In the current study, only sinusoidal oscillations were made according to the following equation:

$$A = A_o + b\sin(t/T + \alpha) \tag{3.10}$$

where A is the area of the drop at a given time t, A_o the initial area of the drop, b the amplitude of oscillations, T the period of oscillation, and α the initial shift factor. The shift factor determines the deviation in area from its initial value before oscillations commence. It was set to zero for all measurements. The period of oscillations, T, is related to the frequency, (f in Hz and ω in rad/s), as follows:

$$T = \frac{1}{f} = \frac{2\pi}{\omega} \tag{3.11}$$

Figure 3.5 presents a schematic of an idealized area profile and the corresponding IFT response. The total modulus is found using Equation (3.7) and the measured area, slope of area versus time, and slope of IFT versus time at any given time. The phase angle is found from the displacement between the peaks of the area and IFT curves.

The measured total modulus depends on a number of experimental parameters including the size of the drop, the amplitude of oscillations, the frequency of oscillations and the interface aging time. As mentioned in Section 3.2.2.2, the initial size of the drop was 22 μL. This corresponds to an interfacial area of approximately 38 mm². Jafari (2005) examined the effect of the amplitude of the oscillation on the measured elastic and viscous moduli. She found that for amplitudes up to 45% of the initial area, a Laplacian drop was maintained and the total modulus did not vary significantly. However, most

experimenters have used amplitudes that do not exceed 10% of the initial area (Aske *et al.*, 2002; Lucassen-Reynders *et al.*, 2001; Freer *et al.*, 2003). In the current work, the amplitude of oscillations was 4 mm^2, or 11% of the initial area, which is within the valid limits measured by Jafari.

The elastic and viscous moduli can be measured as long as the interfacial tension does not change significantly during the interval in which the drop is oscillated. In the current study of asphaltene-solvent/water systems, the minimum time after which measurements were made was 10 minutes; that is, a droplet was formed at the tip of the capillary and the IFT recorded for 10 minutes. No oscillations were applied during the aging time since it has been shown that for systems containing asphaltenes at concentrations exceeding 0.1 kg/m^3, continuous oscillation results in erroneous measurements that are excessively affected by diffusion (Aske *et al.*, 2002; Jafari, 2005). In the current study, the interface aging time was varied from 10 minutes to 24 hours. After the desired aging time had elapsed, the droplet was oscillated at a chosen frequency for a total of ten complete cycles. The frequencies employed in the current study were 0.02, 0.033, 0.1, 0.2 and 0.5 Hz, which corresponds to periods of 50, 30, 10, 5, and 2 s, respectively. Elasticity at a frequency higher than 0.5 Hz could not be measured because there was too much scatter in the IFT response.

Figure 3.6 presents a typical example of the data collected with the DSA. The example system is a droplet of a solution of Athabasca Bitumen 2 Asphaltenes and toluene in a water medium. The droplet was aged for one hour and then oscillated at a frequency of 0.1 Hz (10 s period) with an amplitude of 4.1 mm^2. The initial drop area was 37.8 mm^2. The measured phase angle was 16.6º and the measured total modulus was 10.2 mN/m. Figure 3.6 shows that the DSA data has some scatter, which is a byproduct of minor inertial effects and the finite speed of the motor. However, the data can be smoothed and the phase angle discerned, as shown by the ideal sinusoids imposed on both the area and IFT curves. The Tracker model has a built-in smoothing algorithm. It was found that data

smoothing was important for frequencies exceeding 0.2 Hz and at asphaltene concentrations lower than approximately 0.01 kg/m³; at all other conditions unsmoothed data and smoothed data resulted in the same phase angle and elasticity.

The majority of experiments have been performed for asphaltenes in toluene. Some experiments were made for 25/75 and 50/50 heptol solvents. The asphaltene solutions were prepared and the solvent and aqueous phase equilibrated in the same manner as described previously in Section 3.2.2.1. For concentrations below 0.1 kg/m³, the total modulus varied by ±0.34 mN/m. For concentration greater than 0.1 kg/m³, the total modulus varied by ±0.22 mN/m. At all concentrations, the phase angle varied by ±0.56º. These errors apply at a confidence interval of 95%. The details of the analyses are shown in Appendix A, Section A.5.

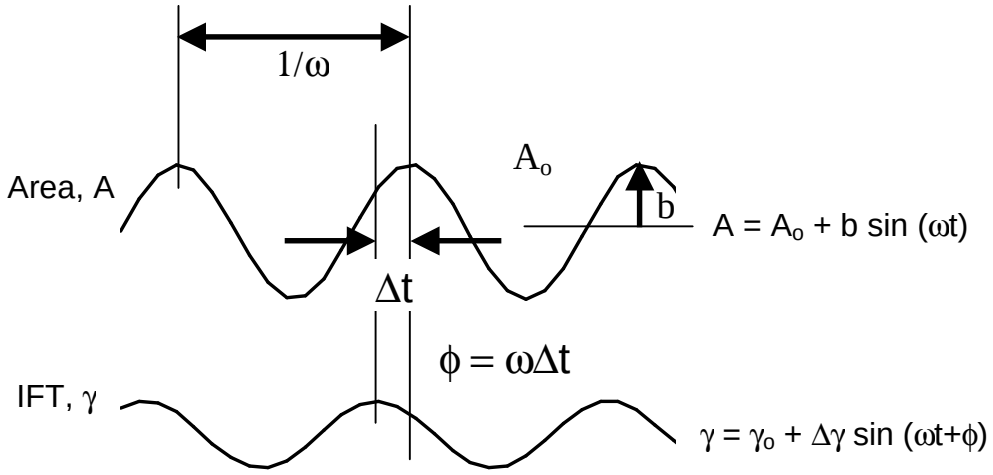

Figure 3.5: Idealized sinusoidal oscillation of drop area and corresponding response in interfacial tension

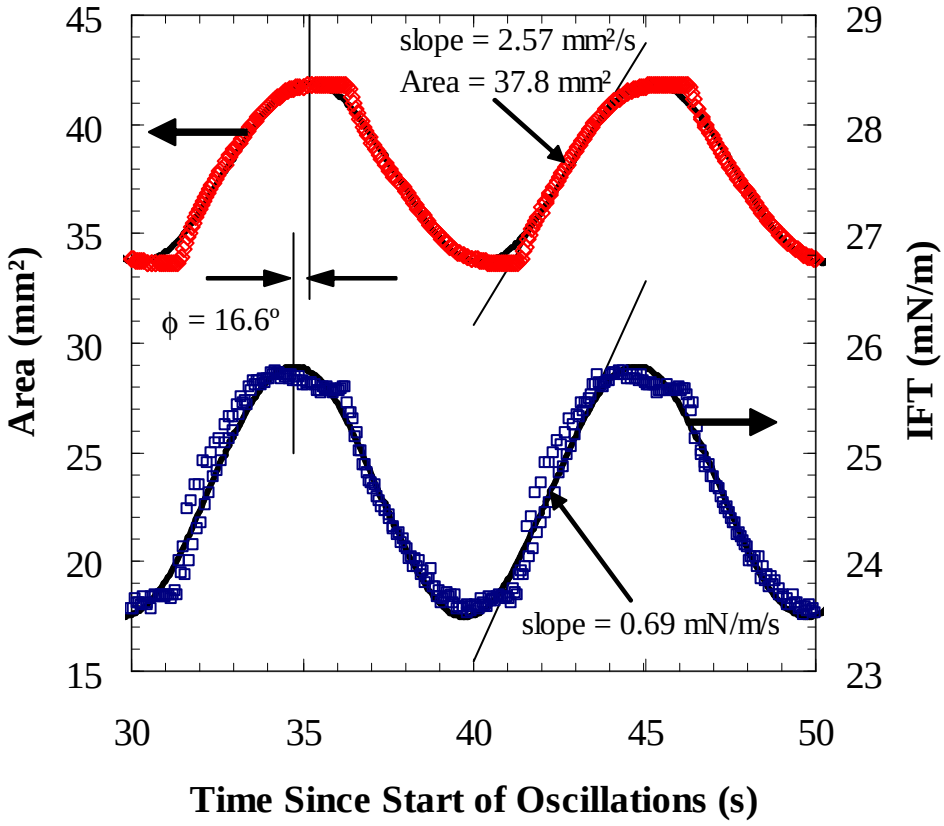

Figure 3.6: Sinusoidal oscillation of drop area and IFT response for 1 kg/m³ Athabasca Bitumen 2 Asphaltenes at a 0/100 heptol/water interface. Interface aging time = 1 hour, ω = 0.1 Hz

3.3 TECHNIQUES UTILIZED TO CHARACTERIZE SOLIDS

3.3.1 Particle Size and Size Distribution Measurements

The particle size and size distribution of Athabasca solids, AEC wellhead solids and IOL refinery rag layer and solids slurry solids were obtained with a Malvern Instrument Model 2000 Mastersizer particle size analyzer. The instrument has a detection range of 0.020 to 2000 μm and measurements must be performed in an aqueous environment. To prepare the solutions, approximately 100 to 200 mg of solids was dispersed in 10 cm^3 of water and the mixture alternately shaken by hand and sonicated. Once the solution appeared to be free of large clumps of solids with no solids floating at the air/water interface, the mixture was introduced into the 2000 Mastersizer apparatus.

The volume frequency distribution was approximated assuming that all of the particles were disc shaped with identical constant thickness. It was further assumed that the measured diameter was equal to the disc diameter. This is a reasonable approximation since the rotation of the solids during the particle size measurement tends to result in a measurement of the diameter rather than the thickness of the disc. The volume frequency is then given by:

$$f_{v,i}^{disc} = \frac{f_{n,i} d_i^2}{\sum_{j=1}^{N} f_{n,j} d_j^2} \tag{3.12}$$

where $f_{v,i}^{disc}$ is the volume frequency, $f_{n,i}$ the number frequency, and d_i the diameter of a given particle.

3.3.2 Particle Size and Shape Assessment

An FEI Company/Philips model XL-30 environmental scanning electron microscope (ESEM) in environmental mode was used to collect several images of solids at various

magnifications. A small dusting of the solids was placed on a 1 cm diameter adhesive wafer. The solids were gold plated in an effort to decrease interference and enhance image quality.

A Philips/FEI Field Emission transmission electron microscope with an accelerating voltage of 200 kV was also employed for the assessment of size and shape of several solid particles. A small drop of toluene, in which solid particles had been dispersed, was placed on a nickel grid and the solvent evaporated. The grid was held in place with a beryllium ring prior to placement in the sample holder.

3.3.3 Mineralogical Assessment

A model *Multiflex 2kW* X-ray diffractometer manufactured by Rigaku was used to perform the X-Ray Diffraction (XRD) analyses of Athabasca solids. The apparatus employs an extra fine copper tube with a 1.542 Å X-ray wavelength. The solids were sampled every 0.02 degrees with a scan speed of 2 deg/minute in continuous mode. For bulk mineralogical characterization, the scan range employed was 2 to 60 degrees on the 2-theta scale, while clays were analyzed from 2 to 40 degrees. The current, voltage, and power utilized during the experiments were 40 mA, 40 kV and 1.6 kW, respectively.

For bulk analyses of solids, approximately 100 to 200 mg of a dry solid sample was placed into a 0.2 mm deep aluminium holder. In order to ensure complete flatness, a glass slide was placed onto the solids, pressed down, and gently removed so as not to disturb the solids. The holders were placed into the *Multiflex* diffractometer and each sample analyzed for thirty minutes. This ensured a complete scan over the 2 to 60 degree range on the 2-theta scale. The mineralogical characterizations were performed using Jade 6.1 software.

In order to better characterize the clay component of the solids, a clay separation was performed on the solids. Approximately 100 mg of solids was placed in a 20 cm^3 vial,

five cm deep. 15 cm^3 of distilled water was added to the solids. The vial was capped, shaken vigorously by hand for approximately 20 seconds, and then placed in a sonication bath. The mixture was alternately sonicated and shaken until most of the solid material had migrated from the air/water interface into the water. The mixture was allowed to stand for four hours, ensuring that solids with an equivalent spherical diameter greater than approximately 2 μm sank to the bottom of the vial. Nearly all of the solids remained in suspension, suggesting that Athabasca solids are predominately composed of clay minerals. The clays remaining in suspension were decanted from the vial and concentrated by centrifugation until the water was nearly clear. The concentrated solids were redispersed in approximately 1 cm^3 of water, and the resultant slurry placed dropwise onto three 2 cm diameter glass discs. The water was allowed to evaporate until a thin covering of solids remained on the discs. The discs were mounted into 0.5 mm deep aluminium holders. One of the samples was analyzed directly, while the other two samples were further treated with either glycolation or heating at 400ºC for one hour. Glycolation and heating treatments can potentially cause specific peaks in the XRD spectra to shift to alternate spacings for certain clay minerals. The presence or absence of peak shifts, as well as potential changes in peak intensity, can be used to verify clay mineralogy and assess if the clay is swelling or non-swelling.

Adsorbed hydrocarbon matter can make the discernment of peaks difficult. To see if adsorbed hydrocarbon matter affected the interpretation of XRD results, two washing techniques were applied to solids. In the first technique, dry solids were dispersed in toluene at approximately a 1:400 g:cm^3 ratio. The mixture was sonicated for five minutes and then centrifuged at 4000 rpm for six minutes. The supernatant, which was nearly colourless, was decanted. The solids were again redispersed in toluene at the same ratio, sonicated and centrifuged. This procedure was repeated a total of three or four times, until the toluene was clear. The solids were dried and stored in glass vials, whereas the solvent from the decanted continuous phase was evaporated. The material removed made up less than 10% of the solids prior to washing with toluene. It was impossible to tell

whether this material consisted of fine solids that remained dispersed in the continuous phase, or purely hydrocarbon matter.

The second technique is more aggressive and uses hydrogen peroxide to bleach the solids and remove adsorbed hydrocarbon materials (Moore and Reynolds, 1997). In this method, approximately 200 mg of solids were placed in a 50 cm^3 beaker. 30% hydrogen peroxide was added dropwise and the mixture slowly stirred with a spatula. Once the hydrogen peroxide began reacting with the organic materials and bubbling was visibly observed, approximately 10 cm^3 of hydrogen peroxide was added to the beaker. The mixture was continuously stirred. A final 10 cm^3 of hydrogen peroxide was added to the beaker. The mixture was left for a period of 24 hours after which bubbling ceased. The beaker was placed in a fume hood and the liquid evaporated. The mass of the material remaining in the beaker was measured and it was found that the mass did not change significantly from the initial value. However, it was observed that the solids were a lighter gray colour than they had been initially.

3.4 EMULSION EXPERIMENTS

3.4.1 Determination of Asphaltene and Solids Surface Coverage

The amount of asphaltenes and solids on the water/oil interface of an emulsion can be calculated from a combination of 1) gravimetric analyses of the continuous phase, 2) droplet diameter measurements of the emulsion phase. The procedure for finding the mass surface coverage of asphaltenes is presented first. Then the additional steps required for systems containing both asphaltenes and solids are described.

The surface coverage of asphaltenes, Γ_A, is defined as the ratio of the mass of asphaltenes adsorbed on the emulsion interface, m_{AI}, to the total area of that interface, A:

$$\Gamma_A = \frac{m_{AI}}{A} \tag{3.13}$$

The mass of asphaltenes on the interface is found from a mass balance and is defined as the difference between the total mass of asphaltenes in the emulsion, m_{AT}, and the mass of asphaltenes remaining in the continuous phase after emulsification, m_{Acp}:

$$m_{AI} = m_{AT} - m_{Acp} \tag{3.14}$$

The total mass of asphaltenes is an experimentally controlled variable and related to the initial concentration of asphaltenes in the continuous phase, C_A^o, by:

$$m_{AT} = C_A^o V_{cp} \tag{3.15}$$

V_{cp} is the total volume of the continuous phase and is also used to relate the mass of asphaltenes remaining in the continuous phase to their equilibrium concentration, C_A^{eq}:

$$m_{Acp} = C_A^{eq} V_{cp} \tag{3.16}$$

Equations (3.14) through (3.16) can be combined and the mass of asphaltenes on the interface related to the initial and equilibrium asphaltene concentrations:

$$m_{AI} = m_{AT}\left(1 - \frac{C_A^{eq}}{C_A^o}\right) \tag{3.17}$$

The other variable in Equation (3.13) is the total emulsion interfacial area which is the sum of the surface areas of all individual drops. It can be related to the total volume of the dispersed phase through the Sauter mean diameter:

$$A = \pi \sum_{i=1}^{N} d_i^2 = \frac{\pi \sum_{i=1}^{N} d_i^3}{d_{32}} = \frac{6V_w}{d_{32}} \tag{3.18}$$

where d_{32} is the Sauter mean diameter and is defined as follows:

$$d_{32} = \frac{\sum_{i=1}^{N} f_i d_i^3}{\sum_{i=1}^{N} f_i d_i^2} \tag{3.19}$$

Equations (3.17) and (3.18) can be combined and the mass surface coverage of asphaltenes defined only in terms of fixed and measurable quantities:

$$\Gamma_A = \frac{m_{AT} d_{32}}{6V_w}\left(1 - \frac{C_A^{eq}}{C_A^o}\right) \tag{3.20}$$

The total mass of asphaltenes, the total volume of water, and the initial asphaltene concentration are experimentally controlled variables. Section 3.4.3 outlines the procedure for determining the equilibrium asphaltene concentration. Section 3.4.4 outlines the procedure for finding the Sauter mean diameter. The application of Equation (3.20) for various initial asphaltene concentrations at a given water content results in plots known as adsorption isotherms. Adsorption isotherms relate the mass surface coverage of asphaltenes to the equilibrium asphaltene concentration.

The same procedure can be followed for emulsions containing both asphaltenes and solids. The asphaltene mass surface coverage is again found from Equation (3.13) but now, if any solids are adsorbed on the water-hydrocarbon interface, the surface coverage will be less than the monolayer coverage. The fact that asphaltenes adsorb as a monolayer will be discussed in detail in Chapter 4.

The fractional area occupied by the asphaltenes on the interface, θ_A, is the ratio of the asphaltene mass surface coverage over the monolayer surface coverage, Γ_A^m:

$$\theta_A = \frac{\Gamma_A}{\Gamma_A^m} \tag{3.21}$$

The solids are assumed to occupy the remainder of the interface so that the fractional area of solids on the interface, θ_s, is equal to $1-\theta_A$.

3.4.2 Preparation of Model Emulsions

Model emulsions were prepared with heptane, toluene, water and one of either AS, asphaltenes, or a mixture of asphaltenes and solids. For emulsions stabilized by asphaltenes or AS, the appropriate mass of either material was placed in a 120 mL glass jar. For emulsions containing mixtures of asphaltenes and solids, solids were extracted from AS and the desired concentration added to the jar containing a pre-measured mass of asphaltenes. As noted in Section 3.2.1.1.1, for emulsions containing asphaltenes and mixtures of solids, the solids were used immediately after extraction from the AS precipitate in order to prevent possible alteration of surface properties upon contact with air.

Toluene was added to the materials in the jar and the mixture sonicated for 20 minutes to ensure asphaltene dissolution and solids dispersion (if solids were present). *n*-heptane was added to the mixture in the desired quantity and the mixture sonicated for a further five minutes to ensure homogeneity. Water in a 40 vol% ratio was added dropwise to the heptol phase while the mixture was homogenized with a *CAT-520D* homogenizer equipped with a 17 mm rotor for five minutes at 18000 rpm. For most experiments, the emulsion was allowed to settle for 1.5 hours following homogenization, during which a continuous phase and a concentrated emulsion phase separated. As will be seen in

Chapter 6, for some experiments, the settling time was increased beyond 1.5 hours in order to gauge the effects of interface aging time. The maximum settling time employed was 24 hours.

3.4.3 Emulsion Gravimetric Experiments

The equilibrium asphaltene concentration, C_A^{eq}, after settling was determined from a gravimetric analysis of the separated continuous phase. As already mentioned, the emulsion divided into a water-free continuous phase on top and a concentrated emulsion phase on the bottom. The continuous phase was decanted from the top of the settled emulsion and its volume measured. After complete solvent evaporation, the mass of the remaining material was determined gravimetrically. If the emulsion was solids-free, the equilibrium asphaltene concentration is simply the residual mass divided by the volume of the decanted continuous phase. If solids were present, the dry residual asphaltene-solids mixture was redispersed in toluene and the solids separated using the centrifugation procedure described previously. The mass of asphaltenes remaining after solids removal was then determined gravimetrically and the equilibrium concentration of asphaltenes calculated as before.

The mass of solids in the settled emulsion was also determined from a mass balance. Note that solids began appearing in the continuous phase after the bulk solids concentration had exceeded ~0.4 kg/m³. However, for all experiments where the solids concentration was greater than 0.4 kg/m³, no more than 2 to 7% of the solids remained with the evolved continuous phase. The majority of the solids was either adsorbed on the water/oil interface or had become trapped between water droplets in the settled emulsion. No solids were observed in the aqueous phase in any experiment. The asphaltene mass surface coverage varies by ±0.0002 g/m² for a confidence interval of 95%. The details are shown in Appendix A, Section A.7.

3.4.4 Emulsion Drop Size Distribution Analysis

The Sauter mean diameter is found from drop size distributions of samples taken from a settled emulsion. After the desired settling time, a drop of the emulsion phase was placed by pipette onto a hanging-drop glass slide. To examine individual drops, a small drop of the continuous phase was added to the slide. The slide was then covered with a slipcover. The drop size distribution was measured with a Carl Zeiss Axiovert S100 inverted microscope equipped with video camera and Image Pro image analysis software. In the current work, approximately 400-500 drops were used, giving an expected error of 5-10% according to Dixon and Massey (1969) and as discussed in detail by Gafonova (2000).

For all experiments except those in which AEC solids were used, the drop size distribution did not change during the 1.5 hour settling period, nor did any water evolve from the emulsion. The drop size distribution did change during the settling period when AEC solids were used as stabilizers and when Athabasca Asphaltene stabilized emulsions were aged beyond 1.5 hours, but no free water was ever observed. Since no free water was observed during a given settling period, the validity of the gravimetric measurements is maintained.

Typical images for the model emulsion systems are shown in Figure 3.7. Figures 3.7 (a), (b), (c) and (d) are micrographs of settled emulsions stabilized by Athabasca Bitumen 1 Asphaltenes at bulk concentrations of 1, 2, 5 and 20 kg/m^3. The results are consistent with the findings of Gafonova (2000) indicating a decrease in drop size with an increase in asphaltene concentration. The average drop size did not change significantly for concentrations exceeding 10 kg/m^3. Note that: 1) emulsions stabilized by Bitumen 1 AS at the same concentrations resulted in nearly identical drop sizes, 2) drop sizes at any given concentration for emulsions stabilized by Athabasca Bitumen 1 asphaltenes were nearly identical to those when Athabasca Bitumen 2 asphaltenes were utilized. The Sauter mean diameter varies by ±0.3 microns for a confidence interval of 95%. The details are shown in Appendix A, Section A.6.

Drop size distributions were also measured for the wellhead emulsion received from AEC and the refinery emulsion received from IOL, Ltd. Because these emulsions were very viscous, a drop of 50/50 heptol was added to the slide in order to disperse the drops and facilitate image analysis.

3.4.5 Assessment of Emulsion Stability

The stability of an emulsion was assessed by measuring the water separated from the emulsion as a function of time. After settling, the concentrated emulsions were transferred to 12 cm^3 centrifuge tubes and capped to prevent evaporation of solvents. The tubes were centrifuged at 4000 rpm (1640 RCF) for five minutes and then placed in a 60 ^oC heating bath. After two hours, the tubes were centrifuged for five minutes and the volume of free water recorded. The tubes were returned to the heating bath and the procedure repeated two more times for a total of four, two hour cycles. The amount of free water is reported as a percentage of the total water in a given emulsion. The relative stability of the emulsions can be assessed by comparing the amount of free water resolved for any given destabilization time. For concentrations exceeding 20 kg/m^3, the free water resolution varies by less than 5%. The details of the analysis are shown in Appendix A, Section A.8.

Note that this procedure can also be applied for the existing wellhead and refinery emulsions. The only modification in the procedure is that the emulsions are placed directly in the centrifuge tubes because a separated continuous phase does not exist for these emulsions.

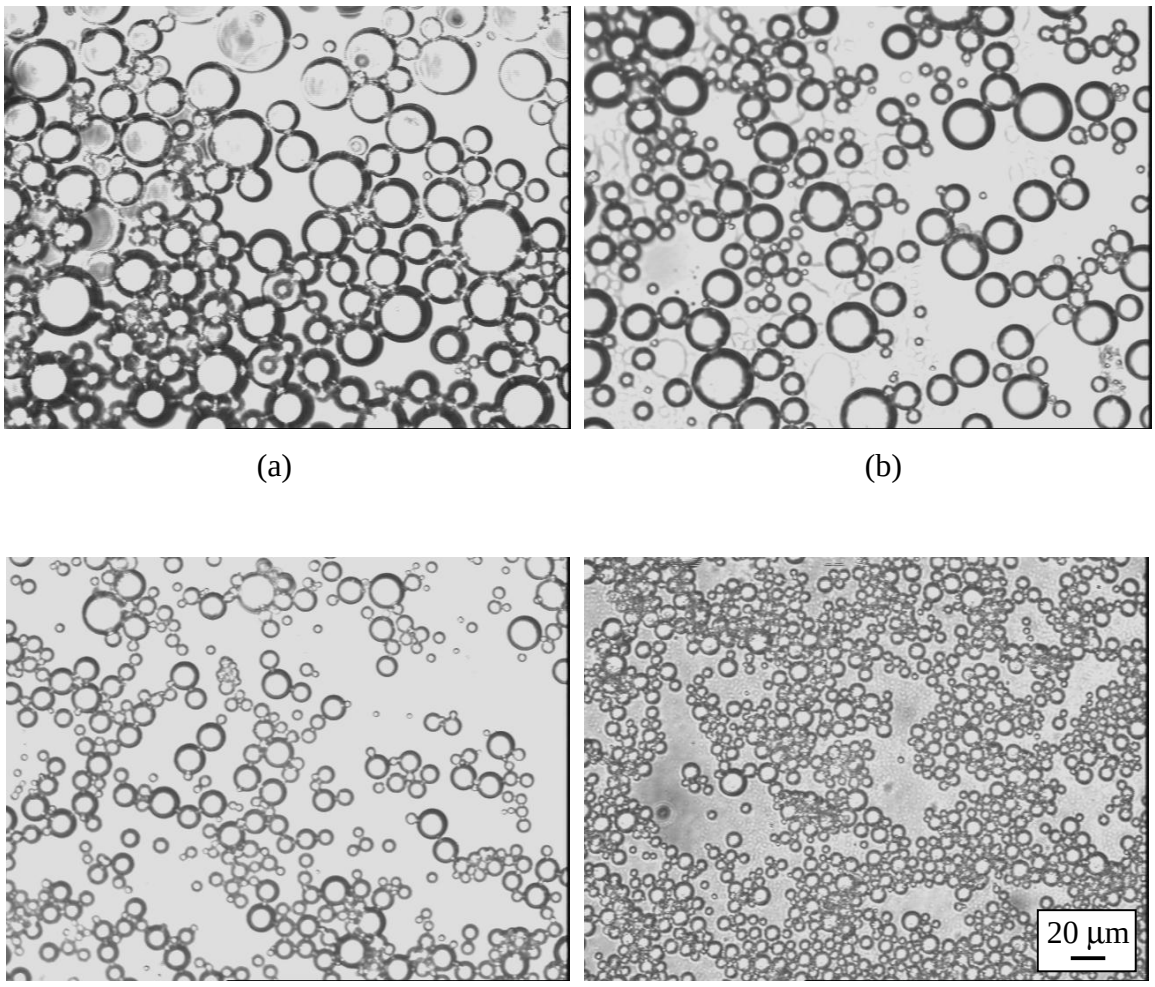

Figure 3.7: Micrographs of settled emulsions stabilized by Athabasca Bitumen 1 Asphaltenes at bulk concentrations of a) 1 kg/m³, b) 2 kg/m³, c) 5 kg/m³, d) 20 kg/m³. 25/75 heptol, 40 vol% water, 1.5 hours settling. Scale bar applies to all micrographs

CHAPTER 4
COMPOSITION AND STRUCTURE OF ASPHALTENE-HEPTOL/WATER INTERFACES

This chapter presents the results of the composition and initial structure of the water/oil interface. The studies were performed on model systems stabilized solely by asphaltenes; that is, interfaces consisting of asphaltenes, heptol, and distilled water. The asphaltene molar mass, interfacial tension of asphaltene solutions over water, and asphaltene adsorption isotherms are presented in Section 4.1, 4.2 and 4.3, respectively. In Section 4.4, the data from these sections is used to interpret the structure of the water/hydrocarbon interface. Section 4.5 contains concluding remarks for this chapter.

The main objective of this chapter is to determine if asphaltenes adsorb as a monolayer or in multilayers. Additionally, the importance of asphaltene self-association on the structural interpretation of the water/oil interface is shown by accounting for a changing asphaltene molar mass in both interfacial tension measurements and in the overall calculation of the number of adsorbed asphaltene layers. The number of asphaltene layers is the ratio between the total number of adsorbed molecules in the interfacial film to the number of molecules in a monolayer. The total number of molecules in the interfacial film can be found from molar mass and emulsion gravimetric measurements. The number of molecules in a monolayer can be found from interfacial tension measurements.

The approach for determining the asphaltene interfacial configuration is demonstrated for the following model emulsion system: Athabasca Bitumen 1 Asphaltenes or Soxhlet-Washed Asphaltenes, 25/75 heptol, 40 vol% water. However, the effects of asphaltene source and solvent quality were also examined in order to see if they had an effect on the interpretation of asphaltene interfacial structure. To summarize, the following experimental variables were considered:

1. *Asphaltene Source and Degree of Washing*: Athabasca Bitumen 1 C_5 Asphaltenes, Asphaltenes, and Soxhlet-Washed Asphaltenes and Athabasca Bitumen 2 Asphaltenes were utilized to complete all desired experiments. Some types of experiments were only performed for Athabasca Bitumen 1 Asphaltenes because their supply was exhausted by the time certain experimental techniques and equipment became available.

2. *Asphaltene Concentration*: For molar mass, interfacial tension, gravimetric and emulsion stability experiments, asphaltene concentrations from 1 to 40 kg/m³ were considered.

3. *Solvent Quality*: The heptane fraction in the heptol was varied from 0 to 50%. Thus, the solvents tested were 0/100, 25/75, and 50/50 heptol.

4. *Temperature*: The effect of temperature was not considered in this work; however, experimental limitations in some procedures prevented the use of a consistent temperature for all measurements. All emulsions were created and analyzed gravimetrically at 23ºC. All interfacial tension measurements were also made at 23ºC. Molar mass of asphaltenes was measured at 50ºC. Emulsion stability experiments were made at 60ºC. Note that emulsion stability experiments are performed at an elevated temperature in order to magnify trends in free water resolution. Recently, Jafari (2005) has shown free water does not resolve in a timely way for a treatment temperature of 23ºC.

4.1 ASPHALTENE MOLAR MASS

The molar mass of Athabasca Bitumen 1 Asphaltenes in toluene at 50ºC is shown in Figure 4.1. The results are generally consistent with previous studies which utilized the same vapour pressure osmometer; however, the initial rise in molar mass is not as steep as measured by others (Agrawala and Yarranton, 2001; Alboudwarej *et al.*, 2002). The asphaltenes used in those studies were from a different batch of Athabasca bitumen. Also, they had been treated with intermittent heptane washing cycles lasting between five and ten days rather than no washing (as in this study). Nonetheless, the trends are consistent with the previous work and show that as the concentration of asphaltenes increases, the molecules self-associate from monomers of approximately 2000 g/mol into 10,000-11,000 g/mol macromolecules at concentrations of 50 to 60 kg/m³. An extrapolation of the curve to infinite dilution shows that the molar mass of an asphaltene monomer is 2060 g/mol, a value consistent with previous work (Agrawala and Yarranton, 2001) but higher than that reported in the literature (Groenzin and Mullins, 2001).

The molar mass of C_5 Asphaltenes and Soxhlet-Washed Asphaltenes in toluene at 50ºC is also shown in Figure 4.1. As expected, the C_5 Asphaltenes have a lower molar mass than the Asphaltenes. This is consistent with the idea that the material precipitated with pentane (C_5 Asphaltenes) is more resinous than that precipitated with heptane (Asphaltenes). Resin molecules are generally smaller than asphaltene molecules so it is expected that the overall molar mass of a sample containing a higher fraction of resin-type molecules will subsequently be smaller. Also, it has been speculated that resin molecules act as “terminator” molecules which limit the extent to which asphaltenes self-associate (Agrawala and Yarranton, 2001). Asphaltenes that have self-associated to a smaller degree will naturally result in a molecule with a smaller molar mass. Conversely, a molecule which has been stripped of its resinous material will result in an asphaltene with more “propagator” sites that facilitate the self-association of asphaltenes. Since a Soxhlet-Washed sample contains asphaltenes which are nearly all “propagator” molecules, self-association continues unimpeded and the molecules form larger and

larger macromolecules as the asphaltene concentration increases. Therefore, Soxhlet-Washed Asphaltenes have a higher apparent molar mass than the Asphaltenes, as shown in Figure 4.1. The molar mass measured here for Soxhlet-Washed Asphaltenes is consistent with the values obtained in a previous work (Akbarzadeh *et al.*, 2004). An extrapolation to infinite dilution yields a monomer molar mass of 2850 g/mol for the Soxhlet-Washed Asphaltenes.

As mentioned previously, two sources of Athabasca bitumen were required for the completion of all experiments. Figure 4.2 compares the molar mass of Athabasca Bitumen 1 and 2 Asphaltenes in toluene at 50ºC. The results show that for concentrations higher than 5 kg/m^3, the asphaltenes extracted from Bitumen 2 have a molar mass approximately 30 to 40% lower than those extracted from Bitumen 1. It can be inferred that Bitumen 2 contains asphaltenes that self-associate to a lesser degree than Bitumen 1. Note, the yield of Athabasca Bitumen 1 Asphaltenes was 2.1% higher than Bitumen 2 Asphaltenes and Bitumen 1 appeared to be more viscous than Bitumen 2. Higher yield and viscosity could indicate higher asphaltene content and also greater self-association of the asphaltenes.

For the structural interpretation, the apparent asphaltene molar masses are required at emulsion conditions; that is, in 25/75 heptol and at 23ºC. However, vapour pressure osmometry can only be employed with pure unmixed solvents, such as toluene. As well, for asphaltenes in toluene, 50ºC is the minimum temperature at which repeatable results can be obtained with the Jupiter 833 instrument. Hence, to apply the measured molar masses at emulsion conditions, the effect of solvent and temperature on molar mass must be considered.

There is some evidence that asphaltene molar mass in heptol is not significantly different than the molar mass in toluene. Moschopedis *et al.* (1976) related the measured asphaltene molar mass at 37°C to the dielectric constant of the solvent. Their results are

reproduced in Figure 4.3. In that study, a correlation between molar mass and the dielectric constant was found for a dielectric constant range between 2 and 35. If the correlation is valid, asphaltenes dissolved in solvents of similar dielectric constant should have a similar molar mass. As shown in the insert of Figure 4.3, the dielectric constants of toluene and *n*-heptane at 37ºC are similar, 2.35 and 1.87, respectively. Hence, the hypothetical molar mass of asphaltenes dissolved in heptane or 25/75 heptol is expected to be similar to or greater than that in toluene. Although the correlation of Moschopedis *et al.* (1976) was developed for aromatic solvents, it has nevertheless been assumed that it is approximately valid for the 25/75 heptol solvent due to the lack of a more appropriate technique for determining asphaltene molar mass in a mixed solvent.

It is known that the apparent asphaltene molar mass decreases with increasing temperature. Agrawala and Yarranton (2001) measured the molar mass of asphaltenes in toluene at two temperatures, 50ºC and 70ºC. Assuming that molar mass changes in proportion to the inverse of the temperature, the molar masses can be extrapolated to 23°C. It was found that the difference between the molar mass at 50ºC and that estimated at 23°C was approximately 20%. Since the form of this extrapolation lacks theoretical justification, the molar masses measured at 50°C are used in this work. These molar masses are probably low but the error is expected to be within 20%.

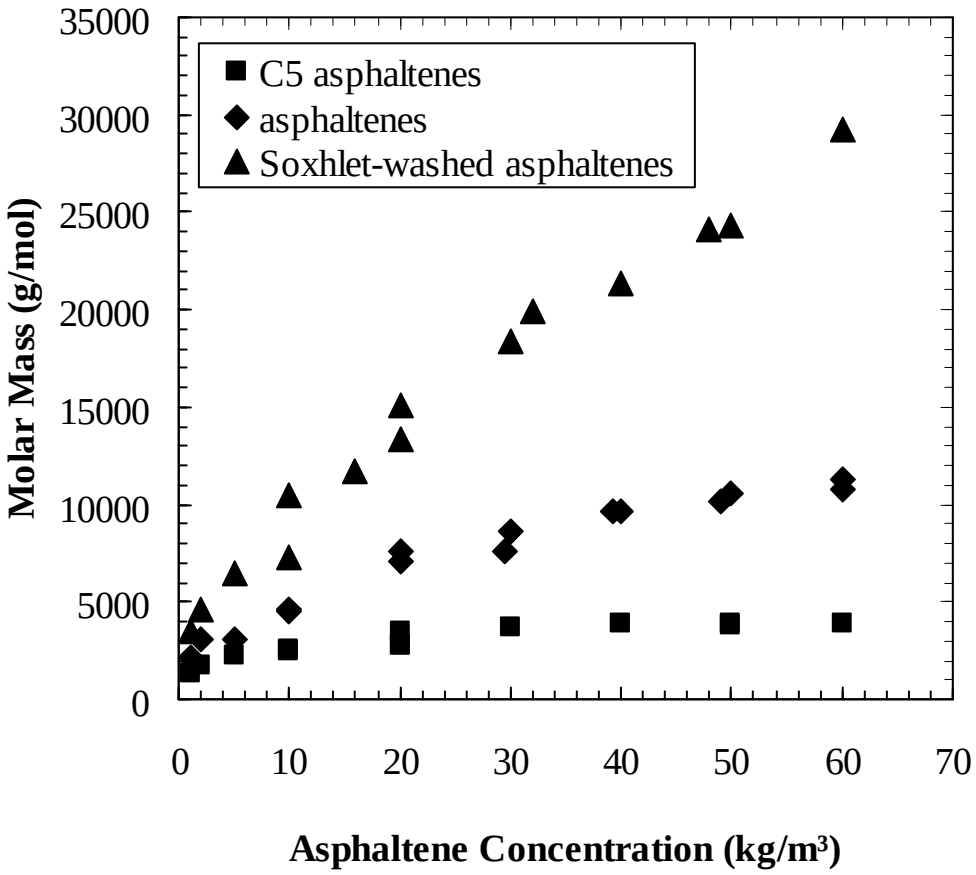

Figure 4.1: Molar mass of C_5 Asphaltenes, Asphaltenes, and Soxhlet-Washed Asphaltenes extracted from Athabasca Bitumen 1. Toluene, 50ºC

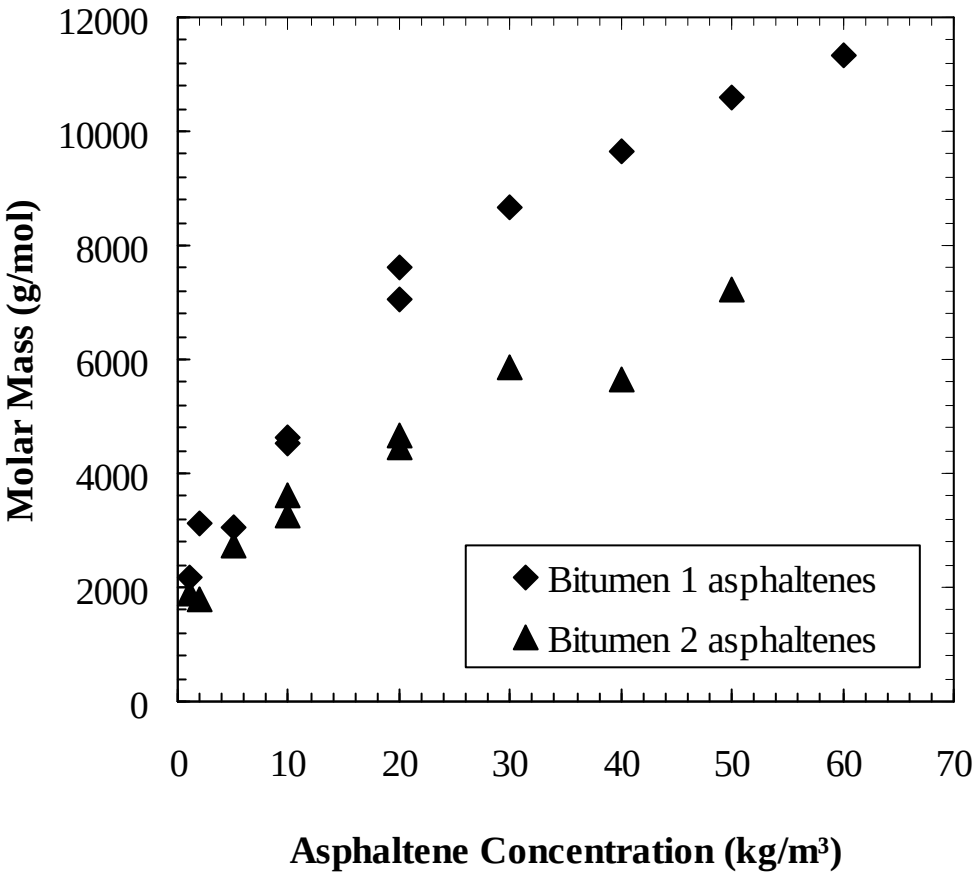

Figure 4.2: Molar mass of Asphaltenes extracted from Athabasca Bitumen 1 and Bitumen 2. Toluene, 50ºC

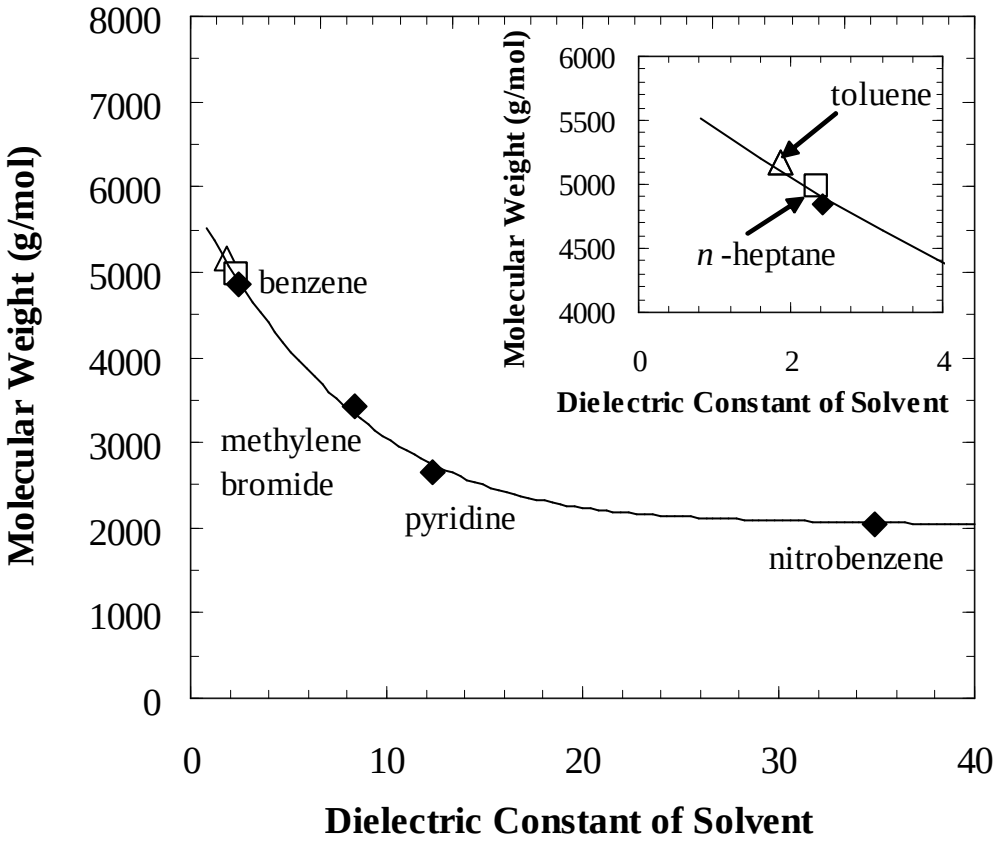

Figure 4.3: Molar mass of asphaltenes in various solvents at 37ºC (Moschopedis *et al.*, 1976)

4.2 INTERFACIAL TENSION OF ASPHALTENE SOLUTIONS

The interfacial tension of asphaltenes in heptol over water has been measured using two techniques: a drop volume tensiometer (DVT) and a drop shape analyzer tensiometer (DSA). The results of the measurements made with the DVT are presented first and then compared to those made with the DSA. Note that, the DVT was used for assessing the interfacial area of Athabasca Bitumen 1 Asphaltenes, whereas the DSA was used for assessing the IFT and interfacial area of Athabasca Bitumen 2 Asphaltenes. Since the two asphaltenes have different molar masses, some differences in the interfacial tensions are to be expected.

4.2.1 Interfacial Tension Measured with DVT

The interfacial tension (IFT) of Athabasca Bitumen 1 Asphaltenes in 25/75 heptol versus water is given in Figure 4.4. Note that the time for the drops to detach from the capillary varied from 45 to 55 seconds. In other words, the interface had aged for less than one minute in these experiments. If the Gibbs' isotherm is assumed to apply, (Equation 4.1), the linearity of the plots suggests that asphaltenes adsorb at the water/hydrocarbon interface with a constant area over a wide concentration range.

$$\frac{d\gamma}{d\ln C} = -\Gamma RT \qquad (4.1)$$

where γ is the interfacial tension, C the concentration, Γ the molecular surface coverage, R the universal gas constant, and T the absolute temperature. There are no deviations from linearity beyond scatter in the data. If micellization occurs, a constant IFT or at least a deviation in the IFT is expected at and above the critical micelle concentration. Hence, there is no indication of micellization, consistent with previous observations (Yarranton *et al.*, 2000a and 2000b). The results for Soxhlet-Washed Asphaltenes in the same solvent are also given in Figure 4.4. At any given concentration, the Soxhlet-Washed Asphaltenes appear to lower the interfacial tension more than the Asphaltenes. However,

as indicated in Figure 4.4 and summarized in Table 4.1, the slope of the two curves is very similar.

The results given in Figure 4.4 were for asphaltene samples that had been treated to remove native solids. The presence of solids can alter the results because solids can potentially adsorb on the interface. Generally, solid particles are not expected to lower the interfacial tension. However, native solids such as the ones removed from the bitumen utilized in this work have been shown to contain a significant quantity of adsorbed humic and petroleum matter (Kotlyar *et al.*, 1998). The presence of these materials may facilitate adsorption of the solids on the interface. Solids on the interface can reduce the interfacial area available for asphaltenes. The adsorption of solids on the interface may manifest itself as a smaller reduction in IFT at any given concentration and hence a smaller slope of the IFT versus log(concentration) plot. A smaller slope may lead to an erroneous interpretation of the area occupied by asphaltene molecules on the interface. The effect of solids is demonstrated in Figure 4.5 and is consistent with the work of Gafonova (2000). The slope of the AS curve is 16% smaller than the Asphaltene curve. The difference between the AS and Asphaltene curves suggests solids have adsorbed on the interface.

The solvent system chosen to demonstrate how the structure of the interface can be interpreted from molar mass, interfacial tension and gravimetric studies was 25/75 heptol. Unless otherwise stated, these experiments were performed with asphaltenes treated to remove solids. In order to assess the effect of solvent on interfacial tension (IFT), the IFT of AS in 0/100, 25/75 and 50/50 heptol was measured and the results shown in Figure 4.6. Note that during the course of these experiments, a sufficient supply of asphaltenes treated to remove solids was not available. Although the slopes may be up to 20% less than those for asphaltenes only, the effect of the solvent can still be established.

The slopes of the curves presented in Figure 4.6 are summarized in Table 4.1. Note that Table 4.1 also contains slopes of curves for 12.5/82.5 and 37.5/62.5 heptol solvents. This graphical data was omitted from Figure 4.6 for clarity but also resulted in linear trends. It appears that as the heptane content in the solvent increases, the slope increases in absolute value. Since the slopes of such curves are inversely proportional to the average area occupied by the molecules, Table 4.1 suggests that individual asphaltene molecules occupy an increasingly smaller area on the interface. Initially, this appears to contradict the idea that a more paraffinic solvent (i.e., more heptane in the heptol) would promote a higher degree of self-association among asphaltenes and that a larger molecule should occupy a larger area. However, the results in Table 4.1 simply show that the average area occupied by a given molecule is larger for "better" solvents (less heptane) and that these asphaltenes are better solvated, less densely packed on the interface, and more surface active.

Table 4.1: Slope of interfacial tension versus concentration plots from DVT

	Slope (mN/m)			
Solvent (H/T heptol)	Bitumen 1 Asphaltenes	Bitumen 1 SW Asphaltenes	Bitumen 1 AS	Bitumen 1 SW AS
0/100			-1.01	
12.5/82.5			-1.21	
25/75	-1.71	-1.79	-1.43	-1.66
37.5/62.5			-1.44	
50/50			-1.64	

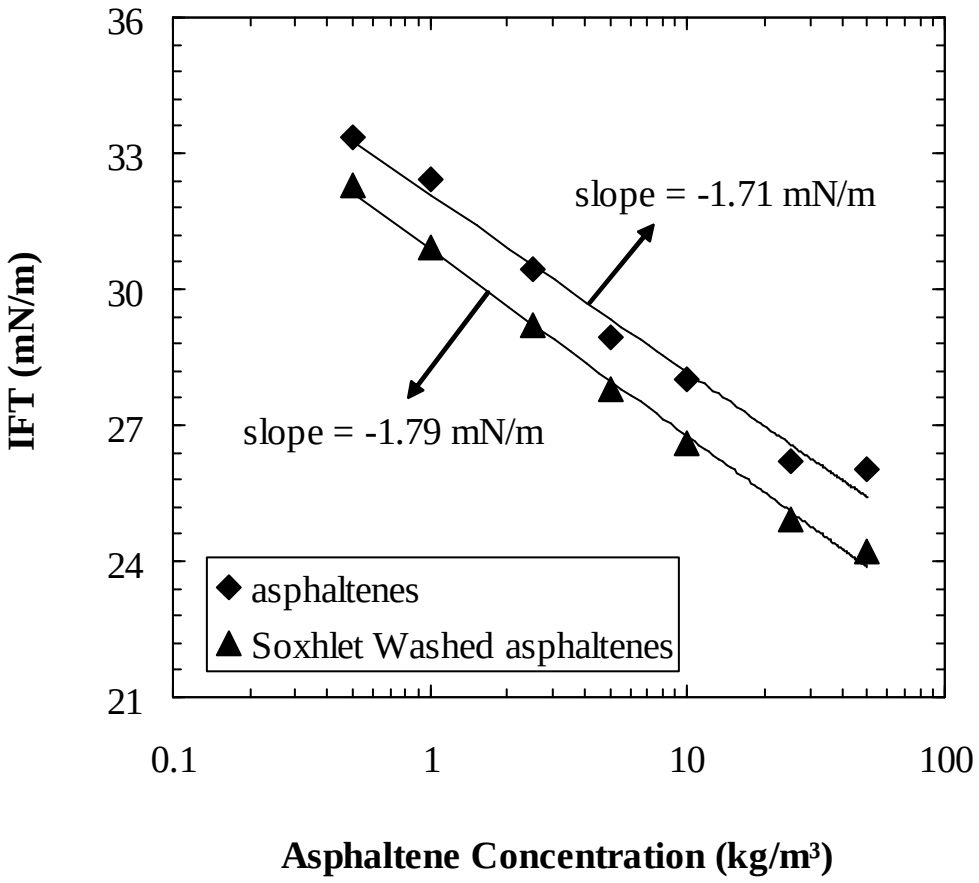

Figure 4.4: Interfacial tension of Athabasca Bitumen 1 Asphaltene- and Soxhlet-Washed Asphaltene-25/75 heptol solutions over water. DVT, 23ºC

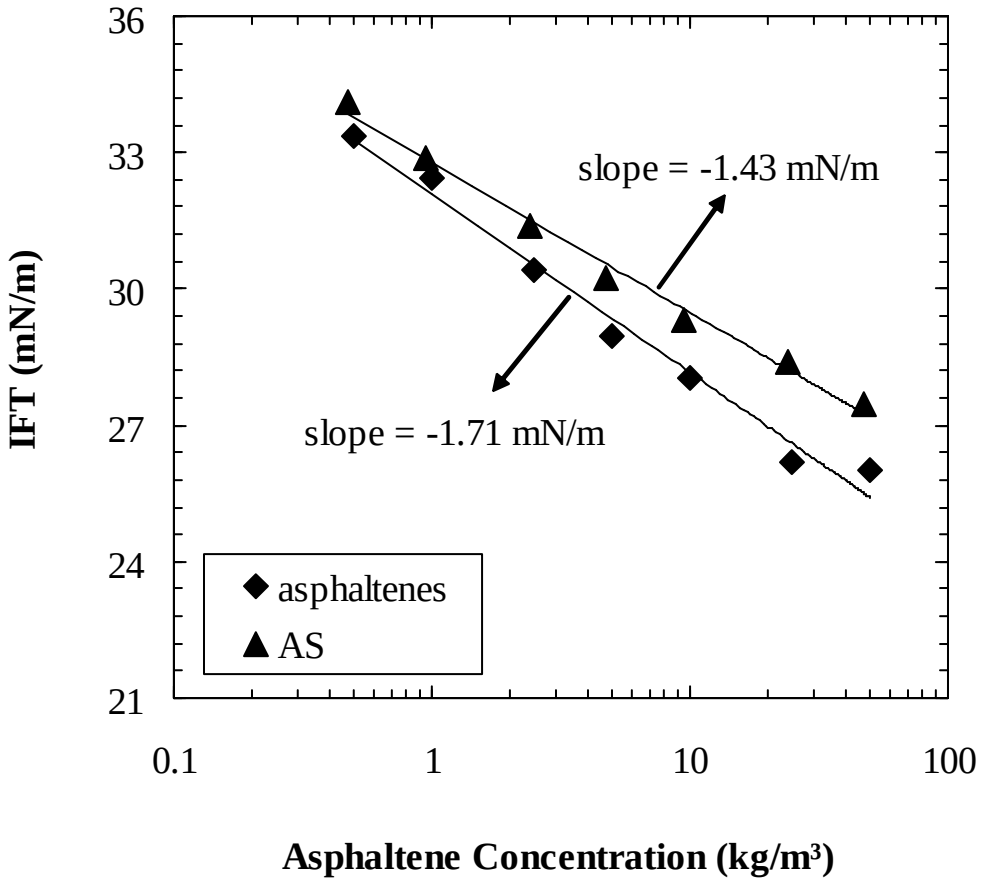

Figure 4.5: Interfacial tension of Athabasca Bitumen 1 Asphaltene- and AS-25/75 heptol solutions over water. DVT, 23ºC

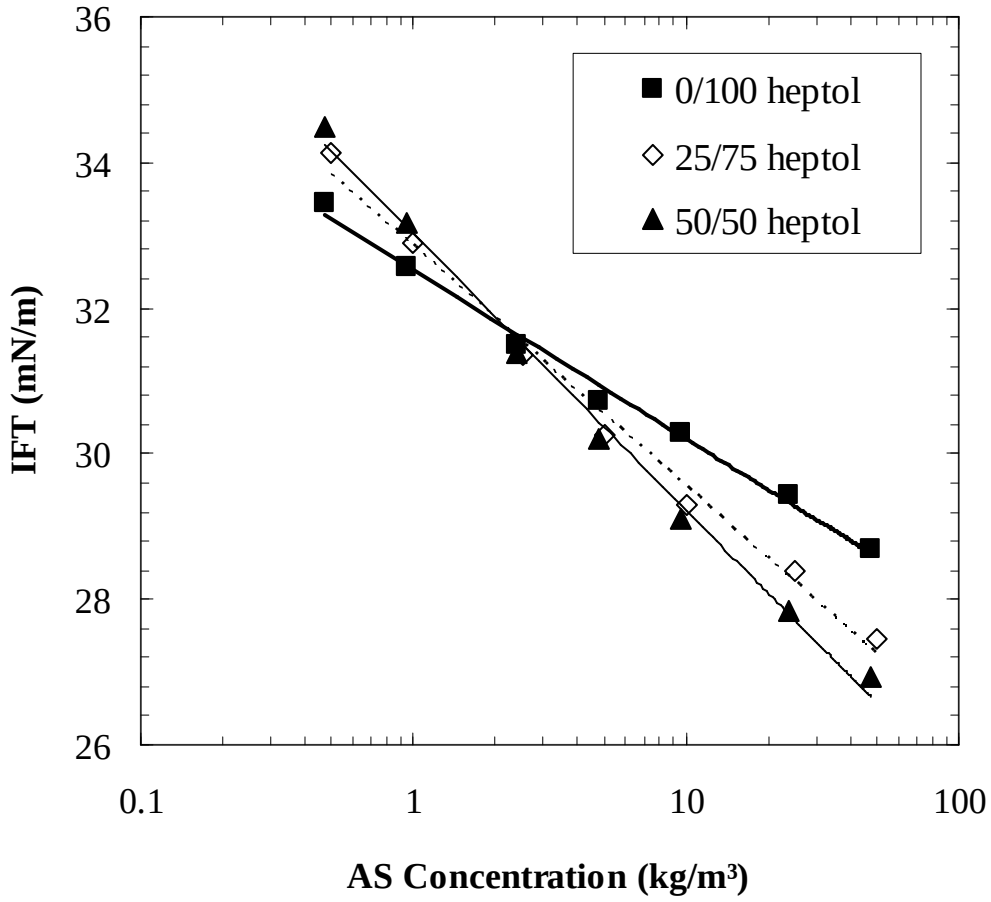

Figure 4.6: Interfacial tension of Athabasca Bitumen 1 AS-heptol solutions over water. DVT, 23ºC

4.2.2 Interfacial Tension Measured with DSA

The interfacial tension of Athabasca Bitumen 2 Asphaltenes in 0/100, 25/75 and 50/50 heptol were measured with the DSA for concentrations varying from 0.001 to 20 or 50 kg/m³. The DSA has been utilized primarily for assessing interfacial rheology; however, it was also used to measure the interfacial tension of asphaltene solutions over water.

Before presenting typical measurements made with the DSA, a comparison is made between the interfacial tension of Athabasca Bitumen 1 and Bitumen 2 Asphaltene solutions over water. The IFT measurement from the DSA is taken at the time that corresponds to the detachment of a drop in the DVT instrument for a given concentration. In this way, the interfacial tensions are compared at the same interface aging time. To reduce the error incurred by solids, asphaltene samples precipitated with *n*-heptane and treated to remove solids were employed for the comparison. Figure 4.7 indicates that the slope of the curve for the Bitumen 2 Asphaltenes is 35% larger than the slope for the Bitumen 1 Asphaltenes. Therefore, Figure 4.7 suggests that the area of a Bitumen 2 molecule is smaller than a Bitumen 1 molecule. This is consistent with the molar mass measurements which showed that the Bitumen 2 Asphaltenes self-associated into smaller molecules.

It was mentioned earlier that the DSA gives interfacial tension versus time for any desired asphaltene concentration. The IFT of Athabasca Bitumen 2 asphaltene in 0/100, 25/75 and 50/50 heptol solutions over water was measured for concentrations varying from 0.001 to 20 kg/m³. The results are too numerous to present here; instead trends in concentration, solvent and time will be presented for typical systems.

Figure 4.8 (a) shows typical IFT curves for Athabasca Bitumen 2 Asphaltenes in 0/100 heptol at several concentrations for times up to ten minutes. The behaviour is similar to that of surfactants: the interfacial tension decays and appears to stabilize at a constant value, at least for the higher concentrations. However, it has been shown that the IFT can

continue to decrease for several hours or even days (Freer and Radke, 2004; Bauget *et al.*, 2001). This is confirmed in Figure 4.8 (b) which shows a substantial decrease in IFT for times exceeding 10 minutes. The decrease is most pronounced at low and intermediate asphaltene concentrations.

The results shown in Figure 4.8 and additional IFTs at higher aging times are summarized in Figure 4.9 by showing the interfacial tension as a function of concentration at 60 seconds, 10 minutes, 1 hour and 4 hours. Although there is scatter, especially at four hours, the results demonstrate the capacity of asphaltenes to lower interfacial tension over long periods of time. It is also interesting to note that for concentrations exceeding roughly 0.01 kg/m^3, the IFT curves at any given time are approximately parallel. If a Gibbs' adsorption is assumed, this suggests that asphaltenes occupy the same area on the interface as the interface ages.

Results similar to those shown in Figure 4.9 were observed for 25/75 and 50/50 heptol solvents. The effect of solvent quality is shown in Figure 4.10 after 10 minutes of interface aging. The trends were similar at shorter and at longer interface aging times. The lack of deviation between the curves at asphaltene concentrations exceeding about 0.1 kg/m^3 suggests that at these concentrations, the interface is dominated by asphaltenes and the solvent that does reside on the interface varies little between the three systems. Perhaps toluene adsorbs preferentially over heptane and hence the IFT measured at a given concentration for any solvent quality is the same. Also, at high concentrations, the interface is dominated by asphaltenes.

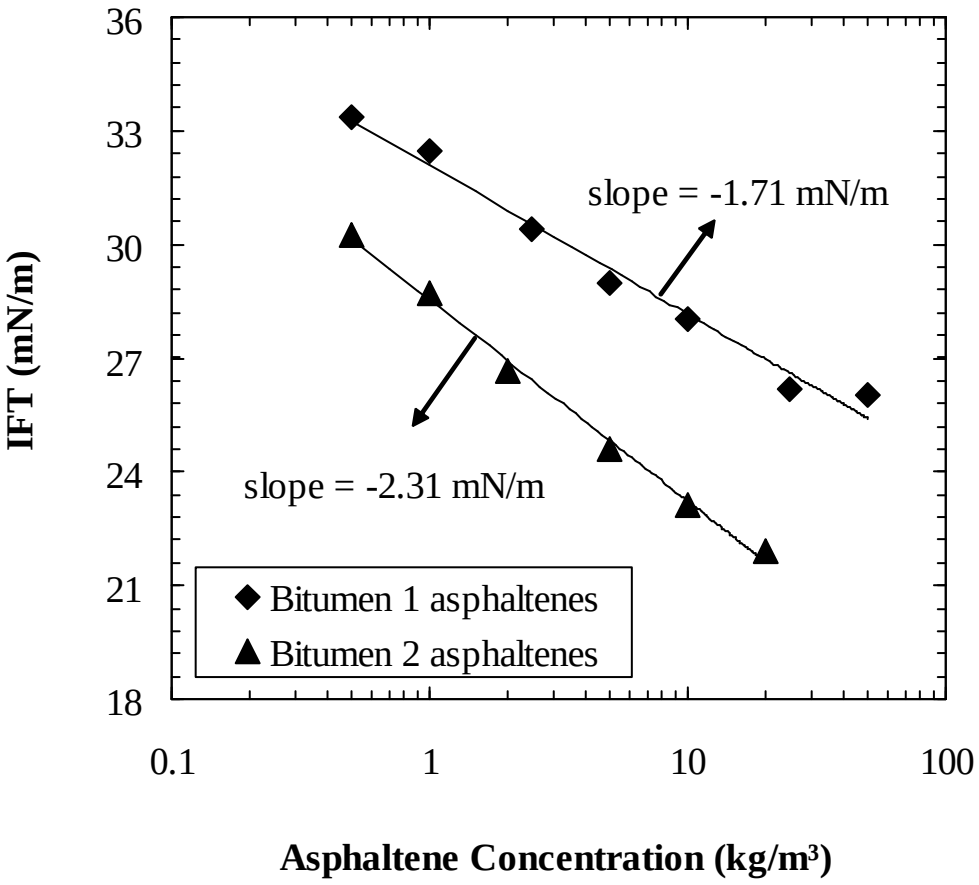

Figure 4.7: Interfacial tension of Athabasca Bitumen 1 and Bitumen 2 Asphaltene-25/75 heptol solutions over water. DSA, 23ºC

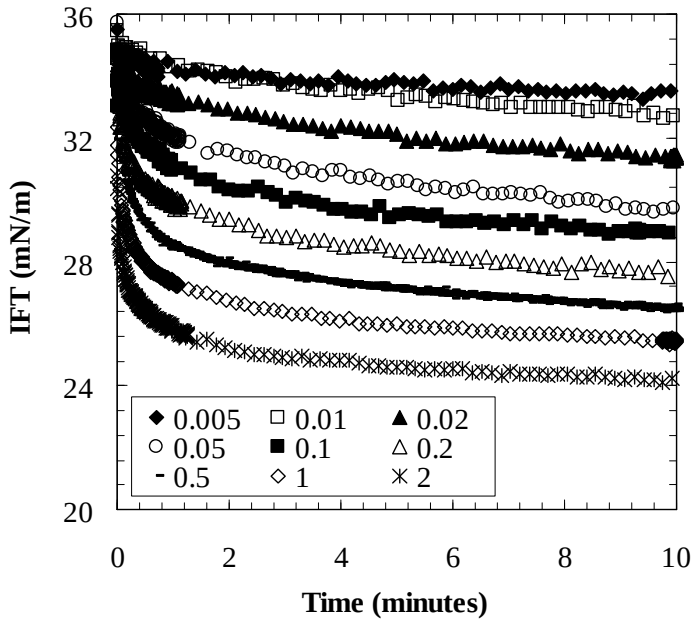

(a)

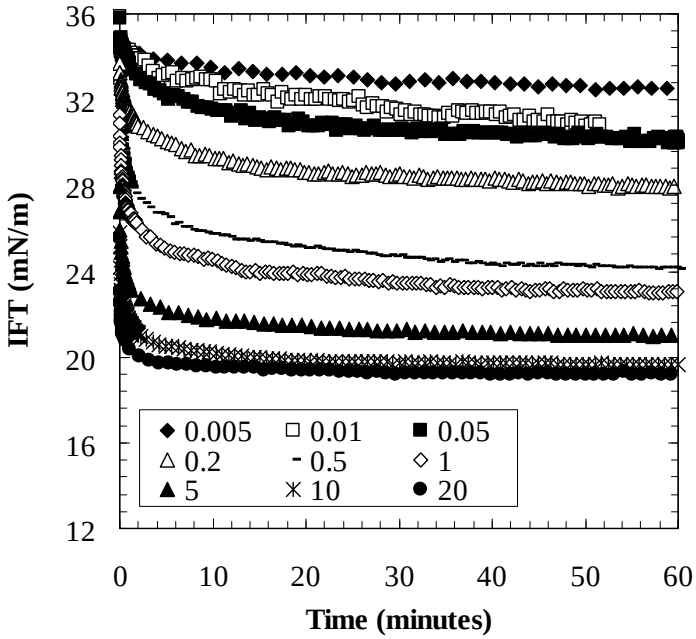

(b)

Figure 4.8: Interfacial tension of Athabasca Bitumen 2 Asphaltenes-0/100 heptol solutions over water. The concentrations are in kg/m³. DSA, 23ºC

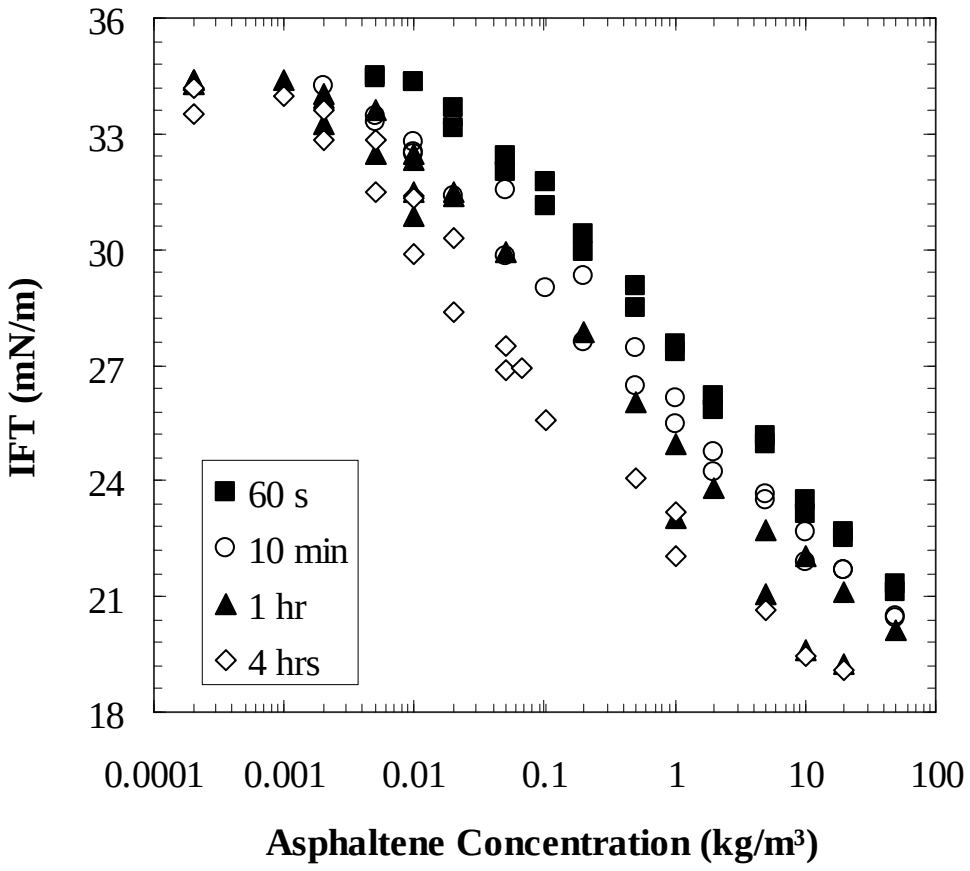

Figure 4.9: Interfacial tension of Athabasca Bitumen 2 Asphaltenes-0/100 heptol solutions over water. DSA, 23ºC

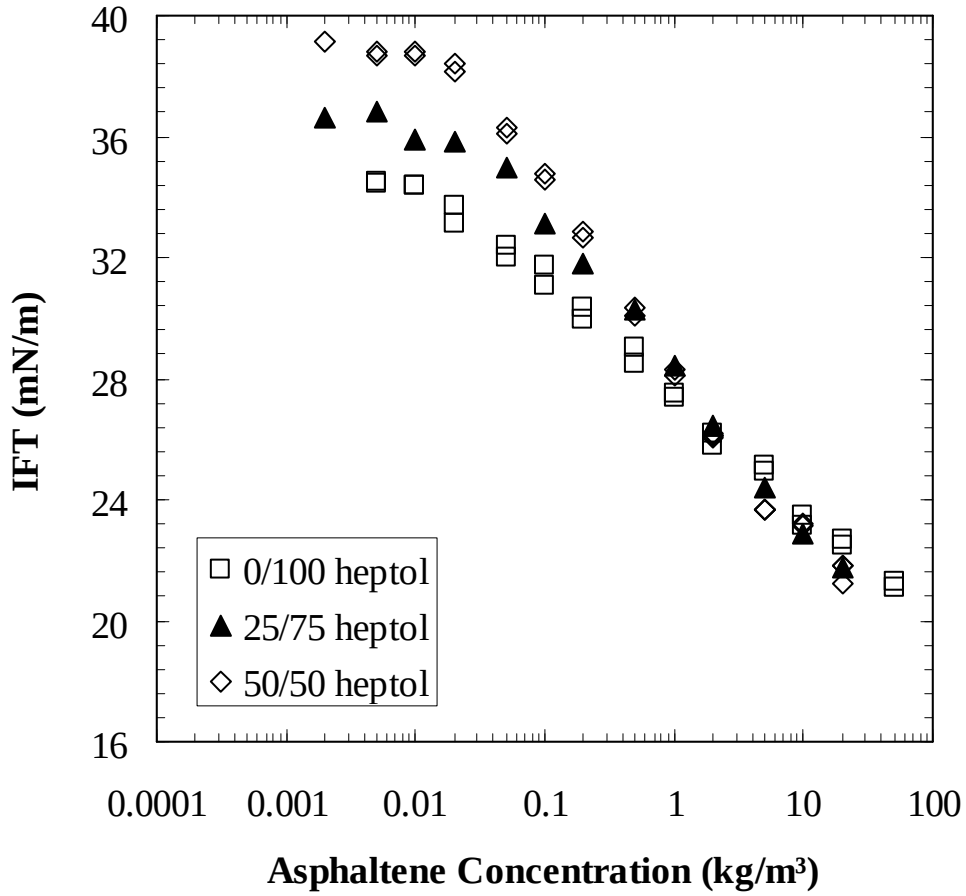

Figure 4.10: Interfacial tension of Athabasca Bitumen 2 Asphaltenes-heptol solutions over water after interface has been aged for 10 minutes. DSA, 23ºC

4.3 ASPHALTENE ADSORPTION ISOTHERMS

Asphaltene adsorption isotherms are used to relate the asphaltene mass surface coverage at the water/hydrocarbon interface to the asphaltene equilibrium concentration of a settled emulsion. They are constructed by applying Equation (3.20) at asphaltene concentrations varying from 1 to 40 kg/m³:

$$\Gamma_A = \frac{m_{AT} d_{32}}{6 V_w}\left(1 - \frac{C_A^{eq}}{C_A^{o}}\right) \tag{3.20}$$

Recall that Γ_A is the asphaltene mass surface coverage, C_A^{eq} and C_A^{o} are the asphaltene equilibrium and bulk concentrations, m_{AT} is the total mass of asphaltenes, V_w is the total volume of water, and d_{32} is the Sauter mean diameter of the dispersed water droplets. The total mass of asphaltenes, their initial concentration, and the volume of water are experimentally controlled variables. The equilibrium concentration is found from a gravimetric analysis of the continuous phase. The Sauter mean diameter is obtained by analyzing the size distribution of the settled drops. The trends in Sauter mean diameter are presented in more detail in the following section because this variable is required not only in equation (3.20) but also important when discussing relative emulsion stability and the effects of film aging on the mass of asphaltenes adsorbed on the interface and the emulsion stability. The effect of film aging on the Sauter mean diameter and the relative emulsion stability is discussed in Chapter 6.

4.3.1 Water Drop Size Distributions of Settled Emulsions

In most of this work, drop size distributions were gathered after a model emulsion had been settled for 1.5 hours. However, the distribution can be gathered at any time as long as free water does not appear during the settling time. In this study, emulsions were aged (i.e., left to settle) up to 24 hours. However, no free water was ever observed during the settling time. The current section presents the drop size distributions and calculated

Sauter mean diameter for emulsions that were aged for 1.5 hours and were stabilized solely by Asphaltenes or AS.

The sample micrographs shown previously in Figure 3.7 indicated that the size of drops decreases with an increase in asphaltene concentration. The droplets also become more uniform in size, as is shown in the frequency histogram of Figure 4.11 for the systems in Figure 3.7. These trends with asphaltene concentration were observed for all heptol contents and all types of asphaltenes. The Sauter mean diameter was assessed at each asphaltene concentration using Equation (3.19).

Figure 4.12 summarizes the Sauter mean diameter at various asphaltene concentrations for emulsions stabilized by Athabasca Bitumen 1 Asphaltenes in 25/75 heptol. At concentrations below approximately 2 kg/m^3, the average diameter is very large because there are insufficient asphaltenes to cover the interface (Yarranton *et al.*, 2000a). Consequently, some of the droplets coalesce immediately following their creation, resulting in a diameter greater than the minimum that can be achieved with the homogenizer at the conditions described in Section 3.4.2. However, as the asphaltene concentration increases, there are sufficient asphaltenes to cover the interface of the drops and the resultant diameter is the minimum that can be created with the homogenizer. Figure 4.12 indicates that the minimum diameter is approximately 8 microns and that it is achieved at a concentration exceeding 10 kg/m^3.

Figure 4.12 also shows other systems and several additional conclusions can be made. First, the presence of solids does not appear to alter the average diameter of the drops since the Asphaltene and AS curves are identical. Chapter 7 will show that native solids found in the AS precipitate do in fact adsorb on the interface (as was already implied by the results of the interfacial tension data in Section 4.2.1); however, it appears that their presence on the interface does not change the average water droplet size.

Second, ultrafine solids also do not alter the drop size, since the diameters for the Asphaltene and Asphaltene-free-of-Ultrafine-Solids emulsions are also identical. Third, asphaltenes containing fewer resinous molecules (i.e., Soxhlet-Washed Asphaltenes) lead to the formation of emulsions containing smaller drops than those stabilized by more "resinous" asphaltenes (i.e., C_5 asphaltenes) at concentrations below 10 kg/m³. Also, the limiting diameter of 8 microns is achieved at 2 kg/m³ for Soxhlet-Washed Asphaltenes, 10 kg/m³ for Asphaltenes, and 20 kg/m³ for C_5 Asphaltenes.

Figure 4.12 suggests that asphaltenes containing fewer resinous materials resist coalescence more. This is consistent with the work of Gafonova (2000) who showed that settled emulsions stabilized by asphaltenes contained smaller drops than those stabilized by mixtures of asphaltenes and resins. The emulsions containing resins were also less stable than those containing asphaltenes alone. As will be seen in Chapter 7, the free water resolution was higher for the C_5 Asphaltene stabilized emulsions than for Asphaltene stabilized emulsions. The Soxhlet-Washed Asphaltene stabilized emulsions were the most stable and experienced minimal free water resolution even at very long treatment times.

The Sauter mean diameters for emulsions stabilized by Athabasca Bitumen 1 and 2 Asphaltenes are compared in Figure 4.13. It appears that the limiting diameter of 8 microns was not achieved for either the Bitumen 2 Asphaltenes or AS, which is consistent with the idea that these are more resinous, smaller asphaltenes perhaps incapable of preventing some coalescence during the 1.5 hours settling period. However, the difference is not great and the water drop sizes of emulsions stabilized by the two Athabasca bitumen samples appear to be similar.

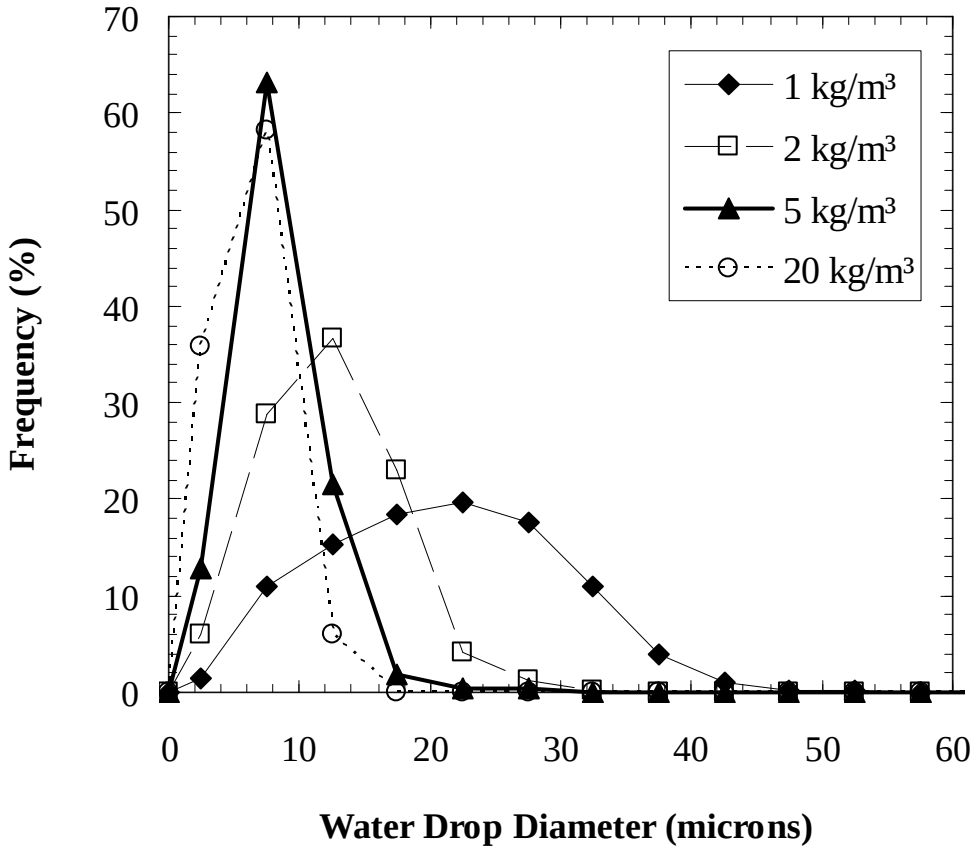

Figure 4.11: Water drop size distributions of settled emulsions stabilized by Athabasca Bitumen 1 Asphaltenes at bulk concentrations of 1 kg/m³, 2 kg/m³, 5 kg/m³, 20 kg/m³. 25/75 heptol, 40 vol% water, 1.5 hours settling

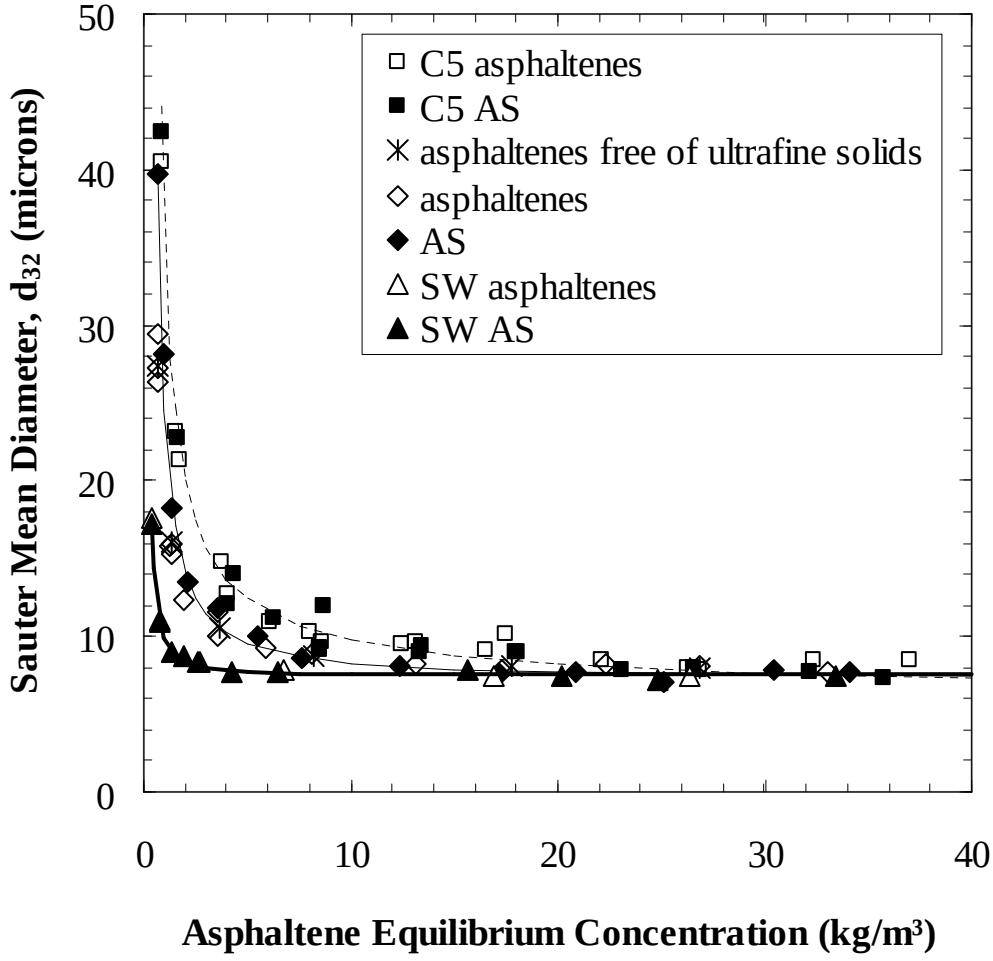

Figure 4.12: Sauter mean diameter of settled emulsions stabilized by Athabasca Bitumen 1 Asphaltenes and AS. 25/75 heptol, 40 vol% water, 1.5 hours settling. The lines are visual aides

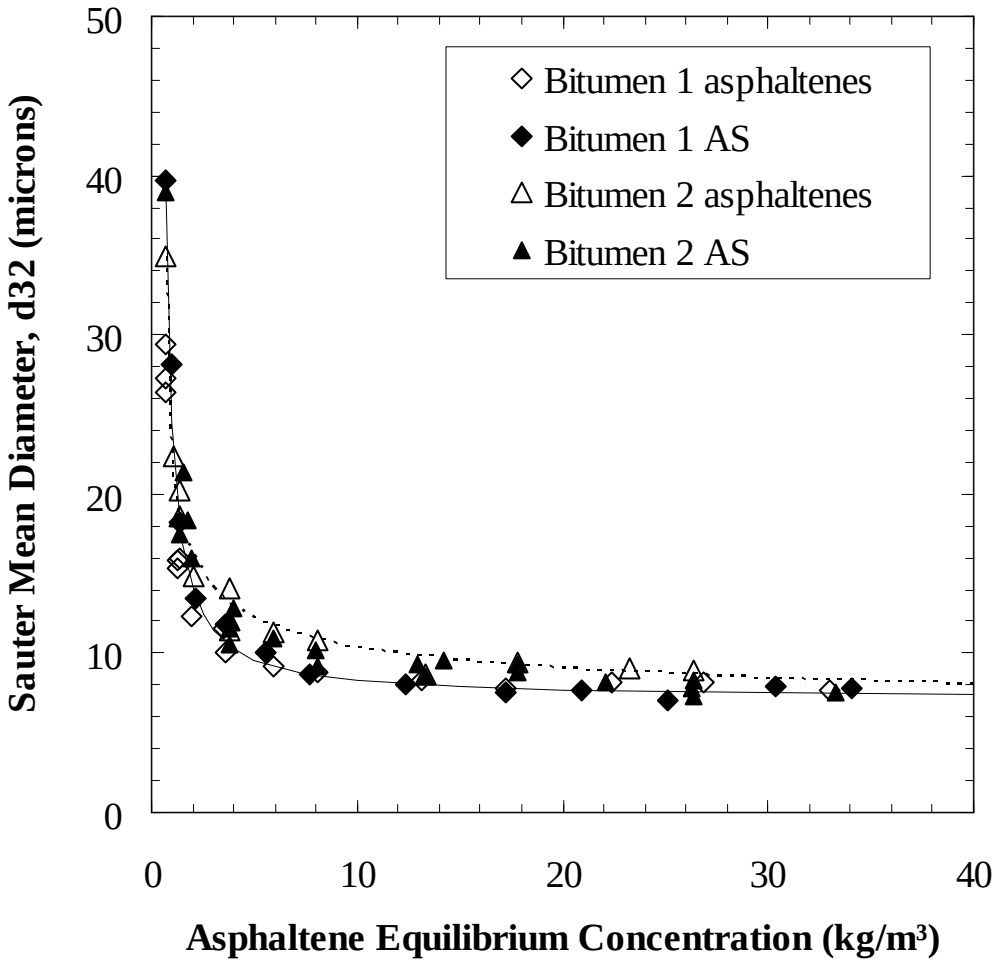

Figure 4.13: Sauter mean diameter of settled emulsions stabilized by Athabasca Bitumen 1 and 2 Asphaltenes and AS. 25/75 heptol, 40 vol% water, 1.5 hours settling. The lines are visual aides

The preceding conclusions regarding the effects of asphaltene extraction procedures and the source bitumen were made based on the results of emulsions with a continuous phase composed of 25/75 heptol. In order to assess the importance of solvent quality on the asphaltene adsorption isotherm, the droplet diameter at each solvent composition is also required. The effect of the solvent quality on the measured Sauter mean diameter of settled emulsions stabilized by Athabasca Bitumen 2 Asphaltenes is shown in Figure 4.14. The average drop size decreases as the heptane fraction in the solvent increases. In a poor solvent such as 50/50 heptol, the asphaltenes are less solvated and occupy a smaller area on the interface, as suggested by the interfacial tension studies. However, they are more densely packed. The resultant film is likely stronger and resists coalescence more, a speculation that will be assessed later in Chapter 6.

4.3.2 Asphaltene Mass Surface Coverage

Equation (3.20) was applied at asphaltene concentrations varying from 1 to 40 kg/m³. The asphaltene adsorption isotherm for Athabasca Bitumen 1 Asphaltenes in a water-in-25/75 heptol emulsion is given in Figure 4.15. The data indicates that the mass of asphaltenes per area increases as the asphaltene concentration in the continuous phase increases. At an equilibrium concentration of approximately 35 kg/m³, the asphaltene surface coverage is just under 0.01 g/m². Previous work (Gafonova and Yarranton, 2001) with 50/50 heptol emulsions demonstrated that, above an equilibrium concentration of 2 kg/m^3, the asphaltene surface coverage followed that of a Langmuir adsorption isotherm. In the current work, it is difficult to assess if the asphaltene surface coverage levels off at a constant value after some equilibrium concentration is reached. Possibly, measurement errors occur above 30 kg/m³ because the concentrated emulsion does not settle effectively and a small fraction of water droplets remains in the continuous phase. In contrast, the settling was effective at all concentrations for the 50/50 heptol emulsions because the density difference between the water and hydrocarbon phases was more pronounced.

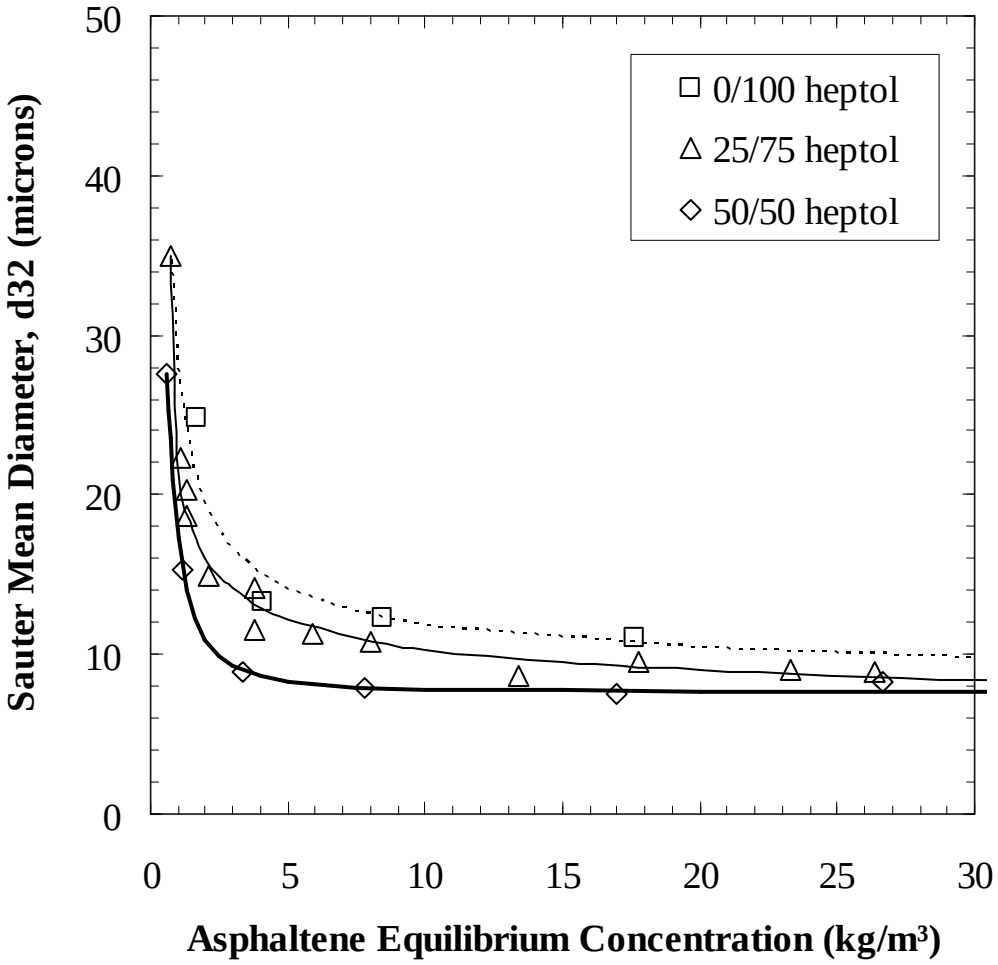

Figure 4.14: Sauter mean diameter of settled emulsions stabilized by Athabasca Bitumen 2 Asphaltenes for 0/100, 25/75 and 50/50 heptol, 40 vol% water, 1.5 hours settling. The lines are visual aides

Figure 4.15 also shows the adsorption isotherm for a 25/75 heptol, 40 vol% water emulsion when C_5 Asphaltenes and Soxhlet-Washed Asphaltenes are the stabilizers. The adsorption isotherms indicate that as the degree of washing increases, the mass of asphaltenes adsorbed per area of the interface also increases. The increase in the mass surface coverage is significant from the C_5 Asphaltenes to the Asphaltenes at high concentrations. However, the mass surface coverage for Asphaltenes and Soxhlet-Washed Asphaltenes is similar, suggesting perhaps that the largest Soxhlet-Washed Asphaltene molecules do not adsorb on the interface. This speculation is discussed in Section 4.3.

Figure 4.16 compares the adsorption isotherm of Athabasca Bitumen 1 and 2 Asphaltenes for a 25/75 heptol, 40 vol% emulsion. For equilibrium concentrations exceeding 25 kg/m³, the mass surface coverage is slightly smaller for the Bitumen 2 Asphaltenes. A smaller mass surface coverage is consistent with the previous observations from vapour pressure osmometry and interfacial tensiometry which indicated that Athabasca Bitumen 2 Asphaltenes are smaller molecules and adsorb with a slightly smaller area on the interface than do Athabasca Bitumen 1 Asphaltenes. However, the differences may also result from the greater experimental error at the high concentrations due to incomplete settling. At concentrations below 25 kg/m³, the surface coverages for the two asphaltenes are within 20% of each other.

The effect of the solvent on the asphaltene adsorption isotherm was found to be marginal for a settling time of 1.5 hours. Figure 4.17 demonstrates that the mass of Bitumen 2 Asphaltenes per area does not vary significantly with solvent.

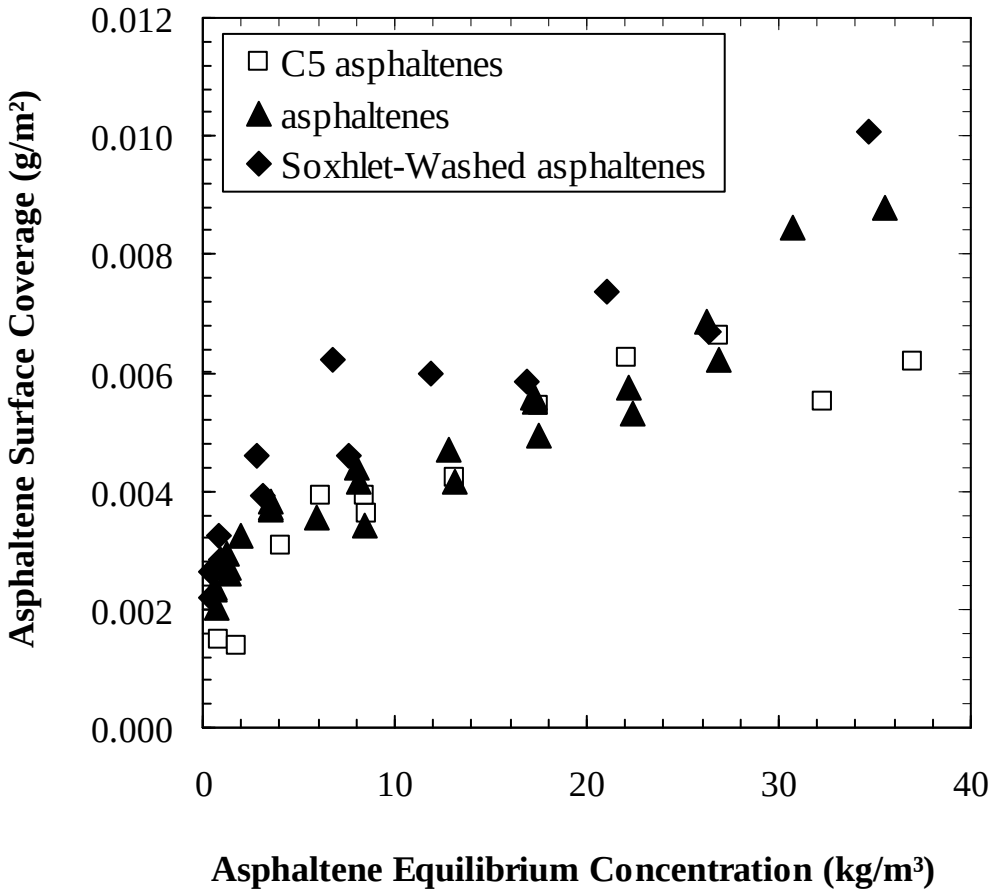

Figure 4.15: Adsorption isotherms of Athabasca Bitumen 1 C_5 Asphaltenes, Asphaltenes and Soxhlet-Washed Asphaltenes in water-in-25/75 heptol emulsions. 40 vol% water, 1.5 hours settling

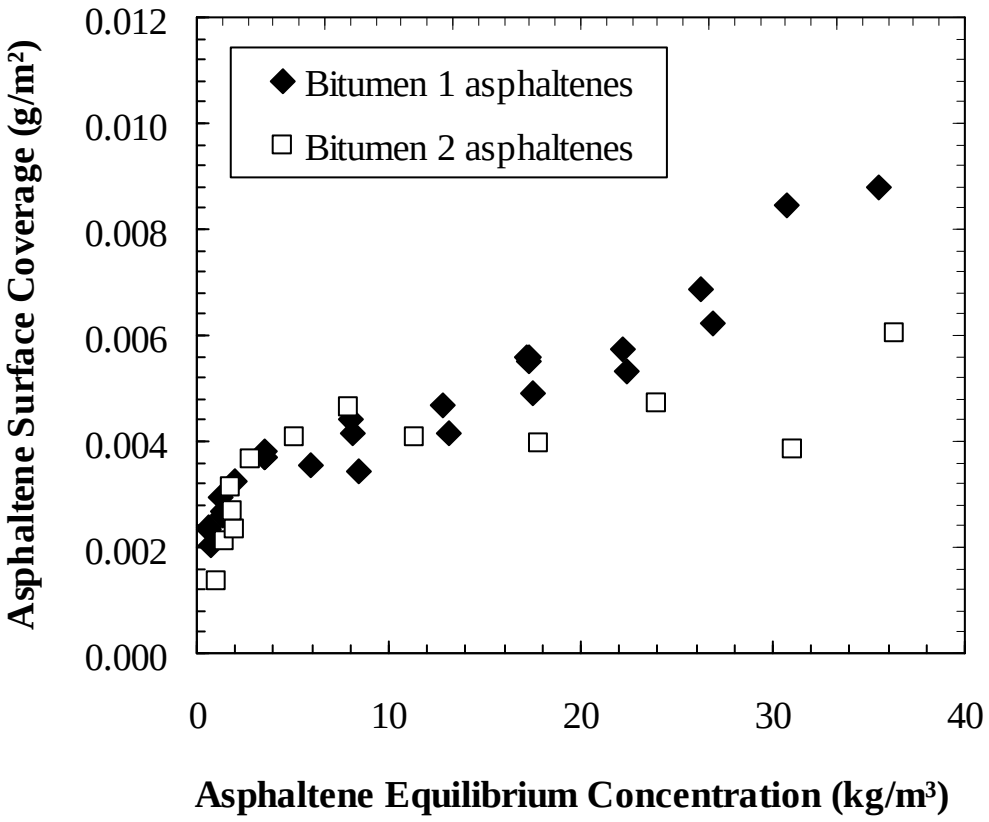

Figure 4.16: Adsorption isotherms of Athabasca Bitumen 1 and 2 Asphaltenes in water-in-25/75 heptol emulsions. 40 vol% water, 1.5 hours settling

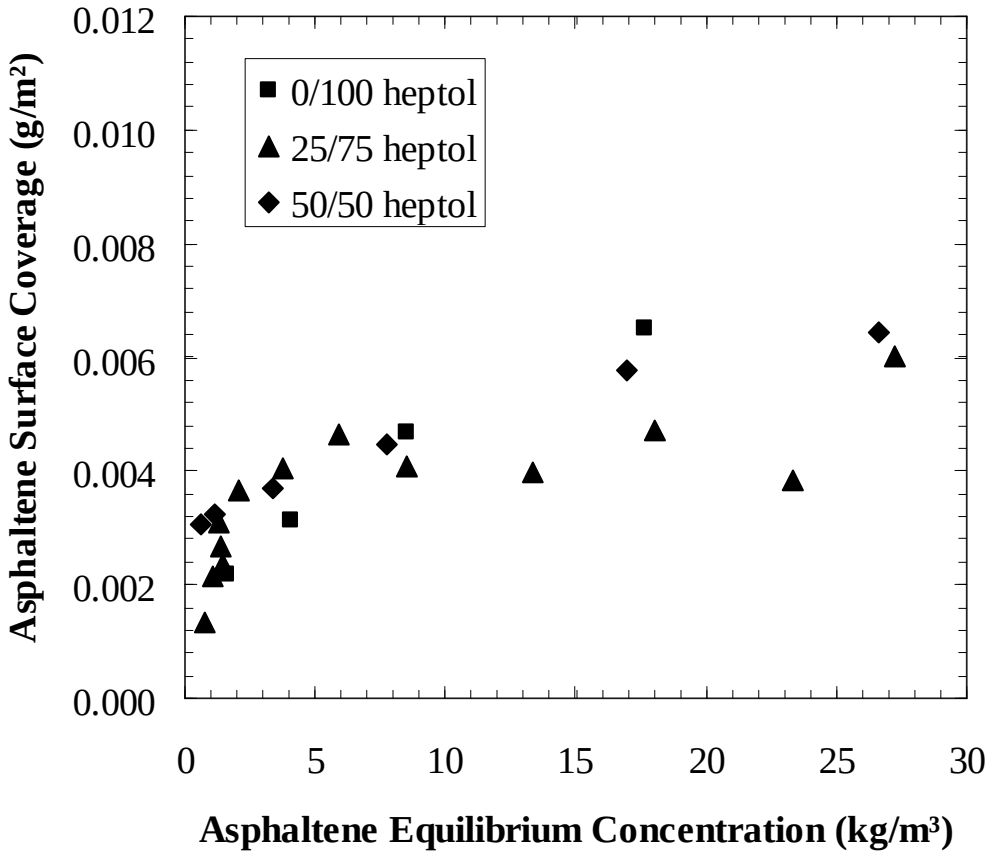

Figure 4.17: Adsorption isotherms of Athabasca Bitumen 2 Asphaltenes in water-in-0/100, 25/75, and 50/50 heptol emulsions. 40 vol% water, 1.5 hours settling

4.4 ASPHALTENE INTERFACIAL CONFIGURATION

The configuration of asphaltenes at the water/oil interface can be examined in part by calculating the number of layers adsorbed at that interface. The number of adsorbed asphaltene layers is the ratio of the total number of adsorbed molecules to the number of molecules in a monolayer. Both the total number of adsorbed molecules and the number of molecules can be determined on a per area basis. The total number of molecules/area of the interfacial film (Γ_t) is the mass of asphaltenes on the interface divided by the mass of a single asphaltene molecule (or molecular aggregate if the asphaltenes have self-associated):

$$\Gamma_t = \frac{\Gamma N_A}{M} \tag{4.1}$$

Γ is the mass surface coverage of asphaltenes on the interface, M is molar mass of an asphaltene molecular aggregate, and N_A is Avogadro's number. The number of molecules per area in a monolayer (Γ^m) is simply the inverse of the cross sectional area of an asphaltene molecule on the interface (A):

$$\Gamma^m = \frac{1}{A} \tag{4.2}$$

The cross sectional area of an asphaltene molecule on the interface can also be determined experimentally using the interfacial tension data from Section 4.2. As long as the molecular packing (interfacial density) does not vary from layer to layer, the number of asphaltene layers adsorbed at the water/oil interface is the ratio of equations (4.1) to (4.2):

$$n = \frac{\Gamma A N_A}{M} \tag{4.3}$$

where n is the number of layers of asphaltenes on the interface.

The interpretation of the interfacial structure will be demonstrated with 25/75 heptol, 40 vol% water emulsions stabilized by either Athabasca Bitumen 1 Asphaltenes or Soxhlet-Washed Asphaltenes. The associated molar masses of these asphaltenes were shown as a function of concentration in Figure 4.1. The asphaltene surface coverage was determined in Section 4.3.2. It remains to determine the area of a molecule on the interface.

4.4.1 Average Molecular Area of Asphaltenes

Interfacial tension measurements can be used to prepare a plot of interfacial tension versus the logarithm of asphaltene concentration as was shown in Figures 4.4 to 4.7. These plots can be used to determine the average area of a molecule adsorbing at the water/hydrocarbon interface. For an ideal mixture of surfactant in a solvent or for mixed surfactant systems as described by Campanelli and Wang (1999), the area is given by Gibbs' isotherm as:

$$A = -\frac{1}{N_A}\frac{RT}{\left(d\gamma/d\ln C\right)} \tag{4.4}$$

where A is the average area per molecule at the interface, N_A is Avagadro's number, R is the universal gas constant, T the absolute temperature, γ the interfacial tension, and C the concentration of surface-active materials. The slope of an IFT versus concentration plot can be used to find the slope required in Equation (4.4). However, the theoretically correct form of concentration is molar concentration although the mass concentration is often used in practice. The distinction between mass and molar concentration becomes important when considering a self-associating material such as asphaltenes. The molar mass measurements in Section 4.1 indicate that self-association is dramatic, particularly for Soxhlet-Washed Asphaltenes.

In order to demonstrate the importance of asphaltene self-association for the interpretation of molecular area, the interfacial tension of asphaltenes in 25/75 heptol

solutions over water are replotted versus both molar and mass concentrations, as demonstrated in Figure 4.18. When a mass concentration plot is employed, the area as calculated from Equation (4.4) is 2.38 nm^2. This area is within the range typically observed for asphaltenes using mass concentration plots. Rogel *et al.* (2000) observed the average interfacial area of asphaltenes in several solvent/water systems to vary from 1 to 4 nm^2. Mohamed *et al.* (1999) obtained similar results with average interfacial area of asphaltenes in solvent/water systems varying from 1.8 to 4.9 nm^2. Sheu (1996) measured an asphaltene interfacial area of 4.5 nm^2 at a pyridine/water interface, while Bhardwaj and Hartland (1994) measured the area at a toluene/water interface to be 2.53 nm^2. Ese *et al.* (1999) calculated the area of an asphaltene molecule at a 2% toluene-98% decane/water interface from surface pressure-area isotherms to be 0.65 nm^2. Although the uncorrected area measured in this work is within the range observed by other researchers, the theoretically valid form of Equation (4.4) employs molar concentration. Utilization of molar concentrations in Equation (4.4) yields an area of 1.55 nm^2, 35% lower than the mass-concentration-based value. The value of 1.55 nm^2 is the correct calculation of area and should be employed in the calculation of the number of layers (Equation 4.3). Note that, an analysis of the Athabasca Bitumen 2 DSA data in this manner results in a molar concentration based area of 1.34 nm^2.

4.4.2 Configuration of Asphaltenes on the Interface

Equation (4.3) has been employed over a wide asphaltene concentration range and the results are shown in Figure 4.19 for Athabasca Bitumen 1 Asphaltenes for a 25/75 heptol solvent. For comparison, results are also shown for calculations made with a constant asphaltene monomer molar mass of 2060 g/mol over the entire concentration range. The "uncorrected" curve also uses the mass concentration based area (i.e., 2.38 nm^2).

Figure 4.19 illustrates the importance of asphaltene self-association when assessing the configuration of asphaltenes at the interface. When a constant molar mass is employed at all asphaltene concentrations, adsorption at the interface appears to occur in a multilayer

fashion with approximately six asphaltene layers adsorbed at concentrations of 40 kg/m^3. However, once self-association in the form of adjusted molar mass data is taken into account, the results indicate monolayer adsorption, even at concentrations as high as 40 kg/m^3. The fact that the number of layers is slightly less than unity at some of the concentrations is likely due to experimental errors in the gravimetric experiments and possibly errors in the molar mass. Molar mass errors directly affect Equation (4.4) and indirectly affect the area determined from IFT analysis.

The configuration of asphaltenes on the interface appears to be a monolayer over the entire range of concentration examined here. An analysis of the Athabasca Bitumen 2 data also resulted in the conclusion that asphaltenes adsorb as a monolayer. Nordli *et al.* (1991) also observed evidence of monolayer formation by the surface-active fractions of crude oil at air/water interfaces.

Although the asphaltenes self-associate into macromolecules as concentration increases, the area of the molecules on the interface does not change. Hence, aggregates appear to extend more into the continuous phase than monomers and a thicker interfacial layer is formed. Assuming a cylindrical shape for adsorbed asphaltene molecules and an asphaltene density of 1181 kg/m³ (Alboudwarej *et al.*, 2002), the thickness of the monolayer ranges from 2 to 9 nm over a concentration range of 1 to 40 kg/m³, as illustrated in Figure 4.20. In a recent study of water/Athabasca-asphaltene-toluene/water thin liquid films, Taylor *et al.* (2002) employed the thin liquid film-pressure balance technique to measure the thickness of asphaltene films. They found that at a bilayer thickness of 8.5 nm (corresponding to a 4.3 nm monolayer), the asphaltene film could no longer be compressed upon the addition of further pressure. The monolayer thickness of 2 to 9 nm found in the current work is of the same order of magnitude as the monolayer thickness of 4.3 nm from their study.

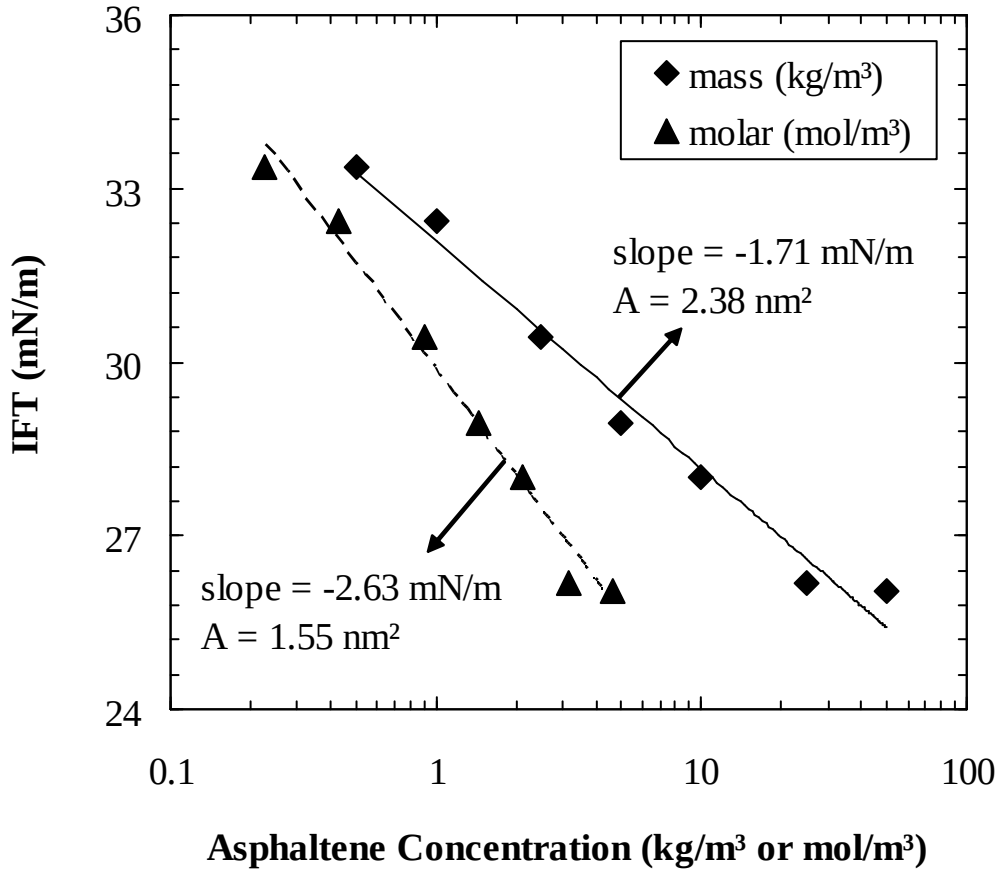

Figure 4.18: Interfacial tension of Asphaltene-25/75 heptol solutions over water plotted on mass and molar concentration bases. Athabasca Bitumen 1 Asphaltenes, DVT, 23ºC

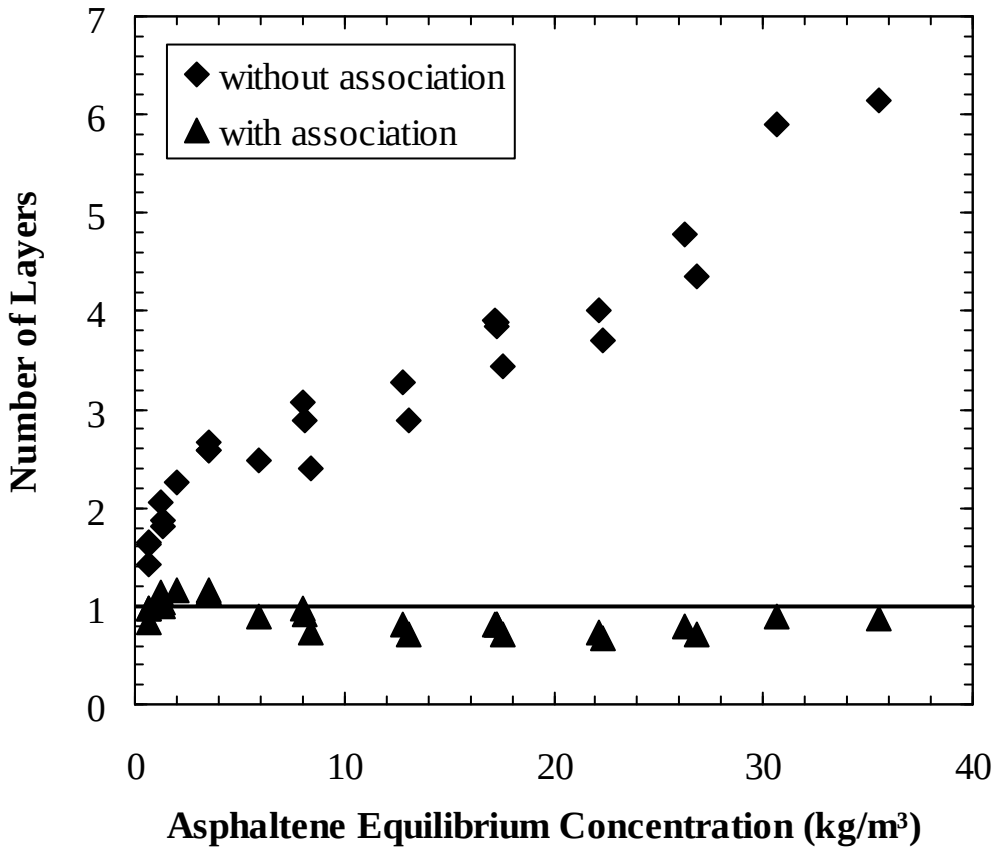

Figure 4.19: Number of layers of adsorbed Athabasca Bitumen 1 Asphaltenes. 25/75 heptol, 40 vol% water, 1.5 hours settling

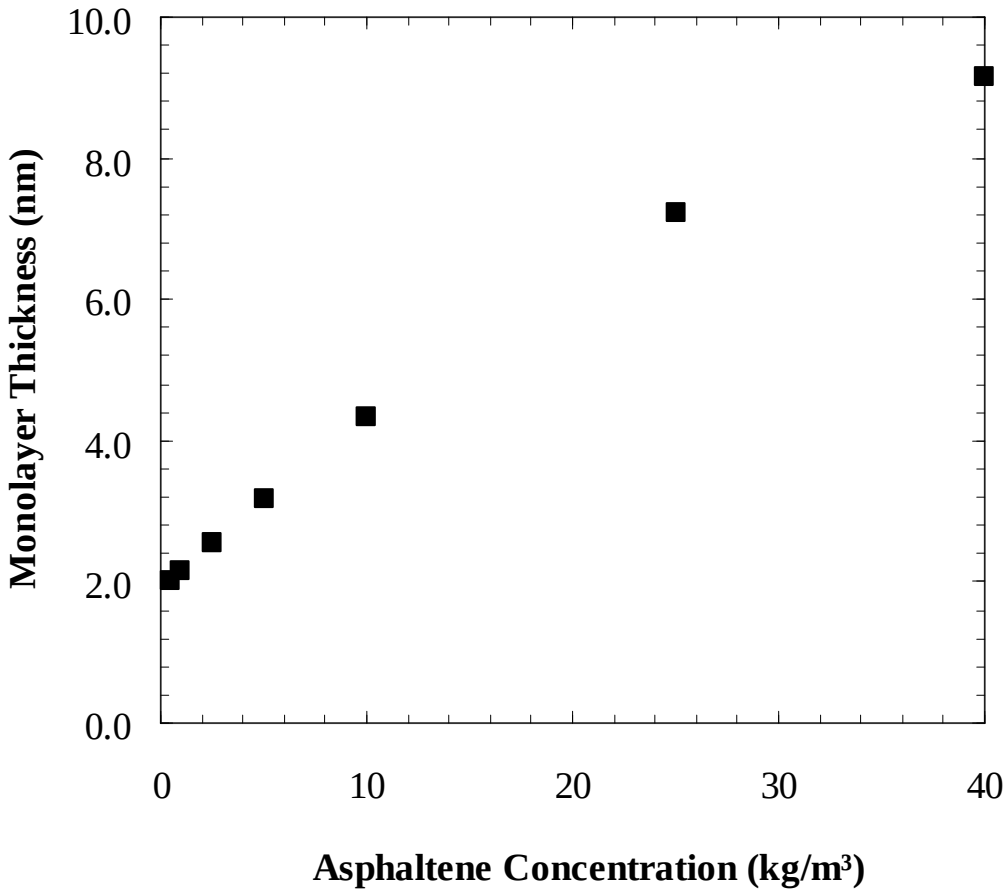

Figure 4.20: Monolayer thickness of Athabasca Bitumen 1 Asphaltenes. 25/75 heptol, 40 vol% water, 1.5 hours settling

4.4.3 Configuration of Soxhlet-Washed Asphaltenes on the Interface

The procedure used to account for asphaltene self-association has also been applied for Soxhlet-Washed Asphaltenes. The interfacial tension of Soxhlet-Washed Asphaltenes in 25/75 heptol over water is shown in Figure 4.21. As for the Asphaltenes, there is no indication of micellization and the linearity in the plot implies asphaltenes adsorb with a constant area over the concentration range tested. The average interfacial area of an asphaltene molecule is 2.27 nm^2 based on mass concentration and 1.26 nm^2 based on the molar concentration calculated from the Soxhlet-Washed Asphaltene molar masses presented in Figure 4.1. The area of 1.26 nm^2 for the Soxhlet-Washed Asphaltenes is smaller than the area of 1.55 nm^2 determined for Asphaltenes. This is a potential inconsistency since the Soxhlet-Washed Asphaltenes are larger than the Asphaltenes and are not expected to have a smaller interfacial area. This inconsistency will be addressed later in this section.

The results of Equation (4.3) applied to the Soxhlet-Washed Asphaltenes are shown in Figure 4.22. The “constant molar mass” curve utilizes a constant molar mass of 2850 g/mol and a mass-basis area of 2.27 nm^2. Recall that the Soxhlet-Washed Asphaltene monomer molar mass of 2850 g/mol was obtained in the same manner as that for the Asphaltenes. If self-association is not taken into account, the calculation from Equation (4.3) seems to suggest multilayer adsorption.

Following the same procedure used for the Asphaltene analysis, Soxhlet-Washed Asphaltene molar mass data was incorporated into Equation (4.3). The results, shown in Figure 4.22 (“Soxhlet-Washed molar mass”) indicate less than monolayer coverage. This outcome is not surprising since the adsorption isotherm and corrected average molecular area for Soxhlet-Washed Asphaltenes are very similar to those of the Asphaltenes, yet a molar mass double that of Asphaltenes has been used.

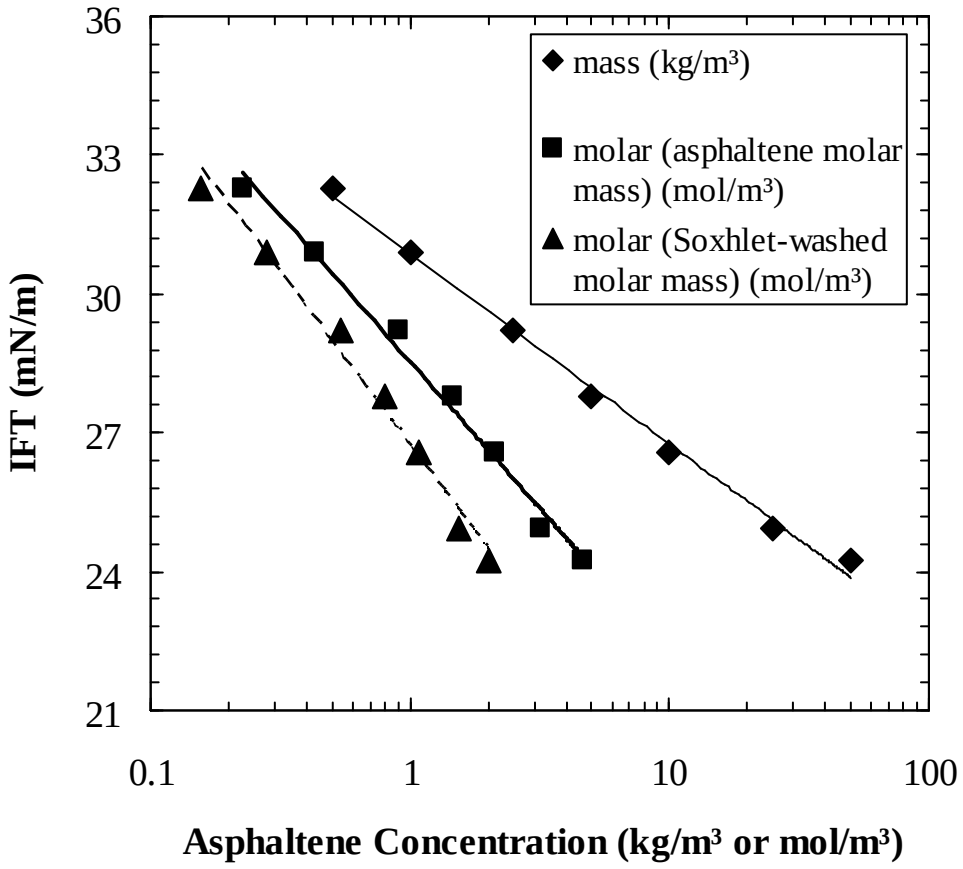

Figure 4.21: Interfacial tension of Soxhlet-Washed Asphaltene-25/75 heptol solutions over water plotted on mass and molar concentration bases. DVT, 23ºC

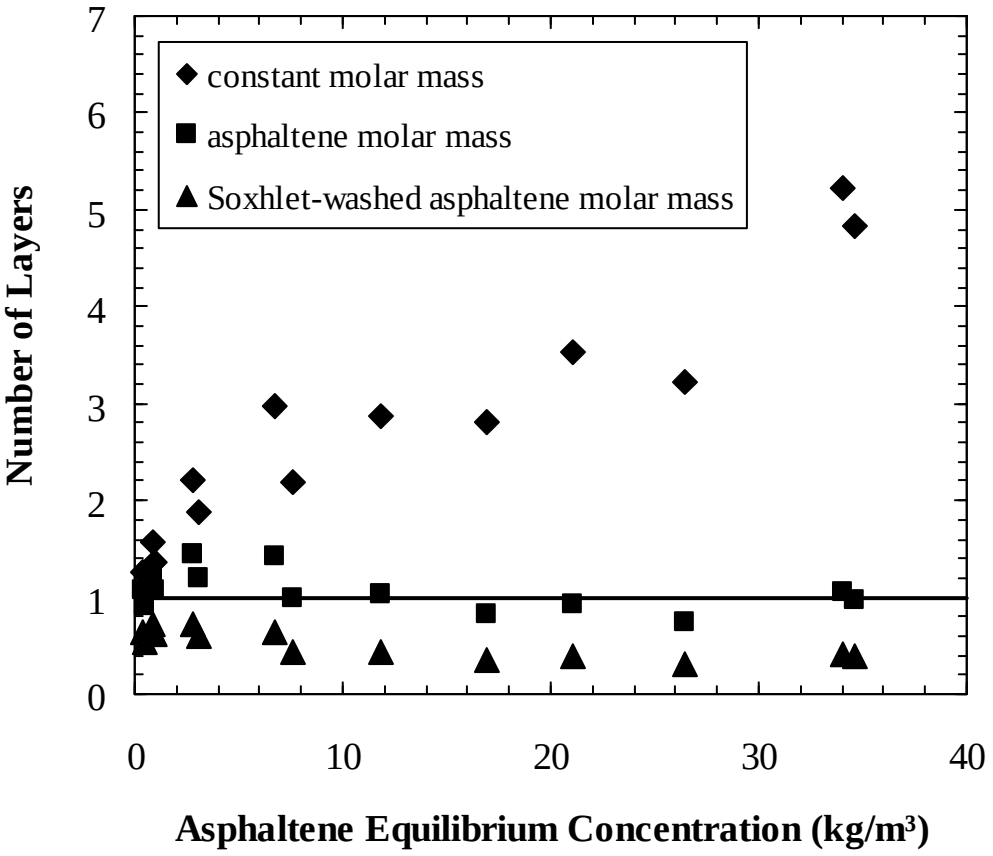

Figure 4.22: Number of layers of adsorbed Athabasca Bitumen 1 Soxhlet-Washed Asphaltenes. 25/75 heptol, 40 vol% water, 1.5 hours settling

It is not plausible that stable emulsions would be obtained when the asphaltenes adsorb significantly below monolayer coverage. Hence, it is probable that the asphaltenes on the interface are smaller than those measured in the VPO experiments.

All of the Soxhlet-Washed Asphaltene data was re-examined assuming that the molar mass was the same as the Asphaltene molar mass. The area per molecule from the IFT plot, Figure 4.22, is 1.46 nm^2. This value is within 10% of the area of 1.55 nm^2 determined for the Asphaltenes; hence, the interfacial areas for Soxhlet-Washed Asphaltenes and Asphaltenes are now consistent within experimental error, as discussed earlier in Chapter 3. Figure 4.22 shows that the calculated number of layers for the Soxhlet-Washed Asphaltenes now corresponds to a monolayer.

Why is it necessary to use Asphaltene molar masses to achieve a consistent interpretation of the Soxhlet-Washed data? One possibility is error in the molar mass measurements. However, the data for both Asphaltenes and Soxhlet-Washed Asphaltenes are similar to previously reported results (Alboudwarej *et al.*, 2002). Also, the solubility of Soxhlet-Washed Asphaltenes has been shown to be lower than Asphaltenes, consistent with the higher molar mass (Yarranton *et al.*, 2002).

Another possibility is that the larger asphaltene aggregates do not adsorb on the interface. They may be sterically hindered from adsorbing or they may diffuse more slowly to the interface. For example, if the smaller asphaltenes form a cross-linked network on the interface before the larger asphaltenes reach the interface, the larger asphaltenes may not be able to adsorb. Yet another possibility is that the adsorption of asphaltenes onto the interface is accompanied by a change in the association state of asphaltenes. For example, the asphaltenes may partially dissociate when they reach the interface. If either interpretation is valid, the molecules that adsorb at the emulsion interface at concentrations up to 40 kg/m^3 are smaller than approximately 10,000 g/mol and they form an interfacial layer of 9 nm thickness.

4.5 CHAPTER CONCLUSIONS

It is necessary to account for asphaltene self-association when interpreting interfacial data. For instance, the interfacial area of asphaltenes on the interface is more accurately determined from a plot of interfacial tension versus the molar concentration of asphaltenes rather than the mass concentration. Using the mass concentration can introduce significant error in the calculated area.

The configuration of asphaltenes at a water-hydrocarbon interface was assessed for Athabasca Bitumen 1 Asphaltenes and Soxhlet-Washed Asphaltenes, two asphaltenes with very different molar mass. Results from vapour pressure osmometry, interfacial tension and emulsion gravimetric studies were combined to calculate the number of layers adsorbed at the interface. Asphaltenes appear to adsorb as a monolayer, even at concentrations as high as 40 kg/m^3. It appears that asphaltenes greater than 10,000 g/mol do not adsorb on the interface. The interfacial tension studies indicate that asphaltenes adsorb as surfactants. The interfacial area of Athabasca asphaltenes is approximately 1.5 nm^2 and does not vary with concentration. However, the mass of the asphaltenes on the interface increases with concentration as the asphaltenes associate into larger aggregates. It appears that higher molar mass asphaltenes simply extend more into the continuous phase. The estimated thickness of the interfacial monolayer ranges from 2 to 9 nm. Figure 4.23 illustrates the hypothesized structure of the water/hydrocarbon interface.

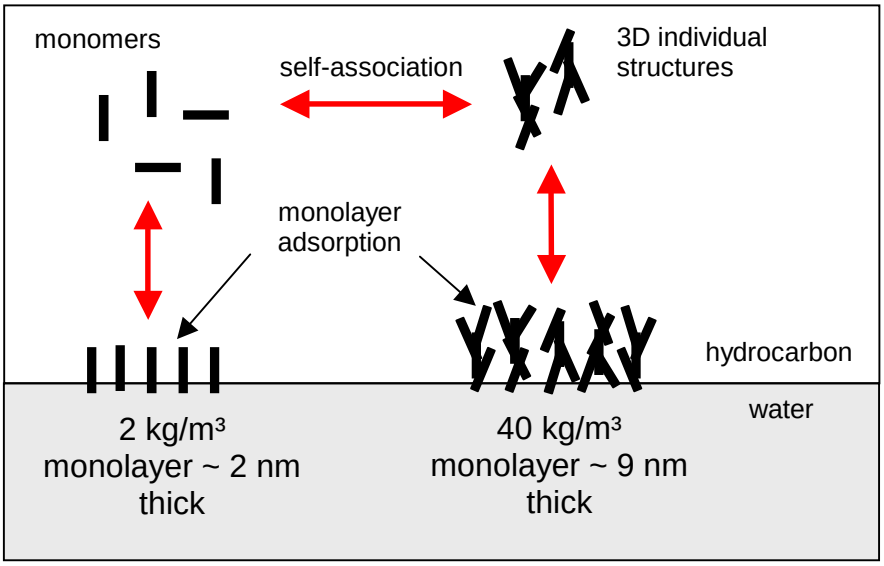

Figure 4.23: Preliminary interpretation of asphaltene configuration at water/hydrocarbon interface

CHAPTER 5

RHEOLOGY OF ASPHALTENE-HEPTOL/WATER INTERFACES

This chapter presents the results of the rheological studies. Section 5.1 presents the experimental elastic and viscous moduli of water/hydrocarbon interfaces stabilized by asphaltenes. The methodology for modeling the elastic and viscous moduli is presented in Section 5.2. Section 5.3 contains concluding remarks for this chapter and proposes a modified interpretation of asphaltene interfacial structure that takes into account the effects of interface aging time.

5.1 RHEOLOGY OF ASPHALTENE SOLUTIONS

The total, elastic and viscous moduli were measured for Athabasca Bitumen 2 Asphaltenes at heptol-water interfaces. The effects of frequency, asphaltene concentration, solvent quality, and interface aging time were examined.

As stated in Chapter 3, the total modulus is a measure of the change in interfacial energy that accompanies a change in interfacial area. The elastic modulus (ε_d) is the real part of the total modulus and represents the energy stored in the system. The viscous modulus ($\omega\eta_d$) is the imaginary part and represents the loss energy. In an oscillating system, the total (ε), elastic, and viscous moduli are related as follows:

$$\varepsilon = \varepsilon_{\mathrm{d}} + \mathrm{i}\omega\eta_{\mathrm{d}} \tag{5.1}$$

$$\left(\left|\varepsilon\right|\right)^2 = \left(\varepsilon_{\mathrm{d}}\right)^2 + \left(\omega\eta_{\mathrm{d}}\right)^2 \tag{5.2}$$

5.1.1 Effect of Frequency

The measured total modulus depends on the frequency of oscillations of the interfacial area. Therefore, before comparing elasticity measurements for different hydrocarbon phases and at different interface aging times, it is necessary to consider the effect of frequency. Figures 5.1 (a) and (b) illustrate the effects of frequency on the total, elastic and viscous moduli. At low frequencies, the interfacial area changes relatively slowly and there is sufficient time for diffusion from the bulk phase or within the interface to affect the measurement. Diffusion acts to reduce the change in interfacial tension and therefore reduces the measured elasticity. Hence, as the frequency approaches zero, the total elasticity approaches zero. As the frequency increases, the total elasticity eventually reaches a plateau where diffusion no longer affects the measurement. Further, the viscous modulus reduces to zero and the elastic modulus approaches a plateau. The plateau can be considered as the instantaneous elasticity, ε_o. The instantaneous elasticity is an intrinsic property of the interfacial film.

The effect of frequency on the measured total modulus of asphaltenes in 0/100 heptol after 10 minutes and 4 hours of interface aging is presented in Figures 5.2 and 5.3, respectively. The results are consistent with the expected trends given in Figures 5.1. Diffusion effects are apparent in all of the measurements except at asphaltene concentrations below 0.01 kg/m^3 and then only at frequencies above 0.1 to 0.2 Hz. Note that the trends with concentration are approximately the same at any given frequency. Hence, the effect of concentration can be examined at any one given frequency.

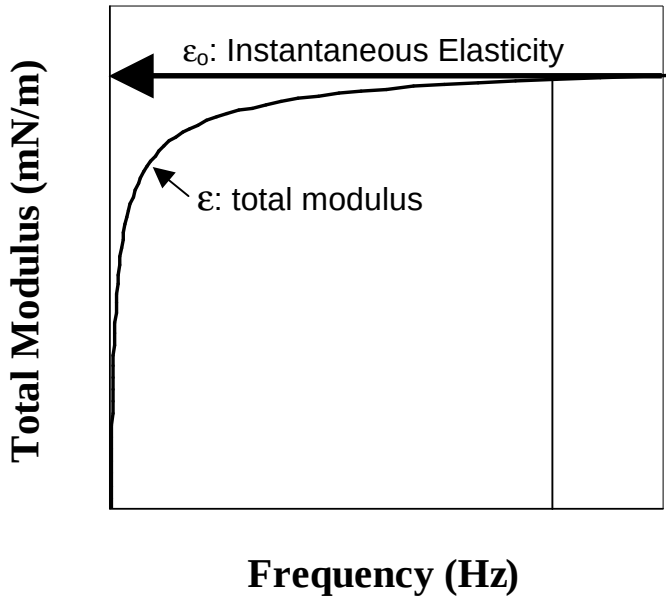

(a)

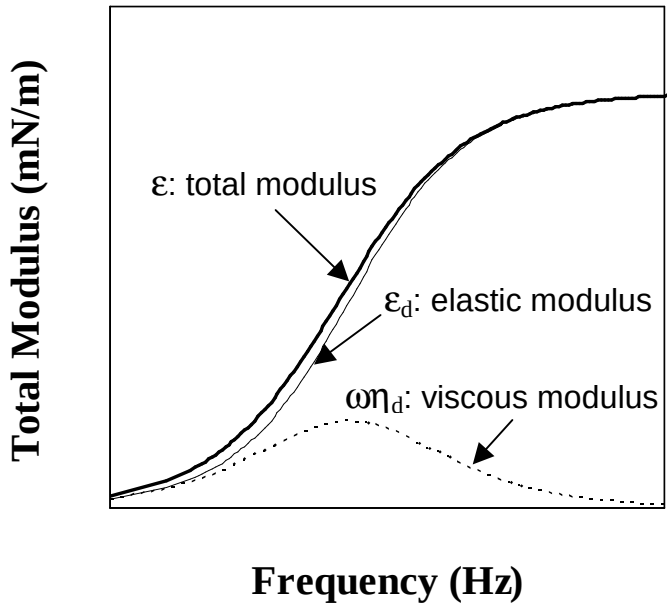

(b)

Figure 5.1: Effect of frequency on a) total modulus, b) elastic and viscous moduli (logarithmic scale)

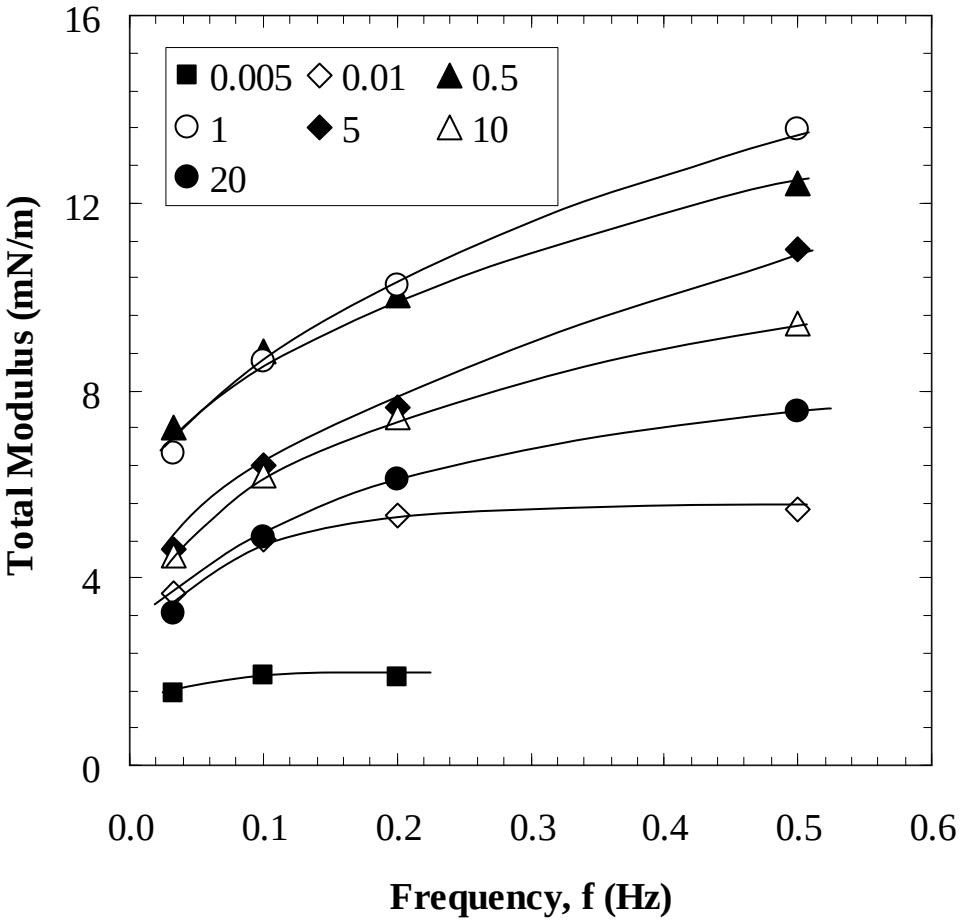

Figure 5.2: Effect of frequency on the total modulus of Athabasca Bitumen 2 Asphaltenes dissolved in 0/100 heptol at concentrations from 0.005 to 20 kg/m³. Interface aged for 10 minutes. The lines are visual aides

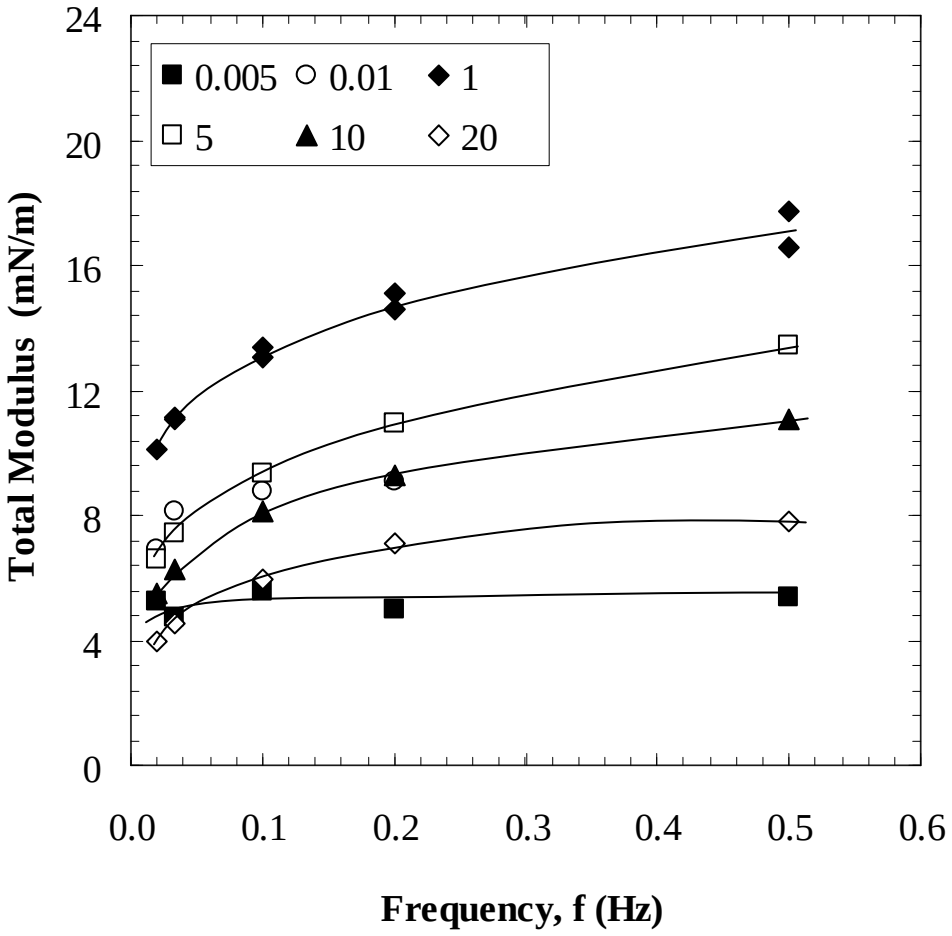

Figure 5.3: Effect of frequency on the total modulus of Athabasca Bitumen 2 Asphaltenes dissolved in 0/100 heptol at concentrations from 0.005 to 20 kg/m³. Interface aged for 4 hours. The lines are visual aides

5.1.2 Effect of Asphaltene Concentration

The effect of concentration on the total modulus is illustrated in Figure 5.4. At low concentrations the measured total modulus corresponds to the instantaneous elasticity since the effects of diffusion are negligible. However, as the concentration (or correspondingly the surface pressure) increases, the effects of diffusion increase. During drop expansion, the interface is stretched and surfactant-free pockets develop on the interface. At high concentrations, there is a large supply of surfactants in the bulk and therefore a large concentration gradient exists between the stretched areas of the interface and the bulk solution. Hence, molecules migrate to the interface quickly; i.e., diffusion is very fast, and interfacial tension increases less than it would if no diffusion occurred. During expansion and contraction, the effect is to reduce the total modulus.

At any given frequency, the total modulus first increases as the instantaneous elasticity increases and then decreases as the asphaltene concentration increases and diffusion dominates. The total, elastic, and viscous moduli versus asphaltene concentration after 10 minutes and 4 hours of interface aging are shown in Figures 5.5 and 5.6, respectively. The comparisons are made for a frequency of 0.033 Hz and a hydrocarbon phase consisting of pure toluene (0/100 heptol). The interface is mostly elastic (i.e., negligible viscous modulus) for asphaltene concentrations less than 0.01 kg/m^3. Diffusion begins to affect the measurements at approximately 0.1 kg/m^3. This is true both at short (10 minutes) and long (4 hours) interface aging times.

For asphaltene concentrations relevant to emulsion stability, i.e., greater than 1 kg/m^3, the total, elastic, and viscous moduli decrease as the asphaltene concentration increases. In fact, the total modulus decreases to half its value as the concentration increases from 1 to approximately 20 kg/m^3.

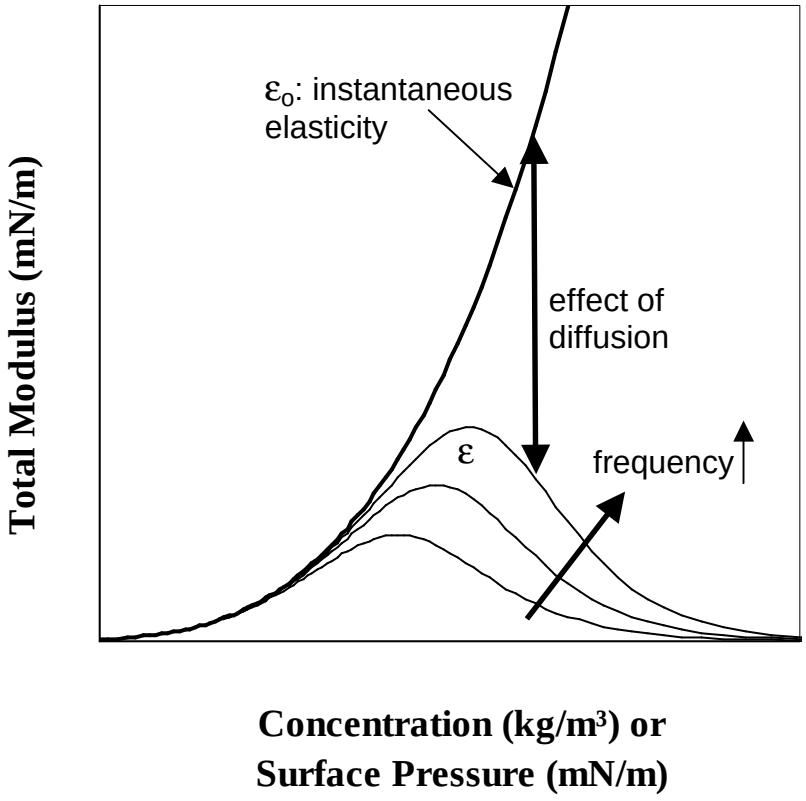

Figure 5.4: Effect of surfactant concentration on total modulus

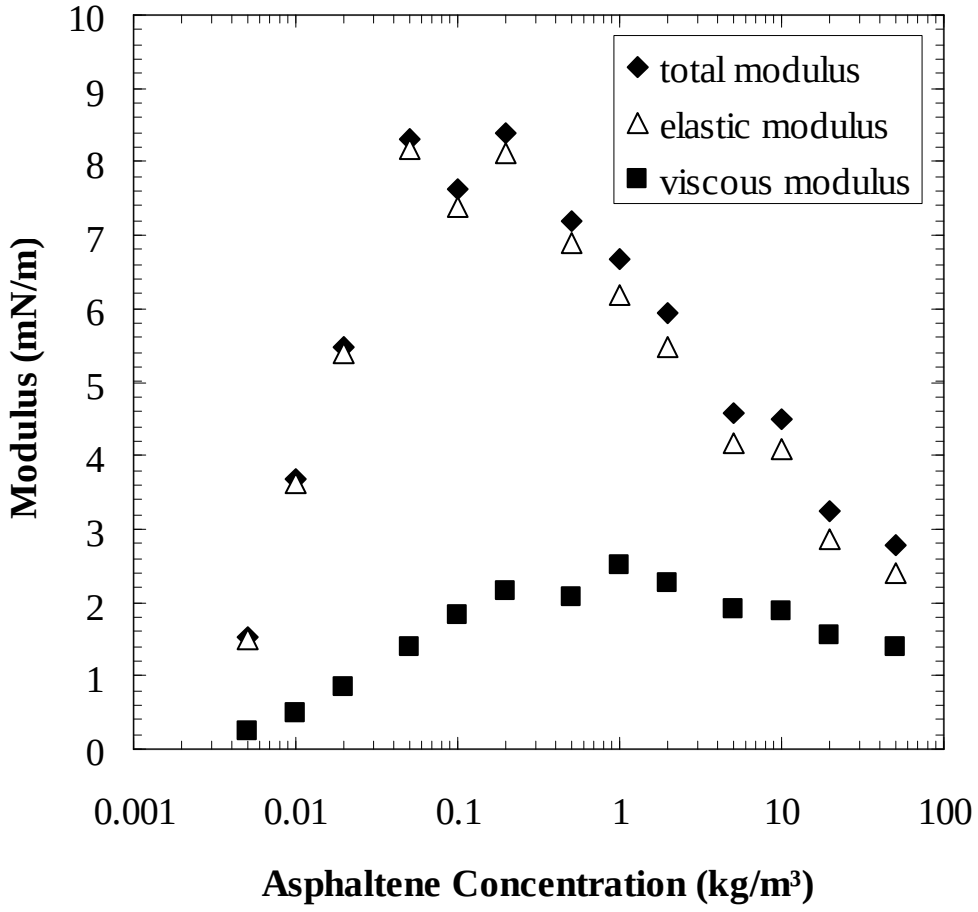

Figure 5.5: Effect of asphaltene concentration on the total, elastic and viscous moduli of Athabasca Bitumen 2 Asphaltenes dissolved in 0/100 heptol at concentrations from 0.005 to 20 kg/m³. Oscillation frequency 0.033 Hz, interface aged for 10 minutes

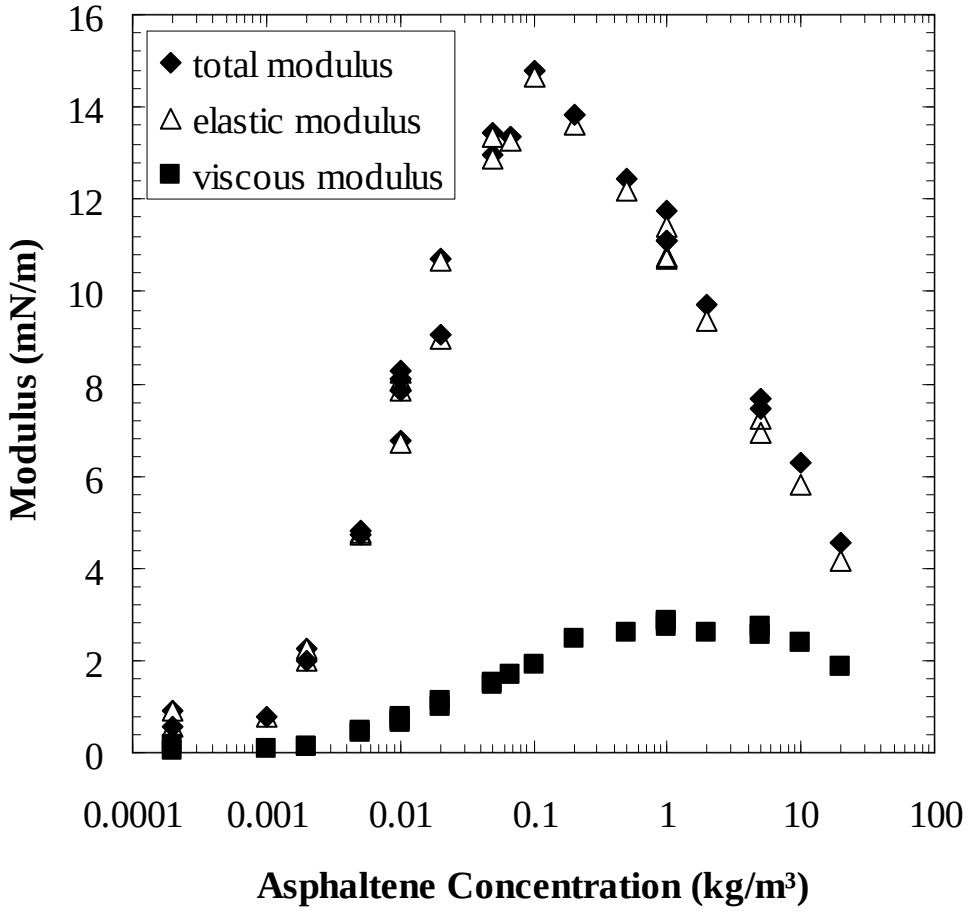

Figure 5.6: Effect of asphaltene concentration on the total, elastic and viscous moduli of Athabasca Bitumen 2 Asphaltenes dissolved in 0/100 heptol at concentrations from 0.005 to 20 kg/m³. Oscillation frequency 0.033 Hz, interface aged for 4 hours

5.1.3 Effect of Solvent

The effect of solvent on the measured elastic and viscous moduli is given in Figure 5.7. Note that, as in Figures 5.5 and 5.6, the measurements were made for an oscillation frequency of 0.033 Hz. The comparisons are shown for interfaces aged for 10 minutes. The viscous and elastic moduli increase as the heptane content increases. At asphaltene concentrations exceeding 0.1 kg/m^3, the moduli increase by 5 to 15% as the heptane fraction increases from 0 to 25% and by 30 to 35% as the heptane fraction increases to 50%.

The trends presented in Figures 5.7 are consistent with the work of Spiecker and Kilpatrick (2004). Using a shear viscometric method, they observed that the elastic modulus increased as the heptane fraction in heptol increased for an asphaltene concentration of 7.5 kg/m^3. For example, after eight hours, the elastic modulus at an oscillation frequency of 0.16 Hz (1 rad/s) for 45/55, 40/60 and 20/80 heptol-water interfaces was approximately 7.5, 5.5 and 3 mN/m. It is speculated that in a poor solvent such as 50/50 heptol, the interface is more rigid because adsorbed asphaltenes cross-link to a higher degree and form a stronger network. In contrast, a good solvent such as 0/100 heptol may result in a more loosely packed, more fluid interface. Therefore, the total elastic modulus for a 50/50 heptol-water interface is higher than for a 0/100 heptol-water interface.

5.1.4 Effect of Interface Aging Time

The elastic and viscous moduli of asphaltenes at a toluene/water interface are given in Figure 5.8 for an oscillation frequency of 0.033 Hz. It is apparent that the elastic modulus increases significantly over 16 hours, whereas the viscous modulus increases marginally. Similar increases in the moduli were observed for 25/75 and 50/50 heptol as shown in Figures 5.9 and 5.10, respectively.

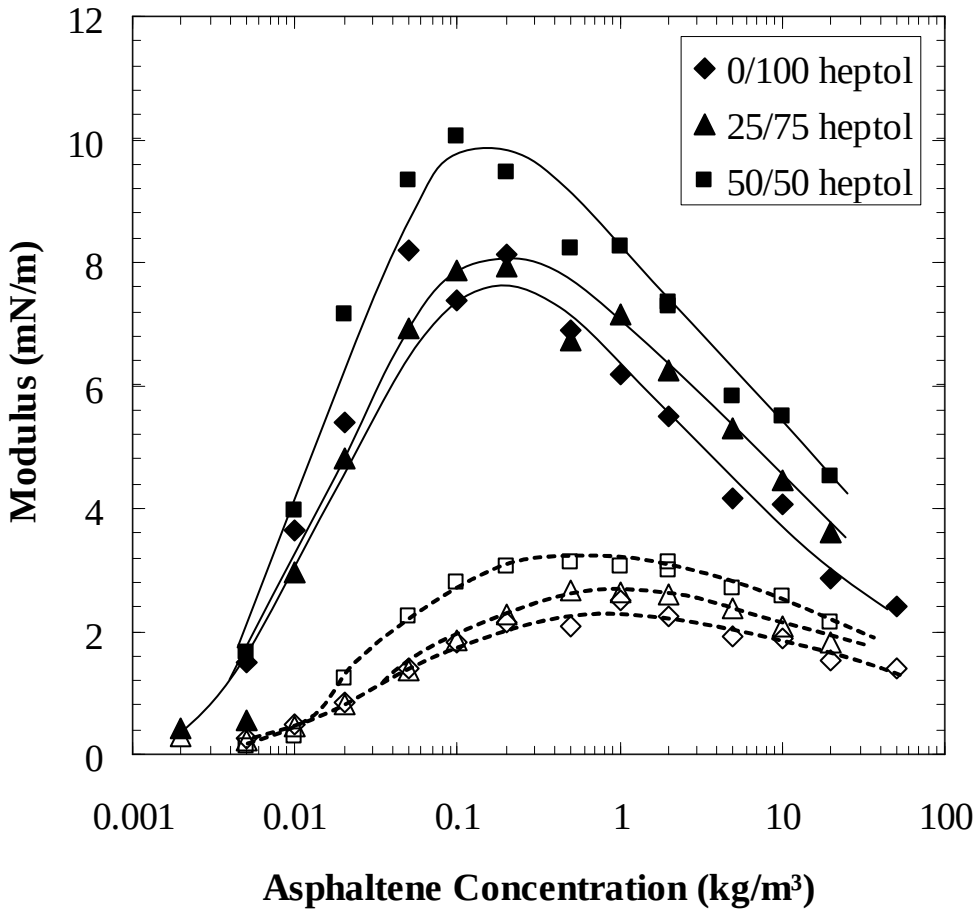

Figure 5.7: Effect of solvent on the elastic and viscous moduli of Athabasca Bitumen 2 Asphaltenes dissolved in heptol. Oscillation frequency 0.033 Hz, interface aged for 10 minutes. closed symbols – elastic modulus, open symbols – viscous modulus. The lines are visual aides

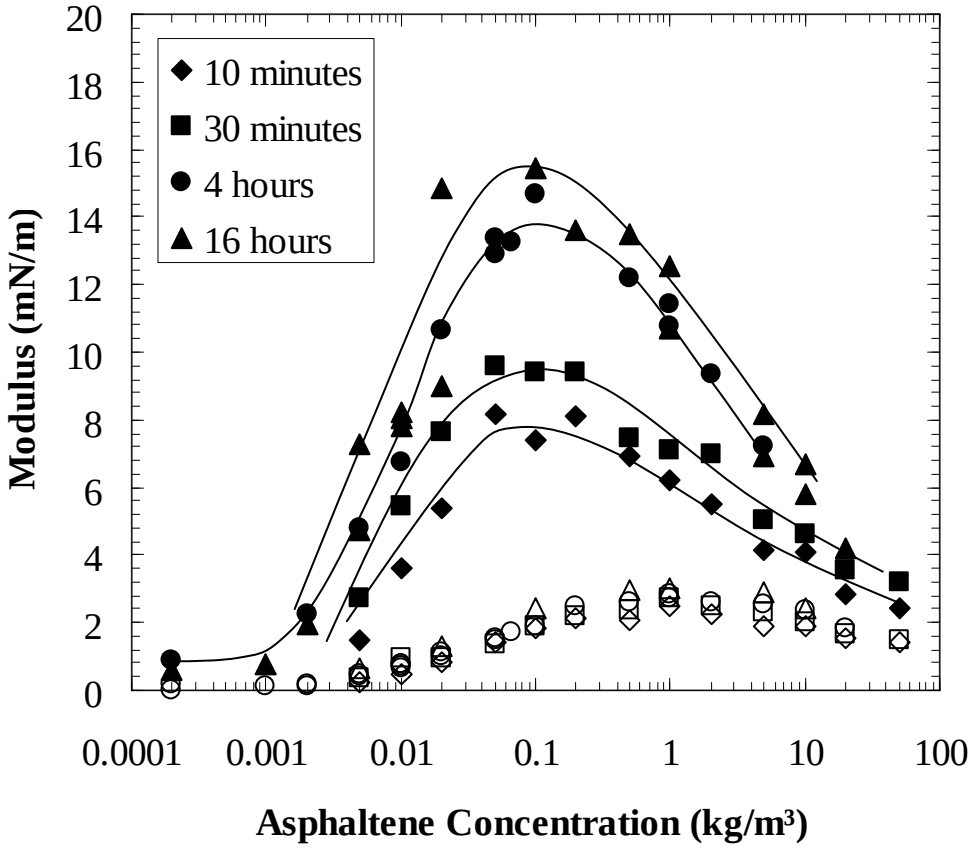

Figure 5.8: Effect of interface aging time on the elastic and viscous moduli of Athabasca Bitumen 2 Asphaltenes dissolved in 0/100 heptol. Oscillation frequency 0.033 Hz. closed symbols – elastic modulus, open symbols – viscous modulus. The lines are visual aides

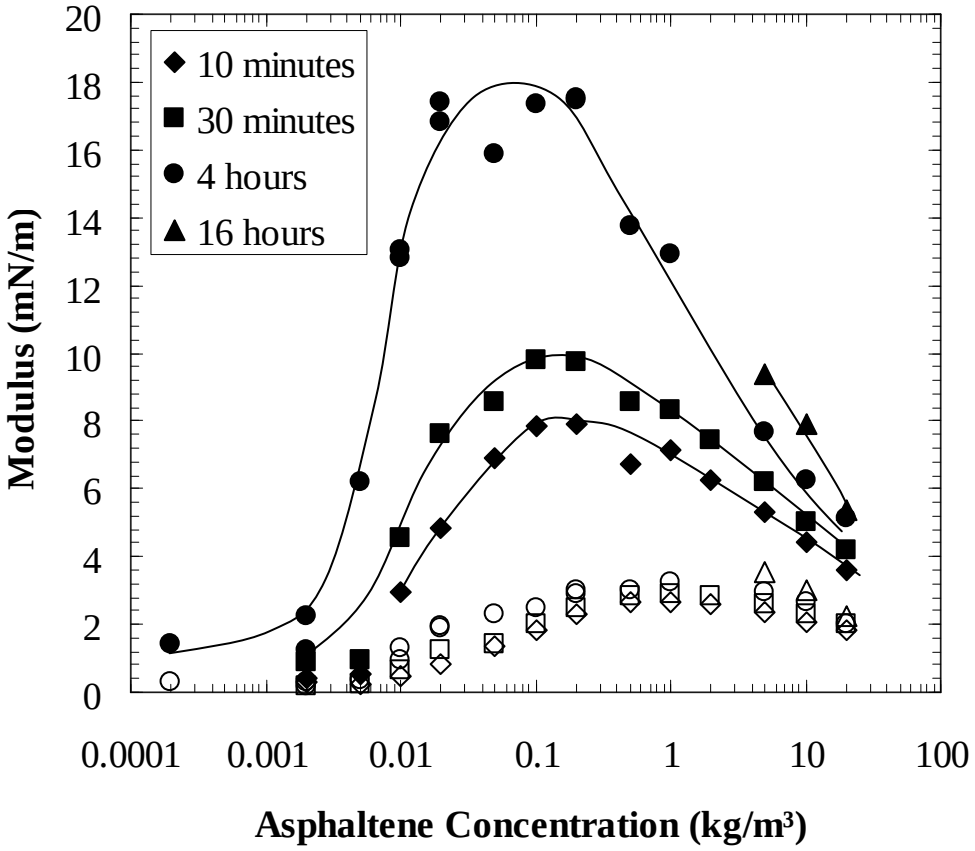

Figure 5.9: Effect of interface aging time on the elastic and viscous moduli of Athabasca Bitumen 2 Asphaltenes dissolved in 25/75 heptol. Oscillation frequency 0.033 Hz. closed symbols – elastic modulus, open symbols – viscous modulus. The lines are visual aides

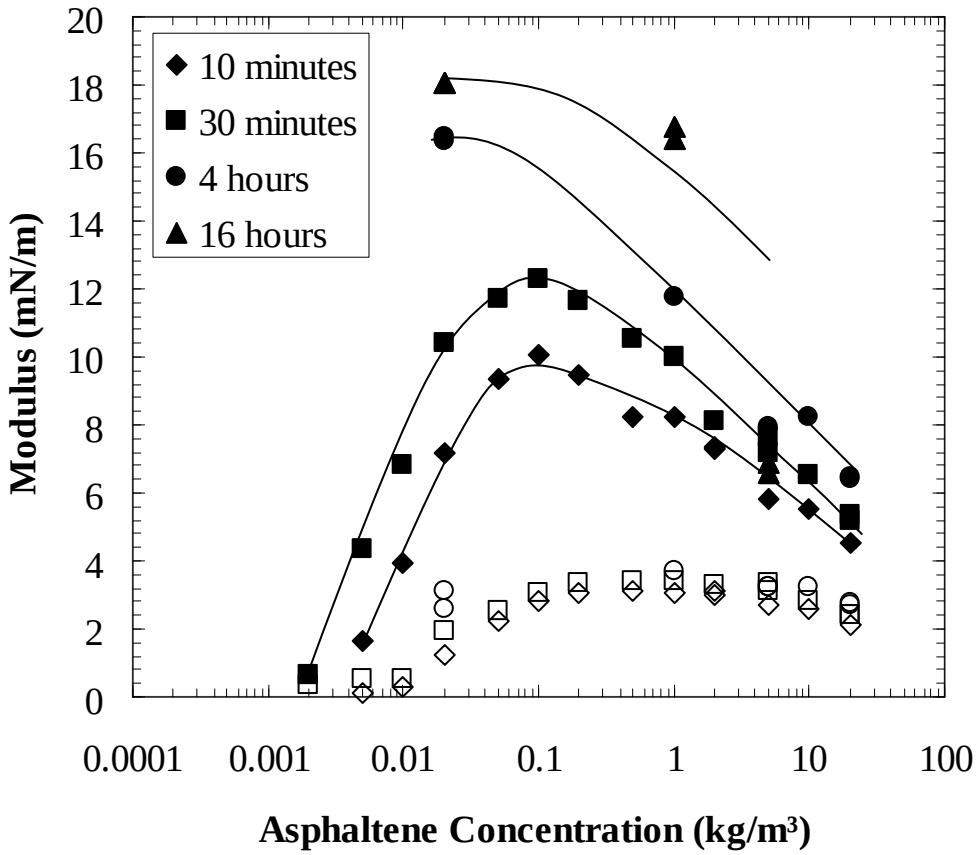

Figure 5.10: Effect of interface aging time on the elastic and viscous moduli of Athabasca Bitumen 2 Asphaltenes dissolved in 50/50 heptol. Oscillation frequency 0.033 Hz. closed symbols – elastic modulus, open symbols – viscous modulus. The lines are visual aides

Note that the elastic and viscous moduli of 25/75 and 50/50 heptol interfaces aged for four and 16 hours were measured only for asphaltene concentrations exceeding 2 kg/m³. As will be seen in Chapter 6, stable emulsions are created once the asphaltene concentration exceeds 2 kg/m³. Therefore, comparisons between rheology and emulsion stability are impossible below asphaltene concentrations of 2 kg/m³; there was no need to collect the rheological data below 2 kg/m³.

Figures 5.8 through 5.10 indicate that as asphaltene-heptol-water interfaces age, the elastic modulus and, to a lesser extent, the viscous modulus increase. The largest increases occur for "intermediate" asphaltene concentrations; that is, concentrations varying between 0.01 and 1 kg/m³. The rise in the moduli is consistent with the work of Spiecker and Kilpatrick (2004), Freer *et al.* (2003), Freer and Radke (2004), Bauget *et al.* (2001) and Aske *et al.* (2001). Unfortunately, a quantitative comparison of the data in Figures 5.8 through 5.10 with the literature is difficult because the asphaltene source, concentration and solvent vary significantly. Further, some of the studies were conducted on crude oil drops rather than asphaltene-heptol drops (Aske *et al.*, 2002; Freer *et al.*, 2003). The effects of resins and other surface-active constituents of oil will impede meaningful comparisons.

5.2 MODELING OF ELASTIC AND VISCOUS MODULI

An attempt to model the interfacial tension and instantaneous, elastic and viscous moduli was made to further understand the experimental rheological measurements. Not only was the validity of the approach assessed for various interface aging times, but the applicability of purely-diffusional relaxation regimes evaluated. The modeling attempt leads to an improvement in the understanding of the structural changes that occur on the interface as the film ages.

5.2.1 Theory

The interfacial tension and elasticity data of the asphaltene/toluene system was modeled

using the Lucassen-Van Den Tempel (LVDT) approach (Lucassen and Van Den Tempel, 1972). There are three main steps:

1) Relate the interfacial tension to the bulk concentration of surfactant,
2) Calculate the instantaneous elasticity,
3) Calculate the elastic and viscous moduli

5.2.1.1 Relation of Interfacial Tension to Surfactant Concentration

First, the interfacial tension is modeled using the binary form of the Butler surface equation of state (SEOS) (Butler, 1932; Lucassen-Reynders *et al.*, 2001):

$$\Pi = \gamma_o - \gamma = -\frac{RT}{a_1}\left[\ln(1-\theta_2) + \left(1-\frac{1}{S_2}\right)\theta_2 + \frac{H}{RT}\theta_2^2\right] \qquad (5.3)$$

where the subscripts "1" and "2" refer to the solvent and surfactant, respectively, Π is the surface pressure; that is, the difference between the interfacial tension between the pure solvent (toluene) and water, γ_o, and the interfacial tension of the solvent and surfactant versus water, γ. R is the universal gas constant, T is temperature, a_1 is the interfacial area of a solvent molecule, S_2 is the ratio of the interfacial area of the surfactant molecule to the area of the solvent molecule, θ_2 is the fractional area surface coverage by the surfactant, and H is the enthalpy of mixing at infinite dilution. The first, second and third terms in Equation (5.3) represent the ideal entropy of mixing, the non-ideal entropy of mixing caused by the difference in size between solvent and surfactant molecules, and the enthalpy of mixing, respectively.

The fractional surface coverage of the solute, θ_2, is related to the surfactant concentration in solution, c_2, through the following:

$$c_2' = \frac{c_2}{c_{2,\theta=0.5}} = \frac{2\theta_2}{[2(1-\theta_2)]^{S_2}} \exp\left[\frac{S_2 H}{RT}(1-2\theta_2)\right] \qquad (5.4)$$

where c'_2 is the reduced concentration and $c_{2,\theta=0.5}$ is the half-saturation concentration. Note that the concentration given in Equation (5.4) is the *molar*, not mass, concentration. Also note that, for ternary or higher order systems, equations similar to Equation (5.4) apply for the reduced concentration of the surfactant molecules in question (Lucassen-Reynders, 1994).

Equation (5.4) reduces to the Frumkin equation when the solvent and surfactant molecules are of equal size (i.e., $S_2 = 1$), and further to the Langmuir equation when the enthalpy of mixing is ignored ($H/RT = 0$). The relationship between the fractional coverage and the reduced concentration is illustrated in Figure 5.11 for Langmuir and Frumkin adsorption.

Figure 5.11 also illustrates the effect of the enthalpy of mixing term on the fractional surface coverage, θ_2. The effect of enthalpy of mixing can be explained as follows: a negative value of H/RT means that the attractive forces between the surfactant and solvent molecules are larger than the attractive forces amongst the surfactant molecules. Conversely, a positive value of H/RT means that the attractive forces amongst surfactant molecules are larger than the attractive forces between solvent and surfactant molecules. When the reduced concentration exceeds unity, more than half the interface is covered by surfactant molecules. At any given concentration, surfactants will resist adsorbing on an interface composed primarily of surfactants if they are more attracted to solvent molecules rather than each other. Therefore, the fractional coverage will be less than if attractive forces between solvent and surfactants are zero (i.e., Langmuir adsorption, $H/RT=0$). Conversely, if surfactants are attracted to each other more than to solvent molecules, they will adsorb more readily on an interface composed primarily of surfactants; the surface coverage will be higher relative to the Langmuir case.

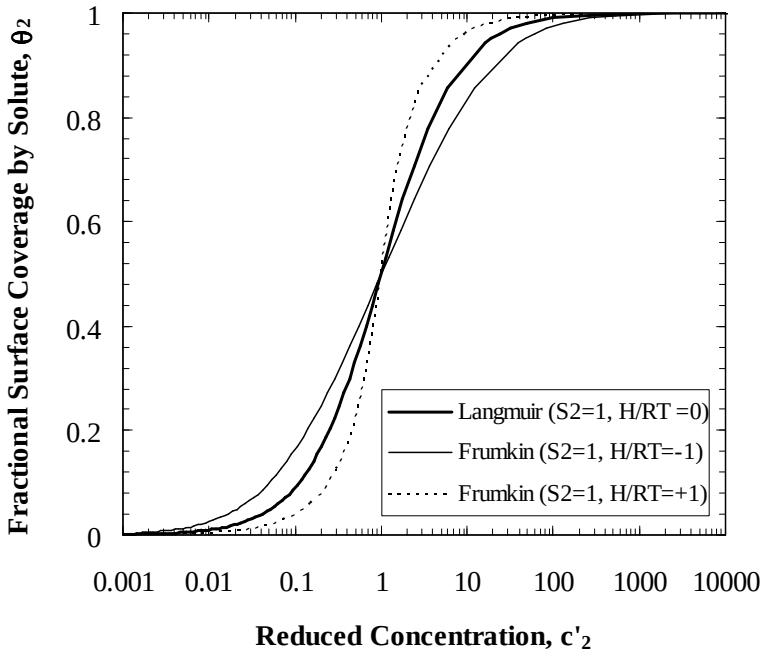

Figure 5.11: Effect of the enthalpy of mixing on the relationship between fractional surface coverage and reduced concentration of surfactant

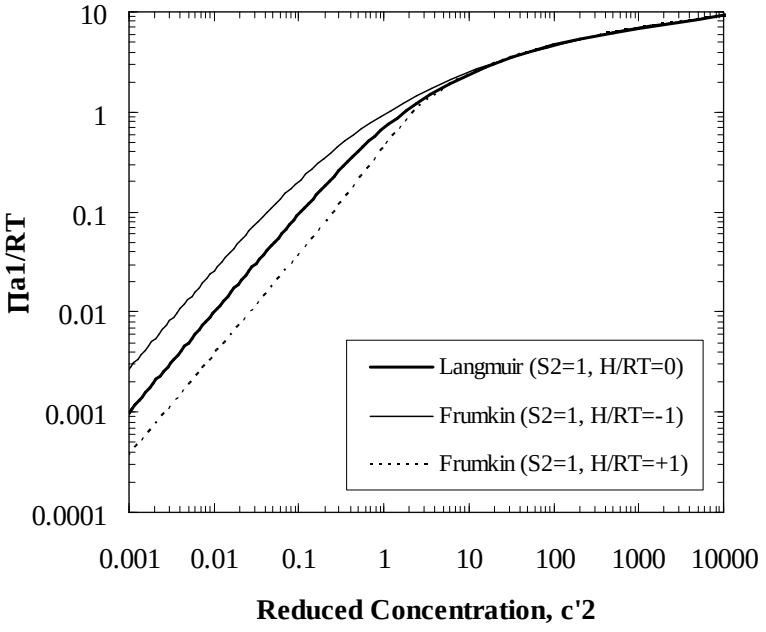

Figure 5.12: Effect of enthalpy of mixing on the dimensionless surface pressure

Similar logic can be used to explain the shapes of the curves at reduced concentrations below unity. Here, less than half the interface is covered by surfactants. At any given reduced concentration, if surfactants are more attracted to solvent molecules than to each other, they will adsorb on the interface with a higher surface coverage compared to Langmuir adsorption. The opposite is true for surfactants attracted more to each other than to solvent molecules: they will adsorb with a lower surface coverage since the interface is composed primarily of solvent molecules.

The effect of the enthalpy of mixing on the dimensionless surface pressure, $\Pi a_1/RT$, is illustrated in Figure 5.12. At a reduced concentration exceeding approximately 10, all of the curves appear to collapse onto one curve. Once the reduced concentration exceeds 10, the interface is saturated with surfactant to a similar degree and therefore the interfacial tensions (and surface pressure) are equal. At reduced concentrations less than unity, the surface coverage is higher for negative H/RT relative to Langmuir adsorption, meaning that the interfacial tension is reduced more. More reduction in interfacial tension results in a higher surface pressure relative to the Langmuir curve, as shown in Figure 5.12. The opposite is true for positive H/RT and the surface pressure is lower relative to the Langmuir curve.

The effect of the size ratio of the surfactant and solvent molecule, S_2, on the fractional surface coverage is illustrated in Figure 5.13. When the reduced concentration is less than unity, less than half the interface is covered by the surfactant. At any given reduced concentration, a larger molecule will occupy more space than a smaller molecule, so the surface coverage for surfactants larger than the solvent exceeds the surface coverage of equal sized surfactant and solvent molecules. When the reduced coverage exceeds unity, more than half the interface is covered by surfactants. At any reduced concentration, it is easier for small ($S_2 = 1$) rather than large ($S_2 > 1$) molecules to adsorb on an interface already composed mainly of surfactants. Therefore, the surface coverage is smaller for larger molecules relative to smaller molecules.

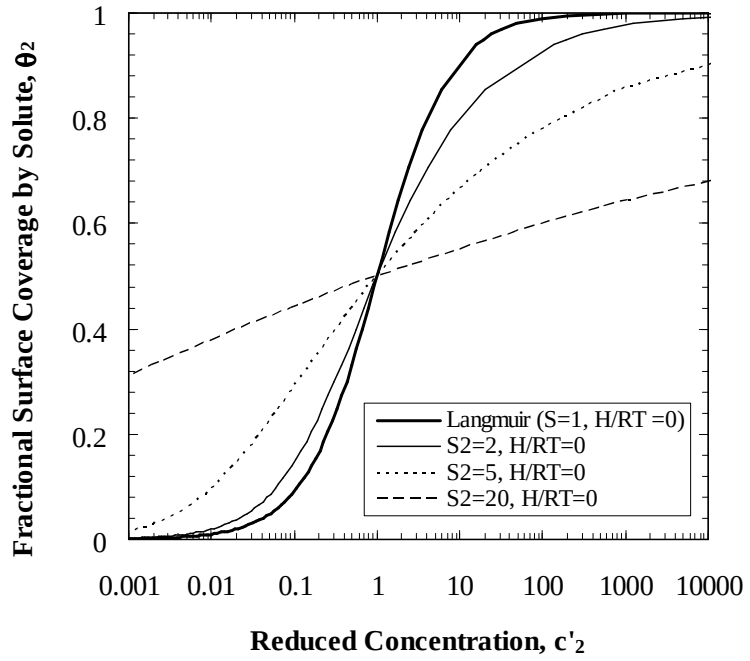

Figure 5.13: Effect of shape factor on the relationship between fractional surface coverage and reduced concentration of surfactant

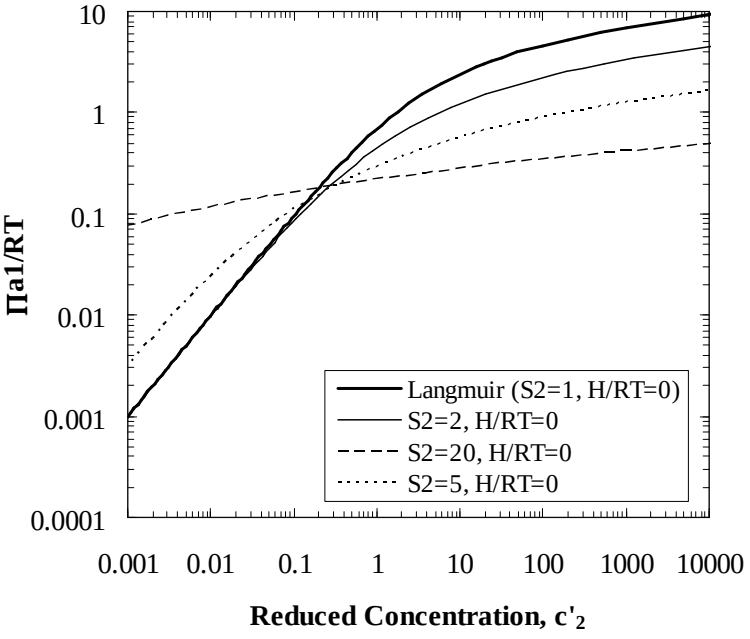

Figure 5.14: Effect of shape factor on the dimensionless surface pressure

The effect of the shape factor on the dimensionless surface pressure is illustrated in Figure 5.14. At low reduced concentrations, the surface pressure increases (i.e., the interfacial tension is reduced more) as the disparity in size between the surfactant molecule and solvent molecule increases (increasing S_2). The higher surface pressure occurs because the surface coverage, θ_2, is higher for larger shape factors. The opposite is true at very high reduced concentrations.

5.2.1.2 Calculation of Instantaneous Elasticity

The SEOS is used to establish the relationship between the surfactant concentration (or fractional surface coverage) and the reduction in interfacial tension (or increase in surface pressure). The second step is to find the instantaneous elasticity, which is given by Equation (5.5):

$$\varepsilon_o = \frac{d\gamma}{d\ln\Gamma} \tag{5.5}$$

or the derivative of interfacial tension (Equation (5.3)) with respect to the natural logarithm of the molar area of the interface, Γ. Note that Equation (5.5) is independent of the SEOS used. For the binary form of the Butler SEOS, the resultant instantaneous elasticity is given by:

$$\varepsilon_o = -\frac{RT}{a_1}\left[\frac{\theta_2}{(\theta_2 - 1)} + \left(1 - \frac{1}{S_2}\right)\theta_2 + 2\frac{H}{RT}\theta_2^2\right] \tag{5.6}$$

5.2.1.3 Calculation of Elastic and Viscous Moduli

The final step is to calculate the total, elastic and viscous moduli. A key assumption is that relaxation is purely diffusional. The effect of diffusion is accounted for as follows (Lucassen and Van Den Tempel, 1972):

$$|\varepsilon| = \frac{\varepsilon_o}{\left[1 + 2\zeta + 2\zeta^2\right]^{1/2}} \tag{5.7}$$

where ζ is a diffusion parameter and given by:

$$\zeta^2 = \frac{D}{2\omega}\left(\frac{dc}{d\Gamma}\right)^2 \tag{5.8}$$

and D is the diffusivity of the surfactant. Also, the characteristic time of diffusion, τ_D, is related to the diffusional parameter and the frequency, ω, through the following:

$$\tau_D = \frac{1}{\zeta^2 \omega} \tag{5.9}$$

The elastic and viscous moduli can be found individually from:

$$\varepsilon' = \varepsilon_d = \varepsilon_o \frac{1 + \zeta}{1 + 2\zeta + 2\zeta^2} \tag{5.10}$$

and

$$\varepsilon'' = \omega\eta_d = \varepsilon_o \frac{\zeta}{1 + 2\zeta + 2\zeta^2} \tag{5.11}$$

Note that for an SEOS and the above elasticity expressions to be valid, the adsorption of the surfactant on the interface must be reversible, equilibrium must be attained, and there can be no mechanical film present.

The effects of the enthalpy of mixing and the shape factor on the dimensionless total modulus are shown in Figures 5.15 and 5.16, respectively. In both figures, the oscillation frequency is 0.1 Hz and the diffusivity 10^{-12} m²/s. Note that this diffusivity is used for illustrative purposes only. From Figure 5.15, it can be said that the total modulus increases as the attractive forces between surfactants increase and decreases when attractive forces between surfactant and solvent molecules increase. Figure 5.16 shows that as the solute molecule increases in size relative to the solvent molecule, the elasticity of the interface is reduced.

The numerical value of the diffusion coefficient also has significant effects on the total modulus, as shown in Figure 5.17. For illustrative purposes, Figure 5.17 was generated for an oscillation frequency of 0.1 Hz and Langmuir adsorption. A lower diffusivity results in a higher total modulus. When surfactants diffuse less rapidly into open areas on the interface, the interfacial tension remains high and so does the elasticity.

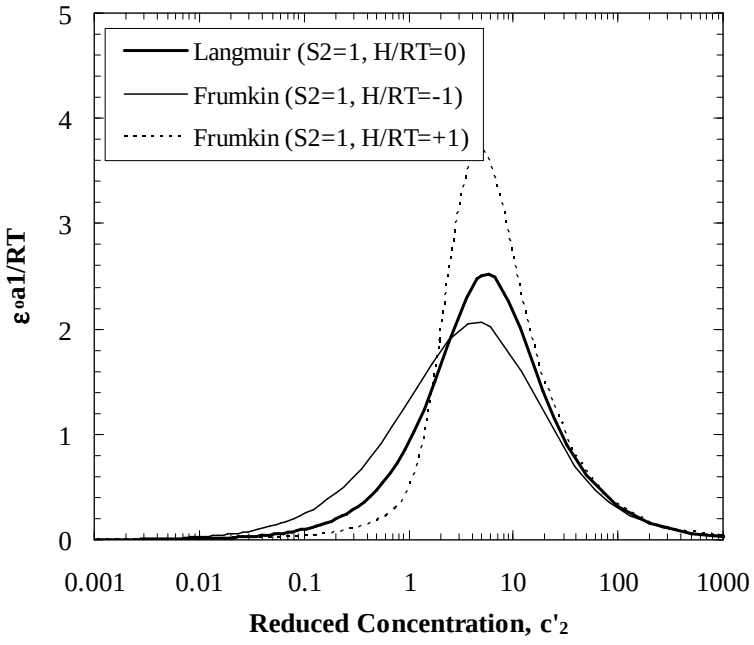

Figure 5.15: Effect of enthalpy of mixing on the dimensionless total modulus

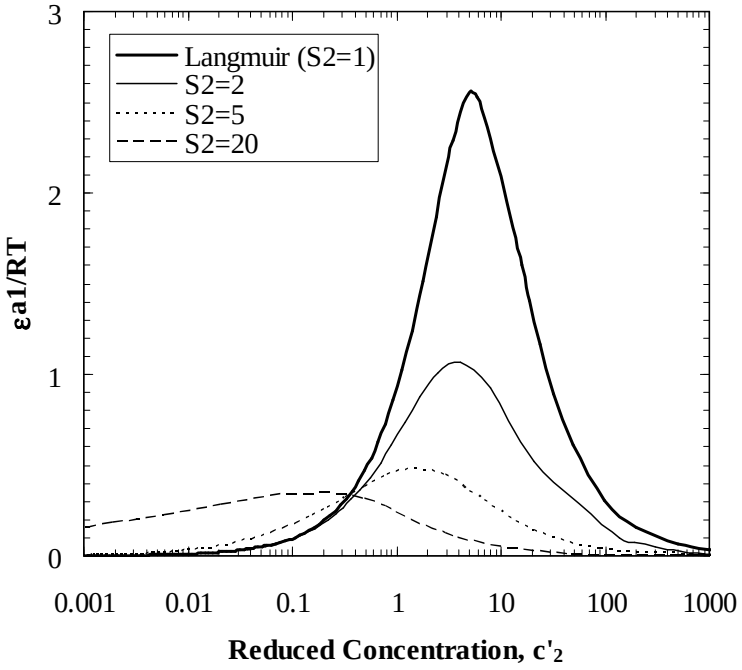

Figure 5.16: Effect of shape factor on the dimensionless total modulus

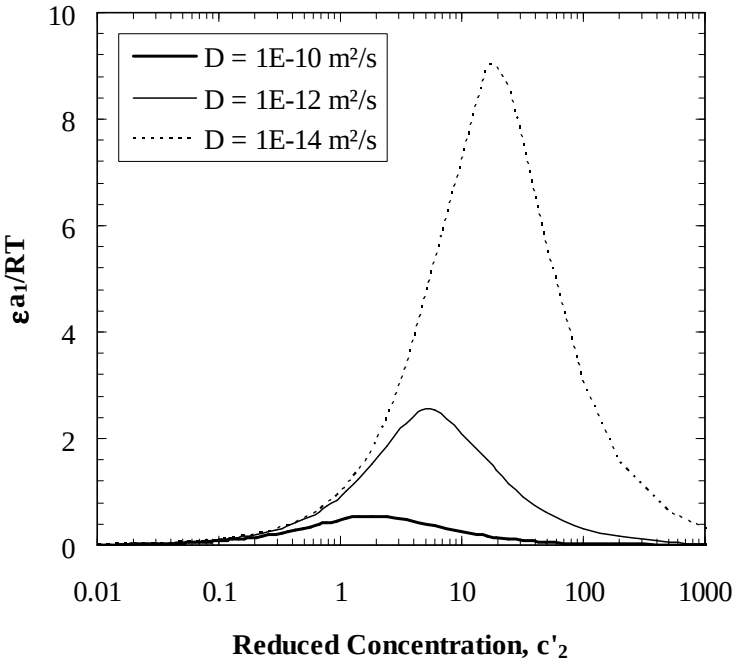

Figure 5.17: Effect of diffusivity on the dimensionless total modulus

5.2.2 Model Match

5.2.2.1 Interfacial Tension

To apply the approach described in the previous section, the SEOS is first fit to interfacial tension data. Since the 0/100 heptol system had the most complete data set, only toluene-water interfaces were modeled. The fit for interfacial tension measurements of asphaltenes in 0/100 heptol versus water after 60 seconds, 10 minutes, and 4 hours of contact is shown in Figure 5.18. Note that the interfacial tension is fit as a function of *molar* concentration. The effects of asphaltene self-association were taken into account using the measured average associated molar mass presented earlier in Figure 4.1.

The fit parameters are the enthalpy of mixing, the area of an asphaltene molecule, the shape factor, and the half saturation concentration. For lack of a better value and the sake of simplicity, the enthalpy of mixing was assumed to be negligible. The interfacial area of an asphaltene was set to 1.4 nm² which is within the range reported in the literature (Rogel et al, 2000; Ese *et al.*, 1999; Bhardwaj and Hartland, 1994). It is interesting that the value of 1.4 nm² is within 5% of the area obtained assuming the Gibbs' isotherm (1.34 nm² for Athabasca Bitumen 2 Asphaltenes, Section 4.4.1). Hence, it appears that the Gibbs' isotherm is a good approximation of the molecular area of an adsorbed asphaltene, even if the Gibbs' isotherm assumes Langmuir-type adsorption (since S_2=1). However, the Gibbs' isotherm would not fit the IFT for concentrations less than 0.01 mol/m³.

The ratio of the molecular areas, S_2, was set to 5 so as to obtain a realistic interfacial area for toluene, 0.28 nm². The area of toluene is expected to be slightly larger than the area of benzene. Based on the lengths of the bonds between carbon atoms in the benzene molecule, the area is about 0.15 nm². As well, the average area of a molecule at an interface will likely be larger than the size of the molecule itself.

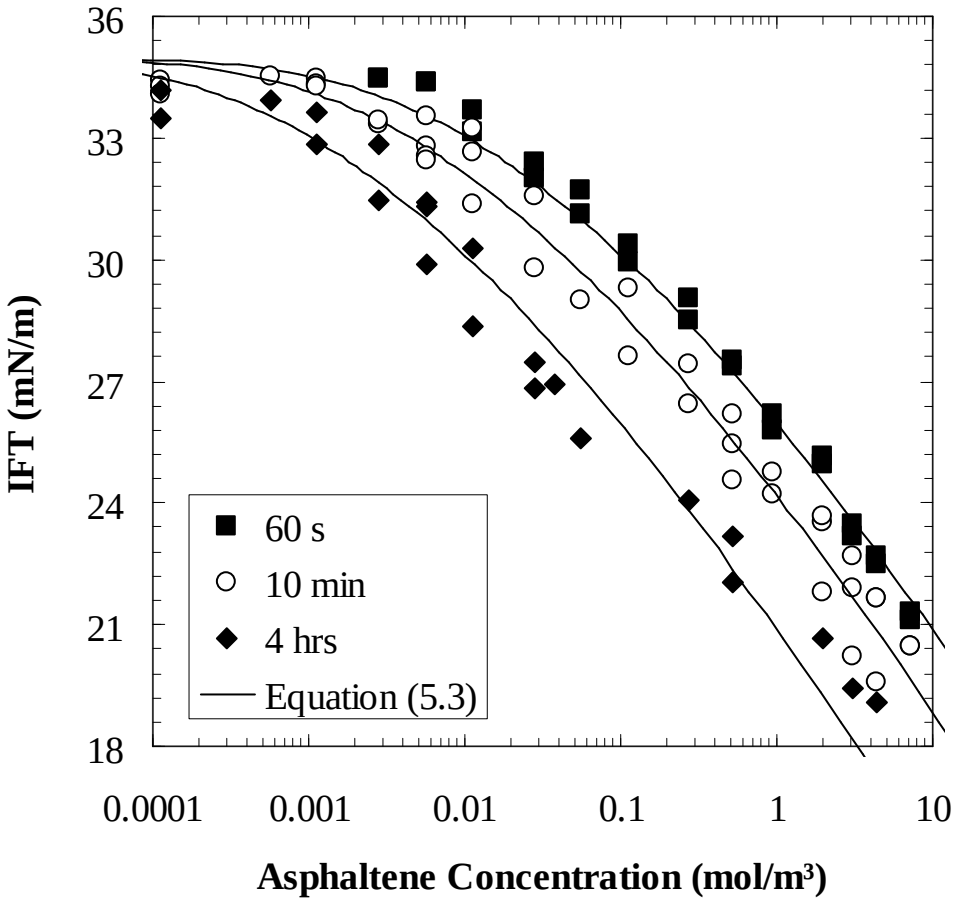

Figure 5.18: Measured and modeled interfacial tension of Athabasca Bitumen 2 Asphaltenes dissolved in 0/100 heptol versus water at 23°C and interface aging times of 60 seconds, 10 minutes and 4 hours

The half-saturation concentrations were then adjusted to fit the data. Concentrations of 0.07, 0.03, and 0.007 mol/m³ were found to fit the data at 60 seconds, 10 minutes, and 4 hours, respectively. Note that theoretically, the half-saturation concentration is applicable at equilibrium and should therefore be constant. However, the equilibrium value of interfacial tension of asphaltene-solutions over water is difficult to assess because mechanical rigidity affects the measurements relatively quickly. Hence, the half-saturation constant has been used as a fitting parameter. In fact, as discussed later in Section 5.2.2.3, the LVDT model is valid only at short interface aging times, i.e., before the formation of mechanical films. Hence, the half-saturation constants are only physically meaningful at very short aging times.

5.2.2.2 Elastic and Viscous Moduli

In order to use the LVDT model, the diffusion coefficient must be known for asphaltene-0/100 heptol solutions over water. The diffusion coefficient, *D*, can be deduced from the interfacial tension at short times using the equation given by Campanelli and Wang (1999):

$$\gamma(t) = \gamma_o - 2RTc_o\sqrt{\frac{3Dt}{7\pi}} \tag{5.12}$$

where γ and γ_o are the interfacial tension of the surfactant-solvent solution and pure solvent over water (or another immiscible liquid), *R* the universal gas constant, *T* the temperature, c_o the bulk concentration of surfactant, and *t* the time. Equation (5.12) shows that for the short time diffusion approximation to apply, a plot of γ versus $t^{1/2}$ should be linear. The diffusion coefficient is then related to the slope of the plot as follows:

$$D = \frac{28\pi}{3}\left(\frac{slope}{RTc_o}\right)^2 \tag{5.13}$$

Figure 5.19 shows the diffusion coefficient as a function of bulk asphaltene concentration. Note that the methodology described in the preceding paragraph is applicable only at low asphaltene concentrations. At asphaltene concentrations greater than 0.2 kg/m³, the interfacial tension decreased during droplet formation. Hence, the value of IFT at time zero, i.e., when the droplet was fully formed, was less than the pure solvent IFT, rendering Equation (5.13) inapplicable. The diffusion coefficients shown in Figure 5.19 are somewhat consistent with the work of Norinaga *et al.* (2001). Using pulsed field gradient spin-echo NMR, they found that the diffusivity of Kafji vacuum residue asphaltenes in pyridine decreased from about 1.4×10^{-10} to 0.9×10^{-10} m²/s when the bulk asphaltene concentration increased from roughly 1 to 20 kg/m³. Although the decrease in diffusion coefficient with concentration also occurs, the data in Figure 5.19 are approximately one order of magnitude smaller than the work of Norinaga *et al.*

Figure 5.20 shows the experimental total, elastic and viscous moduli for 0/100 heptol-water interfaces as a function of asphaltene concentration. The interface aging time is 10 minutes and the oscillation frequency is 0.033 Hz. The model matches for the total, elastic and viscous moduli are also shown in Figure 5.20 and correspond to Equations (5.7), (5.10) and (5.11), respectively. The diffusion coefficient was taken as 3×10^{-11} m²/s, which falls in the range shown in Figure 5.19.

It is obvious from Figure 5.20 that the match was successful only for asphaltene concentrations less than 0.01 kg/m³. To see if the whole range of asphaltene concentration could be matched, the diffusion coefficient was treated as a fitting parameter. It was found that a concentration dependent asphaltene diffusivity of the following power law form was required to fit the elastic and viscous moduli in Figure 5.20:

$$D = ac_2^b \qquad (5.14)$$

where *a* and *b* are constants. The numerical values of *a* and *b* that best fit the elasticity data are 3×10^{-14} m²/s and -0.6, respectively.

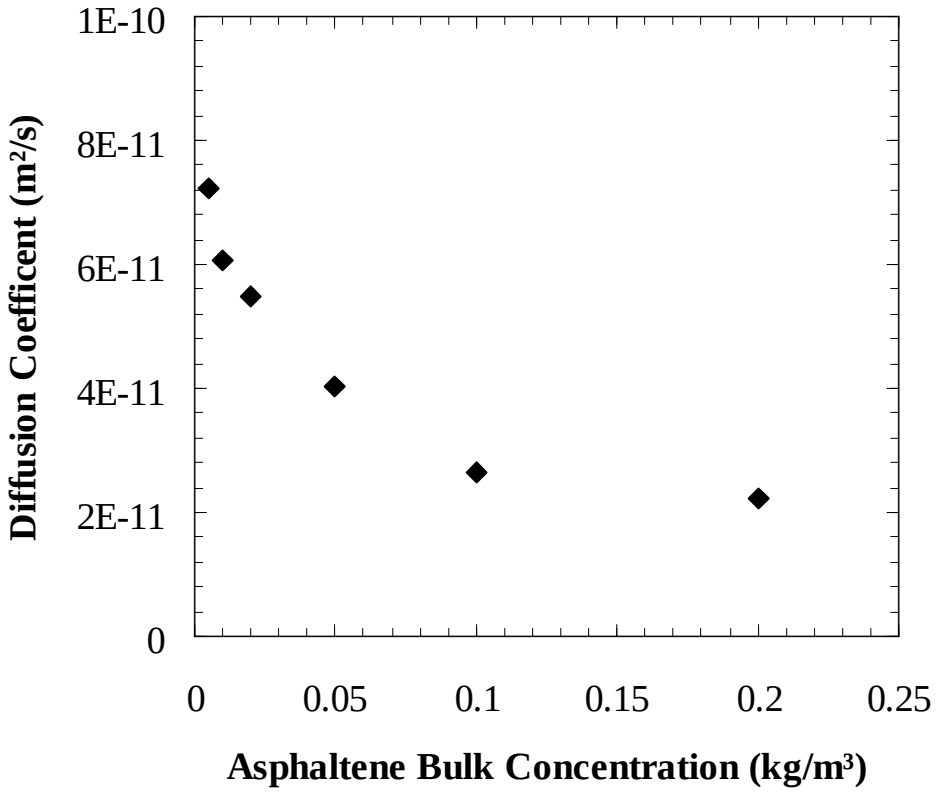

Figure 5.19: Diffusion coefficient for Athabasca Bitumen 2 Asphaltenes dissolved in 0/100 heptol as a function of asphaltene concentration as deduced from Equation (5.13)

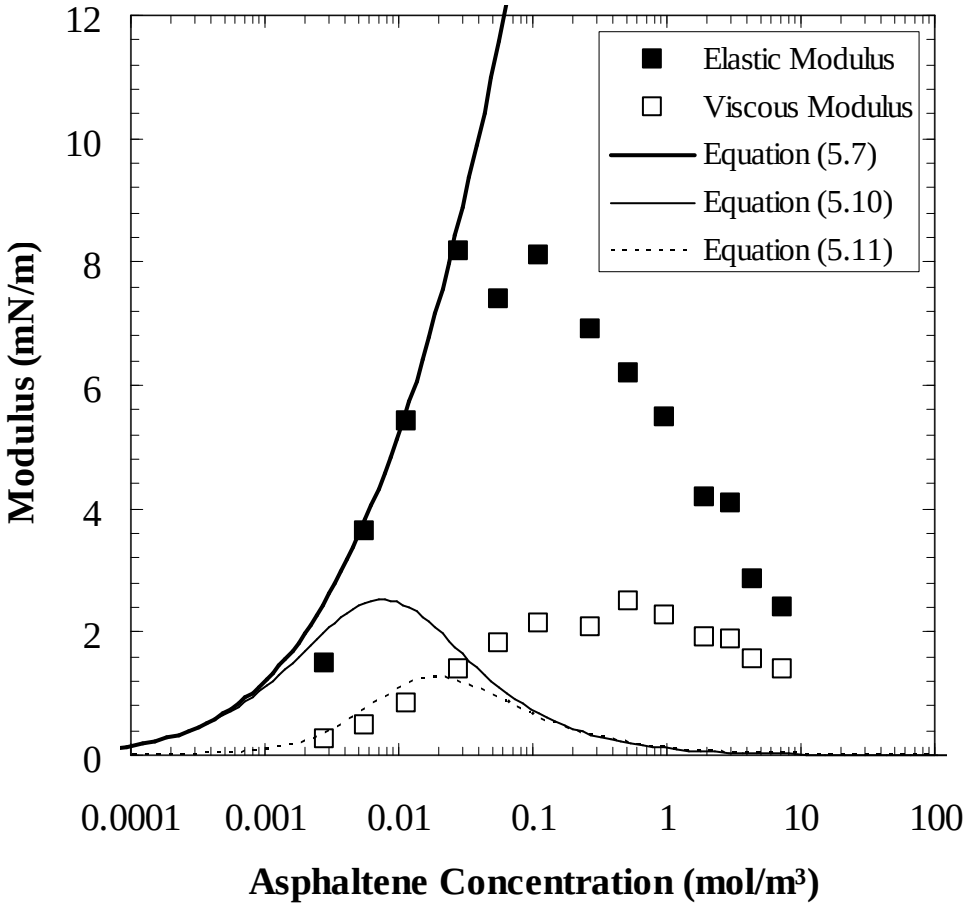

Figure 5.20: Measured and modeled elasticity of Athabasca Bitumen 2 Asphaltenes dissolved in 0/100 heptol solutions over water. Oscillation frequency 0.033 Hz, interfaced aged for 10 minutes. $D = 3 \times 10^{-11}$ m²/s

Equation (5.14) indicates that the diffusivity at the lowest asphaltene concentration shown in Figure 5.20 is approximately 10^{-12} m²/s and decreases to approximately 10^{-14} m²/s at the highest concentrations. Hence, the diffusivity required to match the full range in asphaltene concentration is anywhere from two to four orders of magnitude lower than the values of Norinaga *et al.* (2001) or the values obtained from the short-time diffusion approximation shown in Figure 5.19.

Why is the diffusivity needed to match the full range in asphaltene concentration so much smaller? One reason is that the diffusion coefficient relevant for relaxation of asphaltenes at the interface is not the bulk diffusion coefficient as deduced from the short-time diffusion approximation. Although asphaltenes diffuse to the interface quite quickly, their movement at the interface during droplet expansion/contraction may be retarded due to the formation of skins on the interface. The formation of viscous films may result in slower diffusion along the interface during oscillation and therefore the bulk diffusion may not be representative during interfacial relaxation. Sheu *et al.* (1995) speculated that arrangement of asphaltenes on the interface may be slower than the diffusion process and can therefore become the "bottleneck" of the equilibrium kinetics.

The preceding argument is somewhat supported by the work of Freer and Radke (2004). They measured the elastic and viscous moduli of an asphaltene-toluene-water interface at an asphaltene concentration of 0.05 kg/m³ over six decades of frequency. They used a combination of an LVDT model and a Maxwell visco-elastic model to match their data. Since their data was collected at only one asphaltene concentration, they did not need to predict the instantaneous elasticity from a Surface Equation of State or any other equation that would relate the instantaneous modulus to the concentration. Rather, they regressed ε_o, the characteristic time of diffusion, τ_D, (see Equation (5.9)), and two other parameters that were required for the Maxwell visco-elastic part of the model until a satisfactory match was obtained over the entire frequency range. They found a characteristic diffusion time of 25 s. The expression for the diffusion coefficient used in this thesis results in a

characteristic time of diffusion of 88 s at a concentration of 0.05 kg/m^3. The two diffusion times, and therefore diffusivities, are of similar magnitude.

Figures 5.21 and 5.22 compare the predicted instantaneous, elastic and viscous moduli with experimental data for asphaltene-0/100 heptol over water interfaces aged for 10 minutes. The oscillation frequencies in Figure 5.21 are 0.033 and 0.1 Hz. The frequencies in Figure 5.22 are 0.2 and 0.5 Hz. The same values of *a* and *b* in Equation (5.14) are used for each oscillation frequency. The model matches appear satisfactory, although it is apparent that the viscous modulus is slightly over-predicted at lower frequencies.

5.2.2.3 Effect of Interface Aging Time

Recall that the results in Figure 5.21 and 5.22 were obtained after 10 minutes of contact between the hydrocarbon phase and the aqueous phase. Figure 5.8 showed the increase in the elastic and viscous moduli as the interface aging time increased from 10 minutes to 16 hours. The increase in the moduli over time could not be predicted with the Lucassen-Van Den Tempel model, as shown in Figure 5.23. A possible explanation for the model failure is that irreversible adsorption occurs and a mechanical film forms.

Confirmation was obtained for mechanical film formation in Jafari's (2005) crumpling experiments. In crumpling experiments, the fluid is withdrawn from the asphaltene-solution droplet after some contact (or aging) time and the shape of the droplet observed. Her results are reproduced in Figure 5.24. At short aging times, the droplet surface remained smooth as the drop shrank. After sufficient aging, the droplet surface crumpled when the drop was retracted into the capillary. The aging time required for a crumpling film to appear decreases with increasing asphaltene concentration. The solid line in Figure 5.24 represents a film lifetime of 30 minutes; that is, after droplet contraction, the observed skin persisted for 30 minutes before a smooth surface was restored.

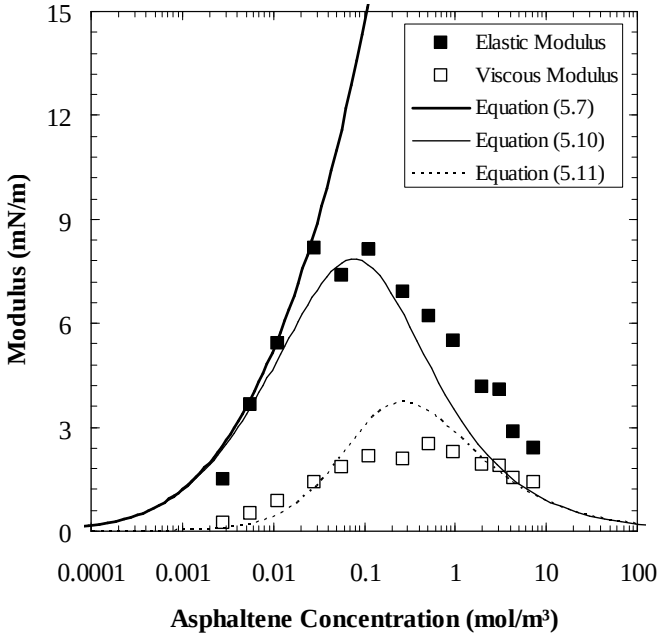

(a) f = 0.033 Hz

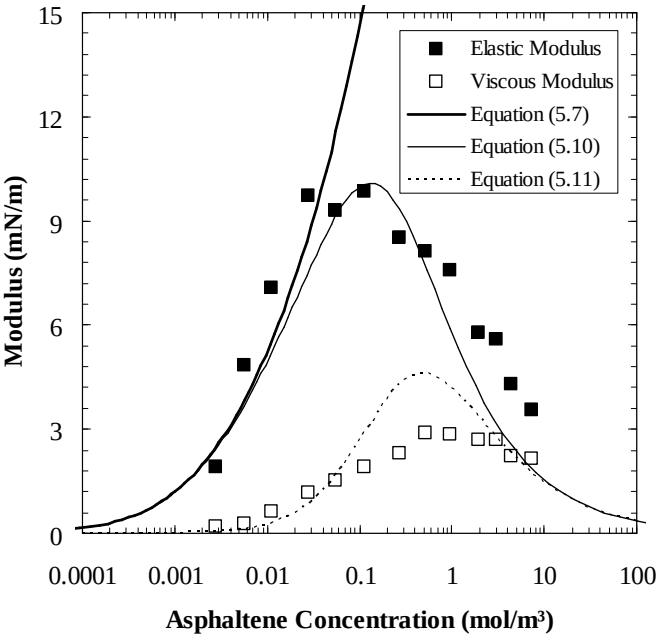

(b) f = 0.1 Hz

Figure 5.21: Measured and modeled elasticity of Athabasca Bitumen 2 Asphaltenes dissolved in 0/100 heptol solutions over water for oscillation frequencies of a) f = 0.033 Hz, b) f = 0.1 Hz. Interface aged for 10 minutes

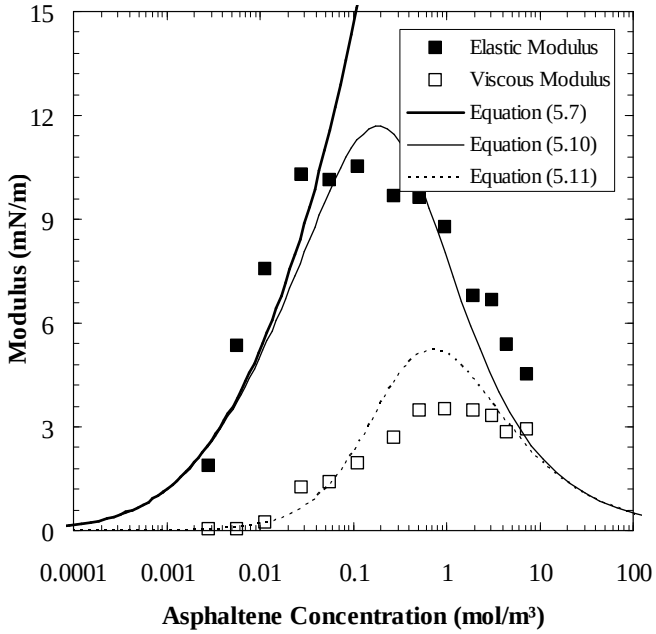

(a) f = 0.2 Hz

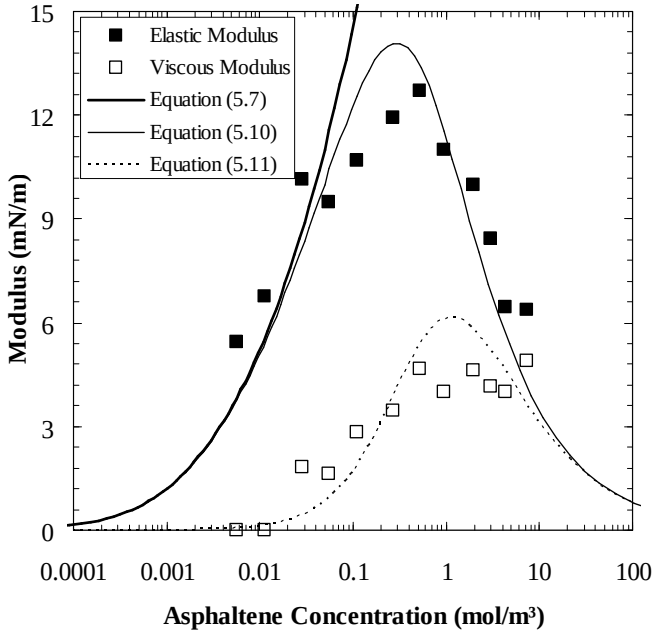

(b) f = 0.5 Hz

Figure 5.22: Measured and modeled elasticity of Athabasca Bitumen 2 Asphaltenes dissolved in 0/100 heptol solutions over water for oscillation frequencies of a) f = 0.2 Hz, b) f = 0.5 Hz. Interface aged for 10 minutes

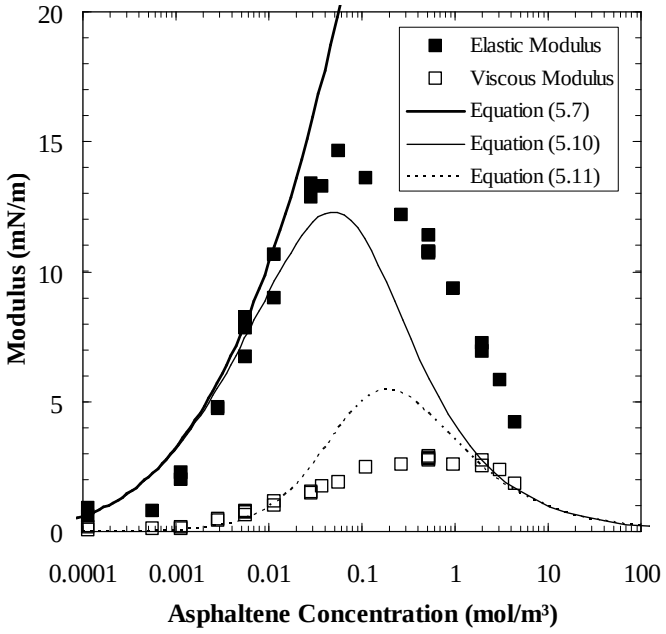

(a) f = 0.033 Hz

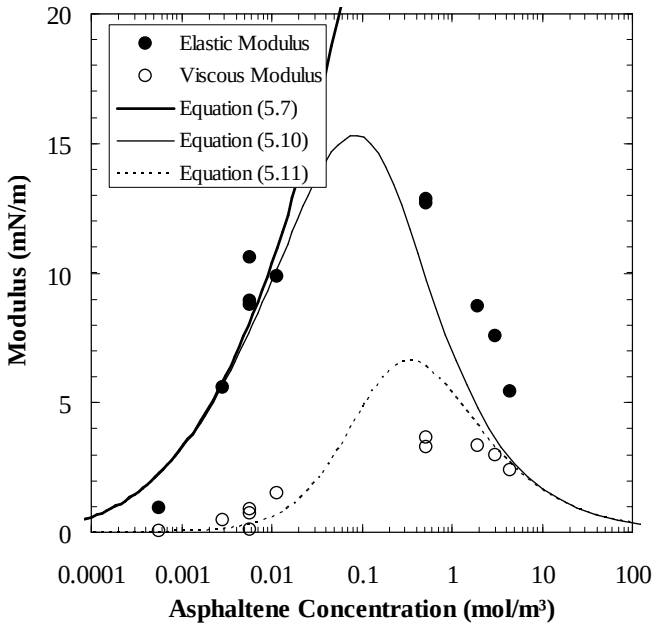

(b) f = 0.1 Hz

Figure 5.23: Measured and modeled elasticity of Athabasca Bitumen 2 Asphaltenes dissolved in 0/100 heptol solutions over water for oscillation frequencies of a) f = 0.033 Hz, b) f = 0.1 Hz. Interface aged for 4 hours

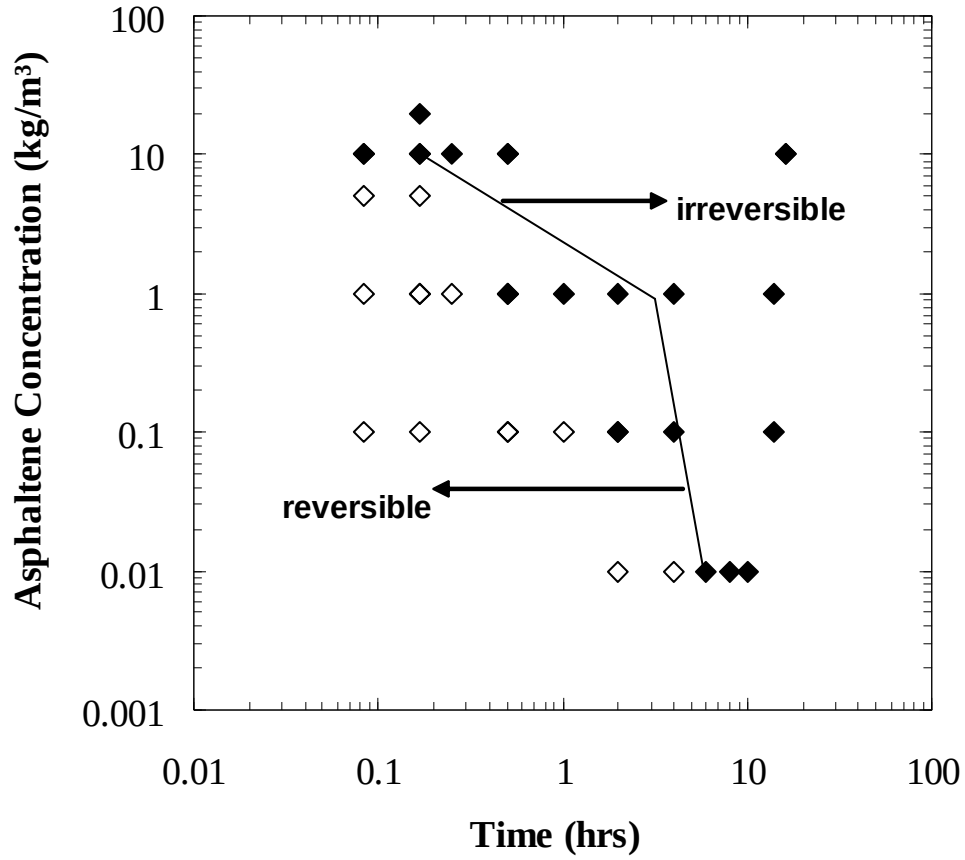

(a) reversible b) irreversible

Figure 5.24: Crumpling of Athabasca Bitumen 2 Asphaltenes dissolved in 0/100 heptol solutions in water as a function of time and asphaltene concentration (Jafari, 2005)

Crumpling is direct evidence of film formation and indirect evidence that asphaltenes have adsorbed irreversibly. For the SEOS-LVDT approach to be valid, asphaltenes must be adsorbed reversibly. Hence, in order to model the entire range of asphaltene concentration (i.e., less than 0.01 up to 20 kg/m³), only moduli measured at interface aging times less than 0.167 hours, or ten minutes, can be considered. It is not surprising that the modeling approach failed at longer times. The small diffusion coefficients required to match the data suggest that asphaltene movement along the interface, rather than bulk diffusion to and from the interface, dominate the rheology. In fact, irreversible effects are probably present even before ten minutes, despite the fact that skins are not observed visually in the crumpling experiments. Therefore, an SEOS-LVDT modeling approach has limited application for asphaltene/heptol interfaces. A visco-elastic model such as the Maxwell model can potentially be used as shown by Freer and Radke (2004). Unfortunately, a predictive model is not yet available. The work of Radke and Freer relied on regression of several parameters for a match of the elastic and viscous moduli of toluene-water interfaces stabilized by asphaltenes.

5.3 CHAPTER CONCLUSIONS

The methodology for assessing interfacial structure, presented in Chapter 4, indicated that asphaltenes initially adsorb on the interface as a monolayer of self-associated macromolecules. The modeling work presented in this chapter showed that the monolayer is probably adsorbed reversibly at early times. Its properties can be modeled using the Lucassen-Van Den Tempel approach when the aging time is less than 10 minutes.

The elasticity measurements suggest that the asphaltenes gradually reorganize on the interface to form a rigid irreversibly adsorbed network, as shown in Figure 5.25. As discussed in Chapter 2, the existence of such a network has been hypothesized in the literature. It has also been observed indirectly in elasticity measurements of similar systems (Freer and Radke, 2004; Spiecker and Kilpatrick, 2004). The recent work of Jafari (2005) also supports asphaltene reorganization at the interface.

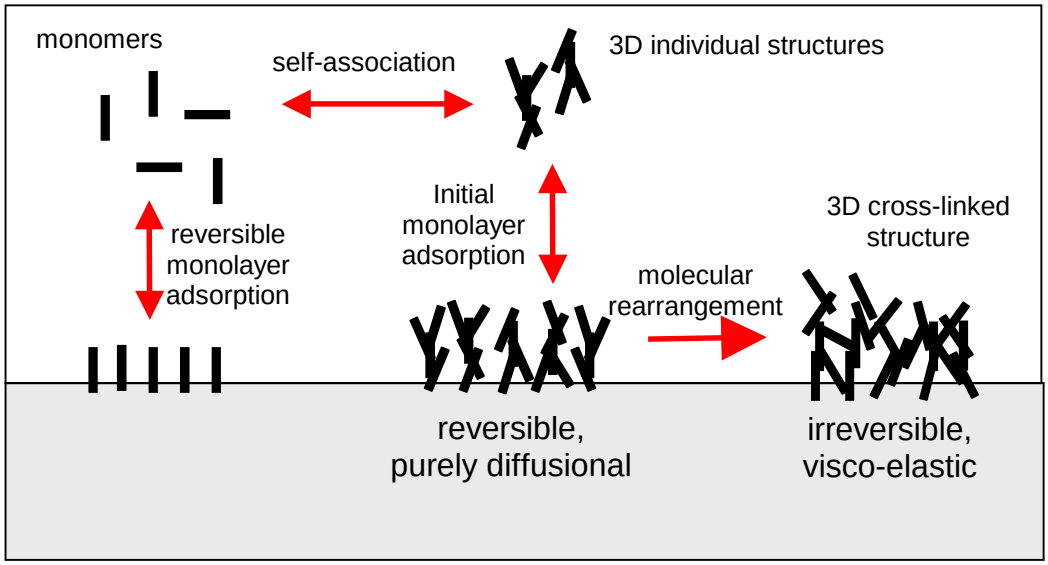

Figure 5.25: Possible steps in the formation of reversible and irreversible asphaltene films on a water-oil interface

CHAPTER 6

THE ROLE OF ASPHALTENES IN EMULSION STABILITY

This chapter attempts to relate the rate of coalescence of an emulsion and ultimate emulsion stability to the rheological properties of the interface. Section 6.1 relates the coalescence rate to the measured total elastic modulus by examining the changes in the droplet size and the total modulus of interfaces aged up to 24 hours. Section 6.2 presents the free water resolution of aged emulsions and attempts to relate emulsion stability to the rheological properties. Section 6.3 provides concluding remarks for this chapter.

6.1 COALESCENCE RATE AND INTERFACIAL ELASTICITY

The stability of an emulsion is at least in part related to the rate of coalescence of the droplets within the emulsion. As described in Chapter 2 and illustrated previously in Figure 2.5, coalescence between two drops occurs in several steps. First, droplets come into close contact through processes such as creaming/sedimentation and/or aggregation. As the droplets approach each other, their surfaces begin to deform such that planar interfaces are created between the drops. Simultaneously, the continuous phase drains from between the drops. As the surface deforms, it stretches and pockets of surfactant-free areas are created. Further drainage from between drops occurs and at some point, when the drops are within a few nanometers of each other, the dispersed phase fluid can bridge the gap between the drops in the surfactant-free areas and trigger coalescence.

The probability of coalescence is reduced if: the droplets do not come into close contact; drainage is hindered; there is strong resistance to dimpling; or the surfactant diffuses rapidly into the dimpled area. For the model water-in-heptol emulsions employed in this thesis, the chances of very poor sedimentation and aggregation are probably low because the viscosity of the continuous phase is relatively small (same order of magnitude as water) and the density difference between the water and continuous phase is appreciable

for each solvent quality tested. Hence, coalescence of the model emulsions is most likely related to the effectiveness of film drainage, dimpling, and the likelihood of asphaltene diffusion into interfacial areas that have stretched as a result of dimpling (i.e., relaxation).

The rheological properties of the film are a factor in both dimpling and relaxation. A high elasticity (that is, total modulus) means that a change in interfacial area significantly increases the interfacial tension and therefore the energy of the system. Hence, there will be more resistance to the dimpling (an area change) and a greater driving force for relaxation processes (high interfacial tension gradient). Therefore, it is hypothesized that as the elasticity of the interface increases, the interfacial film becomes stronger. A stronger interfacial film may reduce the rate of coalescence and increase the overall stability of the emulsion.

In order to see if a correlation between the elasticity and the coalescence rate exists, the elastic and viscous moduli and the droplet diameter of emulsions were measured at various interface aging times. Athabasca Bitumen 2 Asphaltenes, treated to remove solids using the Centrifugation technique, were employed for all rheological measurements and in all emulsion drop size experiments. Three solvents (0/100, 25/75, 50/50 heptol) and three asphaltene concentrations (5, 10, 20 kg/m^3) were tested. The interfaces were aged up to 24 hours. To summarize, three steps were taken to check the existence of a correlation between coalescence rate and interfacial elasticity:

1. Measurement of drop size as a function of time and the calculation of the rate of change of the drop size (*i.e.*, the coalescence rate).
2. Measurement of elastic and viscous moduli as a function of time.
3. Cross-plotting of the coalescence rate and the total modulus.

6.1.1 Sauter Mean Diameter of Aged Emulsions and Droplet Coalescence Rate

In order to calculate the rate of coalescence of water drops, the droplet diameter at any given asphaltene concentration and solvent quality is found as a function of time. For a fair comparison, the initial droplet diameter should be the same at each asphaltene concentration for any given solvent quality. Emulsions with large initial diameters are likely to have a faster coalescence rate than those with smaller diameters because larger droplets are more likely to deform and merge upon collision. Hence, any existing rheological properties may be overshadowed by the large initial diameter. Figure 6.1 (reproduced from Figure 4.14 from Chapter 4) presents the Sauter mean diameter (d_{32}) as a function of asphaltene concentration for 0/100, 25/75 and 50/50 heptol, 40 vol% water, emulsions aged for 1.5 hours. It is apparent that at any solvent quality, the diameter is nearly constant for asphaltene concentrations exceeding 3 to 5 kg/m³. Therefore, the minimum bulk asphaltene concentration utilized in the aging studies was 5 kg/m³. Two other bulk asphaltene concentrations, 10 and 20 kg/m³, were also tested. Note that the minimum Sauter mean diameter that can be created at the experimental homogenization rate and time (18000 rpm and five minutes, respectively) is approximately 7.5 to 8 microns. Therefore, it is likely that during the 1.5 hours settling time, some coalescence of 25/75 and 0/100 emulsions occurred because the limiting Sauter mean diameter for these conditions approaches 9 and 11 microns, respectively. However, when the concentration exceeds 5 kg/m³, the diameter is approximately constant within a given solvent quality.

As an emulsion coalesces, droplets merge producing fewer but larger drops. However, an increase in the Sauter mean diameter may also occur if an emulsion undergoes Ostwald ripening. Recall that in Ostwald ripening, concentration gradients existing at the surfaces of drops prompt mass transfer to occur from smaller to larger drops. The larger drops grow and the smaller drops eventually disappear. Coalescence and Ostwald ripening can be distinguished by comparing the changes in the shape of the drop size distribution over time.

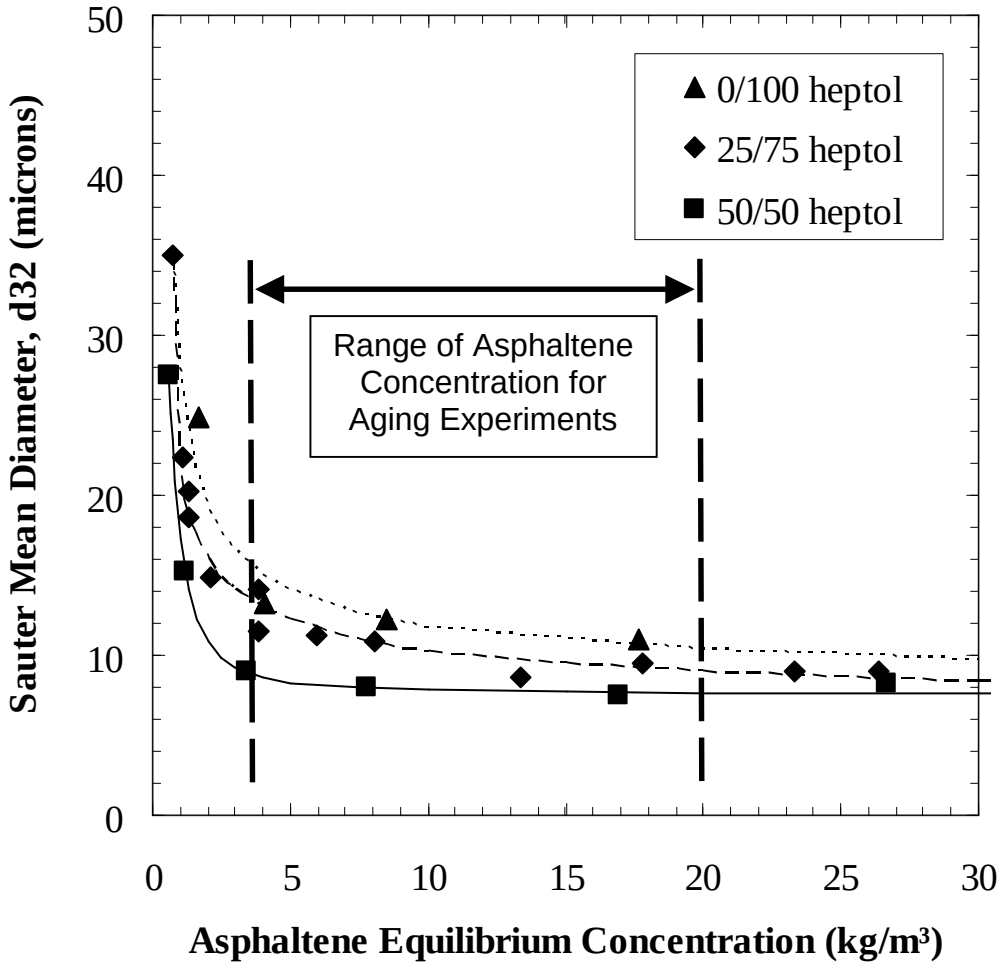

Figure 6.1: Initial Sauter mean diameter of settled emulsions prepared with 40 vol% water and solutions of Athabasca Bitumen 2 asphaltenes dissolved in 0/100, 25/75 or 50/50 heptol. Initial Time = 1.5 hours interfacial aging. The lines are visual aides.

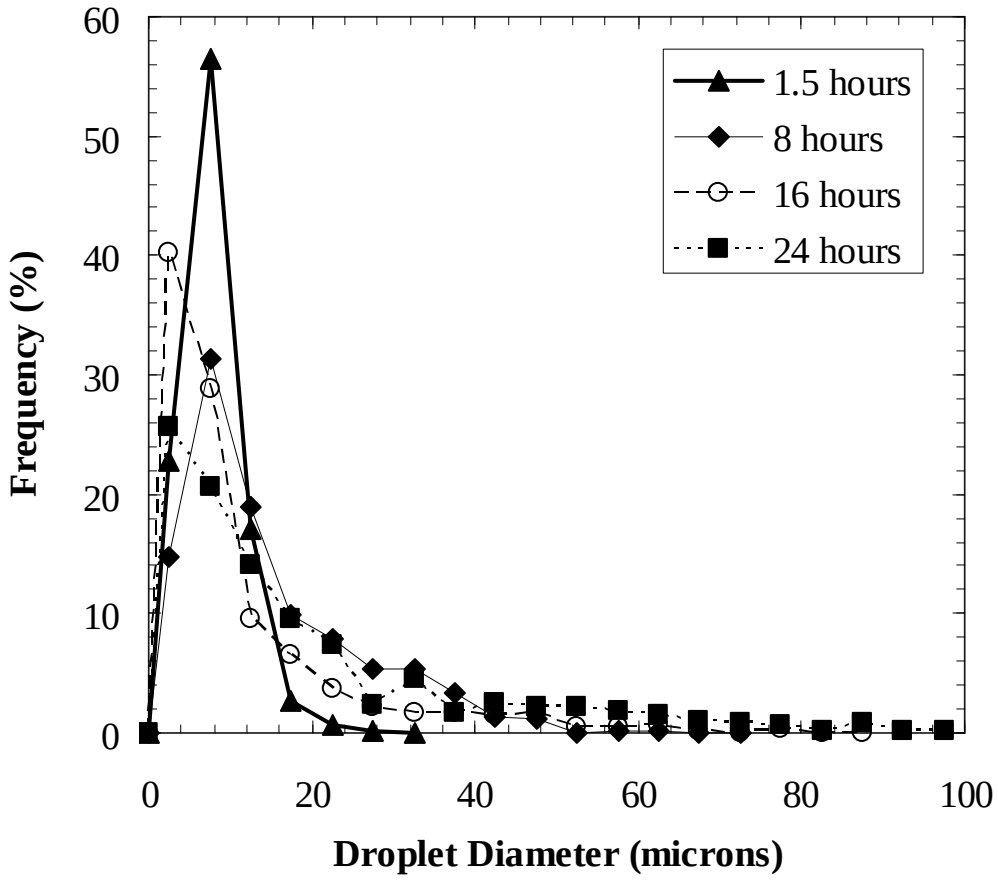

Figure 6.2: Drop size distribution of aged emulsions prepared from 40 vol% water and solutions of Athabasca Bitumen 2 Asphaltenes dissolved in 0/100 heptol. 20 kg/m³ bulk concentration

Coalescence is probabilistic and some small droplets remain intact so that an ever-broadening drop size distribution is observed. During conventional Ostwald ripening, the smaller drops are expected to disappear and the entire drop size distribution shifts to higher diameters. In cases where the small droplets stop shrinking due to rigid film formation, two distinct peaks develop in the drop size distribution (Yarranton, 1997). Figure 6.2 shows the drop size distribution at various times for a bulk asphaltene concentration of 20 kg/m³ and 0/100 heptol. Note that the largest increases in Sauter mean diameter were observed for this system. Although the frequency of small drops decreases with time, a large portion of drops is still less than 20 microns. Also, only one peak is observed in the drop size distribution. Therefore, at aging times below 24 hours, coalescence is likely the only mechanism responsible for the increased Sauter mean diameter. Further, in a study of Athabasca Asphaltene-Solids stabilized water-in-toluene/hexane emulsions, Yarranton (1997) showed that Ostwald ripening only has significant effects on the Sauter mean diameter once the aging time exceeds 100 hours. In that study, coprecipitated solids were not removed from the Asphaltene-Solids. It is possible that solids retard Ostwald ripening; however, the differences are not expected to be great at the concentrations considered here because, in Yarranton's work, the associated solids content at these concentrations was relatively low.

Figures 6.3 (a), (b) and (c) present the Sauter mean diameter as a function of time for emulsions prepared with 40 vol% water and 0/100, 25/75 and 50/50 heptol, respectively. In each figure, the Sauter mean diameter is compared at 5, 10 and 20 kg/m³. Alternatively, the Sauter mean diameter could be compared at each concentration for the different solvent qualities. An example of such a plot is shown in Figure 6.3 (d), which shows the effect of solvent quality on Sauter mean diameter at a bulk asphaltene concentration of 10 kg/m³. It appears that at all asphaltene concentrations and solvent qualities, the droplets increase in size. However, the extent of coalescence is different depending on the bulk asphaltene concentration and solvent quality. One measure of the rate of coalescence is the slope of the Sauter mean diameter (d_{32}) versus time. To

facilitate accuracy when finding the slopes as a function of time, equations of the form given in Equation (6.1) were first fit to the data in Figure 6.3:

$$d_{32} = \frac{1}{2}\left(at^2 + bt\right) + \frac{1}{2}\left(d \ln t\right) + c \qquad (6.1)$$

Equation (6.1) is the average of a quadratic and logarithmic function. The constants *a*, *b*, *c* and *d* are fit parameters. Note that neither the form of Equation (6.1) nor the fit parameters have any physical meaning; simply, through trial and error, it was found that this equation gave satisfactory matches for all asphaltene concentrations and solvent qualities. The results of the fits are shown as lines in Figure 6.3. The AARD of all of the fits is less than 5%, as shown in Appendix A, Section A.6.

The derivative of Equation (6.1) gives the coalescence rate. The coalescence rate as a function of time is shown in Figures 6.4 (a), (b) and (c) for 0/100, 25/75 and 50/50 heptol at the three bulk asphaltene concentrations of interest. Figure 6.4 (d) shows the coalescence rate for a bulk asphaltene concentration of 10 kg/m³ for the three solvent qualities. The following observations can be made from Figures 6.3 and 6.4:

1. coalescence rate decreases as the interface is aged
2. the coalescence rate decreases as the heptane content increases
3. the coalescence rate increases at higher asphaltene concentration except in the 50/50 heptol system

Before interpreting these trends, the interfacial elastic moduli are considered at the same conditions.

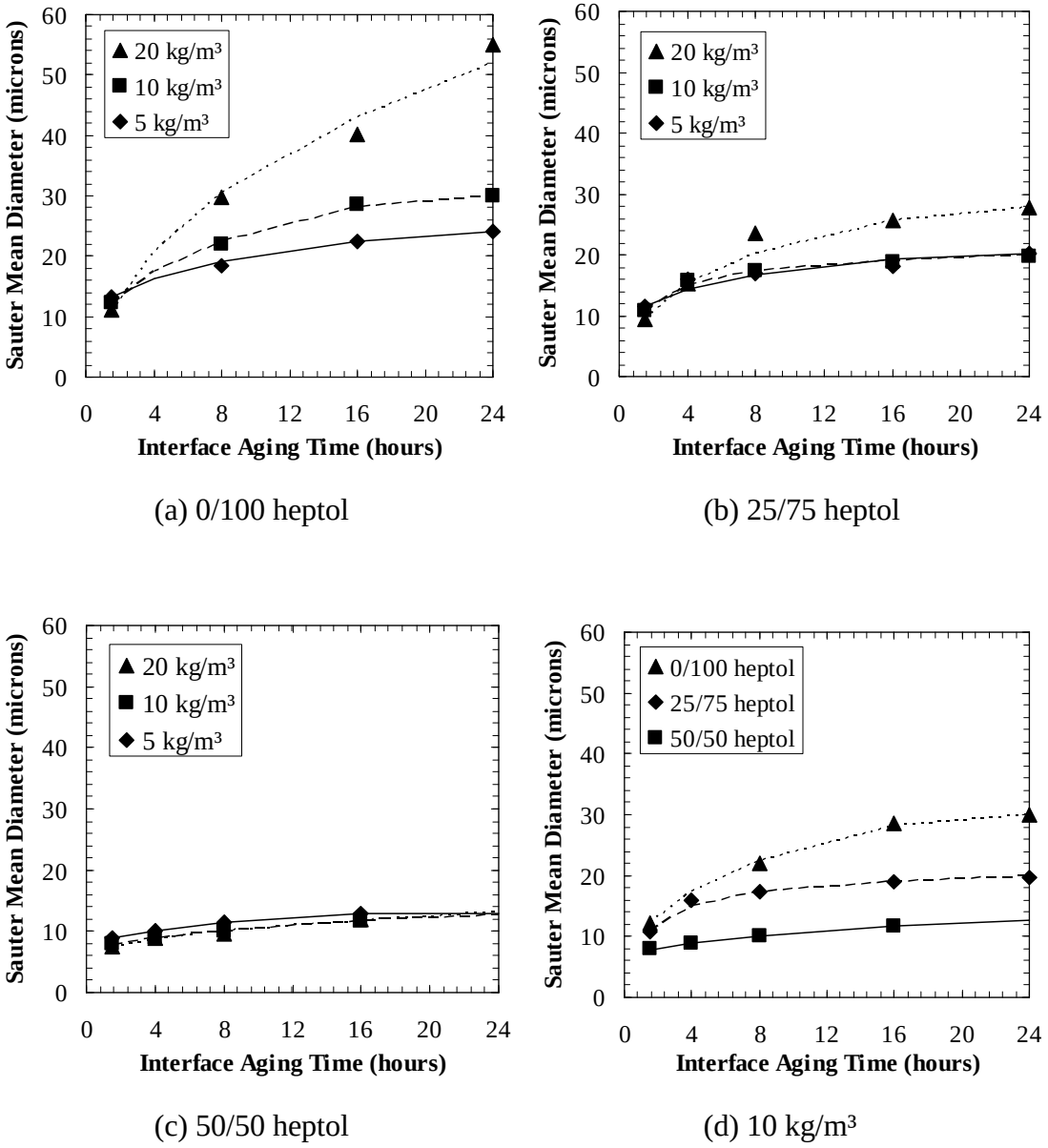

Figure 6.3: Sauter mean diameter for aged emulsions prepared from 40 vol% water and solutions of Athabasca Bitumen 2 asphaltenes in a) 0/100 heptol, b) 25/75 heptol, c) 50/50 heptol. The data at 10 kg/m³ bulk asphaltene concentration are replotted in (d) for 0/100, 25/75 and 50/50 heptol. The lines are curve fits using Equation (6.1).

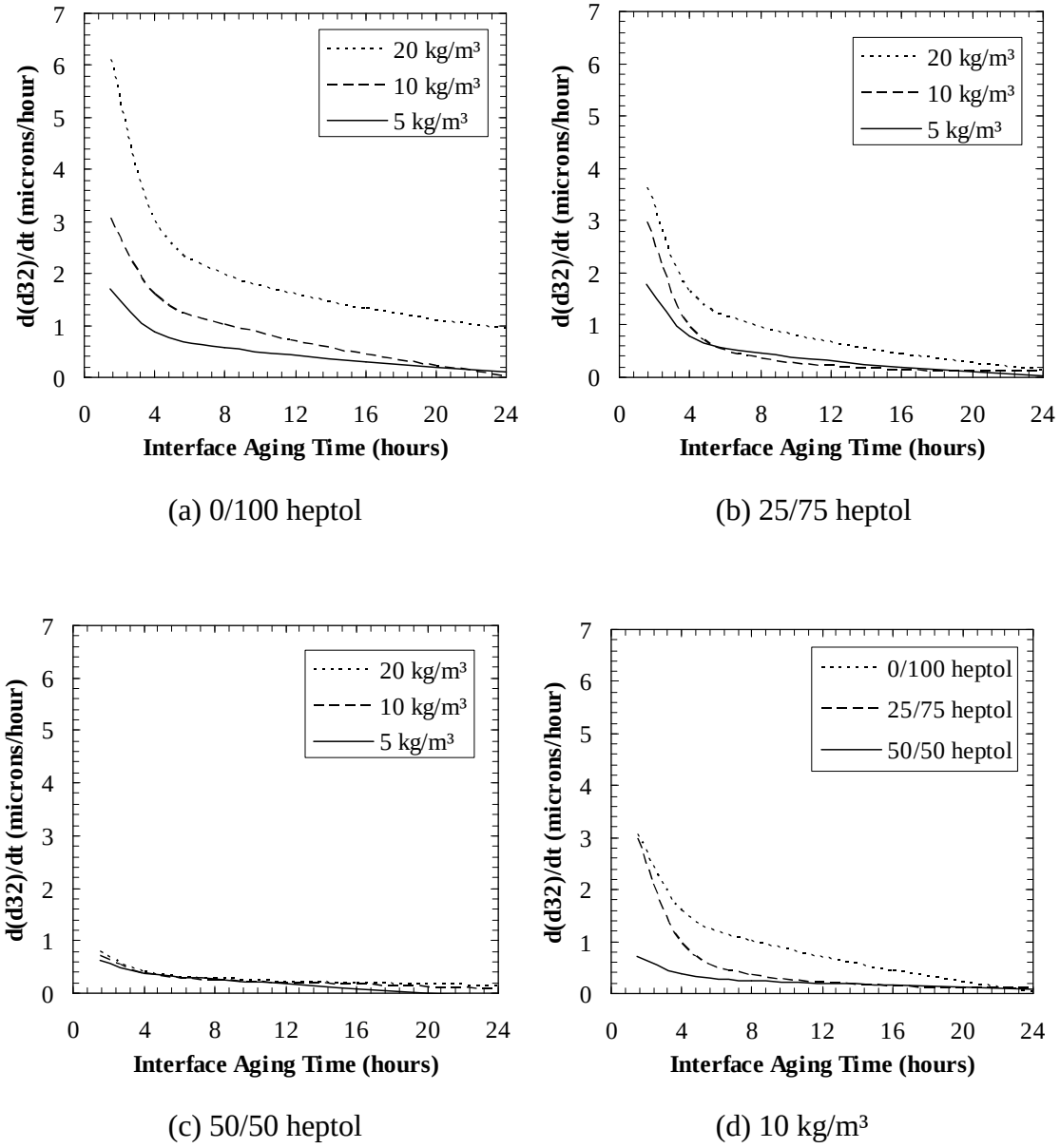

(a) 0/100 heptol

(b) 25/75 heptol

(c) 50/50 heptol

(d) 10 kg/m³

Figure 6.4: Coalescence rate for aged emulsions prepared from 40 vol% water and solutions of Athabasca Bitumen 2 Asphaltenes dissolved in a) 0/100 heptol, b) 25/75 heptol, c) 50/50 heptol. The data at 10 kg/m³ bulk concentration are replotted in (d) for 0/100, 25/75 and 50/50 heptol. The lines correspond to the derivative of Equation (6.1) with respect to time

6.1.2 Total Elastic Modulus of Aged Interfaces

Figures 6.5 (a), (b) and (c) present the total modulus measured at an oscillation frequency of 0.033 Hz for 0/100, 25/75 and 50/50 heptol-water interfaces, respectively. In each figure, the modulus is presented for 5, 10 and 20 kg/m³ at each solvent quality. The effect of solvent quality at 10 kg/m³ bulk asphaltene concentration is shown in Figure 6.5 (d). The following observations can be made from Figures 6.5:

1. the total modulus increases as the interface is aged
2. the total modulus increases as the heptane content increases
3. the total modulus decreases as asphaltene concentration increases

The trends in coalescence and elasticity appear to be consistent. Recall that an increase in the total modulus is believed to be the result of increased film rigidity (Freer and Radke, 2003; Freer and Radke, 2004; Spiecker and Kilpatrick, 2004). Figure 5.25 illustrated how an initially adsorbed asphaltene monolayer could undergo molecular rearrangement and form a three dimensional, cross-linked network structure on the interface. It is speculated that increased film rigidity should result in interfaces that are more difficult to rupture. Hence, the rate of coalescence should also be reduced.

The first set of observations from Figures 6.4 and 6.5 showed that as the interface ages, the total modulus increases and the rate of coalescence decreases. The development of more rigid films with time is consistent with a reduction in the rate of coalescence. The second set of observations indicated that when the heptane fraction in heptol increases, the total modulus increases and the rate of coalescence decreases. It is to be expected that a more rigid film is formed in a less aromatic solvent (a poorer solvent for asphaltenes) because the asphaltenes are more likely to strongly adsorb and cross-link in a poorer solvent. Hence, the probability of coalescence is reduced in a poorer solvent. In fact, the final Sauter mean diameter of the water droplets is significantly less for a more paraffinic continuous phase.

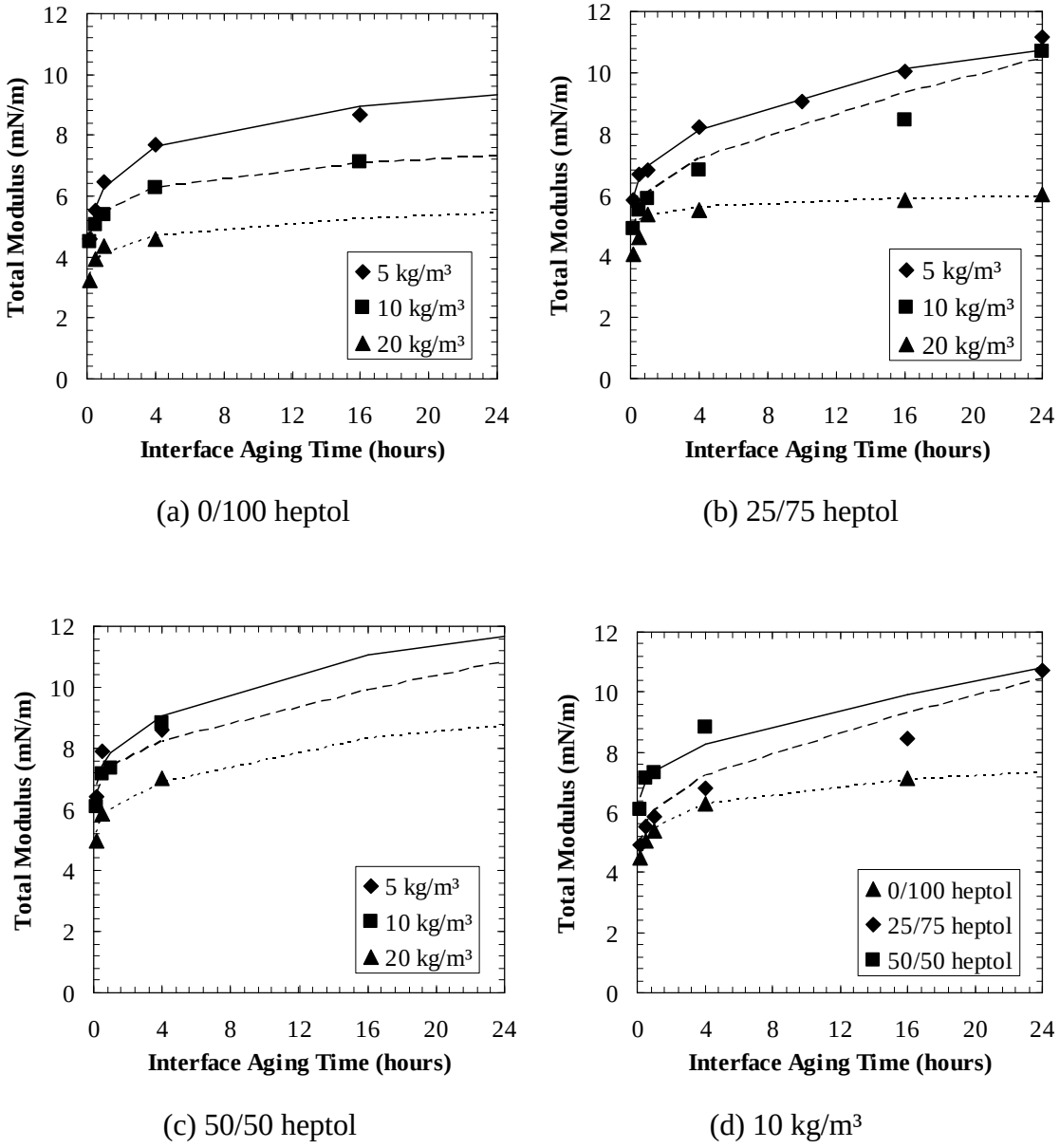

(a) 0/100 heptol

(b) 25/75 heptol

(c) 50/50 heptol

(d) 10 kg/m³

Figure 6.5: Total modulus for Athabasca Bitumen 2 Asphaltenes dissolved in a) 0/100 heptol, b) 25/75 heptol, c) 50/50 heptol over water. The data at 10 kg/m³ bulk concentration are replotted in d) for 0/100, 25/75 and 50/50 heptol. The lines are curve fits using Equation (6.1)

The third set of observations showed that as the asphaltene concentration decreases, the total modulus increases and the rate of coalescence decreases. Note that the asphaltene concentrations considered here are those relevant for emulsion stability, i.e., higher than 2 kg/m³. Also, note that the rate of coalescence for a 50/50 heptol solvent was independent of asphaltene concentration; it is likely that a 50/50 heptol continuous phase is sufficient to limit coalescence regardless of the asphaltene concentration. In general, film rigidity is reduced at higher asphaltene concentrations. At first glance, this result is surprising given that the mass surface coverage increases with concentration, as was shown in Figure 4.17. This trend is also in contrast to other studies which suggest that an increase in asphaltene concentration will result in more rigid films (Jeribi *et al.*, 2002; Bauget *et al.*, 2001; Li *et al.*, 2002). However, reduced film rigidity with an increase in the concentration of surface-active species is consistent with the work of Yeung *et al.* (1999). It appears that the high concentrations increase diffusional flux from the bulk phase and relaxation on the interface sufficiently to weaken the interfacial film. Note that the overall diffusion increases (elasticity decreases) with concentration even though the diffusivity appears to decrease.

The preceeding observations suggest that there is a correlation of coalescence rate to the total modulus. An increase in the total modulus and a decrease in the coalescence rate occur when the interface is aged, the heptane fraction in heptol increases, and the asphaltene concentration decreases. To see the strength of the correlation, the data from Figures 6.4 and 6.5 are cross-plotted in a single figure.

Before examining the cross-plotted data, it is important to note that there is some scatter in the total modulus versus time curves. Further, measuring the total modulus is very time consuming because a fresh drop must be made for each time point. To reduce the number of measurements, some of the intermediate aging times were interpolated from curves of the form given by Equation (6.1) fit to the total modulus versus time data. The AARD of the fits is less than 6% for all cases, as shown in Appendix A, Section A.5. The fits are shown as lines in Figure 6.5 and serve primarily as visual aides. Although the curves in

Figure 6.5 suggest that the most rapid increase in the total modulus occurs in the first four to eight hours, it is difficult to speculate about the shape of the total modulus curve beyond 24 hours. For example, Freer *et al.* (2003) observed two different trends in the elastic and viscous moduli in an oscillatory rheological study of crude oil/water interfaces. For oil "AS", the elastic modulus increased rapidly from ~4.5 to ~5.5 mN/m over the course of an hour, but then remained constant for the next 25 hours. The viscous modulus had the same trend but was lower in magnitude. The second oil, oil "AH", had similar initial trends in the elastic and viscous moduli: a rapid initial increase in the moduli over the first hour (from ~3.5 to 7 mN/m) was followed by constant values for the next ~15 hours. However, over the next 50 hours, the moduli increased an additional 35% (from 7 to 9.5 mN/m). It was speculated that the surface active components (likely asphaltenes) in oil AH caused formation of rigid skins that developed over time.

Also note that the total modulus could not be measured at interface aging times beyond four hours for the 50/50 heptol-water interfaces. In the 50/50 heptol solvent, the droplets that formed at the tip of the capillary deformed at long aging times and the shape was no longer Laplacian. A non-Laplacian drop invalidates the shape analysis. It is possible that a highly rigid skin formed that prevented meaningful measurements. Therefore, the moduli beyond four hours were extrapolated. As will be seen in Figure 6.6, even if the extrapolation is inaccurate, the cross-plot of modulus and coalescence rate will not be significantly altered. Most of the coalescence occurs in the first four hours for the 50/50 heptol/water emulsions, where the moduli are known.

6.1.3 Relationship between Total Modulus and Coalescence

Figure 6.6 cross-plots the coalescence rate for the aging times given in Figure 6.3 (i.e., 1.5, 4, 8, 16 and 24 hours) with the total modulus measured at the same aging time. Note that the total modulus was taken from the curve fits in Figure 6.5 if it was not available at the aging times of the emulsion droplet diameter measurements. Figure 6.6 shows that there is a general correlation between coalescence rate and the total modulus of the

heptol-water interface. Time is embedded in the data and increases along any concentration-solvent curve as the total modulus increases and coalescence rate decreases. Figure 6.6 shows that coalescence is reduced as the total modulus increases. Although a general correlation exists in Figure 6.6, the data seem to be grouped. The data from Figure 6.6 are reproduced in Figure 6.7 and divided into three groups as follows: Curve (a): 5 kg/m³, 0/100, 25/75, 50/50 heptol; 10 kg/m³, 25/75 and 50/50 heptol. Data falling between Curves (b): 10 kg/m³, 0/100 heptol; 20 kg/m³, 0/100 and 25/75 heptol. The 20 kg/m³, 50/50 heptol data appears to fall partially on Curve (a) and partially between Curves (b). It is examined independently and labeled as Curve (c) in Figure 6.7.

6.1.4 Expulsion of Asphaltene Mass from the Interface

The groupings of the data shown in Figure 6.7 are related to the extent to which asphaltenes are expelled from the water/oil interface during coalescence. Figures 6.8 (a), (b) and (c) present the mass of asphaltenes adsorbed on the interface as a function of time for emulsions prepared with 40 vol% water and 0/100, 25/75 and 50/50 heptol, respectively. In each figure, the mass on the interface is compared at 5, 10 and 20 kg/m³. Figure 6.8 (d) shows how mass on the interface varies with solvent quality for a bulk asphaltene concentration of 10 kg/m³. In these plots, the mass of asphaltenes on the interface, m_{AI}, is considered instead of the asphaltene mass surface coverage, Γ. Since the size of the droplets is significantly different at aging times beyond 1.5 hours for the various conditions examined, m_{AI} is a more relevant comparison. Also, note that m_{AI} depends on the total volume of emulsion. Therefore, comparisons of m_{AI} were made for the same total initial emulsion volume, which was 50 cm³.

The trends in Figure 6.8 are first compared for the systems in which the modulus-coalescence rate cross-plot point fell on Curve (a). For the 5 kg/m³ 0/100 heptol and 25/75 heptol systems, the mass on the interface remains constant with time for all solvent qualities. This is also true of the 10 kg/m³ 50/50 heptol and 25/75 heptol points, as indicated by Figures 6.8 (b) and (c), respectively. Therefore, as the emulsions coalesce, asphaltenes do not leave the interface.

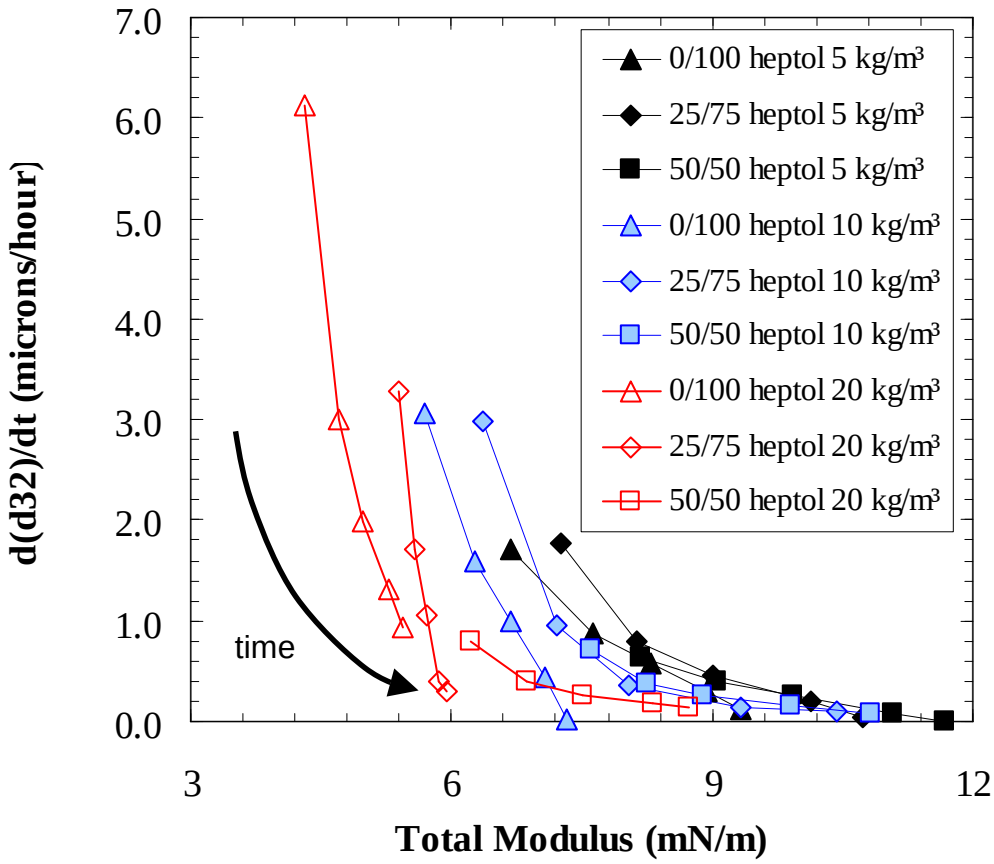

Figure 6.6: Cross-plot of change in Sauter mean diameter with total modulus.

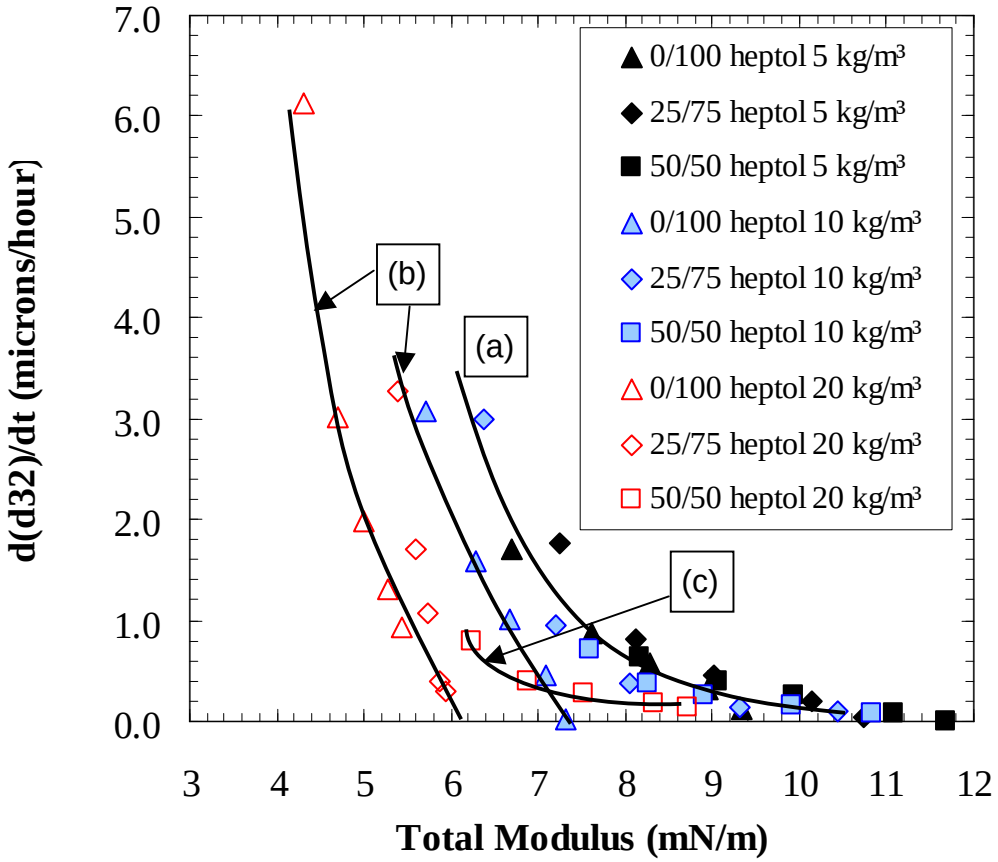

Figure 6.7: Crossplot of change in Sauter mean diameter with total modulus. Identification of three regimes

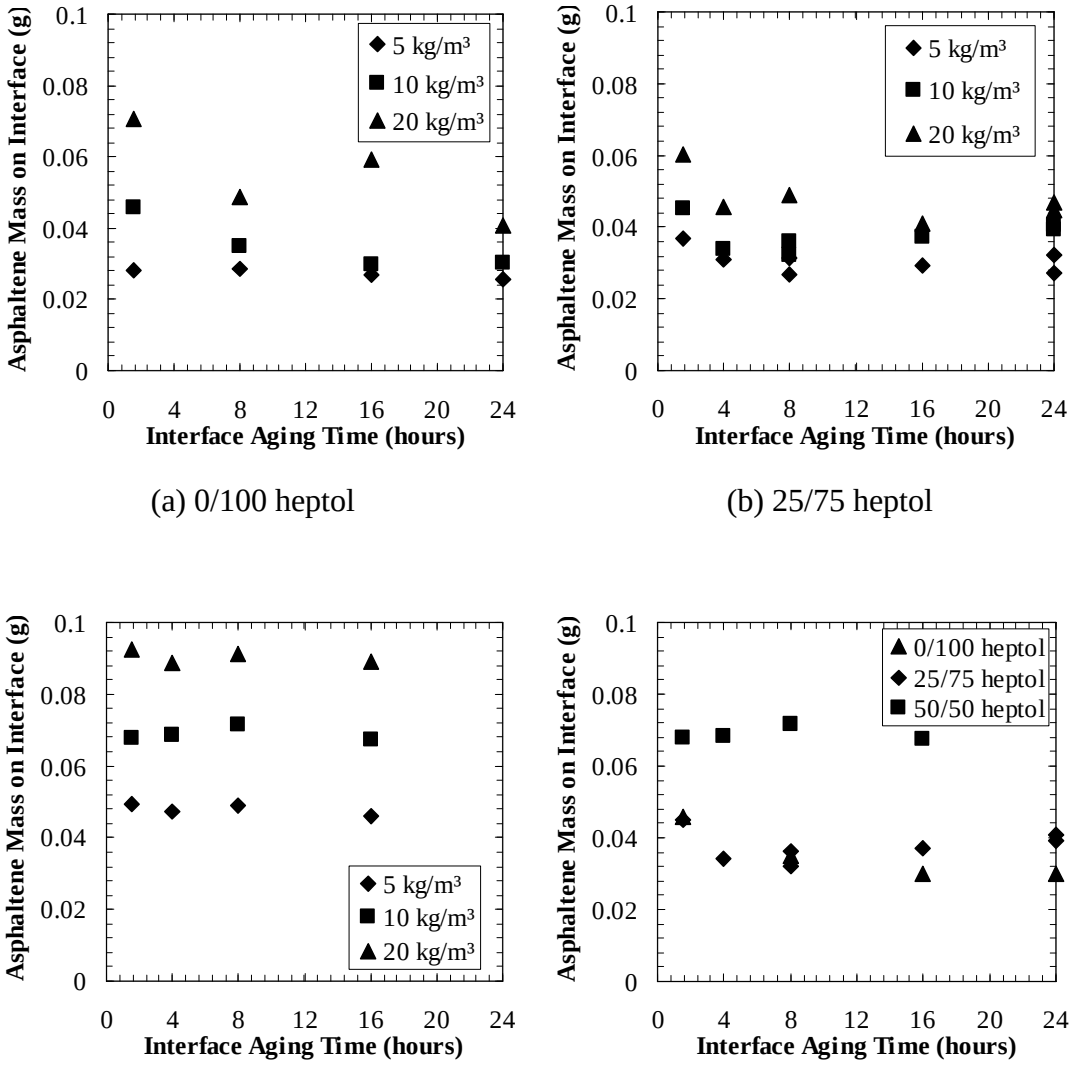

(a) 0/100 heptol

(b) 25/75 heptol

(c) 50/50 heptol

(d) 10 kg/m³

Figure 6.8: Mass of asphaltenes on the interface for aged emulsions prepared from 40 vol% water and solutions of Athabasca Bitumen 2 Asphaltenes dissolved in a) 0/100 heptol, b) 25/75 heptol, c) 50/50 heptol. The data at 10 kg/m³ bulk asphaltene concentration are replotted in (d) for 0/100, 25/75 and 50/50 heptol

The moduli along Curve (a) can therefore be thought of as measurements that accurately reflect the rheology of an aging interface because mass does not leave the interface either in the rheology or emulsion experiments.

The systems in which the cross-plot points fell between Curves (b) are compared next. For the 10 kg/m³ 0/100 heptol system, the mass of asphaltenes on the interface appears to decrease from 0.045 to 0.035 g over the 24 hour time period, as shown in Figure 6.8 (a). For the 20 kg/m³ 0/100 heptol and 25/75 heptol systems, there is also a decrease in the asphaltene mass adsorbed on the interface over the 24 hour period. Therefore, for the systems falling between Curves (b), mass is expelled from the interface during droplet coalescence. Since the extent of expulsion differs for each system, the cross-plot points do not all fall on one curve; rather, they appear to shift to the left hand side of the plot. The apparent shift can be explained as follows. During expulsion, some of the material is removed from the interface. The asphaltenes that are expelled are likely the ones most easily removed from the interface, whereas the remaining asphaltenes are the ones most difficult to remove. It is speculated that the remaining asphaltenes are those that can crosslink to the highest degree and form the strongest interfacial film. A stronger interfacial film exhibits a higher total modulus. Hence, a shrinking area in which asphaltenes are expelled will have a larger total modulus than one in which no material is removed. The total modulus measured with the Drop Shape Analyzer is indicative of a drop in which no mass has been expelled from the interface. Therefore, the moduli are under predicted and the cross-plot points fall to the left of Curve (a).

One way to check if removal of asphaltene mass results in an interface with higher rheological properties is to measure the total modulus for a drop in which the total interfacial area is reduced stepwise over the desired aging time. A reduction in droplet area is related to droplet coalescence in an emulsion because upon coalescence, the total area of the emulsion decreases. It is recommended that such experiments should be

performed in the future in order to account for coalescence and in order to accurately relate rheology to emulsion properties.

The final data left to analyze in Figure 6.7 is Curve (c). Figure 6.8 (c) shows that for the 20 kg/m³, 50/50 heptol emulsion, no mass is removed from the interface over the course of 16 hours. Hence, one would expect the cross-plot points to fall along Curve (a). Although this is possibly true for the furthest two points on the right hand side (which correspond to 8 and 16 hours), the points on the left hand side (1.5 and 4 hours) appear to fall between Curves (b). One possible explanation for Curve (c) is related to the formation of irreversible asphaltene skins on the interface; that is, films which crumple when contracted. As the heptane fraction in heptol increases, asphaltenes form irreversible rigid skins at lower asphaltene concentrations and earlier interface aging times (Jafari, 2005). Hence, it is possible that an irreversible rigid skin was formed very rapidly for the 20 kg/m³, 50/50 heptol emulsion. Irreversible rigid skins may prevent coalescence. Therefore, it appears that coalescence is related not only to the rheological properties of the interface, but also the formation of skins. Skin formation may have a significant effect on the ultimate stability of emulsions.

6.2 STABILITY OF ASPHALTENE-STABILIZED EMULSIONS

The cross-plot shown in Figure 6.7 demonstrated that coalescence in an emulsion is retarded when the rigidity of the interface is increased; i.e., when the total modulus increases. Since the total modulus correlated with the coalescence rate, a relationship between the total modulus and ultimate emulsion stability should also exist.

To see if a correlation between the total modulus and emulsion stability exists, the free water resolution was recorded after two hours of treatment for water-in-heptol emulsions stabilized by asphaltenes at 5, 10 and 20 kg/m³ and for interface aging times varying between 1.5 and 24 hours. Before examining the cross-plot of free water resolution and total modulus, the stability of the model emulsions aged from 1.5 to 24 hours is shown as

a function of asphaltene concentration. Figures 6.9, 6.10 and 6.11 show the free water resolution for water-in-0/100, 25/75 and 50/50 heptol emulsions, respectively.

Figure 6.9 shows that beyond the scatter of the data, the effect of aging time on the stability of water-in-0/100 heptol emulsions is negligible. Figure 6.10 and Figure 6.11 show that the relative emulsion stability increases as water-in-25/75 and 50/50 heptol emulsions are aged. Note that below 3 kg/m^3, the initial size of emulsion drops is quite large, i.e., between 25 and 35 microns (see Figure 6.1). Therefore, the emulsion does not survive centrifugation and the free water is relatively high. However, once the asphaltene equilibrium concentration exceeds approximately 3 kg/m^3, the relative stability decreases as the asphaltene concentration increases. The largest relative decreases in free water occur at bulk concentrations of 5 and 10 kg/m^3 for 25/75 heptol and at 20 kg/m^3 for 50/50 heptol. For the water-in-50/50 or 25/75 heptol emulsions, the free water decreases as the asphaltene concentration decreases and as the interface aging time increases.

Recall that an increase in the total modulus was observed when the asphaltene concentration decreased and when the interface was aged. An increase in the total modulus is believed to be a result of increased film rigidity. The results in Figures 6.10 and 6.11 are consistent and show that a more rigid interface reduces coalescence, which in turn increases emulsion stability. To confirm this relationship, the free water resolution after two hours of treatment is cross-plotted against the total modulus for a given solvent quality, asphaltene concentration, and interface aging time. The cross-plot is shown in Figure 6.12. Interface aging time is embedded in the data and increases as the total modulus increases. The lines in Figure 6.12 are visual aides and show that there is some correlation within each solvent quality. However, there is no single correlation independent of solvent. In fact, the 0/100 heptol curve and some of the points on the 25/75 heptol curve are expected to shift even further to the right since the total measured modulus is thought to be under-predicted for these systems.

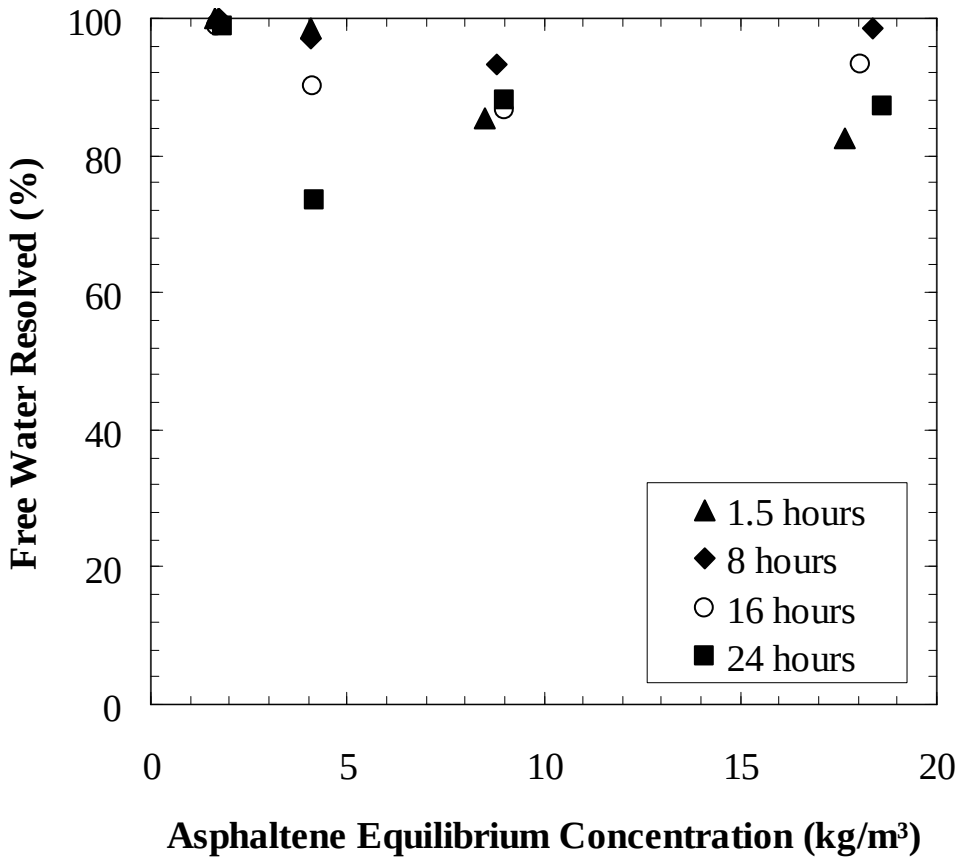

Figure 6.9: Free water resolution after two hours of treatment for model emulsions prepared from 40 vol% water and solutions of Athabasca Bitumen 2 Asphaltenes in 0/100 heptol. The emulsions were aged up to 24 hours

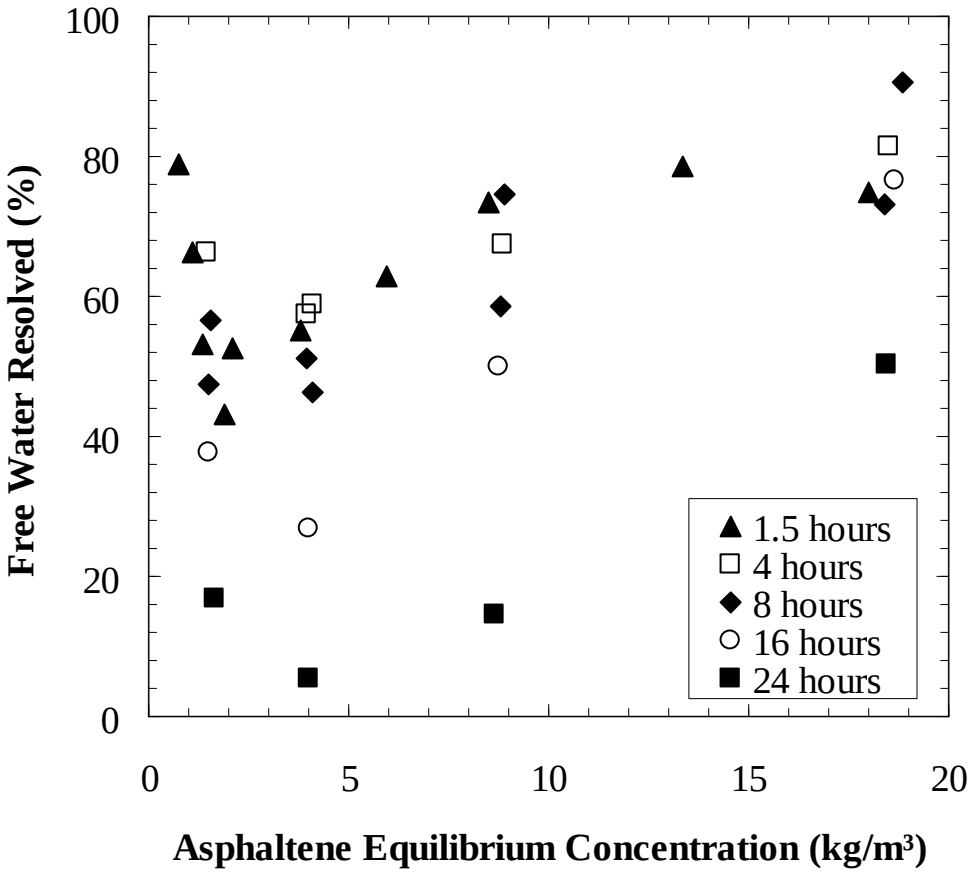

Figure 6.10: Free water resolution after two hours of treatment for model emulsions prepared from 40 vol% water and solutions of Athabasca Bitumen 2 Asphaltenes in 25/75 heptol. The emulsions were aged up to 24 hours

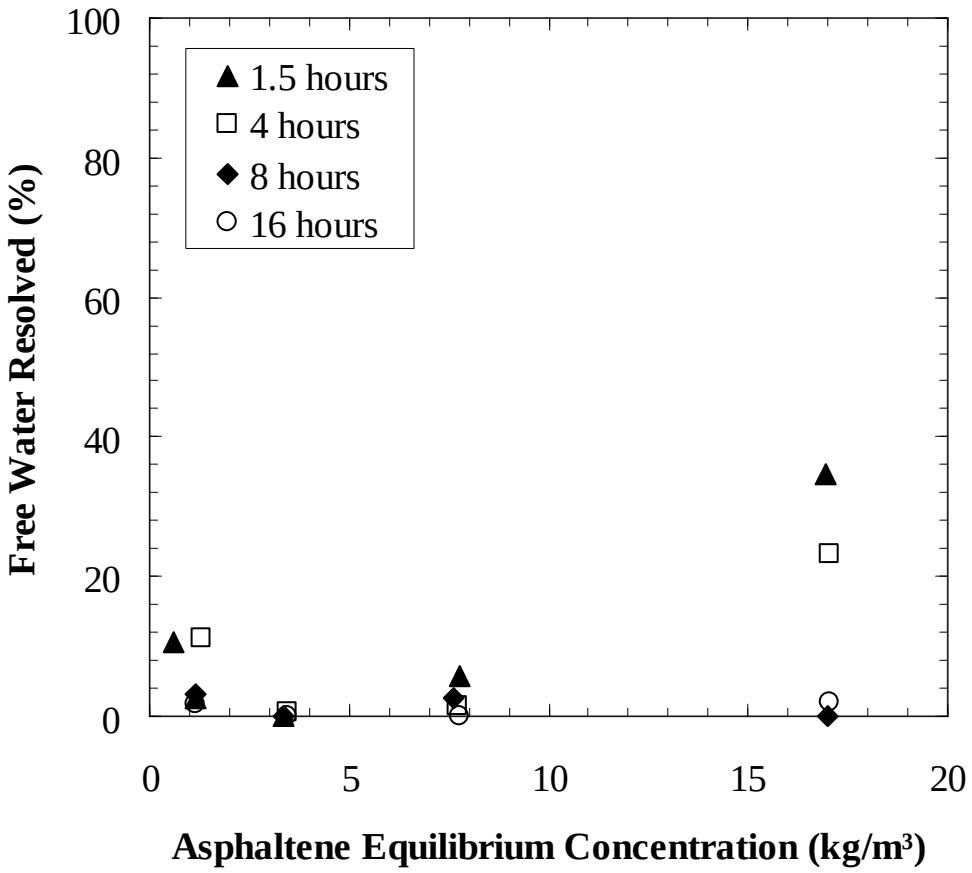

Figure 6.11: Free water resolution after two hours of treatment for model emulsions prepared from 40 vol% water and solutions of Athabasca Bitumen 2 Asphaltenes in 50/50 heptol. The emulsions were aged up to 16 hours

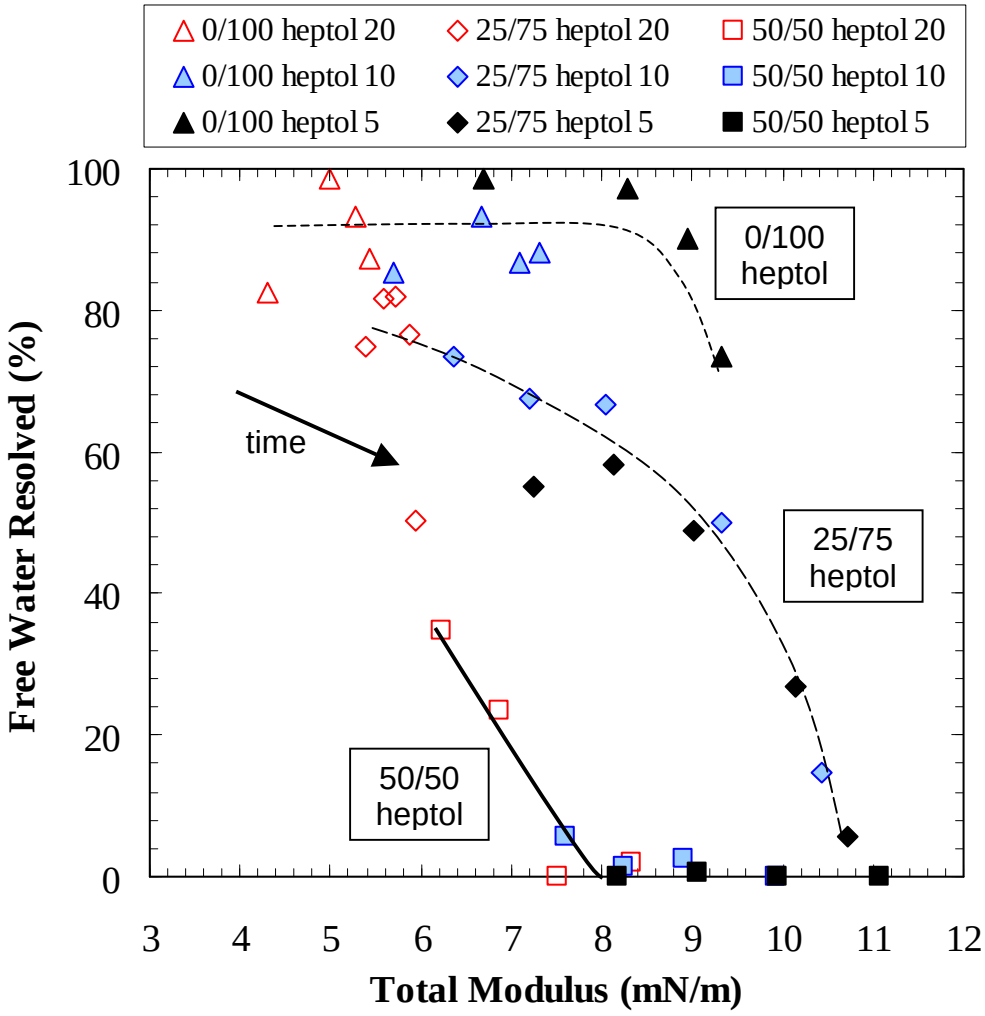

Figure 6.12: Cross-plot of free water resolution after two hours treatment with the total modulus.

Recall that the rheology measurements did not take into account asphaltene mass expulsion from the interface during coalescence. It was speculated earlier that expelled mass results in increased rigidity, i.e., a higher total modulus, because the asphaltenes least likely to form strong networks are expelled most easily.

Figure 6.12 suggests that there is a factor or factors in addition to rheology and the rate of coalescence that determine ultimate emulsion stability. The lack of one consistent curve in the free water versus total modulus cross-plot can be explained in several ways. First, it is possible that there may be a limiting droplet diameter beyond which the interfacial film can no longer shrink. The limiting diameter may be lower for a "poor" solvent such as 50/50 heptol and higher for a "good" solvent such as 0/100 heptol. Recently, Jafari's (2005) crumpling experiments revealed that the ratio of the final area to which an asphaltenes-heptol droplet can be shrunk before crumpling is visibly observed to the drop's initial area increases as the heptane fraction in the heptol increases. Hence, coalescence during the 60ºC treatment may cease for the 50/50 heptol emulsions at some droplet diameter but continue unimpeded for the 0/100 heptol emulsions.

Second, it is possible that the rheology of the interface is altered when the emulsions are placed in the 60ºC heating bath. Bouriat *et al.* (2004) observed that the elastic modulus of asphaltene-cyclohexane/water interfaces decreased when the temperature increased. At an oscillation frequency of 0.033 Hz, the elastic modulus decreased from nearly 50 to 5 mN/m when the temperature increased from 15 to 55ºC. Further, if the rheology does change with temperature, it is possible that the extent of reduction in the modulus is different for the three solvent qualities. For example, the modulus may be reduced significantly for 0/100 heptol-water interfaces but only marginally for 50/50 heptol-water interfaces. The rate of coalescence may also be increased when the temperature is elevated to 60ºC. Again, the degree to which the coalescence rate is increased may be less for water-in-50/50 heptol emulsions than for water-in-0/100 heptol emulsions. Further, a

combination of altered rheology and crumpling diameter may contribute to the lack of a single curve in Figure 6.12.

6.3 CHAPTER CONCLUSIONS

The rigidity of the interface, i.e., the total modulus, increases when the interface is aged and when the continuous phase becomes more paraffinic. For the concentrations relevant to emulsion stability, the interfacial rigidity also increases when the asphaltene concentration decreases. Faster diffusion at high concentrations likely relaxes the interface.

Increased film rigidity reduces the rate of coalescence in a water-in-oil emulsion. For systems in which asphaltenes do not leave the interface during coalescence, the rate of coalescence can be related to the measured total modulus through one single curve. This curve accounts for interface aging time, asphaltene concentration, and solvent quality. When asphaltenes are expelled from the interface, the measured total modulus is under-predicted. It is speculated that a lack of expulsion results in a more fluid film because the asphaltenes least likely to contribute to strong, network formation remain on the interface. However, in an emulsion, the non-network forming asphaltenes are expelled during droplet coalescence. A more accurate reflection of interfacial rheology in a coalescing system may result if the droplet is shrunk stepwise during the aging time and the elasticity then measured.

Emulsion stability increases when the interface becomes more rigid. Increased stability may occur even if the Sauter mean diameter increases. Although the total modulus correlated well with free water resolution within a given solvent quality, an overall correlation was not found. It is possible that other effects such as crumpling and skin formation contribute to ultimate emulsion stability. Further, it is possible that rheological properties and the rate of coalescence change when the temperature is increased. The relative changes may be different for each solvent quality.

CHAPTER 7
THE ROLE OF SOLIDS IN EMULSION STABILITY

This chapter presents the results of the studies on the characterization of oilsands, wellhead, and refinery solids as well as their relationship to emulsion stability. Section 7.1 describes the source emulsions and the particular problems associated with destabilizing each. Characteristics such as size and size distribution, shape, morphology, and concentration are discussed for the solids from each sample. Section 7.2 and 7.3 present the compositional, structural and stability results of emulsions stabilized by "fine" and "coarse" particles, respectively. The appropriate choice of treatment method for emulsions stabilized by asphaltenes and solids is discussed in Section 7.4. Section 7.5 provides some concluding remarks regarding solids stabilized oilfield emulsions.

7.1 SOURCE EMULSIONS AND THEIR SOLIDS

7.1.1 Coker-Feed Bitumen

It has been well established that the bitumen product from Syncrude's froth treatment process contains approximately 1 to 3 wt% water in the form of droplets less than 10 microns in diameter (Taylor *et al.*, 2002; Kotylar *et al.*, 1998; Yan *et al.*, 1999; Chen *et al.*, 1999; Wu, 2003). This emulsion may be at least partially stabilized by solids and survives centrifugation at process temperatures. After naphtha recovery, these solids remain in the product coker feed bitumen, making up approximately 0.4 to 0.5 wt% of the bitumen (Kotlyar *et al.*, 1998; Chen *et al.*, 1999). The froth treatment product stream was not available for testing of the emulsion's stability but the solids were recovered from the coker-feed bitumen for model emulsion tests as described in Section 3.1.2.2.

Figure 7.1 (a) is a typical ESEM micrograph of the oil sands solids. Some individual particles can be discerned and appear to be platelets with diameters ranging from

approximately 200 nm to one or two micrometers. The resolution is insufficient to clearly distinguish many individual particles but the micrograph illustrates how the particles can aggregate into micron scale clusters when dried. Particle size measurements of dried samples are likely to yield aggregate size distributions rather than individual particle size distributions.

Figure 7.1 (b) is a TEM micrograph of individual particles. The particles have an irregular plate-like morphology. The platelet diameters range from approximately 70 to 350 nm. These results are consistent with Kotlyar et. al's (1998) TEM analysis of solid particles separated from a bitumen sample that had been recovered from an oil sand using a batch extraction unit (BEU). They observed crystallites with a lateral extension of less than 200 nm and a thickness of at most 10 nm. In a similar TEM examination of colloidal solids separated from fine tailings, Kotlyar *et al.* (1993) observed that solid particles varied anywhere from 50 to 400 nm and were primarily plate-like with an irregular morphology.

Figure 7.2 presents the particle size distribution of Athabasca solids on a number-frequency basis. The solids vary between 35 and 400 nm in diameter, a range consistent with the TEM observations. The cumulative number frequency distribution indicates that 90% of the particles are smaller than 120 nm, and the volume frequency was calculated using Equation 3.12. Figure 7.2 shows that approximately 90% of the particles are less than 300 nm and 98% less than 1 micron on a volume basis.

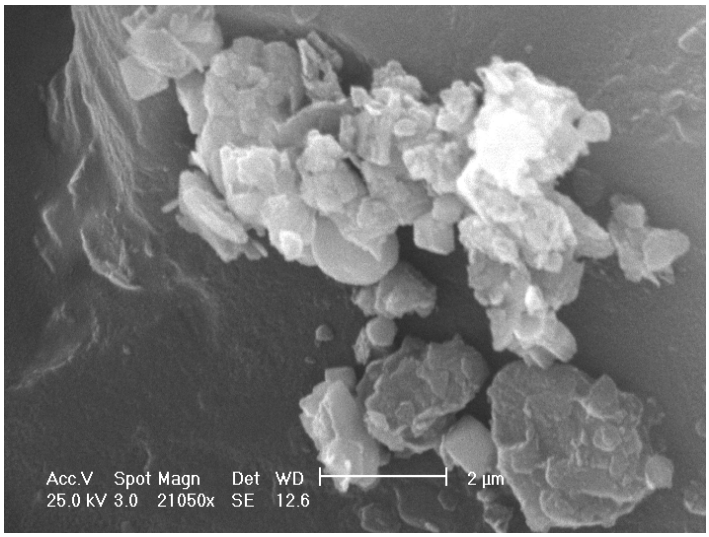

(a)

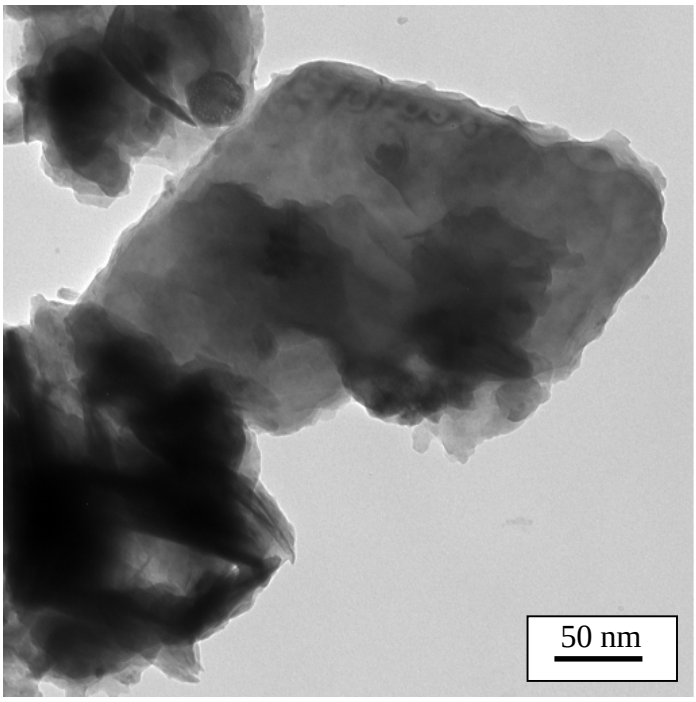

(b)

Figure 7.1: a) SEM micrograph of Athabasca solids, b) TEM micrograph of Athabasca solids

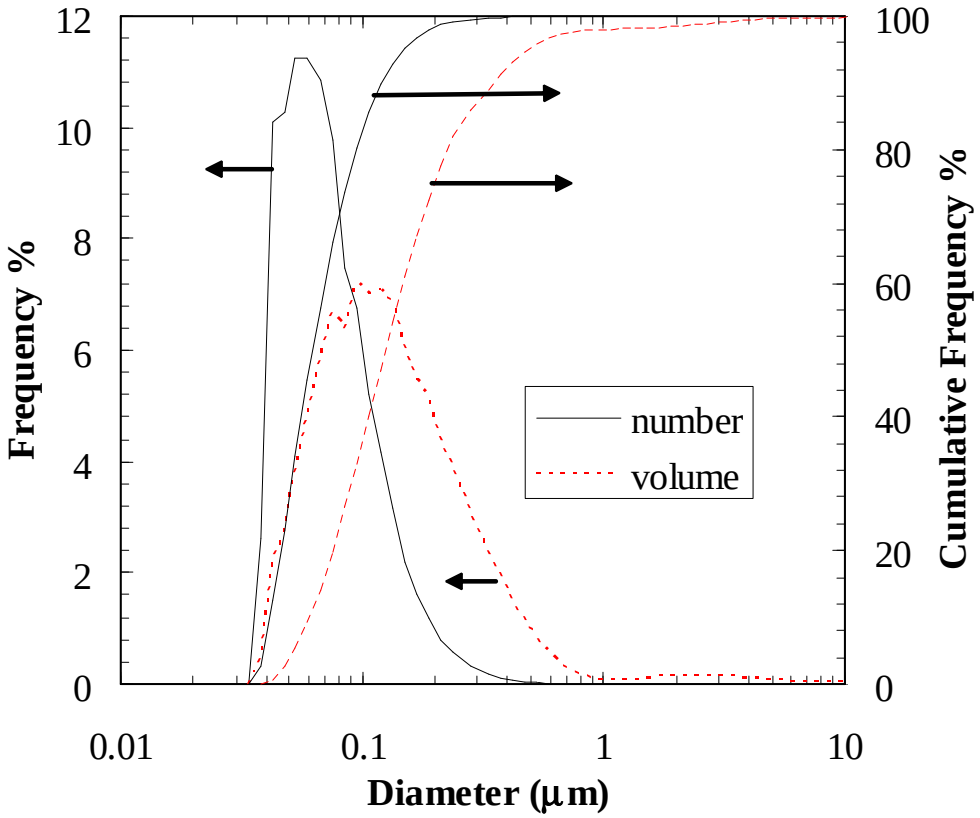

Figure 7.2: Particle size distribution for number frequency and volume frequency assuming disc-shaped particles of Athabasca solids

Figure 7.3 shows the XRD spectra for a random oriented sample of unwashed solids, solids washed with toluene, and solids bleached with hydrogen peroxide. The results indicate little variation between the three spectra: there is no difference between the unwashed and toluene washed samples, suggesting that any materials adsorbed on the surfaces of the clays cannot be removed with toluene washing. For the hydrogen peroxide bleached sample, only the peaks at 32º 2-theta are missing. These peaks correspond to titanium oxide. Apparently, bleaching removed this material. Since titanium is often a heavy metal associated with asphaltenes, its removal may indicate bleaching removes adsorbed hydrocarbon matter. However, the rest of the spectrum is the same, so identification of non-clay minerals was performed on the unwashed sample.

Figure 7.4 shows the XRD spectra for the bulk (unwashed) solids sample and the locations of the peaks corresponding to the three main non-clay minerals identified. Very good matches for pyrite, quartz and titanium oxide are indicated (note that other peaks correspond to the clay minerals). These results are consistent with those observed by Kotlyar *et al.* (1998), who identify pyrite as the source of sulfur and titanium oxide as the source of titanium in bitumen solids.

Figure 7.5 shows the XRD spectra for the separated clays. The clays are predominantly composed of kaolin-type crystallites, such as kaolinite and dickite, and of a mica mineral, such as muscovite. When this XRD spectrum was compared to the XRD spectra of the clay samples after 1) glycolation, and 2) heating to 400ºC, as shown in Figure 7.6, no shifts in peaks or changes in peak intensity were observed. The absence of peak shifts suggests that the clay material is non-swelling, consistent with the identification of kaolinite and muscovite. The clay minerals identified in the current work are also consistent with those identified by Kotlyar *et al.* (1993) who examined the XRD spectra of glycerolated subfractions of fine tailings. They identified kaolinite and mica as the major components of the 50 to 400 nm subfraction of the fine tailings with traces of smectite and vermiculitic minerals in the finest particles. They also noticed an increase in

the non-crystalline content for the finer particles. In a PAS-FTIR analysis of bitumen solids, Bensebaa *et al.* (2000b) also identified the presence of kaolinite.

The oil sands solids appear to be plate-like particles predominantly composed of kaolin minerals. Although non-clay minerals such as pyrite, quartz and titanium oxide were also identified, these minerals are probably present in a much smaller quantity. Nearly all of the solids remained in suspension during the separation of the clays from the bulk solids, implying that most of the solids were clays rather than non-clays. Furthermore, the similarity in XRD spectra between the bulk solids sample and the clays, as well as the fact that the non-clays did not register excessively high intensities in the bulk scan suggests a primarily clay-like nature.

The oil sands solids appear to be similar to other reservoir solids thought to contribute to emulsion stability. Kaolinite has been identified as one of the most common clay minerals in oil-sands reservoirs (Gunter, 1992) and kaolin clays with adsorbed asphaltenes have been identified as emulsion stabilizers (Yan *et al.*, 2001).

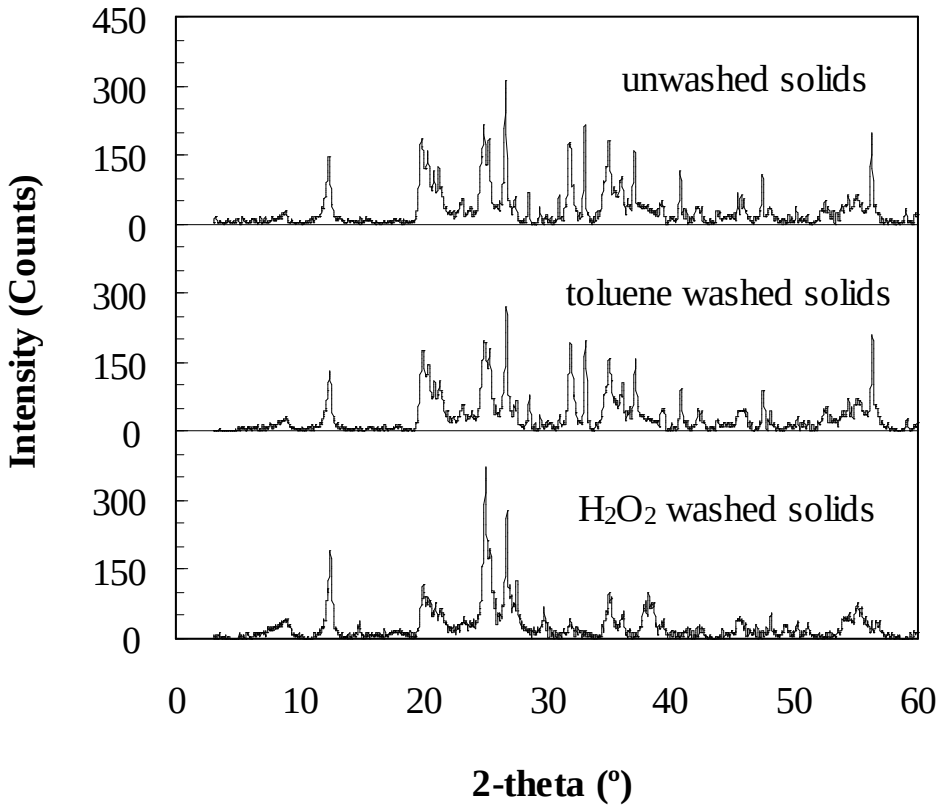

Figure 7.3: XRD spectra of Athabasca solids that are a) unwashed, b) toluene washed, c) bleached with hydrogen peroxide

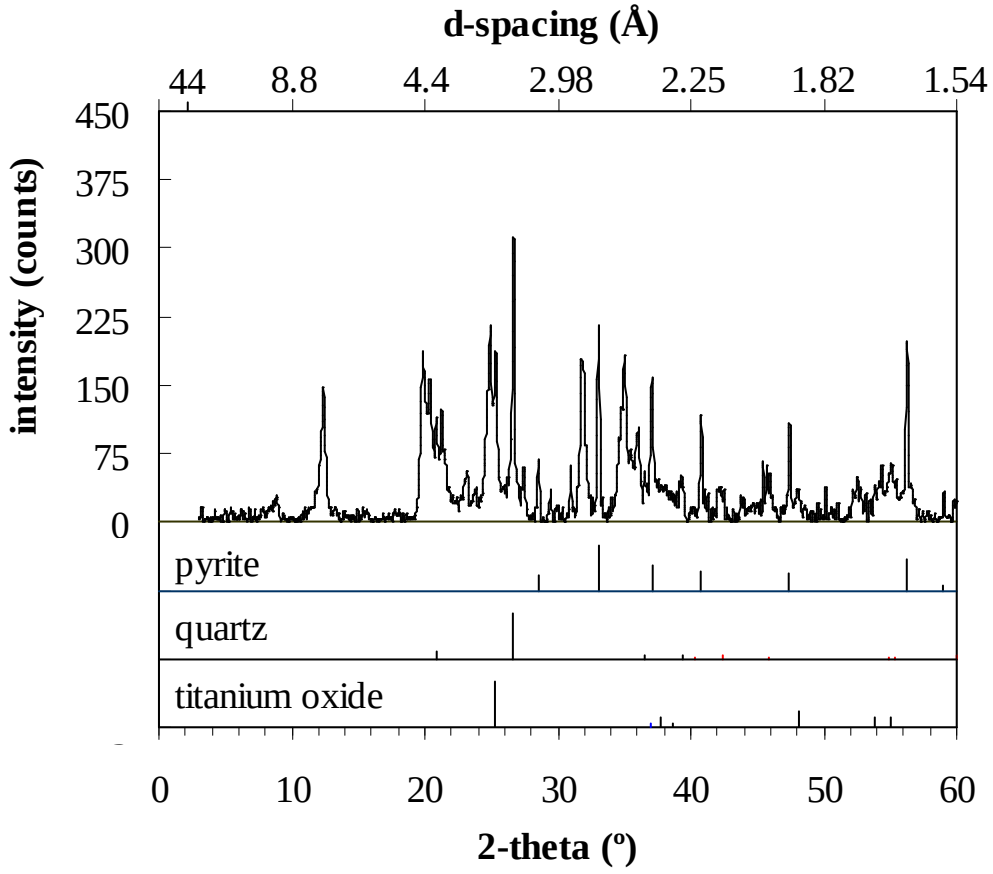

Figure 7.4: XRD spectra of air-dried Athabasca solids identifying non-clay minerals

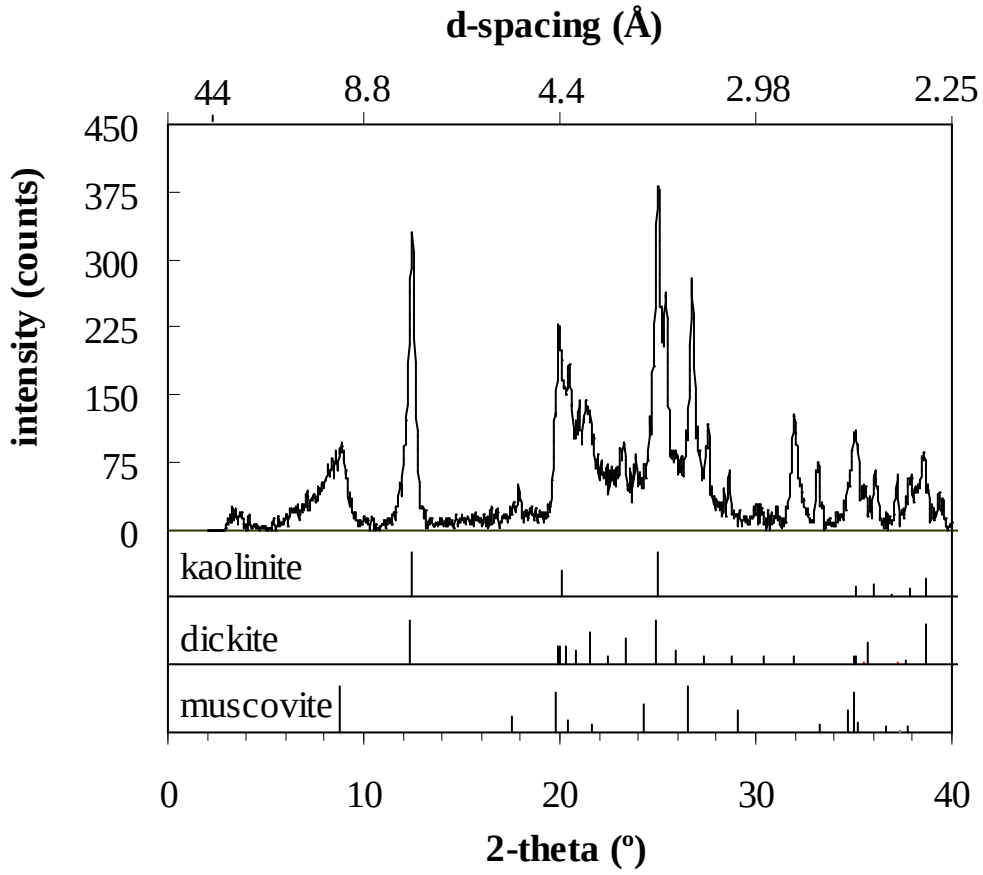

Figure 7.5: XRD spectra of air-dried clays separated from Athabasca solids identifying clay minerals

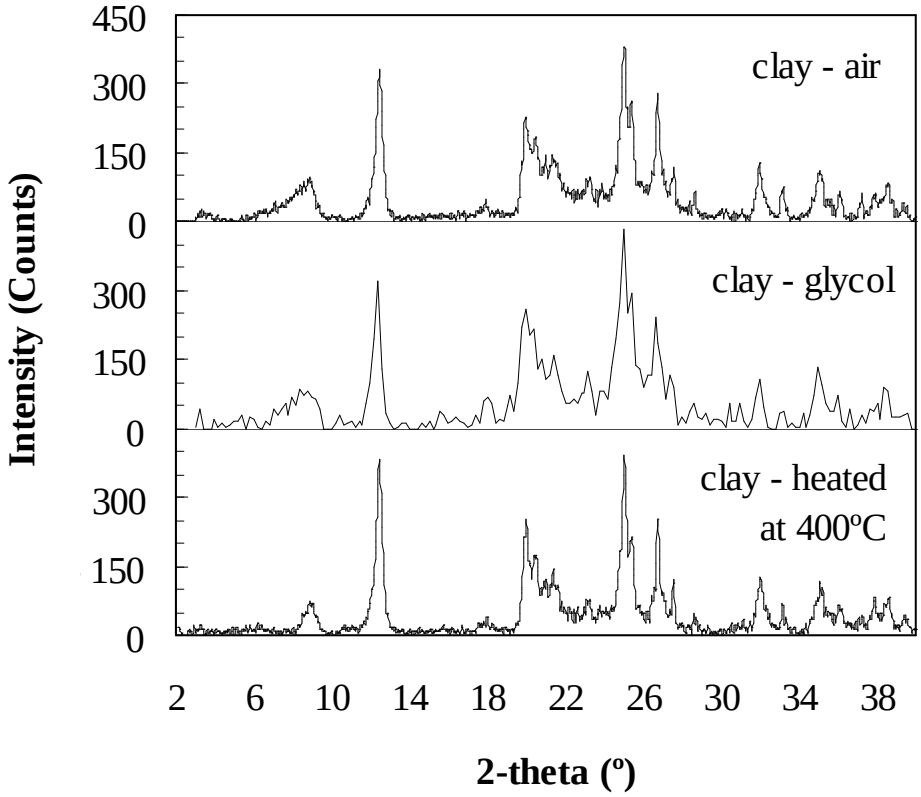

Figure 7.6: XRD spectra of clays after a) drying in air, b) glycolation, c) heating at 400ºC

7.1.2 AEC Wellhead Emulsion

The AEC wellhead emulsion contains 35 vol% water and the non-aqueous phase contains 1.9 wt% solids. Due to the high viscosity and opacity of the emulsion, microscopic examination of the emulsion was difficult and therefore an average droplet diameter could not be determined with any certainty. However, by adding one or two drops of a 50/50 heptol solution to a small emulsion sample, droplets varying from 1 to 50 microns could be discerned as indicated in Figure 7.7.

Figure 7.8 shows the free water resolution with time for the AEC emulsion, as received. The emulsion is very stable with only 12% of the water resolved after 8 hours of treatment. The unresolved water remained dispersed in the continuous phase. The high viscosity of this emulsion and the relatively small droplet size likely contribute to the relatively high stability of this emulsion. Note that, the free water for the IOL refinery sample is also shown and will be discussed in more detail in Section 7.1.3.

Figure 7.9 (b) shows a TEM image of the solids recovered from the AEC emulsion. An additional TEM micrograph of Athabasca solids is shown in Figure 7.9 (a) for comparison. Figure 7.10 shows the particle size distribution and cumulative distribution of the solids from the AEC emulsion on number and volume frequency bases. The particles appear to be irregularly shaped platelet structures with diameters between 1 and 10 μm. The XRD analysis was similar to that obtained for the Athabasca solids and is therefore not shown here. The solids were primarily clays. However, they are approximately fifty times greater in diameter than the Athabasca solids, on average. 90% of the particles are smaller than 4 microns and smaller than 7 microns on number and volume frequency bases, respectively.

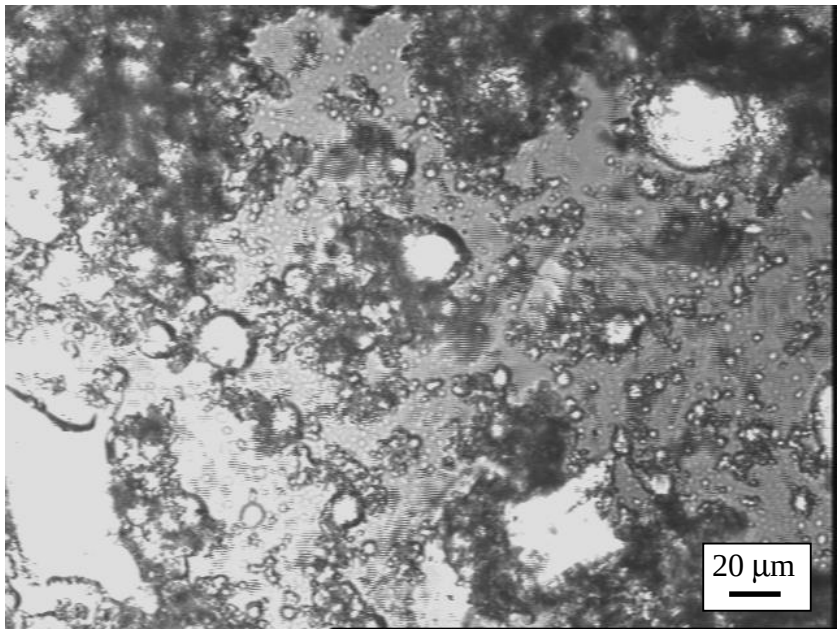

Figure 7.7: Micrograph of AEC emulsion diluted with a drop of 50/50 heptol

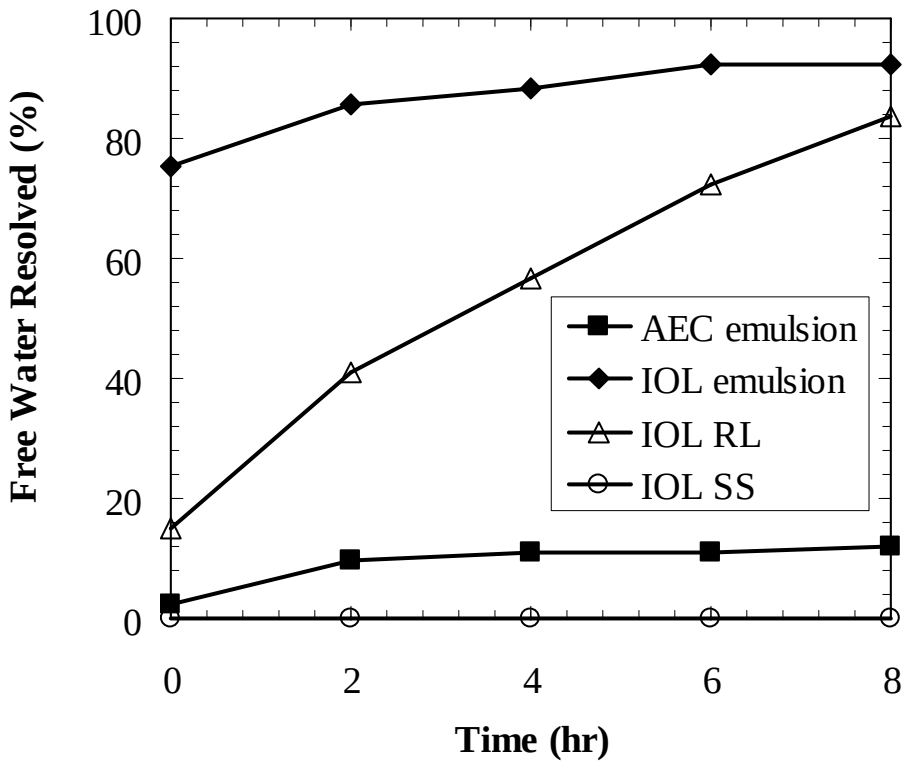

Figure 7.8: Free water resolution as a function of time of AEC wellhead emulsion, IOL refinery emulsion, IOL refinery rag layer and IOL refinery solids slurry

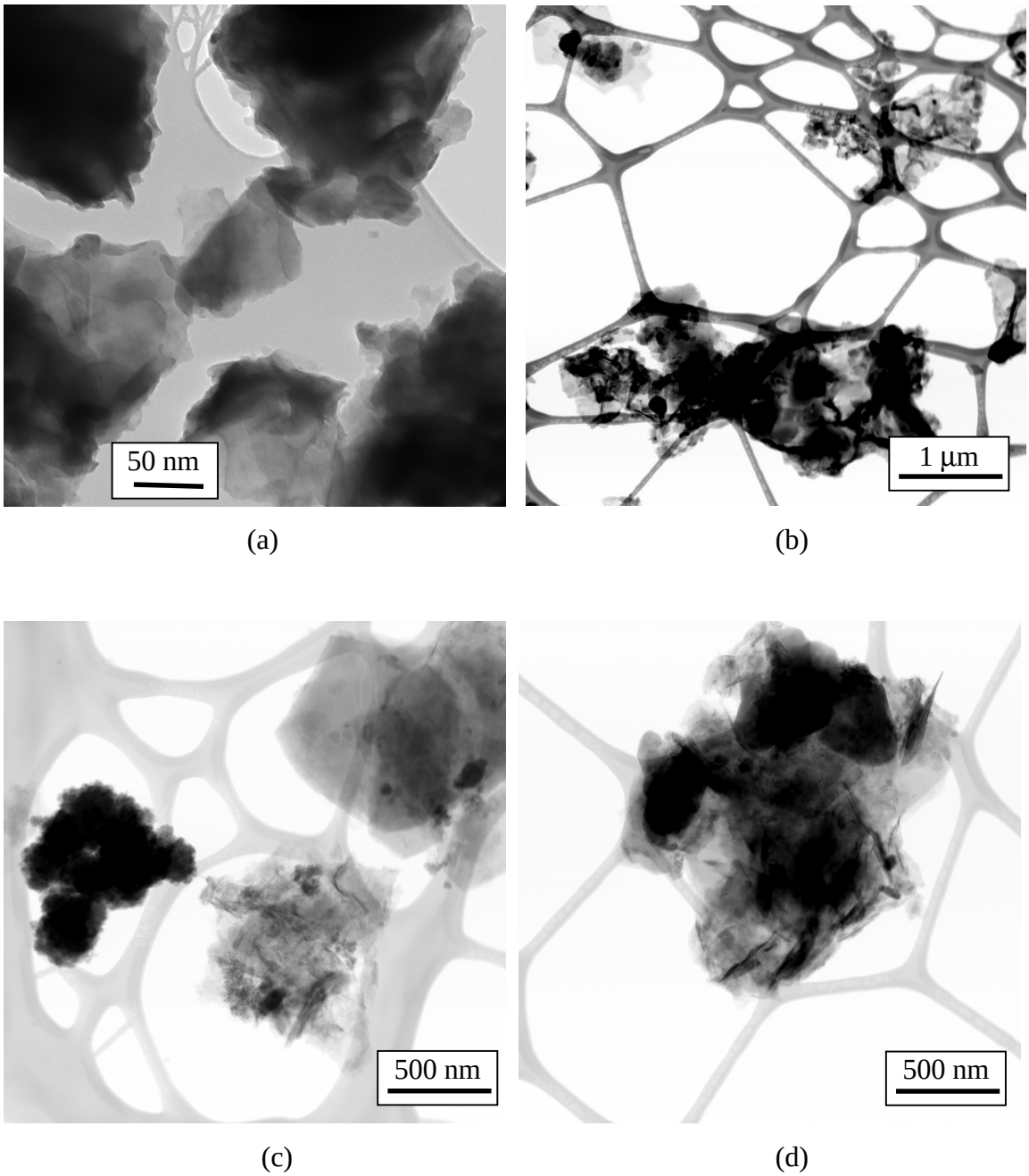

Figure 7.9: TEM micrograph of a) Athabasca oil-sands solids b) AEC wellhead solids, c) IOL refinery rag layer solids, d) IOL refinery solids slurry solids. Solids are dispersed on carbon-webbing

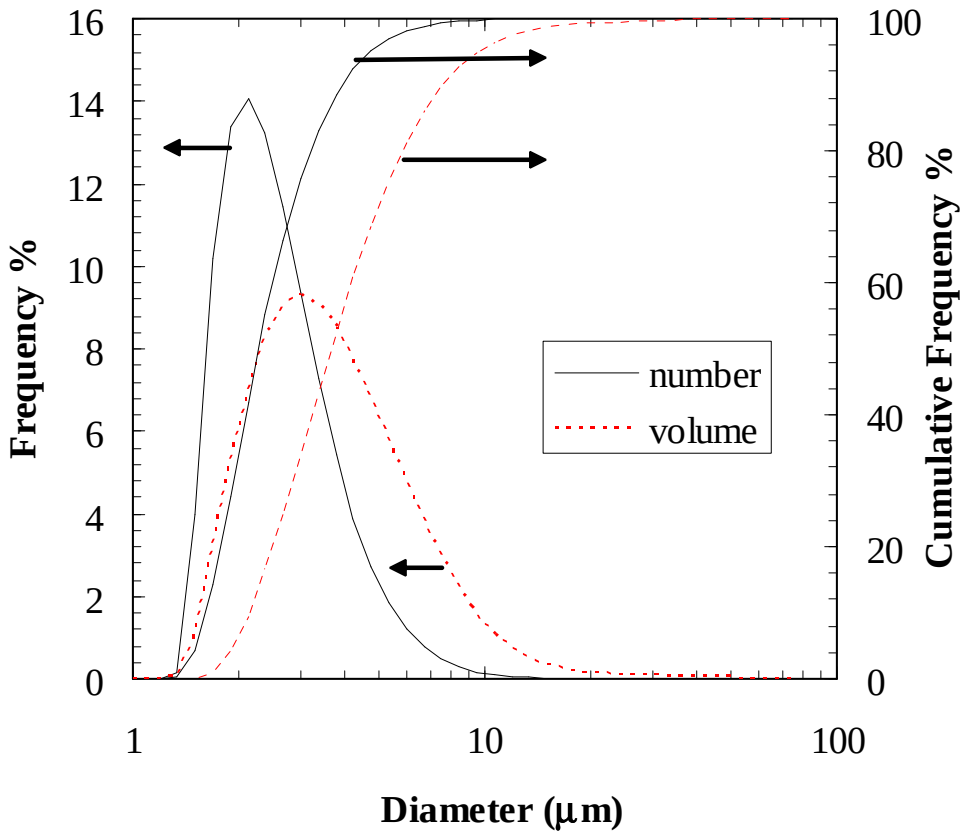

Figure 7.10: Particle size distribution for number frequency and volume frequency assuming disc-shaped particles of AEC solids

7.1.3 IOL Refinery Emulsion

The IOL refinery emulsion contains 43 vol% water and the non-aqueous phase contains 2.1 wt% solids. Microscopic examination of the emulsion was possible although the addition of a droplet of 50/50 heptol greatly facilitated drop size analysis. Figure 7.11 (a) and (b) show micrographs of the IOL emulsion as received and after the addition of a drop of the heptol solvent, respectively. The micrographs show water droplets varying from less than 10 up to 350 microns. The drop size distribution for the total emulsion is shown in Figure 7.12 and results in a Sauter mean diameter of 146 microns.

This emulsion was very stable under normal gravity but, as shown in Figure 7.8, it is quite unstable after heating and centrifugation. Approximately 80% of the water was resolved after five minutes of centrifugation and the emulsion was 90 to 95% resolved after six to eight hours of treatment. This emulsion is significantly less stable than the AEC emulsion.

As was mentioned previously in Section 3.1.4, four distinct phases separated during this first centrifugation step: a continuous phase, a rag layer (RL), a free water phase, and a solids slurry (SS). Representative micrographs of the rag layer and solids slurry are given in Figure 7.11 (c) through (f) and the droplet size distributions are shown in Figure 7.12. The rag layer accounted for 9 vol% of the total emulsion with a Sauter mean diameter of 30 microns. The solids slurry made up 7 vol% of the total emulsion with a Sauter mean diameter of only 8.1 microns. The continuous phase was free of water.

Table 3.4 showed that the solids content of the continuous phase, the rag layer and solids slurry were 0.11, 1.8 and 11.8 wt%, respectively. The stability of the rag layer and solids slurry emulsions was also assessed and is shown in Figure 7.8. After eight hours of treatment, 85% of the water from the rag layer was resolved while zero water was resolved from the solids slurry. The micrographs of Figure 7.11 and the drop size

distributions given in Figure 7.12 are consistent with the stability results given in Figure 7.8; the smaller the droplets, the lower the free water resolution.

It appears that the IOL emulsion consists of or separates into two distinct emulsions. As outlined in Section 3.1.4, solids were recovered from each of these distinct emulsions. Figures 7.9 (c) and (d) are TEM micrographs of the solids separated from the IOL emulsion rag layer and solids slurry, respectively. Figures 7.13 (a) and (b) show the particle size distributions of the same two solids samples based on number and volume frequencies.

A comparison of the particle size distributions of the four solid samples shows that the rag layer solids are similar in size and shape to the “fine” solids from the Athabasca bitumen sample while the solids in the solids slurry are similar to the “coarse” AEC wellhead sample solids. Figure 7.14 demonstrates this more clearly by comparing the number frequency particle size distribution of each sample.

7.1.4 Summary of Solids Characteristics

There appear to be two classes of native solids 1) fine solids less than 500 nm in diameter; 2) coarse solids from 1 to 10 microns in diameter. “Fine” solids were observed in the oilsands particles extracted from Athabasca bitumen and the solids extracted from the IOL rag layer. “Coarse” solids were observed in the AEC emulsion and in the IOL solids slurry. It is interesting to note that the IOL emulsion appears to contain two distinct sizes of solids. It is possible that this emulsion is a combination of two or more different emulsions, (for example, emulsions similar to the oilsands and AEC emulsions), and that each contain a specific size class of solids. Both types of solids have platelet structures and are predominantly clays. The role of fine and coarse solids in emulsion stability is considered next.

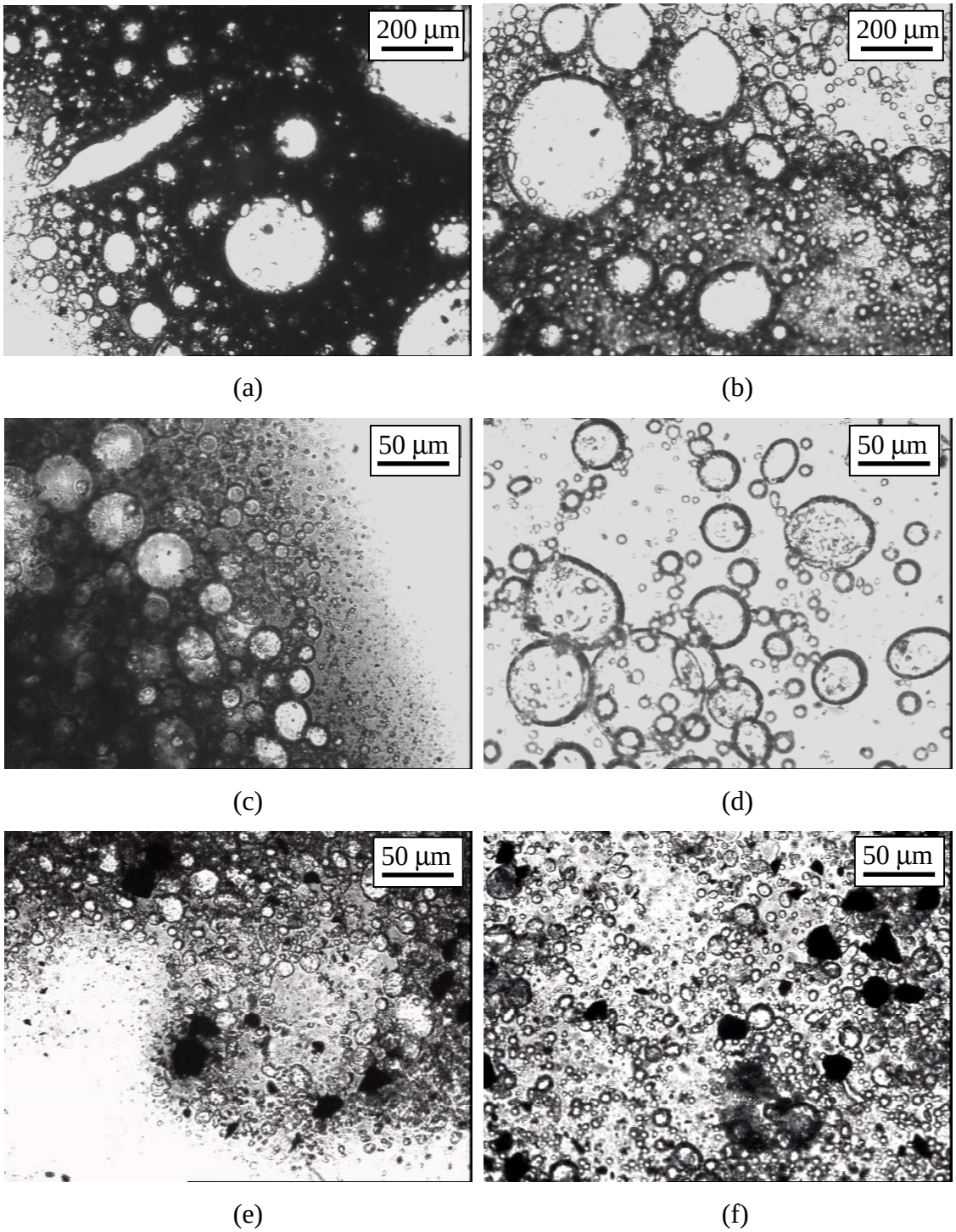

Figure 7.11: Micrographs of IOL a) total emulsion, b) total emulsion and 50/50 heptol drop, c) rag layer, d) rag layer and 50/50 heptol drop, e) solids slurry, f) solids slurry and 50/50 heptol drop

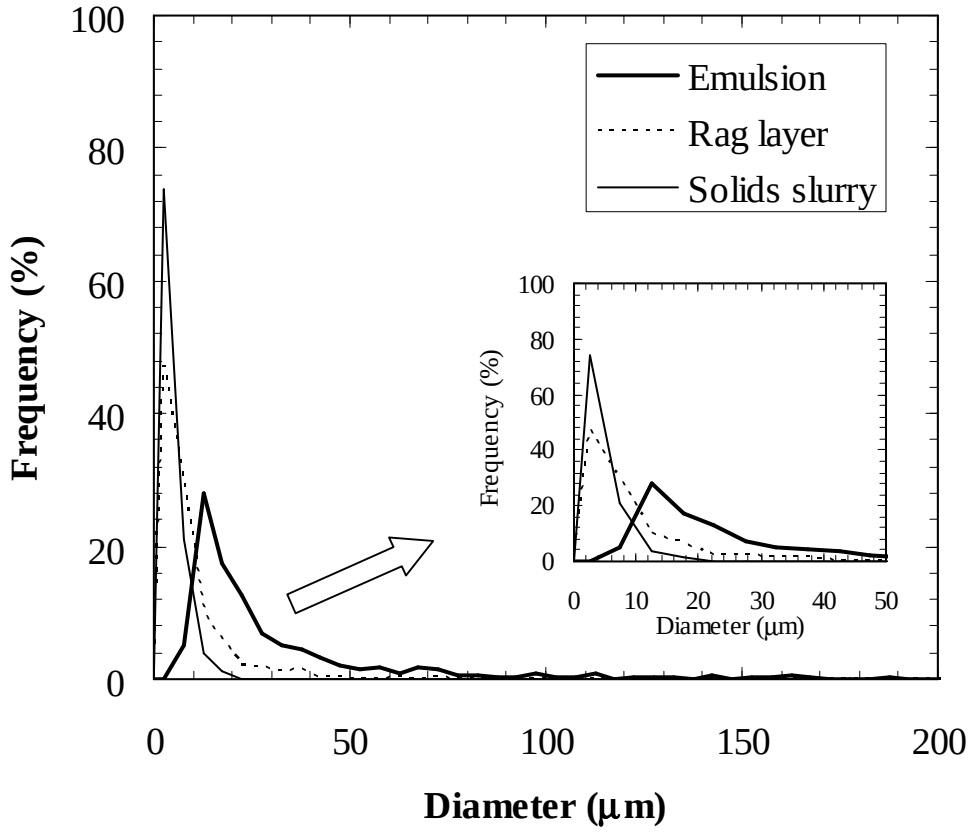

Figure 7.12: Water drop size distribution for IOL emulsion, IOL rag layer, and IOL solids slurry

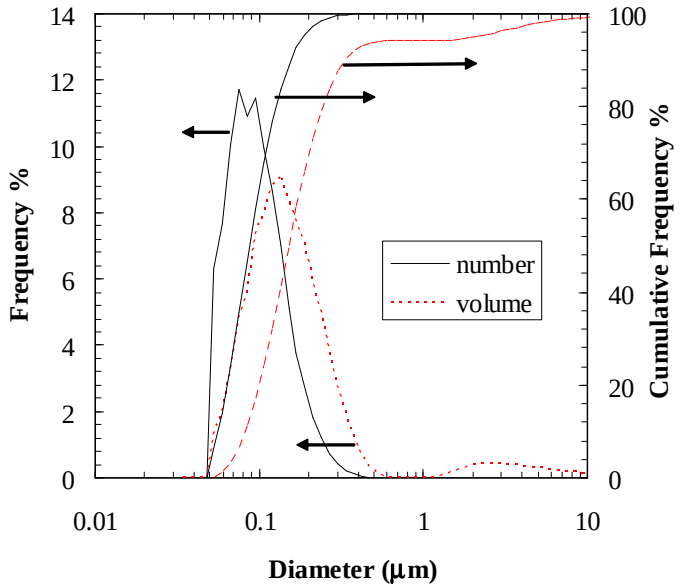

(a)

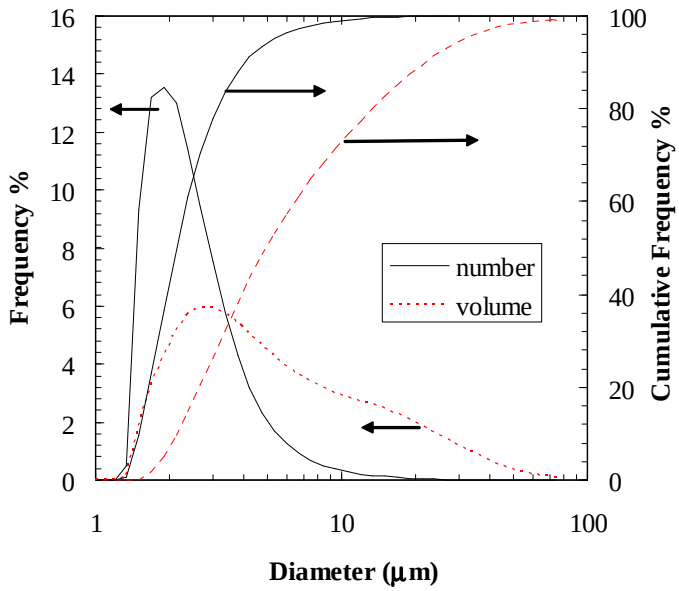

(b)

Figure 7.13: Particle size distribution for number frequency and volume frequency assuming disc-shaped particles of a) IOL rag layer solids, b) IOL solids slurry solids

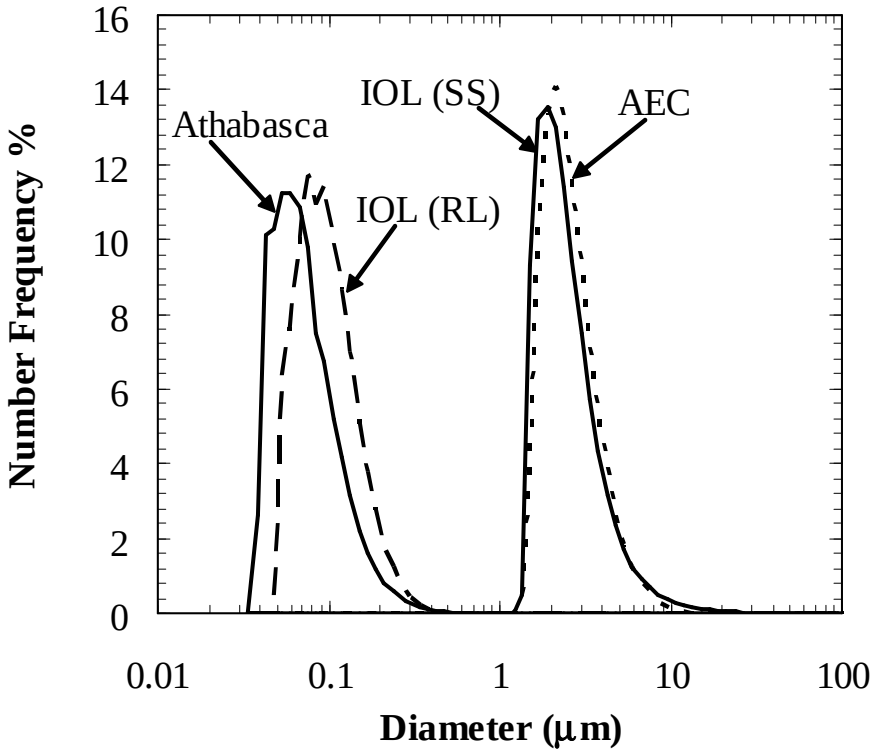

Figure 7.14: Particle size distributions of Athabasca fine solids, AEC wellhead solids, IOL refinery rag layer solids and IOL refinery solids slurry solids

7.2 THE ROLE OF FINE SOLIDS

7.2.1 Stability of Fine Solids-Stabilized Emulsions

Before examining the interfacial behavior of fine solids, it was necessary to confirm that they acted as emulsion stabilizers. As discussed previously in Section 3.1.2.2, two techniques were applied for the extraction of solids. Figure 3.3 showed that the effect of ultrafine solids (or the small fraction of asphaltenes precipitated) was marginal and did not alter the trends in the free water resolution. Figure 3.1 also indicated that wet solids had to be utilized in order to reproduce emulsion stability.

The effect of fine oilsands solids on the free water resolution of model emulsions stabilized by Athabasca Bitumen 1 Asphaltenes and AS is given in Figures 7.15 (a). The free water resolution of model emulsions at the same concentration of asphaltenes is also shown for C_5 and Soxhlet-Washed Asphaltenes and AS in Figures 7.15 (b) and (c).

The trends in Figure 7.15 suggest that fine solids, even in low concentrations, can increase the relative stability of Asphaltene and C_5 Asphaltene stabilized emulsions significantly. At asphaltene equilibrium concentrations exceeding approximately 25 kg/m^3, the free water resolution decreases by 30% for systems containing solids and either Asphaltenes or C_5 Asphaltenes. However, the solids appear to contribute marginally to emulsion stability for Soxhlet-Washed Asphaltene samples. It is likely that the high molecular weight Soxhlet-Washed Asphaltenes are sufficient to reduce the free water resolution to very low levels, i.e., approximately 10%. Continuous washing of an AS sample with heptane strips all resinous materials and leaves an asphaltene that results in a very strong film resistant to coalescence. Further, a 25/75 heptol ratio corresponds to the onset of precipitation for Soxhlet-Washed Asphaltenes. It has been suggested that asphaltenes near their incipient point of precipitation can lead to the formation of the most stable emulsions (McLean and Kilpatrick, 1997; Eley *et al.*, 1988). If the Soxhlet-Washed Asphaltenes are at their incipient point of precipitation, they may stabilize

emulsions more effectively than the Asphaltenes which not only contain more “resinous” molecules, but are also not near their point of precipitation in a 25/75 heptol solvent. Recall that Figure 3.2 showed that Asphaltenes are at their point of precipitation when the heptane fractin in heptol is approximately 50%.

Since the model emulsions stabilized by Asphaltenes and C_5 Asphaltenes gave consistent trends, only Asphaltenes and AS, i.e., samples precipitated with n-heptane, are used for all subsequent model emulsion studies. Soxhlet-Washed Asphaltene samples were not utilized because the differences in stability between samples containing solids and those without were trivial.

The completion of all emulsion stability experiments required the use of two different Athabasca Bitumen samples. Figure 7.16 compares the free water resolution after two hours of treatment for model emulsions created from Asphaltenes and AS extracted from Bitumen 1 and 2. While the difference in stability is modest under the imposed treatment, the enhanced stability can potentially be significant; for example, in a conventional heater-treater. Figure 7.16 shows that the emulsions prepared from the Athabasca Bitumen 2 Asphaltenes are less stable than the emulsions prepared from Bitumen 1 Asphaltenes. The molar mass of Athabasca Bitumen 1 and Bitumen 2 Asphaltenes was compared in Figure 4.1. The Bitumen 2 Asphaltenes have a molar mass 30% smaller than that of the Bitumen 1 Asphaltenes confirming that asphaltene properties have a significant impact on emulsion stability even for emulsions partially stabilized by solids.

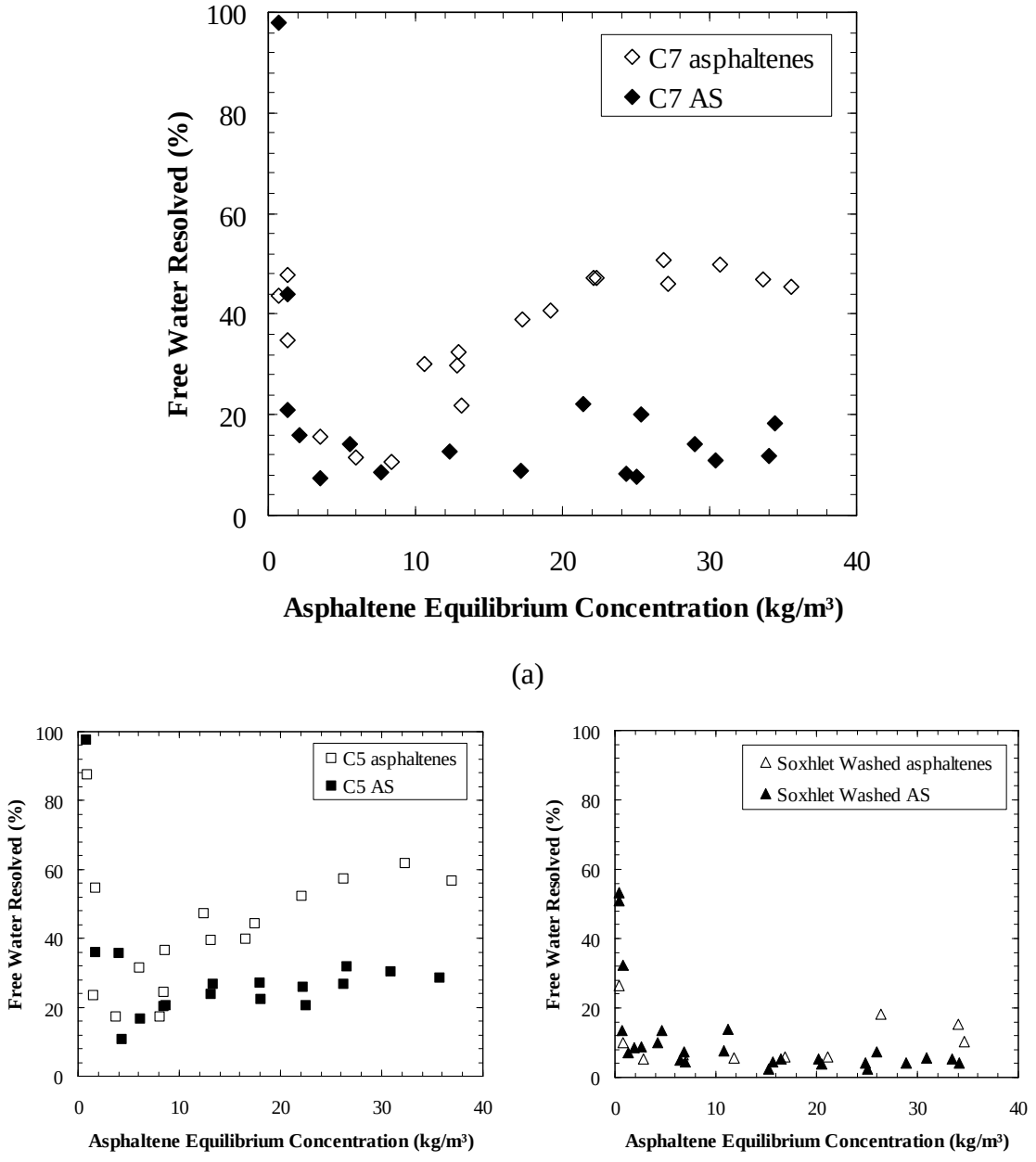

Figure 7.15: Free water resolution after eight hours of treatment of model emulsions stabilized by Athabasca Bitumen 1 a) Asphaltenes and AS, b) C_5 Asphaltenes and AS, c) Soxhlet-Washed Asphaltenes and AS. 25/75 heptol, 40 vol% water, 1.5 hours settling

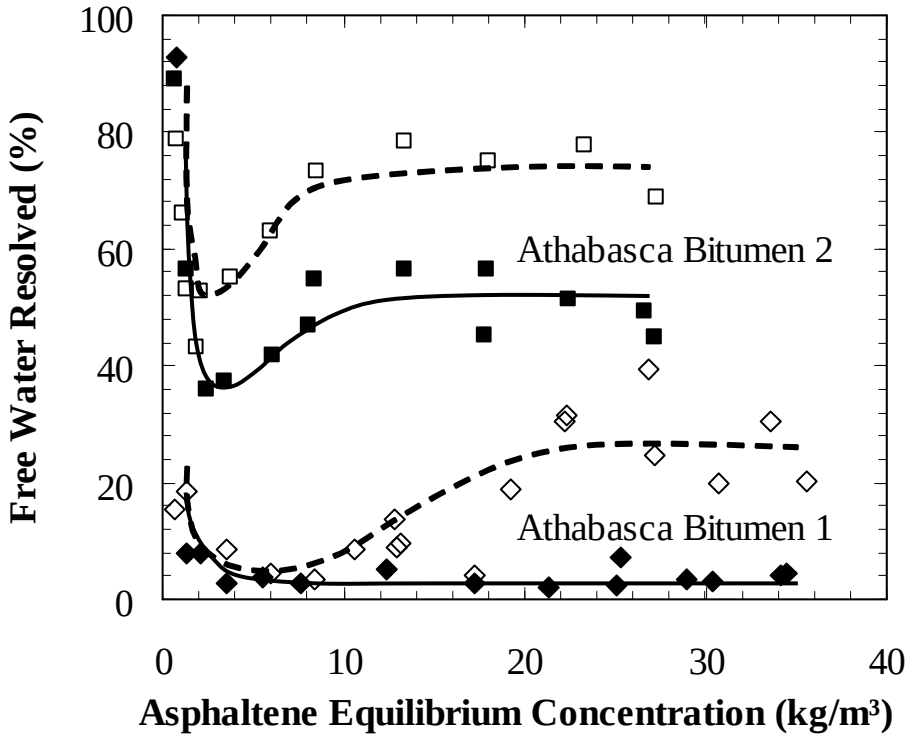

Figure 7.16: Free water resolution after two hours of treatment for model emulsions stabilized by Athabasca Bitumen 1 Asphaltenes and AS (diamonds), Athabasca Bitumen 2 Asphaltenes and AS (squares). 25/75 heptol, 40 vol% water, 1.5 hours settling. The closed symbols indicate AS and the open symbols indicate asphaltenes only. The lines are visual aides

There are several ways in which solids can contribute to emulsion stability. These include steric stabilization due to adsorbed solids on the interface or on the asphaltene film, as well as stabilization due to trapped particles. In order to better understand which scenario(s) are possible, it is necessary to examine the composition of the interface.

7.2.2 Interfacial Composition of Fine Solids-Stabilized Emulsions

Since Athabasca and IOL fine solids appear to be similar in size and composition and there was a limited supply of the IOL fine solids, only Athabasca fine solids were used for these experiments. For the data shown in Figures 7.15 and 7.16, the solid concentration in the AS emulsions varies from approximately 0.05 to 1.7 kg/m³. In order to assess interfacial composition, experiments were performed at a fixed asphaltene concentration of 1.9 kg/m³ and solids concentrations in the range indicated by Figures 7.15 and 7.16.

Figure 7.17 indicates that the enhanced stability is a function of the concentration of the solids. At a treatment time of two hours, emulsion stability increases as the solids concentration increases up to approximately 1.5 kg/m³. At all times, stability decreases at solids concentrations greater than 2 kg/m³.

The fractional surface coverage of Asphaltenes (and by difference of solids) was determined from Equations 3.20 and 3.21 for emulsions consisting of Athabasca Bitumen 1 Asphaltenes at a concentration of 1.9 kg/m³ and Athabasca fine solids varying from 0 to 2.8 kg/m³. The asphaltene monolayer coverage determined from Equation 3.20 and shown in Figure 4.15 was found to be 0.00265 g/m² at an asphaltene concentration of 1.9 kg/m³. The fractional solids surface coverage is shown in Figure 7.18.

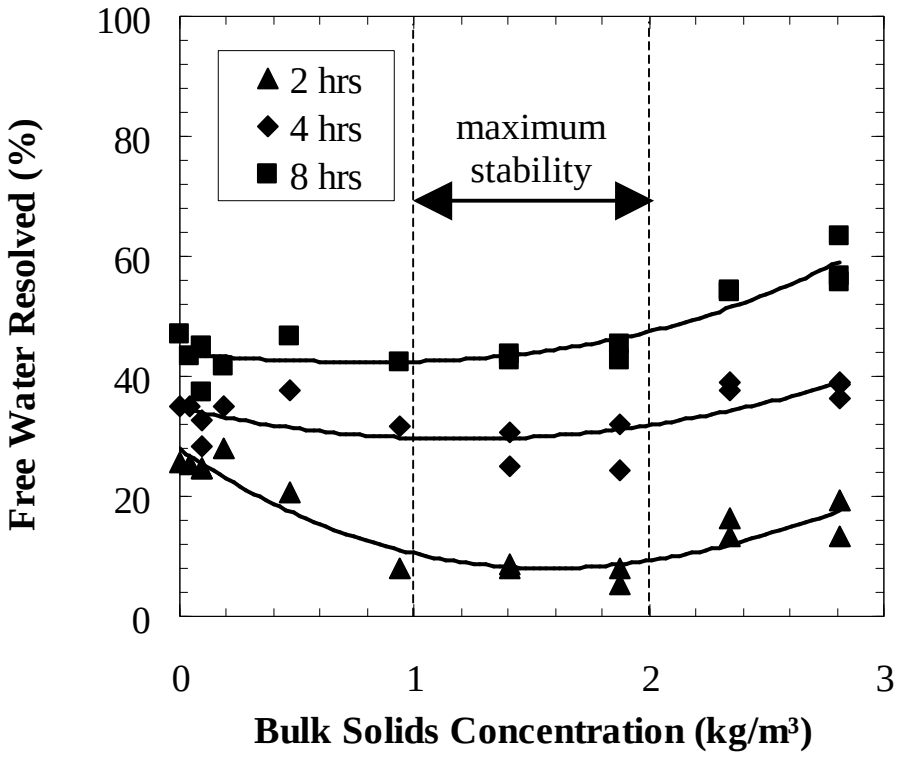

Figure 7.17: Free water resolution after two, four and eight hours of treatment for model emulsions stabilized by Athabasca Bitumen 1 Asphaltenes and fine solids. 25/75 heptol, 40 vol% water, 1.5 hours settling. The lines are visual aides

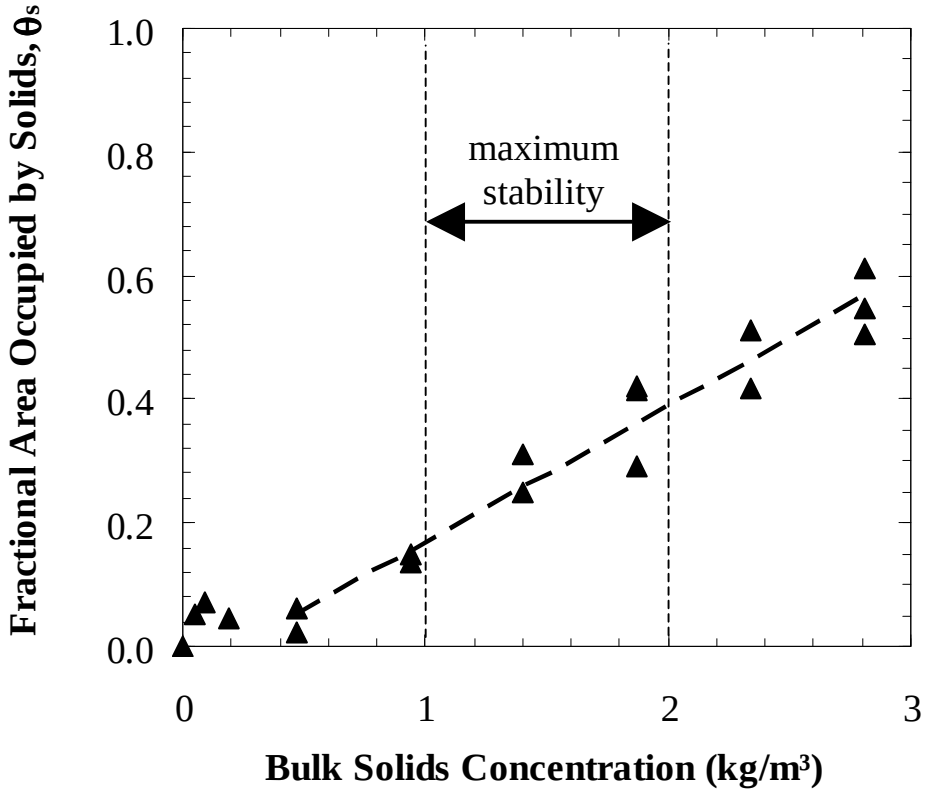

Figure 7.18: Fractional area occupied by solids on water-oil interface for model emulsions stabilized by Athabasca Bitumen 1 Asphaltenes and fine solids. 25/75 heptol, 40 vol% water, 1.5 hours settling. The line is a visual aide

Note that the solids concentration in both Figure 7.17 and 7.18 is the bulk concentration prior to emulsification. The equilibrium solids concentration after emulsification could not be determined since the solids concentration in the decanted continuous phase is not necessarily the same as the solids concentration in the continuous phase of the settled emulsion. Some of the solids may be trapped in the settled emulsion whether or not they adsorb on the water droplets.

Figure 7.18 confirms that at least some of the solids adsorb directly on the water/hydrocarbon interface. There appears to be competitive adsorption between the asphaltenes and solids since the solids surface coverage increases monotonically with solids concentration. At a solids concentration of 3 kg/m³, the solids have displaced asphaltenes from approximately 50% of the interfacial area. The most stable emulsions (least free water) occur when 60 to 80% of the area of the water/oil interface is covered by asphaltenes and 20 to 40% is covered by solids; that is, approximately a 2:1 fractional area ratio of asphaltenes to solids. It appears that a combination of asphaltenes and solids result in the most stable emulsions, consistent with the observations of Zaki *et al.* (2000) and Yan *et al.* (1999). The region of maximum emulsion stability is shown in Figures 7.17 and 7.18.

7.2.3 Interfacial Structure of Fine Solids-Stabilized Emulsions

The average thickness of solids adsorbed at the interface can be estimated from a combination of a material balance on the solids and a consideration of particle shape. It is assumed that the solids are a collection of monodisperse particles and that the asphaltenes in solution do no adsorb onto the particle surfaces. The ratio of the volume, V_s, of an individual particle to its area, A_s, is then given by:

$$\frac{V_s}{A_s} = \frac{1}{6}\frac{m_s(1-f_t)d_{32}}{\rho_s V_w(1-\theta_A)} \tag{7.1}$$

where m_s is the mass of solids on the interface, ρ_s is the density of the solids, θ_A is the fractional area occupied by asphaltenes on the interface, and f_t is the fraction of trapped and/or attached solids. If some of the solids are trapped between water droplets or are adsorbed on the outside of the asphaltene interfacial film, then the mass of solids adsorbed on the interface is less. The adsorbed solids equal $m_s(1-f_t)$.

To calculate the average size of the particles, a geometrical configuration for the solids must be assumed. In the current study, a disc-shaped geometry is assumed. A disc is the simplest approximation of a platelet and requires only two lengths for definition: the radius and thickness. The average thickness, t_s, for cylindrical particles on the interface is given by:

$$t_s = \frac{1}{6}\frac{m_s(1-f_t)d_{32}}{\rho_s V_w(1-\theta_A)} \qquad (7.2)$$

However, several simplifying assumptions must be made. First, it is assumed that all of the solids in the settled emulsion have adsorbed on the interface; that is, the fraction of trapped solids is zero. Second, the solids layer is uniform with a density of 2600 kg/m³, the density of koalinite. The average interfacial thickness of the adsorbed solids can then be determined from Equation (7.2). The calculated average thickness is plotted versus solids concentration in Figure 7.19. Note that for concentrations less than 0.4 kg/m³, the thickness is not presented because at high values of θ_A, the error in the thickness calculation is very large.

Figure 7.19 indicates that for all of the solids concentrations considered here, the average thickness of the solids adsorbed on the water/oil interface is 8 ±2 nm. This thickness is very close to the thickness of clay platelets. For example, TEM observations of aluminosilicate clays from oil sands indicated that the platelets were less than 10 nm thick (Bensebaa *et al.*, 2000). At first glance, it seems likely that the clays adsorb as individual platelets lying flat on the interface.

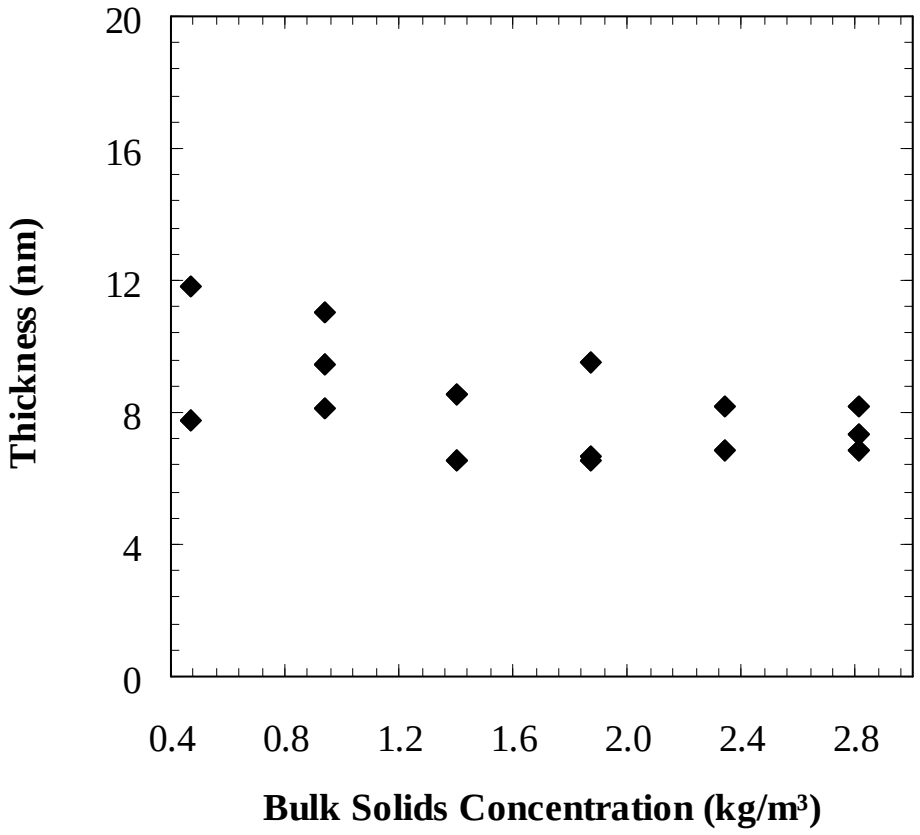

Figure 7.19: Thickness of Athabasca solids adsorbed at model interface. 25/75 heptol, 40 vol% water

It was assumed that all of the solids in the settled emulsion adsorbed on the interface. If this assumption is relaxed, the calculated thickness is even less. For example, if the concentration of trapped solids is assumed to be the same as the concentration of solids in the decanted continuous phase, the thickness of the solids layer decreases by 4%. If the fraction of trapped solids is assumed to be 25, 45, and 70%, the thickness of the solids layer decreases to 6, 4, and 2 nm, respectively. Kotlyar *et al.* (1998b) have observed platelets as thin as 1, 3 and 4 nm in a study of the properties of mature fine tailings. The most plausible interpretation is that the average thickness of the solids layer is at least 3 nm and the fraction of trapped solids is less than 50%.

Figure 7.20 illustrates how a combination of adsorbed solids and asphaltenes might contribute to emulsion stability. The thickness of the asphaltene layer at an asphaltene concentration of 1.9 kg/m^3 is approximately 2 nm as discerned from Figure 4.20. This is consistent with that reported by Taylor *et al.* from thin liquid film-pressure balance studies on systems of asphaltenes, toluene and water (Taylor *et al.*, 2002). The average thickness of the solids is less than 10 nm but the solids have irregular morphology so that local thickness may be greater than 10 nm as shown in Figure 7.20 (b). The solid platelets have a diameter upwards of 300 nm. The solids may act as mountainous islands that prevent very close contact between the droplets. Also, a bridge between droplets cannot form where a solid resides on the interface. With two approaching interfaces, a 25% fractional solids surface coverage on each interface may reduce the area for potential bridging by 50% as shown in Figure 7.20 (b). The presence of trapped solids between the approaching interfaces could prevent close contact between the droplets and enhance this stabilization mechanism as shown in Figure 7.20 (c).

It was assumed that the solids layer was uniform and consisted solely of solids; that is, zero porosity. It is possible that the clays form loose clusters that adsorb on the interface in a much thicker layer. However, once a partial monolayer of adsorbed solids is accounted for, the maximum average number of particles per aggregate is less than two.

It seems that solids aggregation can be ruled out. It is also possible that the solids add to the mechanical strength and rigidity of the interfacial film. However, a fractional solids surface coverage of 25% is probably insufficient to significantly alter the mechanical properties of the interface.

Hence, the most likely explanation is that there is a synergy between the asphaltenes and the solids; asphaltenes maintain a rigid interface while the solids form a barrier between the water droplets. At lower solids to asphaltene ratios, there are insufficient solids to form an effective barrier, while at higher ratios insufficient asphaltenes remain on the interface to immobilize the solids on the interface.

7.3 THE ROLE OF COARSE SOLIDS

7.3.1 Stability of Coarse Solids-Stabilized Emulsions

Since only a limited supply of IOL coarse solids were extracted from the solids-slurry and the coarse IOL and AEC solids are similar in size and nature, only the AEC solids were considered for these experiments. Table 3.3 indicated that the solids content of the AEC emulsion was 1.9 wt% or an equivalent solids concentration of approximately 19 kg/m^3. Hence, to reproduce the original AEC emulsion stability, it was necessary to utilize a solids concentration ten times greater than that used for the fine solids emulsions discussed in the previous section.

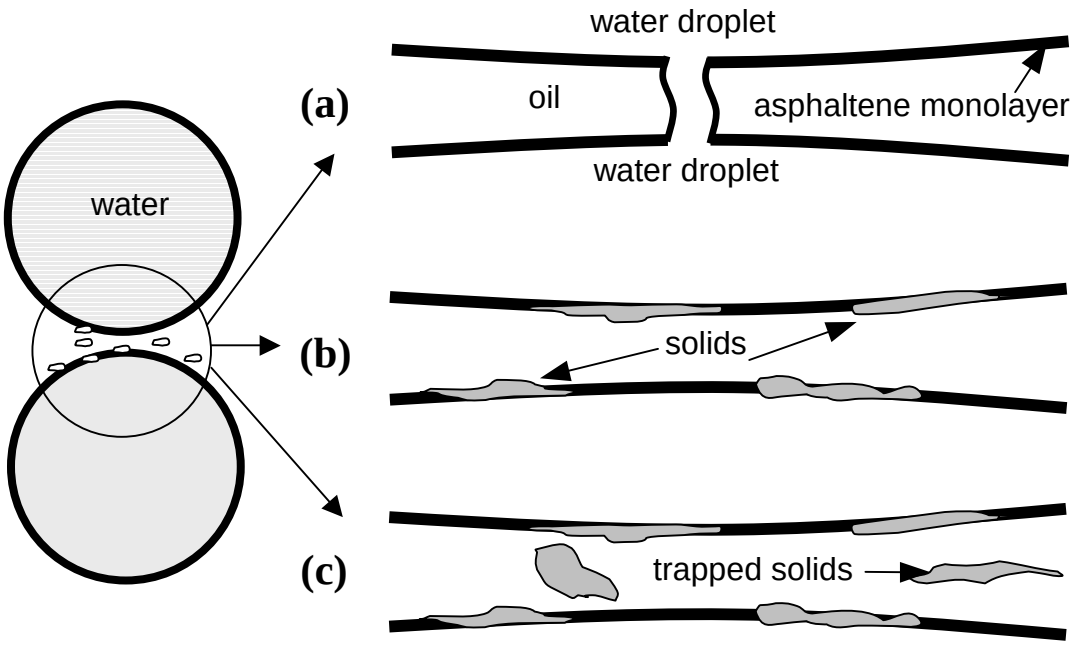

Figure 7.20: Possible configuration of fine solids in interfacial region: a) bridging of asphaltene film between two water droplets, b) adsorbed solids prevent bridging, c) trapped solids prevent close contact between droplets

Figure 7.21 shows the stability of emulsions created from Athabasca Bitumen 2 Asphaltenes at a concentration of 1.9 kg/m³ and solids varying in concentration from 0.01 to 25 kg/m³. When AEC solids are present in concentrations less than 5 kg/m³, unstable emulsions will result with complete water resolution after eight hours for emulsions containing less than 1 kg/m³ solids. However, as the solids concentration increases, the free water resolution decreases, a result consistent with the work of others (Menon and Wasan, 1988; Yan *et al.*, 1999; Tambe and Sharma, 1993; Menon and Wasan, 1984; Abend *et al.*, 1998; Schulman and Leja, 1954; Bowman, 1967; Gelot *et al.*, 1984; Yan and Masliyah, 1995; Binks and Lumsdon, 2001; Sullivan and Kilpatrick, 2002). For solids concentrations exceeding 10 kg/m³, the free water resolution of the model emulsion is approximately the same as that of the original AEC emulsion.

It is interesting to note that although the asphaltene concentration for the model system (1.9 kg/m³) and the actual emulsion (160 kg/m³) is markedly different, the actual emulsion stability can be reproduced. This result suggests that in high enough concentrations, coarse solids alone are sufficient to impart long term stability to an emulsion. This is confirmed by the additional results in Figure 7.21 which show that emulsions consisting solely of AEC solids at bulk concentrations exceeding 5 kg/m³ have the same free water resolution as those containing both asphaltenes and solids.

7.3.2 Interfacial Composition of Coarse Solids-Stabilized Emulsions

Figure 7.22 indicates that AEC solids replace all asphaltenes on the interface for bulk solids concentrations exceeding 1 kg/m³. Although the interface appears to be predominantly occupied by asphaltenes at bulk solids concentrations below 0.5 kg/m³, the emulsions are very unstable and are completely broken after eight hours of treatment. Note that an emulsion stabilized by 1.9 kg/m³ Athabasca Bitumen 2 Asphaltenes with no solids had only 63% resolved water after 8 hours of treatment. The high free water resolution of these emulsions with low AEC solids concentrations is linked to the large average droplet size as indicated in Figure 7.23.

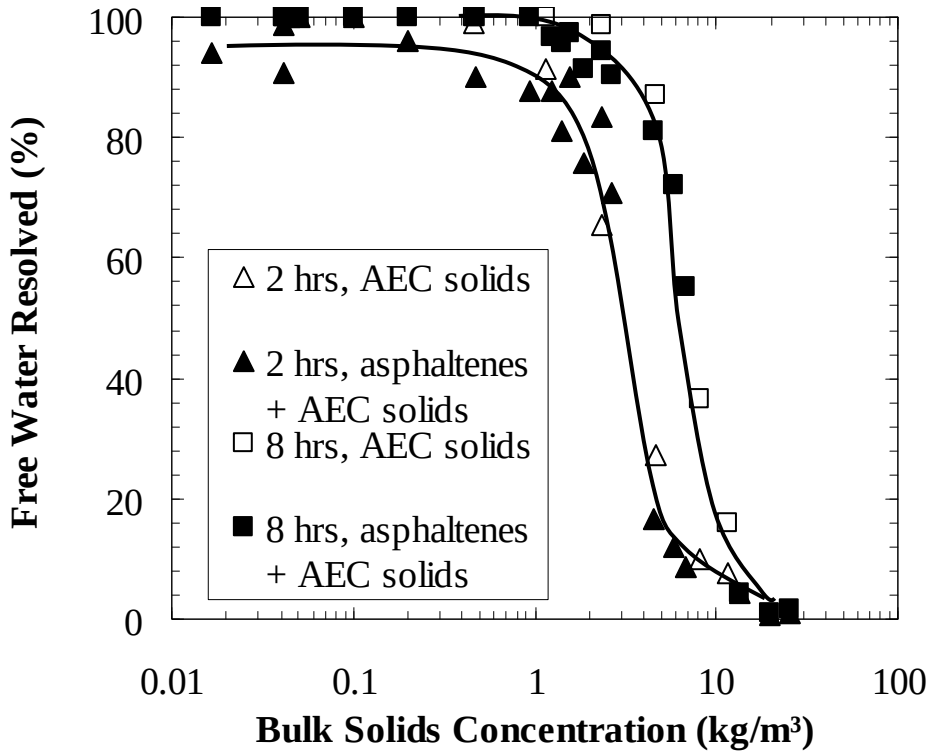

Figure 7.21: Free water resolution after two and eight hours of treatment for model emulsions stabilized by Athabasca Bitumen 2 Asphaltenes and AEC coarse solids and by AEC coarse solids. 25/75 heptol, 40 vol% water, 1.5 hours settling. The lines are visual aides

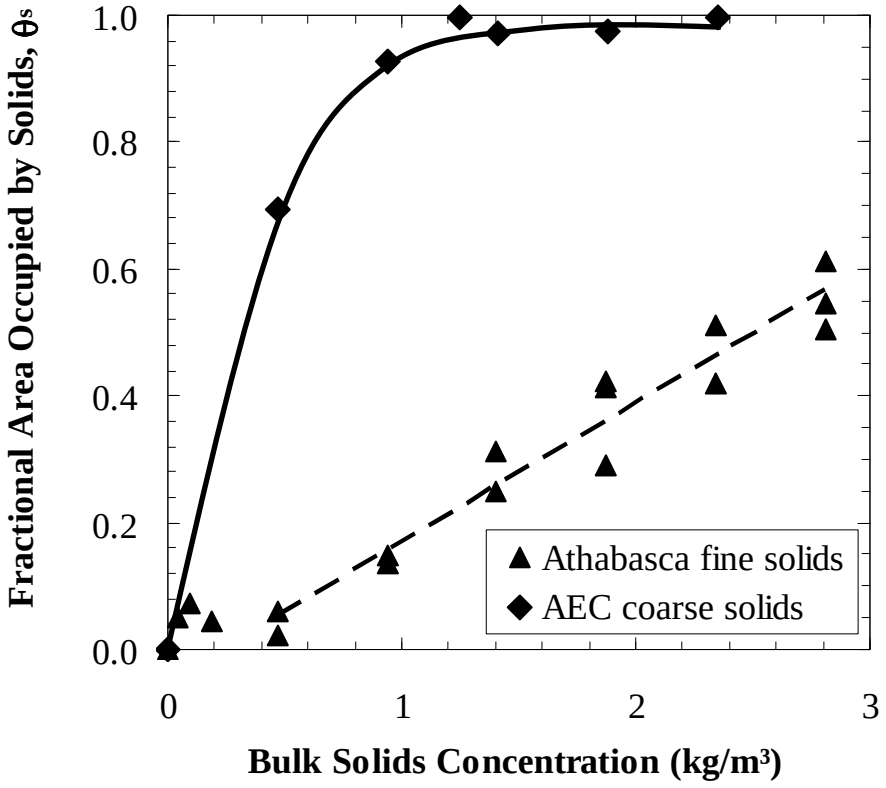

Figure 7.22: Fractional area occupied by solids on water-oil interface for model emulsions stabilized by Athabasca Bitumen 1 Asphaltenes and fine solids and by Athabasca Bitumen 2 Asphaltenes and AEC coarse solids. 25/75 heptol, 40 vol% water. The lines are visual aides

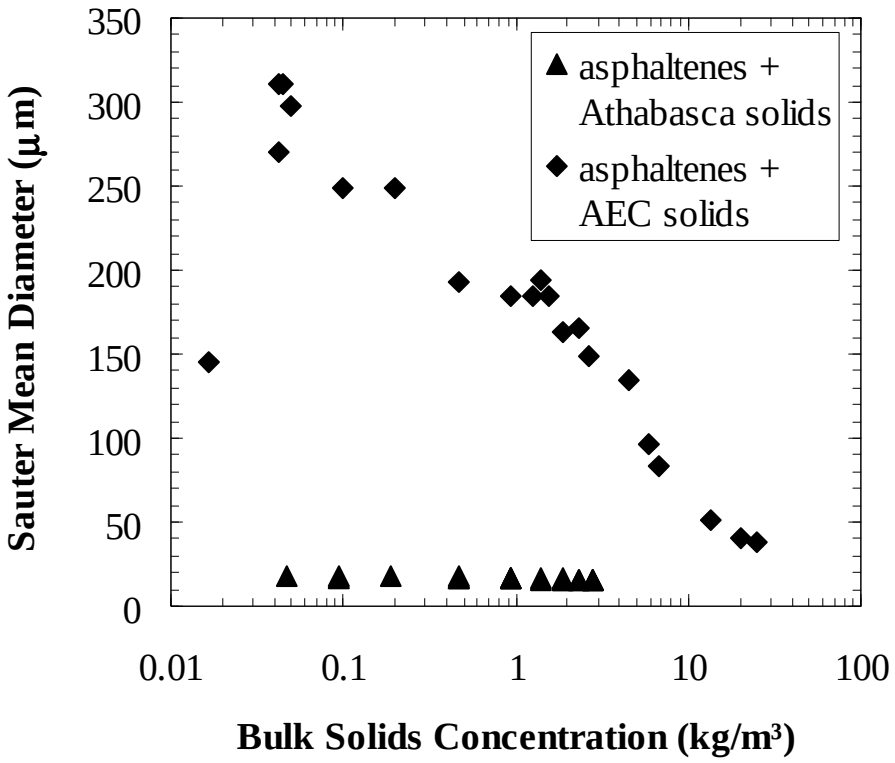

Figure 7.23: Sauter mean diameter of model emulsions stabilized by Athabasca Bitumen 1 Asphaltenes and fine solids (triangles), Athabasca Bitumen 2 Asphaltenes and AEC coarse solids (diamonds). 25/75 heptol, 40 vol% water, 1.5 hours settling

The droplet diameters are approximately ten times larger than those encountered in Asphaltene or Asphaltene and fine solids stabilized emulsions for low bulk solids concentrations, as illustrated in Figure 7.24.

Figures 7.23 and 7.24 suggest that there is significant coalescence of droplets during the settling period even though the interface is primarily occupied by asphaltenes. It is speculated that the few coarse solids that do adsorb on the interface act as bridges between water droplets and facilitate coalescence. To test this hypothesis, AEC solids at a concentration of approximately 0.5 kg/m^3 were gently stirred into a settled emulsion stabilized solely by Athabasca Bitumen 2 Asphaltenes. The Sauter mean diameter increased from 17 to approximately 180 microns within minutes. Hence, it appears that the AEC solids are capable of acting as bridges and facilitate coalescence at low concentrations.

When the solids concentration surpasses 1 kg/m^3 and continues to increase, particles can potentially form either a multilayer around the droplet or become trapped in the continuous phase between adjacent water drops. Trapped droplets or a thicker steric barrier prevent aggregation among water droplets and direct bridging of solids between interfaces, thus reducing coalescence and the overall free water resolution. Reduced coalescence is confirmed by the decrease in the Sauter mean diameter at higher solids concentrations, as shown in Figure 7.23. It appears that film rigidity imparted by asphaltenes adsorbed on the interface is unnecessary for achieving high emulsion stability if solids are present in high enough concentrations.

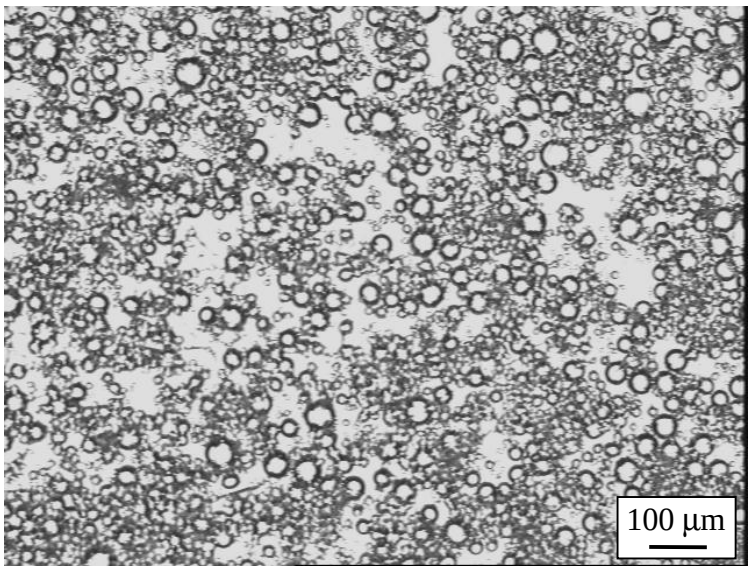

(a)

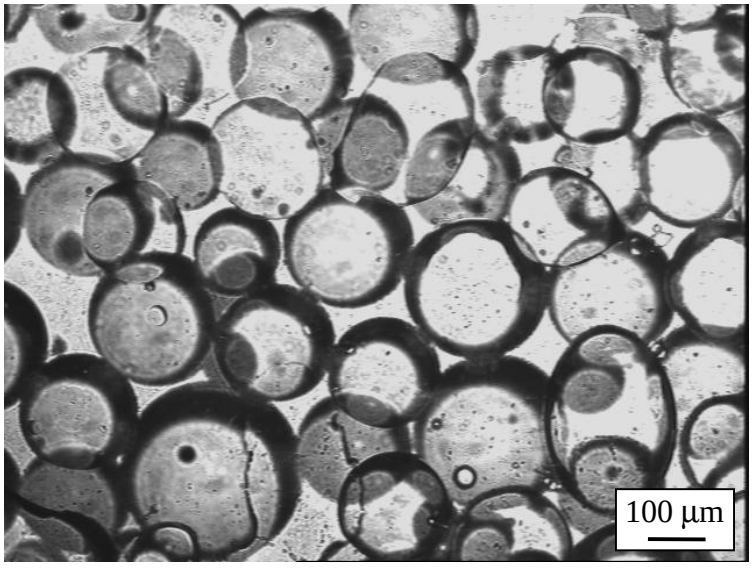

(b)

Figure 7.24: Micrographs of model emulsions stabilized by a) Athabasca Bitumen 1 Asphaltenes at 1.9 kg/m³ and Athabasca solids at 1 kg/m³, b) Athabasca Bitumen 2 Asphaltenes at 1.9 k/gm³ and AEC solids at 1 kg/m³. 25/75 heptol, 40 vol% water, 1.5 hours settling

7.4 TREATMENT OF SOLIDS-STABILIZED EMULSIONS

Figure 7.25 summarizes the hypothesized configurations of fine and coarse solids in the near interfacial region of an emulsion. The location of solids in an emulsion has consequences for emulsion treatment. If solids or asphaltenes are located on the interface, it is desirable to weaken the interface; for example, by introducing a chemical capable of replacing these particles with a material that will promote droplet coalescence. If, however, solids are not located on the interface but enhance an emulsion's stability by trapping or multilayer formation, a treatment based on particle flocculation would be more beneficial. If solids can be flocculated and concentrated in such a way that they do not hinder the aggregation of droplets, the interface of such an emulsion may be weak enough for coalescence. Two preliminary treatments based on these principles are considered here: toluene dilution and heptane dilution.

There is evidence that when the continuous phase is either strongly aromatic or strongly paraffinic, emulsions with low stability are created (McLean and Kilpatrick, 1997; Gafonova and Yarranton, 2001). Similarly, unstable emulsions result when asphaltenes are either in a mostly soluble or insoluble range (Yang *et al.*, 2004). Hence, it is speculated that it may be possible to destabilize an existing emulsion if excess toluene (aromatic) or heptane (paraffinic) are added. In a good solvent such as toluene, asphaltenes are more mobile and form a weaker, less elastic interface. Excess toluene may further weaken the interface and promote droplet coalescence. In a poor solvent such as heptane, asphaltenes may precipitate and flocculate and be less likely to adsorb on and stabilize the interface. Heptane may also cause solids to flocculate and become less effective stabilizers.

The effect of toluene and heptane dilution is discussed below for emulsions stabilized by asphaltenes, asphaltenes and fine solids, and asphaltenes and coarse solids.

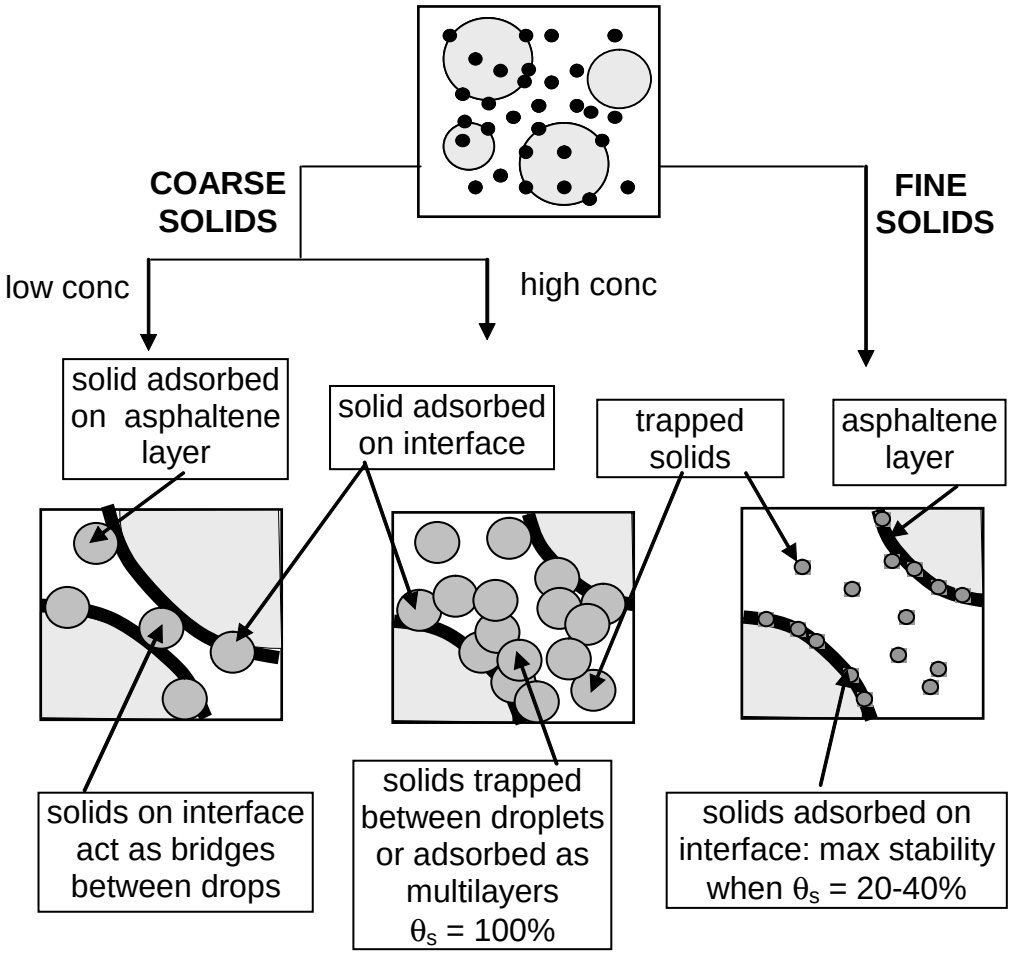

Figure 7.25: Possible distributions of coarse and fine solids in an emulsion

7.4.1 Effect of Solvent Dilution on Asphaltene-Stabilized Emulsions

Model emulsions were prepared from Athabasca Bitumen 2 Asphaltenes at 5 kg/m³ in 25/75 heptol and allowed to settle for 1.5 hours. The continuous phase that evolved during the settling time was decanted until only concentrated emulsion remained. Toluene or heptane was then added to the concentrated emulsion at ratios varying from 0.2 to 2.8 cm³/cm³ solvent/emulsion, which corresponds to a solvent/continuous phase ratio of 0.6 to 7 cm³/cm³. The mixtures were shaken in a shaker table for approximately two minutes to ensure the solvents were entirely dispersed throughout the emulsion. The mixtures were poured into centrifuge tubes, capped and subjected to the destabilization treatment outlined in Section 3.4.5. Note that the free water resolution for these experiments is reported after two hours.

Figure 7.26 shows that the addition of toluene increases the free water resolution by 30% once the toluene/continuous phase ratio exceeds 1 cm³/cm³. The addition of toluene does appear to weaken the interface and promote coalescence. On the other hand, heptane dilution results in very stable emulsions with no free water resolution for dilution ratios exceeding 1 cm³/cm³ heptane/continuous phase. Note that the heptane content of the continuous phase at the lowest and highest dilution ratios was 60 and 95%, respectively, which is above the onset of precipitation (at 50% heptane).

At first glance, the increased stability contradicts previous work (McLean and Kilpatrick, 1997; Gafonova and Yarranton, 2001) indicating that if sufficient heptane to precipitate asphaltenes is added *prior* to emulsification, the emulsions are unstable. However, in this case, the heptane was added *after* emulsification. It appears that as the continuous phase becomes a poor solvent, the asphaltenes adsorbed on the interface become trapped on the interface and are not precipitated. They appear to form a stronger film that provides more resistance to coalescence.

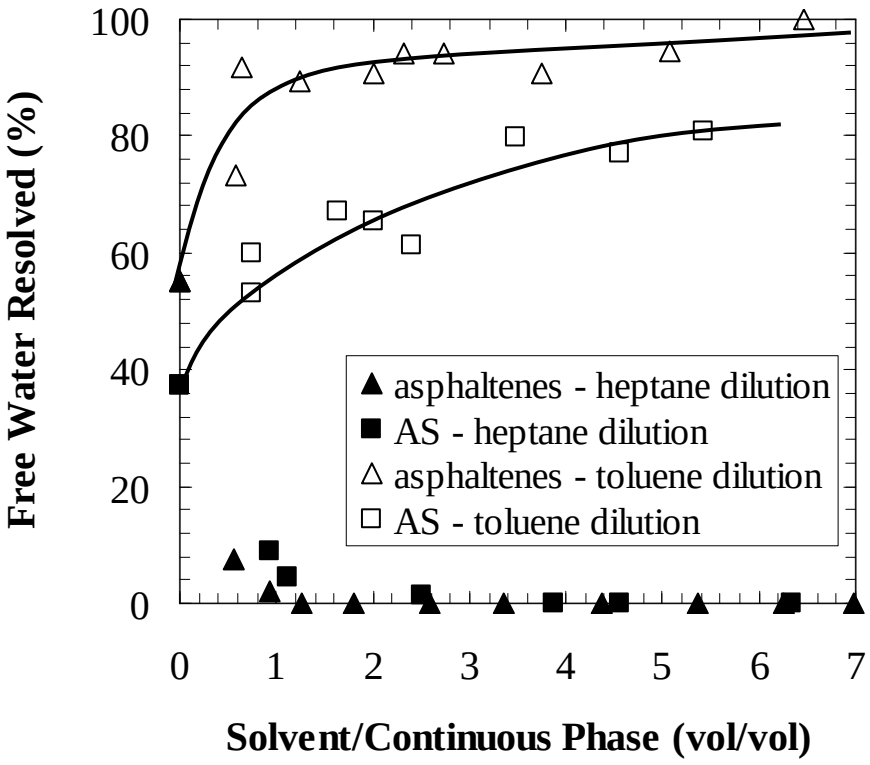

Figure 7.26: Effect of solvent and solvent concentration on free water resolution of model emulsions stabilized by Athabasca Bitumen 2 Asphaltenes and AS after two hours of treatment. 25/75 heptol, 40 vol% water, 1.5 hours settling. The lines are visual aides

7.4.2 Treatment of Emulsions with Fine Solids

Model emulsions were prepared from Athabasca Bitumen 2 AS at a total concentration of 5 kg/m³ in 25/75 heptol. As noted in Table 3.2, the solids made up 3.1 wt% of the AS and hence the solids concentration is 0.15 kg/m³. The emulsions were settled for 1.5 hours and the continuous phase decanted. The concentrated emulsions were diluted at ratios similar to those used for the asphaltene-stabilized emulsions. The free water resolution was again reported after two hours.

Figure 7.26 shows that the addition of toluene results in an additional 30% free water when the dilution ratio exceeded 2 cm³/cm³ toluene:continuous phase. Heptane dilution results in very stable emulsions with no free water resolution for heptane ratios greater than 1 cm³/cm³. While the presence of solids increases emulsion stability in general, it appears that the effect of the diluent on the asphaltenes is the dominant factor in the treatment. Toluene addition weakens the interface and results in more coalescence. Heptane addition strengthens the interface and results in less coalescence than no treatment at all.

As a comparison, the IOL rag layer was also treated with 1:1 volume ratio of solvent to emulsion dilutions (2 cm³/cm³ solvent:continuous phase). The rag layer was stabilized by asphaltenes and fine solids with a solids concentration of 33 kg/m³. The toluene and heptane treatments achieved 84% and 29% free water resolution, respectively. The results are consistent with those for the model emulsions prepared from Athabasca AS. Hence, even at relatively high fine solids concentrations, the effect of the solvent on the asphaltenes appears to be the dominant factor in the treatments.

7.4.3 Treatment of Emulsions with Coarse Solids

Figure 7.27 shows the effect of toluene and heptane dilution on the AEC emulsion. Toluene addition did not destabilize the emulsion even at high dilution ratios and after eight hours of treatment. However, heptane addition significantly destabilized the

emulsion even at dilution ratios below the onset of asphaltene precipitation, i.e., at a dilution ratio of 1.3 wt/wt heptane:bitumen (2.0 cm^3/cm^3 heptane:continuous phase). In fact, the maximum free water resolution is experienced just below the onset of precipitation. Recall that coarse solids in high concentrations appeared to stabilize the emulsion by preventing contact between droplets. They also dominated the interface so that asphaltenes are not expected to play a significant role in stabilizing the emulsion. It is speculated that heptane addition causes the solids to flocculate. Flocculated solids are far less likely to form a continuous barrier between the water droplets; and hence, coalescence can occur.

A brief test in which heptane was added to wet AEC solids indicated that they flocculated into aggregates varying from 20 to approximately 200 μm in size, as indicated by the micrograph in Figure 7.28 (a). The flocculation of coarse solids in heptane confirms that they have some adsorbed hydrocarbon matter. Figure 7.28 (b) shows that the solids did not flocculate in toluene. The toluene treatment is therefore ineffective because the primary stabilization mechanism remains in place. Note that with sufficient dilution and agitation, any solvent could likely break this emulsion simply by reducing the concentration of the solids (see Figure 7.21). However, flocculation of the solids clearly promotes the emulsion breaking.

With the heptane treatment, the maximum in the free water resolution occurred at the onset of asphaltene precipitation. It is possible that precipitated asphaltene particles simply add to the total concentration of particles increasing the stability of the AEC solids-stabilized emulsion. It is also possible that as heptane is added some asphaltenes are driven to the interface and that at high heptane dilutions they enhance emulsion stability. In either case, the maximum in free water would occur at the onset of precipitation.

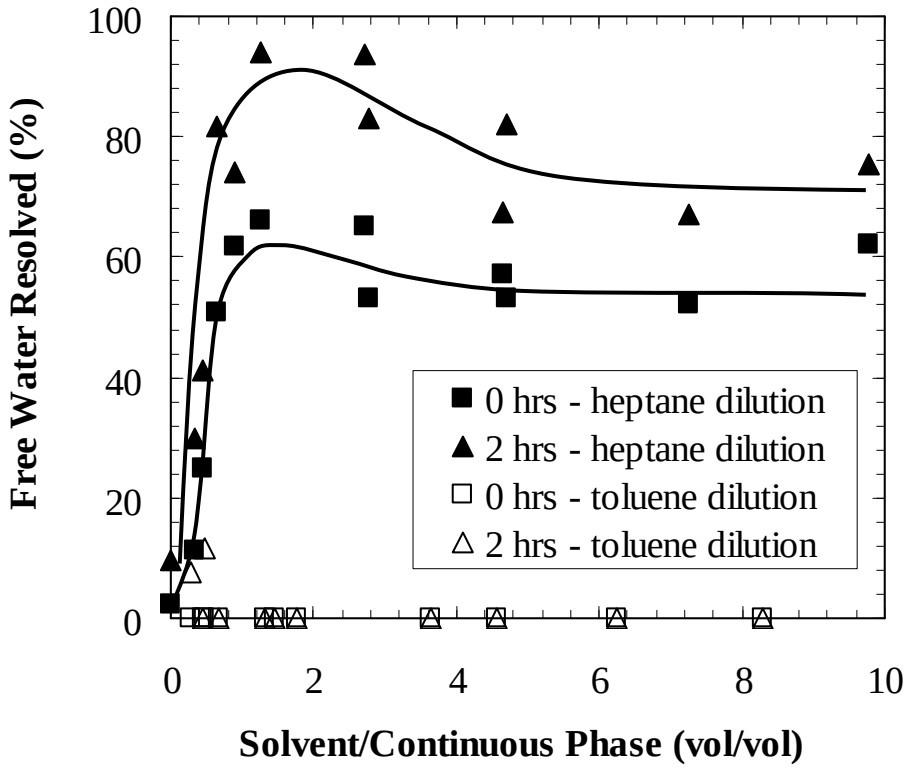

Figure 7.27: Effect of solvent and solvent concentration on free water resolution of AEC emulsion. The lines are visual aides

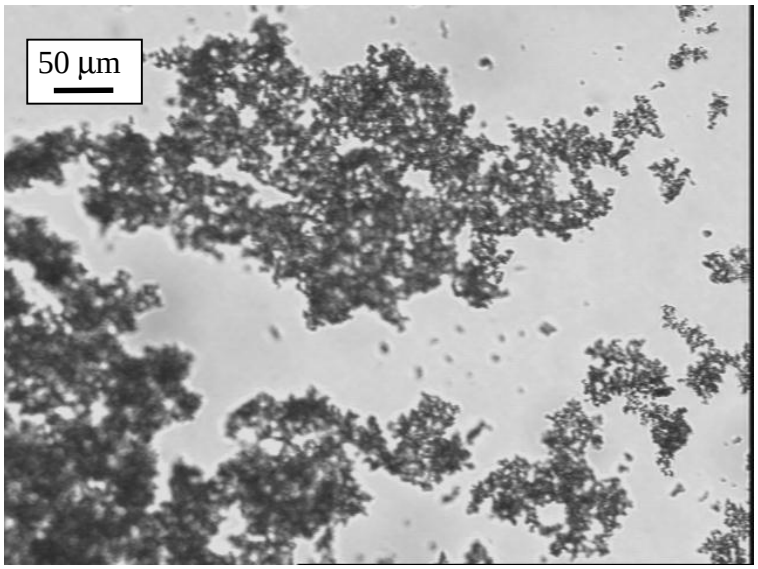

(a)

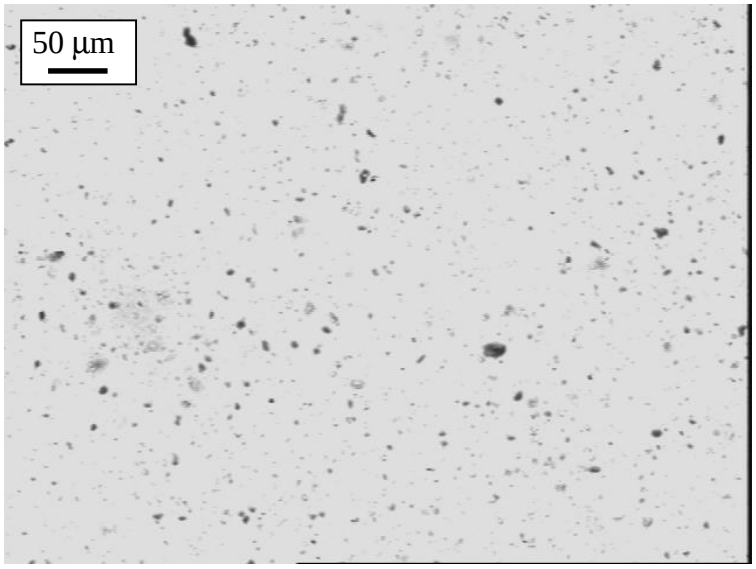

(b)

Figure 7.28: Micrographs of AEC solids dispersed in a) pure heptane, b) pure toluene

The IOL solids slurry was also treated with 1:1 volume ratio of solvent to emulsion dilutions (2 cm^3/cm^3 solvent:continuous phase). The toluene and heptane treatments achieved 13% and 23% free water resolution, respectively. The toluene treatment results are consistent with those for the AEC emulsion. Although the heptane treatment outperformed the toluene treatment, it was less effective than the heptane treatment of the AEC emulsion. It is possible that additives present in the IOL solids slurry reduce the effectiveness of the heptane treatment.

7.5 CHAPTER CONCLUSIONS

Fine solids, i.e., platelet shaped particles ranging from 50 to 500 nm, compete with asphaltenes to adsorb on the interface. Fine solids adsorb flat on the interface and likely form a partial barrier to water bridging between droplets. A combination of asphaltenes and fine solids at the water/oil interface in a 2:1 fractional area ratio creates a maximum in emulsion stability. If there are too few solids, there is an insufficient surface coverage to provide extra stability, whereas too many solids results in an interface that is not rigid enough to maintain stability.

Relatively low concentrations of coarse clays destabilize emulsions because they replace asphaltenes on the interface and cannot stabilize small water droplets. Coarse solids may also act as bridges between individual water droplets, increasing the mean diameter of water droplets and the overall coalescence rate. Conversely, relatively high concentrations of coarse clays strongly stabilize emulsions because they prevent close contact between water droplets or form multilayers on the interface.

The most effective treatments for emulsions stabilized by fine clays appear to be those that weaken the interfacial film or replace the solids and asphaltenes on the interface with a poorer stabilizer. Emulsions stabilized by coarse particles are most effectively broken when solids are flocculated so that they can no longer prevent close contact between

water droplets. Refinery emulsions containing both types of solids may require more than one type of treatment for effective water resolution.

CHAPTER 8
CONCLUSIONS AND RECOMMENDATIONS

The main objective of this work was to investigate the compositional, structural and rheological properties of the water/hydrocarbon interface and to relate them to the stability of model asphaltene and solids-stabilized emulsions. The conclusions from this study and recommendations for future research are presented below.

8.1 THESIS CONCLUSIONS

Asphaltenes

1. Results from vapour pressure osmometry, interfacial tension and emulsion gravimetric studies were combined to calculate the number of asphaltene layers adsorbed at the water/oil interface. Asphaltenes appear to initially adsorb as a monolayer of self-associated molecular aggregates, even at concentrations as high as 40 kg/m^3. The interfacial area of Athabasca asphaltenes is approximately 1.5 nm² and does not vary with concentration. However, the mass of the asphaltenes on the interface increases with concentration as the asphaltenes associate into larger macromolecules. Higher molar mass asphaltenes extend more into the continuous phase. The estimated thickness of the interfacial monolayer ranges from 2 to 9 nm.

2. The assessment of the interfacial configuration of Soxhlet-Washed Asphaltenes revealed that it is unlikely that asphaltenes greater than 10,000 g/mol adsorb on the interface.

3. It is necessary to account for asphaltene self-association when interpreting interfacial data. For instance, the correct method to determine the interfacial area of asphaltenes at the interface is from a plot of interfacial tension versus the molar concentration of asphaltenes rather than the mass concentration. Using the mass concentration is only valid for non-associating molecules and can introduce significant error in the calculated area for asphaltenes.

4. The asphaltene monolayer is adsorbed reversibly only at short interface aging times. The elastic and viscous moduli can be modeled using the Lucassen-van den Tempel (LVDT) approach when the aging time is less than 10 minutes. However, asphaltenes gradually reorganize on the interface to form a rigid, irreversibly adsorbed network, which can no longer be modeled with a Surface Equation of State and the LVDT approach. Increased film rigidity can be detected with an increase in the total elastic modulus of the water/oil interface.

5. The total modulus, and therefore the film rigidity, increases as the interface is aged, the heptane fraction in the heptol increases, and the asphaltene concentration decreases.

6. Increased film rigidity reduces the rate of coalescence in an emulsion. For systems in which asphaltenes do not leave the interface during coalescence, the rate of coalescence can be related to the measured total modulus through a single curve which accounts for interface aging time, asphaltene concentration, and solvent quality. When asphaltenes are expelled from the interface, the measured total modulus is under-predicted. It is hypothesized that expulsion results in a more rigid film because the asphaltenes least likely to contribute to strong, network formation leave the interface whereas those most likely to contribute to strong network formation remain on the interface.

7. Increased film rigidity and reduced coalescence result in increased overall emulsion stability. Emulsions become more stable when the interface aging time increases, the heptane fraction in heptol increases, and the asphaltene concentration decreases (for asphaltene concentrations relevant for emulsion stability, i.e., greater than 2 kg/m^3). Emulsion stability could not be correlated to the rheological properties of the interfacial film alone. It is likely that other factors such as the crumpling ratio also influence emulsion stability.

8. Asphaltenes extracted from two sources of Athabasca bitumen (Bitumen 1 and 2) resulted in model emulsions with markedly different emulsion stability. Although the trends with asphaltene concentration are consistent (decreasing stability with increasing concentration once the minimum in free water is surpassed), the free water resolution appears to decrease when the emulsion is stabilized with asphaltenes that have a higher molar mass and higher average interfacial area (Bitumen 1 Asphaltenes). Additionally, the rheological properties of Bitumen 1 and Bitumen 2 Asphaltene-stabilized water/hydrocarbon interfaces may be different. It is speculated that Bitumen 1 Asphaltenes may form interfaces with a higher total modulus than interfaces stabilized by Bitumen 2 Asphaltenes, hence resulting in emulsions with lower free water resolution.

Solids

9. It appears that exposure of solids to air alters the surface properties of the solids. In order to reproduce emulsion stability, freshly extracted, “wet” solids must be used in emulsion experiments.

10. Fine solids, i.e., platelet shaped particles ranging from 50 to 500 nm, compete with asphaltenes to adsorb on the interface. Fine solids adsorb flat on the interface and likely form a partial barrier to water bridging between droplets. A

combination of asphaltenes and fine solids at the water/oil interface in a 2:1 fractional area ratio creates a minimum in free water resolution. Too few solids result in insufficient surface coverage to provide extra stability, whereas too many solids results in an interface that is not rigid enough to maintain emulsion stability.

11. Coarse solids, i.e., platelet shaped particles ranging from 1 to 10 microns destabilize emulsions in low concentrations but significantly increase emulsion stability in high concentrations. Relatively low concentrations of coarse solids destabilize emulsions because they replace asphaltenes on the interface and therefore cannot stabilize small water droplets. In low concentrations, coarse solids may act as bridges between individual water droplets, increasing the mean diameter of water droplets and the overall coalescence. Conversely, relatively high concentrations of coarse clays strongly stabilize emulsions because they prevent close contact between water droplets or form multilayers on the interface.

12. The most effective treatments for emulsions stabilized by fine clays appear to be those that weaken the interfacial film or replace the solids and asphaltenes on the interface with a poorer stabilizer. Emulsions stabilized by coarse particles are most effectively broken when solids are flocculated so that they can no longer prevent close contact between water droplets. Refinery emulsions containing both types of solids may require more than one type of treatment, or even process step, for effective water resolution.

8.2 NOVELTY OF THE RESEARCH AND INDUSTRIAL IMPLICATIONS

The conclusions regarding the effects of asphaltenes and native oilfield solids on the formation of interfacial films and on ultimate emulsion stability have important consequences on the direction of future research. Additionally, the observations and conclusions made in this thesis have direct impact on or application to industrial processes.

Asphaltenes

The current research has shown that although asphaltenes adsorb initially at the water/oil interface as a monolayer, they quickly begin rearranging and forming rigid, three dimensional networks that strengthen as the interface is aged. The application of the LVDT model showed that reversible adsorption of asphaltenes occurs at relatively short interfacial aging times. Rigid film formation was observed directly as an increase in the total modulus of asphaltene-in-heptol/water interfaces. Mechanical effects were observed indirectly when the LVDT model failed to match predicted and experimental elastic and viscous moduli at interface aging times exceeding ten minutes. Consistent with the work of others (Freer and Radke, 2004), it was concluded that irreversible adsorption had occurred and that mechanical films had formed at the interface. Most importantly, it was shown that mechanical effects are very fast and therefore, the LVDT model should not be used to predict elasticity except at short aging times. Consequently, development of predictive models should be aimed primarily at incorporating mechanical interfacial effects.

In the present study, the total modulus was also shown to correlate with the coalescence rate over a range of asphaltene concentrations, solvent qualities, and interface aging times. Although the total modulus did not correlate to the ultimate free water resolution with a single curve, correlation within each solvent quality was possible over a range of

asphaltene concentrations and interface aging times. Interestingly, it was found that an increase in asphaltene concentration results in more fluid interfacial films (lower total modulus), which finally explained why emulsion stability decreases (free water resolution increases) when the asphaltene concentration increases. Often, speculations in the literature imply that film rigidity increases when asphaltene concentration increases, and that therefore the emulsion stability should also increase. The current work has shown that this is not an accurate hypothesis. Note that it is possible that some of the observations in the literature regarding the effects of asphaltene concentration on emulsion stability were based on emulsions stabilized by not only asphaltenes, but also associated solids. Therefore, the current research has also shown that assessment of the effects of asphaltenes on film rigidity and emulsion stability must be performed on a solids-free basis.

The present study also showed that emulsions stabilized by asphaltenes can be destabilized if the rigidity of the interface is reduced. The addition of an aromatic solvent such as toluene was shown to increase the free water resolution of Asphaltene-stabilized emulsions by 30%. Although many commercial demulsifiers are aimed at flocculating water droplets or solid materials trapped in the continuous phase, demulsifiers are also used to promote coalescence of water droplets by reducing the rigidity of the interface. The effectiveness of a chemical demulsifier depends on its chemical nature and concentration. Its effectiveness is also related to the age of the emulsion. Since this study showed that asphaltenes form rigid interfacial films relatively quickly, the timing of chemical demulsifier addition is probably critical. A demulsifier aimed at replacing interfacial material and reducing the rigidity of the interface should be added as soon as possible in order to avoid or reduce the formation of strong asphaltene networks on the interface. As the delay between emulsification and demulsifier addition increases, the effectiveness of the demulsifier will likely be reduced and possibly more demulsifier will be required in order to penetrate very viscous, asphaltene stabilized films.

Since the total modulus was shown to correlate with coalescence rate and to a lesser extent with the ultimate free water resolution, measurements of total, elastic and viscous moduli can be used to estimate the degree of coalescence and free water resolution in existing emulsions and, more importantly, assess the potential effectiveness of chemical demulsifiers. A reduction in total modulus upon demulsifier addition can be used to narrow down conditions required for testing (i.e., type of chemical demulsifier, concentration) and reduce the number of bottle tests. Additionally, the effects of emulsion age (i.e., interface aging time) can be assessed for each demulsifier. Perhaps some demulsifiers are effective only at short interface aging times, prior to the formation of very rigid interfacial films, while others are effective even at long aging times. Therefore, measurement of rheological properties can be used to optimize demulsifier type and concentration. In order to apply this commercially, a study of the effects of selected families of demulsifiers on interfacial rheological properties must be conducted.

Solids

When fine clays less than 500 nm in diameter are present in crude oil, they can adsorb at water/oil interfaces and increase emulsion stability beyond that observed for asphaltene-stabilized emulsions. The current work showed that when 20 to 40% of the interface is occupied by solids, a synergistic effect occurs between asphaltenes and solids, resulting in emulsions with minimum free water resolution. Therefore, if possible, it is desirable to avoid a situation in which the surface coverage of solids is such that emulsion stability is a maximum. At low solids surface coverage, the emulsion can be treated by reducing the rigidity of the asphaltene interface (either with dilution with an aromatic solvent, or with the addition of a chemical designed to replace the asphaltenes on the interface).

When coarse clays varying from approximately 1 to 10 microns are present in the crude oil, they too can adsorb at the water/oil interface. The current work showed that in relatively low concentrations, these clays do not contribute to emulsion stability.

However, in large concentrations coarse clays were shown to create very stable emulsions by becoming trapped between water droplets. It was also shown that emulsions stabilized by high concentrations of coarse solids can be destabilized if the solids are flocculated through the addition of a paraffinic solvent.

Knowledge of the location of fine and coarse solids in an emulsion and their mechanisms of stabilization can be important for oilfield operations. For example, in Alberta's oil sands industry, bitumen recovery is performed in two stages: the extraction stage, and the froth treatment stage. In the extraction stage, bitumen froth is recovered when hot water, oil sands and other chemicals such as sodium hydroxide are mixed and settled. The bitumen froth contains emulsified water and suspended solids. In the froth treatment stage, the bitumen froth is processed to remove these solids and water and recover clean bitumen. Currently, two processes exist for treating froth: the Syncrude and Albian process (Shelfantook, 2004). In the Syncrude process, an aromatic solvent (naphtha) is added to the bitumen froth and the mixture is then centrifuged. Addition of naphtha reduces viscosity and promotes water coalescence. In the Albian process, a paraffinic solvent is added to the bitumen froth and the mixture is allowed to settle. Dilution with a paraffinic solvent promotes aggregation of water drops and the removal of solids since many of the solids are known to adsorb at the water/oil interface. Typically, the bitumen recovery from the Syncrude process is 5 to 10% higher than the Albian process (Shelfantook, 2004), but the bitumen recovered with the Albian process is cleaner (less water and solids).

The Syncrude process is effective in breaking water-in-oil emulsions except possibly when fine solids are present. The presence of fine solids may partially explain why an emulsion of two micron water droplets survives the froth treatment process. The Albian process is effective at obtaining clean bitumen, but the separated emulsion may be difficult to break because the asphaltene film is surrounded by a paraffinic solvent and dispersed solids.

8.3 RECOMMENDATIONS FOR FUTURE RESEARCH

Although this research has helped to reveal the structural and rheological properties of water/oil interfaces and their relation to emulsion stability, several new questions arose during the study. The following are recommendations for future avenues of research.

1. Theoretical work aimed at modeling the interfacial rheology of asphaltene stabilized water/oil interfaces should concentrate on visco-elastic or mechanical models. The SEOS-LVDT approach is limited for interface aging times less than 10 minutes. However, the approach may be useful for systems containing chemical demulsifiers; the interaction of demulsifiers with asphaltenes and their influence on the rheology may be illuminated even with a short-time modeling approach.

2. The model emulsion aging tests revealed that asphaltenes leave the interface during coalescence for certain systems. It was speculated that removal of asphaltenes from the interface would result in a higher total modulus than measured in experiments where the interfacial area is fixed and no expulsion occurs. One way to check if asphaltene expulsion affects the interfacial rheology is to perform elasticity measurements on a drop that is shrunk stepwise over the course of the desired aging time. Stepwise shrinking mimics coalescence and may result in a more accurate reflection of the interfacial rheology of real emulsion systems.

3. Although it was possible to relate the rheology of the interface to the rate of coalescence in an emulsion, the correlation between rheology and ultimate emulsion stability was less obvious. One possible reason for the lack of a single relationship is the discrepancy between the emulsion treatment temperature, 60ºC, and the temperature at which rheological measurements were made, 23ºC. It is

possible that the rheology of the interface changes when the temperature increases. Therefore, the total, elastic and viscous moduli of water/oil interfaces should be measured at 60ºC over the concentration range relevant for emulsion stability. The effect of solvent quality should also be assessed in order to gauge the relative changes in moduli with temperature for each solvent.

4. There is considerable debate in the literature as to the role of resins in emulsion stability. The total, elastic, and viscous moduli of water/oil interfaces stabilized by resins and combinations of resins and asphaltenes should be measured in order to assess the effect of resins. A consistent rheological study would not only quantify the effects of resins on elasticity, but also help relate the interfacial properties of films containing resins to emulsion stability.

5. Emulsions stabilized by asphaltenes and fine solids should be destabilized with a treatment aimed at replacing or removing the surface-active materials from the interface. Emulsions stabilized by coarse solids in high concentrations should be destabilized with a treatment aimed at flocculating the solids. The proposed heptane and toluene treatments resulted in promising results; however, they need to be assessed in more detail. Specifically, it would help to test these methods on existing oilfield emulsions. Further, as demonstrated by the IOL refinery emulsion, it is possible that emulsions are stabilized by more than one type of solid and stabilization mechanism. Combinations of the proposed treatments, or perhaps more than one process step, may be beneficial for the optimization or design of treatments that rely less on chemical demulsifiers.

REFERENCES

Abend, S., Bonnke, N., Gutschner, U., and Lagaly, G., "Stabilization of Emulsions by Heterocoagulation of Clay Minerals and Layered Double Hydroxides," *Colloid Polym. Sci.*, **276**, 730-737 (1998).

Acevedo, S., Escobar, G., Gutierrez, L.B. and Rivas, H., "Isolation and Characterization of Natural Surfactants from Extra Heavy Crude Oils, Asphaltenes, and Maltenes. Interpretation of Their Interfacial Tension-pH Behaviour in terms of Ion Pair Formation," *Fuel*, **71**, 619-623 (1992).

Acevedo, S., Escobar, G., Gutierrez, L.B., Rivas, H. and Gutierrez, X., "Interfacial Rheological Studies of Extra-Heavy Crude Oils and Asphaltenes: Role of the Dispersion Effect of Resins in the Adsorption of Asphaltenes at the Interface of Water-in-Crude Oil Emulsions," *Colloids Surfaces, A: Physicochem. Eng. Aspects*, **71**, 65-71 (1993).

Acevedo, S., Escobar, G., Ronaudo, M.A. and Gutierrez, L.B., "Discotic Shape of Asphaltenes Obtained from GPC Data," *Fuel*, **73**, 1807-1809 (1994).

Acevedo, S., Ranaudo, M.A., Escobar, G., Gutierrez, L. and Ortega, P., "Adsorption of Asphaltenes and Resins on Organic and Inorganic Substrates and their Correlation with Precipitation Problems in Production Well Tubing," *Fuel*, **74**, 595-598 (1995).

Agrawala, M. and Yarranton, H.W., "An Asphaltene Association Model Analogous to Linear Polymerization," *Industrial and Engineering Chemistry Research*, **40 (21)**, 4664-4672 (2001).

Akbarzadeh, K., Amandeep, D., Svrcek, W.Y. and Yarranton, H.W., "Method for the Characterization and Modeling of Asphaltene Precipitation from Heavy Oils Diluted with n-Alkanes," *Energy Fuels*, **18**, 1434-1441 (2004).

Alboudwarej, H., Beck, J., Svrcek, W. Y., Yarranton, H. W. and Akbarzadeh, K., "Sensitivity of Asphaltene Properties to Separation Techniques" *Energy Fuels*, **16(2),** 462-469 (2002).

Alboudwarej, H. "Asphaltene Deposition in Flowing Systems," Ph.D. Thesis, University of Calgary (2003).

Anderson, S.I. and Birdi, K.S., "Aggregation of Asphaltenes as Determined by Calorimetry," *J. Colloid and Interface Sci.*, **142(2)**, 497-502 (1991).

Aske, N., Orr, R. and Sjoblom, J., "Dilatational Elasticity Moduli of Water-Crude Oil Interfaces Using the Oscillating Pendant Drop," *Journal of Dispersion Science and Technology*, **23(6)**, 809-825 (2002).

Aveyard, R., Binks, B.P., and Clint, J.H., "Emulsions Stabilized Solely by Colloidal Particles," *Adv. Colloid Interface Sci.*, **100-102**, 503-546 (2003).

Aveyard, R., Clint, J.H. and Horozov, T.S., "Solid Particles as Emulsion Stabilisers," *Progr. Colloid Polym. Sci.*, **121**, 11-18 (2002).

Bantignies, J.L., Cartier dit Moulin, C. and Dexpert, H.J., "Asphaltene Adsorption on Kaolinite Characterized by Infrared and X-Ray Absorption Spectroscopies," *Journal of Petroleum Science and Engineering*, **20(3&4)**, 233-237 (1998).

Bauget, F., Langevin, D. and Lenormand, R., "Dynamic Surface Properties of Asphaltenes and Resins at the Oil-Air Interface," *J. Colloid and Interface Sci.*, **239**, 501-508 (2001).

Bensebaa, F., Kotlyar, L.S., Sparks, B.D. and Chung, K.H., "Organic Coated Solids in Athabasca Bitumen: Characterization and Process Implications," *Can. J. Chem. Eng.*, **78 August**, 610-616 (2000).

Bensebaa, F., Kotlyar, L., Pleizier, G., Sparks, B., Deslandes, Y. and Chung, K., "Surface Chemistry of End Cuts from Athabasca Bitumen," *Surf. Interface Anal.*, **30**, 207-211 (2000b).

Bestougeff, M.A. and Byramjee, R.J., "Chemical Constitution of Asphaltenes," in Asphaltenes and Asphalts, 1., T.F. Yen and G.V. Chilingarian Eds., Elsevier Science, Amsterdam (1994).

Bhardwaj, A. and Hartland, S., "Dynamics of Emulsification and Demulsification of Water in Crude Oil Emulsions," *Ind. Eng. Chem. Res.*, **33**, 1271-1279 (1994).

Binks, B.P. and Kirkland, M., "Interfacial Structure of Solid-Stabilized Emulsions Studied by Scanning Electron Microscopy," *Phys. Chem. Chem. Phys.*, **4**, 3727-3733 (2002).

Binks, B.P. and Lumsdon, S.O., "Influence of Particle Wettability on the Type and Stability of Surfactant-Free Emulsions," *Langmuir*, **16**, 8622-8631 (2000).

Binks, B.P.; Lumsdon, S.O., "Pickering Emulsions Stabilized by Monodisperse Latex Particles: Effects of Particle Size," *Langmuir*, **17**, 4540-4547 (2001).

Bouriat, P., N. El Kerri, Graciaa, A. and Lachaise, A., "Properties of a Two-Dimensional Asphaltene Network at the Water-Cyclohexane Interface Deduced from Dynamic Tensiometry," *Langmuir*, **20**, 7459-7464 (2004).

Bowman, C.W., "Molecular and Interfacial Properties of Athabasca Tar Sands," *Proc. 7th World Petroleum Congress*, Mexico City, Mexico, April 2–8, 1967; Elsevier: Amsterdam **3**, 583-603 (1967).

Butler, J.A.V., "The Thermodynamics of the Surfaces of Solutions," *Proceedings of the Royal Society of London, Series A.*, **135**, 348-375 (1932).

Calemma, V., Rausa, R., D'Antona, P. and Montanari, L., "Characterization of Asphaltenes Molecular Structure," *Energy Fuels*, **12**, 422-428 (1998).

Campanelli, J.R. and Wang, X.H., "Dynamic Interfacial Tension of Surfactant Mixtures at Liquid-Liquid Interfaces," *J. Colloid Interface Sci.*, **213,** 340-351 (1999).

Carnahan, N.F., Salager, J-L., Anton, R. and Davila, A., "Properties of Resins Extracted from Boscan Crude Oil and their Effect on the Stability of Asphaltenes in Boscan and Hamaca Crude Oils," *Energy Fuels*, **13**, 309-314 (1999).

Castillo, J., Goncalves, S., Fernandez, A. and Mujica, V., "Applications of Photothermal Displacement Spectroscopy to the Study of Asphaltenes Adsorption," *Optics Communications*, **145**, 69-75 (1998).

Chen, F., Finch, J.A., Xu, Z. and Czarnecki, J., "Wettability of Fine Solids Extracted from Bitumen Froth," *J. Adhesion Sci. Technol.*, **13 No.10**, 1209-1224 (1999).

Crouch, F.W., Sommer, C.S., Galobardes, J.F., Kraus, S., Schmauch, E.M., Galobardes, M., Fatmi, A., Pearsall, K. and Rogers, L.B., "Fractionations of Nonporphyrin Complexes of Vanadium and Nickel from Boscan Crude Oil," *Separation Sci. Technol*., **18(7)**, 603-634 (1983).

da Silva Ramos, A.C., Haraguchi, L., Notrispe, F.R., Loh, W. and Mohamed, R.S., "Interfacial and Colloidal Behavior of Asphaltenes Obtained from Brazilian Crude Oils," *Journal of Petroleum Science and Engineering*, **32**, 201-216 (2001).

Dickie, J.P. and Yen, T.F., "Macrostructures of the Asphaltic Fractions by Various Instrumental Methods," *Anal. Chem.*, **39**, 1847-1852 (1967).

Dixon, W.J. and Massey, F.J. Introduction to Statistical Analysis; McGraw-Hill, New York, New York (1996).

Dow, D.B., "Oil-Field Emulsions," *U.S. Dept. Comm. Bull*., **250** (1926).

Eley, D.D., Hey, M.J. and Lee, M.A., "Rheological Studies of Asphaltene Films Adsorbed at the Oil/Water Interface," *Colloids and Surfaces*, **24**, 173-182 (1987).

Eley, D.D, Hey, M.J. and Symonds, J.D., "Emulsions of Water in Asphaltene-Containing Oils: Droplet Size Distribution and Emulsification Rates," *Colloids Surfaces*, **32**, 87-101 (1988).

Erdman, J.G., Pollak, S.S. and Yen, T.F., "Investigation of the Structure of Petroleum Asphaltenes by X-Ray Diffraction" *Anal. Chem*. **33(11)**, 1587 - 1594 (1961).

Espinat, D. and Ravey, J.C., "Colloidal Structure of Asphaltene Solutions and Heavy-Oil Fractions Studied by Small-Angle Neutron and X-Ray Scattering," Proceedings of the 1993 SPE International Symposium on Oilfield Chemistry, *Soc. Pet. Eng*., **SPE#25187**, 365-373 (1993).

Ese, M-H., Galet, L., Clausse, D. and Sjoblom, J., "Properties of Langmuir Surface and Interfacial Films Built up by Asphaltenes and Resins: Influence of Chemical Demulsifiers," *J. Colloid and Interface Sci.*, **220**, 293-301 (1999).

Ese, M-H., Yang, X. and Sjoblom, J., "Film Forming Properties of Asphaltenes and Resins. A Comparative Langmuir-Blodgett Study of Crude Oils from North Sea, European Continent and Venezuela," *Colloid Polym. Sci*., **276**, 800-809 (1998).

Fenistein, D., Barre, L., Broseta, D., Espinat, D., Livet, A., Roux, J-N. and Scarsella, M., "Viscometric and Neutron Scattering Study of Asphaltene Aggregates in Mixed Toluene/Heptane Solvents," *Langmuir*, **14**, 1013-1020 (1998).

Fingas, M.F., Kyle, D. and Tennyson, E.: "Dispersant Effectiveness: Studies into the Causes of Effectiveness Variations," in The Use of Chemicals in Oil Spill Response, ASTM 1252, Peter Lane, Ed., American Society for Testing and Materials, Philadelphia (1995).

Freer, E.M. and Radke, C.J., "Relaxation of Asphaltenes at the Toluene/Water Interface: Diffusion Exchange and Surface Rearrangement," *Journal of Adhesion*, **80**, 481-496 (2004).

Freer, E.M., Svitova, T. and Radke, C.J., "The Role of Interfacial Rheology in Reservoir Mixed Wettability," *Journal of Petroleum Science and Engineering*, **39**, 137-158 (2003).

Gafonova, O.V., "Role of Asphaltenes and Resins in the Stabilization of Water-in-Hydrocarbon Emulsions," M.Sc. Thesis, University of Calgary, (2000).

Gafonova, O.V. and Yarranton, H.W., "The Stabilization of Water-in-Hydrocarbon Emulsions by Asphaltenes and Resins," *J. Colloid and Interface Sci*., **241**, 469 (2001).

Gelot, A., Friesen, W., and Hamza, H.A., "Emulsification of Oil and Water in the Presence of Finely Divided Solids and Surface-Active Agents," *Colloids Surfaces*, **12**, 271-303 (1984).

Grace, R., in Emulsions – Fundamentals and Applications in the Petroleum Industry, L.L. Shcramm, Ed., p. 319. AM. Chemi.Soc., Washington, DC, (1992).

Grim, R.E., "Concepts of the Composition of Clay Materials," in Clay Mineralogy, 2nd Edition, McGraw-Hill, New York, New York (1968).

Groenzin, H. and Mullins, O.C., "Molecular Size and Structure of Asphaltenes," *Pet. Sci and Technol.*, **19(1&2)**, 219-230 (2001).

Gunter, W.D., Zhou, Z. and Perkins, E.H., "Modeling Formation Damage Caused by Kaolinite From 25 to 300º Centigrade in the Oil Sand Reservoirs of Alberta," Proc. Int. Symp. Form. Damage Control, *Soc. Pet. Eng.*, **SPE 23786**, 205-215 (1992).

Hammami, A., Ferworn, K. and Nighswander, J., "Asphaltenic Crude Oil Characerization: an Experimental Investigation of the Effect of Resins on the Stability of Asphaltenes," *Pet. Sci. Technol*., **16**, 227-249 (1998).

Herzog, P., Tchoubar, D. and Espinat, D., "Macrostructure of Asphaltene Dispersions by Small-Angle X-ray Scattering," *Fuel*, **67**, 245-250 (1988).

Hirschberg, A., Dejong, L.N., Schipper, B.A. and Meijer, J.G., "Influence of Temperature and Pressure on Asphaltene Flocculation," *Soc. Pet. Eng. J.*, **June**, 283-293 (1984).

Houache, O. and Yaghi, B., "Effect of Temperature and Solids on Rheology of Water-in-Oil Emulsions," *Pet. Sci. Technol.*, **21** (7&8), 1207-1218 (2003).

Jafari, M., in preparation, M.Sc. Thesis, University of Calgary (2005).

Jeribi, M., Almir-Assad, B., Langevin, D., Henaut, I. and Argillier, J.F., "Adsorption Kinetics of Asphaltenes at Liquid Interfaces," *J. Colloid and Interface Sci.*, **256**, 268-272 (2002).

Jones, T.J., Neustadter, E.L. and Whittingham, K.P., "Water-in-crude Oil Emulsion Stability and Emulsion Destabilization by Chemical Demulsifiers," *JCPT*, **April-June**, 100-108 (1978).

Kabalnov, A.S. and Shchukin, E.D., "Ostwald Ripening Theory. Applications to Fluorocarbon Emulsion Stability," *Advances in Colloid and Interface Science*, **38**, 69-97 (1992).

Kawanaka, S., Leontaritis, S., Park, S.J. and Mansoori, G.A., "Thermodynamic and Colloidal Models of Asphaltene Flocculation," ACS Symp. Series, 396, Oilfield Chemistry, Chapter 24, American Chemical Society, Washington DC, 443-458 (1989).

Khadim, M.A. and Sarbar, M.A., "Role of Asphaltene and Resin in Oil Field Emulsions," *J. Pet. Sci. Eng.*, **23**, 213-221 (1999).

Khristov, Khr., Taylor, S.D. and Masliyah, J., "Thin Liquid Film Technique – Application to Water-Oil-Water Bitumen Emulsion Films," *Colloids Surfaces, A: Physicochem. Eng. Aspects*, **174**, 183-196 (2000).

Kim, H.G. and Long, R.B., "Characterization of Heavy Residuum by Small-Angle X-ray Scattering Technique," *Ind. Eng. Chem. Fund*., **18**, 60-63 (1979).

Kokal, S., Tang, T., Schramm, L. and Sayegh, S., "Electrokinetic and Adsorption Properties of Asphaltenes", *Colloids Surfaces A: Physicochem. Eng. Aspects*, **94**, 253-265 (1995).

Koots, J.A. and Speight, J.G., "Relation of Petroleum Resins to Asphaltenes," *Fuel*, **54**, 179-184 (1975).

Kotlyar, L.S., Sparks, B.D., Woods, J.R. and Chung, K.H., "Solids Associated with the Asphaltene Fraction of Oil Sands Bitumen," *Energy Fuels*, **13**, 346-350 (1999).

Kotlyar, L.S., Deslandes, Y., Sparks, B.D., Kodama, H. and Schutte, R., "Characterization of Colloidal Solids from Athabasca Fine Tails," *Clays Clay Minerals*, **41**, 341-345 (1993).

Kotlyar, L.S., Sparks, B.D., Woods, J.R., Raymond, S., LePage Y. and Shelfantook, W., "Distribution and Types of Solids Associated with Bitumen," *Pet. Sci. Technol*., **16(1&2)**, 1-19 (1998).

Kotlyar, L.S., Sparks, B.D., LePage, Y., and Woods, J.R., "Effect of Particle Size on the Flocculation Behaviour of Ultra-Fine Clays in Salt Solutions," *Clay Minerals*, **33**, 103-107 (1998b).

Leon, O., Rogel, E., Espidel, J and Torres, G., "Asphaltenes: Structural Characterization; Self-Association and Stability Behaviour," *Energy Fuels*, **14**, 6-10 (2000).

Levine, S. and Sanford, E., "Stabilisation of Emulsion Droplets by Fine Powders," *Can. J. Chem. Eng.*, **62 April**, 258-268 (1985).

Li, B. and Fu, J., "Interfacial Tensions of Two-Liquid-Phase Ternary Systems," *Journal of Chemical and Engineering Data*, **37(2)**, 172-174 (1992).

Li, M., Xu, M., Ma, Y., Wu, Z. and Christy, A., "Interfacial Film Properties of Asphaltenes and Resins," *Fuel*, **81**, 1847-1853 (2002).

Lucassen, J. and Van Den Tempel, M., "Dynamic Measurements of Dilational Properties of a Liquid Interface," *Chem. Eng. Sci.*, **27**, 1283-1291 (1972).

Lucassen-Reynders, E.H., "Competitive Adsorption of Emulsifiers 1. Theory of Adsorption of Small and Large Molecules," *Colloids Surfaces, A: Physicochem. Eng. Aspects*, **91**, 79-88 (1994).

Lucassen-Reynders, E.H., Cagna, A. and Lucassen, J. "Gibbs Elasticity, Surface Dilational Modulus and Diffusional Relaxation in Nonionic Surfactant Monolayers," *Colloids Surfaces*, **186**, 63-72 (2001)

Lyklema, J.: "Adsorption at Solid-Liquid Interfaces with Special Reference to Emulsion Systems," *Colloids Surfaces, A: Physicochem. Eng. Aspects*, **91**, 25-38 (1994).

Masliyah, J.H., Electrokinetic Transport Phenomena, AOSTRA Technical Publication Series #12, *AOSTRA* (1994).

McLean, J.D. and Kilpatrick, P.K., “Effects of Asphaltene Aggregation in Model Heptane-Toluene Mixtures on Stability of Water-in-Oil Emulsions,” *J. Colloid & Int. Sci.*, **196**, 23-34 (1997a).

McLean, J.D., and Kilpatrick, P.K., “Effects of Asphaltene Solvency on Stability of Water-in-Crude-Oil Emulsions,” *J. Colloid Interface Sci.* **189**, 242 (1997b).

Menon, V.B. and Wasan, D.T., “Coalescence of Water-in-Shale Oil Emulsions,” *Sep. Sci. Technol.*, **19** (8&9), 555-574 (1984).

Menon, V.B. and Wasan, D.T., “Particle-Fluid Interactions with Application to Solid-Stabilized Emulsions Part I. The Effect of Asphaltene Adsorption,” *Colloids Surfaces*, **19**, 89-105 (1986).

Menon, V.B. and Wasan, D.T., “A Review of the Factors Affecting the Stability of Solids-Stabilized Emulsions,” *Pet. Sci. Technol.*, **23** (12&13), 2131 (1988).

Mitchell, D.L. and Speight, J.G., “The Solubility of Asphaltenes in Hydrocarbon Solvents,” *Fuel*, **52**, 149-152 (1973).

Mitra-Kirtley, S., Mullins, O.C., Van Elp, J., George, S.J., Chen, J., and Cramer, S.P., “Determination of the Nitrogen Chemical Structures in Petroleum Asphaltenes using XANES Spectroscopy,” *J. Am. Chem.. Soc*. **115**, 252-258 (1993).

Mohamed, R.S., Ramos, A.C.S., and Loh, W., “Aggregation Behavior of Two Asphaltenic Fractions in Aromatic Solvents,” *Energy Fuels*, **13**, 323-327 (1999).

Mohammed, R.A., Bailey, A.I., Luckham, P.F. and Spencer, S.E., "Dewatering of Crude Oil Emulsions: 1. Rheological Behaviour of the Crude Oil-Water Interface," *Colloids Surfaces, A: Physicochem. Eng. Aspects*, **80**, 223-235 (1993).

Mohammed, R.A., Bailey, A.I., Luckham, P.F. and Spencer, S.E., "Dewatering of Crude Oil Emulsions: 2. Interfacial Properties of the Asphaltic Constituents in Crude Oil," *Colloids Surfaces, A: Physicochem. Eng. Aspects*, **80**, 237-242 (1993b).

Moore, D.M. and Reynolds, R.C. Jr. "Sample Preparation Techniques for Clay Minerals," in X-Ray Diffraction and the Identification and Analysis of Clay Minerals, 2nd Edition, Oxford University Press (1997).

Moschopedis, S.E. and Speight, J.G., "Investigation of Hydrogen Bonding by Oxygen Functions in Athabasca Bitumen," *Fuel*, **55(3)**, 187-192 (1976).

Moschopedis, S.E. and Speight, J.G., "Investigation of Nitrogen Types in Athabasca Bitumen," *Preprints - Division of Petroleum Chemistry, American Chemical Society*, **24(4)**, 1007-1008 (1979).

Moschopedis, S.E., Fryer, J.F., and Speight, J.G., "Investigation of Asphaltene Molecular Weights," *Fuel*, **55**, 227-232 (1976).

Murgich, J. and Strausz, O., "Molecular Mechanics of Aggregates of Asphaltenes and Resins of the Athabasca Oil," *Pet. Sci. Technol.,* **19(1&2)**, 231-243 (2001).

Murzakov, R.M., Sabanekov, S.A. and Synyaev, Z.I., "Influence of Petroleum Resins on Colloidal Stability of Asphaltene-Containing Disperse Systems," *Chem. Tech. Fuels Oils,* **16**, 674-677 (1980).

Nalwaya, V., Tangtayakom, V., Piumsomboon, P. and Fogler, S., "Studies of Asphaltenes through Analysis of Polar Fractions," *Ind. Eng. Chem. Res*., **38**, 964-972 (1999).

Nellensteyn, F.J. "The Colloidal Structure of Bitumens," in The Science of Petroleum, **4**, Oxford University Press, 2760-2763 (1938).

Nicksic, S.W., and Jeffries-Harris, M.J. "Acid Precipitation of Crude Oil Asphaltenes – Structural Implications," *J. Inst. Petroleum*, **54**, 107- 114 (1968).

Nordli, K.G., Sjöblom, J., Kizling, J., and Stenius, P., "Water-in-Crude Oil Emulsions from the Norwegian Continental Shelf 4. Monolayer Properties of the Interfacially Active Crude Oil Fraction," *Colloids Surfaces*, **57**, 83 (1991).

Norinaga, K., Wargardalam, V.J., Takasugi, S., Iino, T. and Matsukawa, S., "Measurement of Self-Diffusion Coefficient of Asphaltene in Pyridine by Pulsed Field Gradient Spin-Echo ^{1}H NMR," *Energy Fuels*, **15**, 1317-1318 (2001).

NRC (National Research Council): Using Oil Spill Dispersants on the Sea, National Academy Press, Washington, DC (1989).

Nushtaeva, A.V. and Kruglyakov, P.M., "Investigation of Model Emulsion Films Stabilized by Solid Particles: Thickness of Films, Their Stability and Interfacial Tension," *Colloid Journal*, **66(4)**, 456-465 (2004).

Overfield, R.E., Sheu, E.Y., Sinha, S.K. and Liang, K.S., "SANS Study of Asphaltene Aggregation," *Fuel Sci. Tech. Int*., **7**, 611-624 (1989).

Papirer, E., Bourgeois, C., Siffert, B. and Balard, H., “Chemical Nature and Water/Oil Emulsifying Properties of Asphaltenes,” *Fuel*, **61**, 732-734 (1982).

Peramanu, S., Pruden, B.B. and P. Rahimi, “Molecular Weight and Specific Gravity Distributions for Athabasca and Cold Lake Bitumens and Their Saturate, Aromatic, Resin, and Asphaltene Fractions,” *Industrial and Engineering Chemistry Research*, **38** (8), 3121-3130 (1999).

Pickering, S.U., “Emulsions,” *J. Chem. Soc.*, **91,** 2001- 2021 (1907).

Pfeiffer, J. Ph. and Saal, R.N.J., “Asphaltic Bitumen as Colloid System,” *J. Phys. Chem*., **44**, 139-149 (1940).

Ramsden, W., “Separation of Solids in the Surface-Layers of Solutions and ‘Suspensions’ (Observations on Surface-Membranes, Bubbles, Emulsions, and Mechanical Coagulation) – Preliminary Account,” *Proc. R. Soc*., **72**, 156-164 (1903).

Ravey, J.C., Ducouret, G. and Espinat, D., “Asphaltene Macrostructure by Small-Angle Neutron Scattering,” *Fuel*, **67**, 1560-1567 (1988).

Reerink, H., “Size and Shape of Asphaltene Particles in Relationship to High-Temperature Viscosity,” *Ind. Eng. Chem. Res. Dev*., **12**, 82-88 (1973).

Reisberg, J. and Doscher, T.M., “Interfacial Phenomena in Crude-Oil-Water Systems,” *Producers Monthly*, **November**, 43-50 (1956).

Ritchie, R. George S., Roche, R. S., and Steedman, W., “Pyrolysis of Athabasca Tar Sands: Analysis of the Condensible Products from Asphaltene,” *Fuel*, **58(7)**, 523-530 (1979).

Rogacheva, O.V., Rimaev, R.N., Gubaidullin, V.Z. and Khakimov, D.K., "Investigation of the Surface Activity of Asphaltenes of Petroleum Residues, *Kolloidnyi Zhurnal*, **42(3)**, 586-589 (1980).

Rogel, E., León, O., Torres, G., and Espidel, J., "Aggregation of Asphaltenes in Organic Solvents Using Surface Tension Measurements," *Fuel*, **79**, 1389-1394 (2000).

Roux, J-N., Broseta, D. and Dume, B., "SANS Study of Asphaltene Aggregation: Concentration and Solvent Quality Effects," *Langmuir*, **17**, 5085-5092 (2001).

Sabbagh, A.B. and Lesser, A.J., "Effect of Particle Morphology on the Emulsion Stabilty and Mechanical Performance of Polyolefin Modified Asphalts," *Polym. Eng. Sci.,* **38** No. 5, 707 (1998).

Schildberg, Y., Sjöblom, J., Christy, A.A., Volle, J-L., and Rambeau, O., "Characterization of Interfacially Active Fractions and their Relation to Water-in-Oil Emulsion Stability," *J. Disp. Sci. Techn.,* **16(7)**, 575-605 (1995).

Schramm, L.L.: "Petroleum Emulsions, Basic Principles" in Emulsions: Fundamentals and Applications in the Petroleum Industry, L.L. Schramm, Ed., American Chemical Society, Washington DC (1992).

Schulman, J.H. and Leja, J., "Control of Contact Angles at the Oil-Water Solid Interface," *Trans. Faraday Soc.*, **50**, 598-605 (1954).

Sethumadhavan, G., Bindal, S., Nikolov, A. and Wasan, D., "Stability of Thin Liquid Films Containing Polydisperse Particles," *Colloids Surfaces A: Physicochem. Eng. Aspects*, **204**, 51-62 (2002).

Shaw, J.M., Maham, Y., Chodakowski, M.G. and Zhang, X. “Asphaltene Phase Behavior: Prediction at a Crossroads,” presented at the 54th Canadian Chemical Engineering Conference, Calgary, Alberta, Canada, October 3 – 6 (2004).

Shelfantook, W.E., “A Perspective on the Selection of Froth Treatment Processes,” *Can. J. Chem. Eng.,* **82(4)**, 704-709 (2004).

Sheu, E.Y., DeTar, M.M., Storm, D.A. and DeCanio, S.J., “Aggregation and Kinetics of Asphaltenes in Organic Solvents,” *Fuel*, **71**, 299-302 (1992).

Sheu, E.Y., “Physics of Asphaltene Micelles and Microemulsions - Theory and Experiment,” *Phys. Condens Matter*, **8**, A125 (1996).

Sheu, E.Y., Storm, D.A, and Shields, M.B., “Adsorption Kinetics of Asphaltenes at Toluene/Acid Solution Interface,” *Fuel*, **74**, 1475-1479 (1995).

Sheu, E.Y. and Shields, M.B., “Asphaltene Surface Activity at Oil/Water Interfaces”, SPE Int. Symp. Oilfield Chem., *Soc. Pet. Eng.*, **SPE #28995**, 523-532 (1995).

Siffert, B., Bourgeois, C., and Papirer, E., “Structure and Water-Oil Emulsifying Properties of Asphaltenes,” *Fuel*, **63**, 834-837 (1984).

Singh, S., McLean, J.D., and Kilpatrick, P.K., “Fused ring aromatic solvency in destabilizing water-in-asphaltene-heptane-toluene emulsions,” *J. Dispersion Sci. and Technology*, **20**(1&2), 279-293 (1999).

Sirota, B., “Swelling of Asphaltenes,” *Pet. Sci. Technol.*, **16(3&4)**, 415-431 (1998).

Smith, H.V. and Arnold, K.E. “Crude Oil Emulsions,” in Petroleum Engineering Handbook, Bradley, H.B., Ed., Richardson, TX, USA (1987).

Speight, J.G. “Asphaltenes” in The Chemistry and Technology of Petroleum, Marcel Dekker, Inc., New York (1999).

Speight, J.G., “The Desulfurization of Heavy Oils and Residua,” Marcel Dekker, New York (1981).

Spiecker, P.M. and Kilpatrick, P.K., “Interfacial Rheology of Petroleum Asphaltenes at the Oil-Water Interface,” *Langmuir*, **20**, 4022-4032 (2004).

Strassner, J.E., “Effect of pH on Interfacial Films and Stability of Crude Oil-Water Emulsions,” *J. Pet. Technol.*, **20**, 303-312 (1968).

Strausz, O.P., “Bitumen and Heavy Oil Chemistry,” in Technical Handbook on Oil Sands, Bitumen and Heavy Oils, L.G. Helper and C. His Eds., AOSTRA, Edmonton, Canada (1989).

Strausz, O.P., Mojelsky, T.W. and Lown, E.M., “The Molecular Structure of Asphaltene: an Unfolding Story,” *Fuel*, **71**, 1355-1362 (1992).

Sullivan, A.P. and Kilpatrick, P.K., “The Effects of Inorganic Solid Particles on Water and Crude Oil Emulsion Stability,” *Ind. Eng. Chem. Res.*, **41,** 3389-3404 (2002).

Tadros, T.F. and Vincent, B., “Emulsion Stability” in Encyclopedia of Emulsion Technology, Basic Theory, Becker, P. Ed, Marcel Dekker, Inc. New York, New York, **1**, 272-273 (1983).

Tambe D.E. and Sharma M.M., “Factors Controlling the Stability of Colloid-Stabilized Emulsions: I. An Experimental Investigation”, *J. Colloid Interface Sci*, **157**, 244-253 (1993).

Tambe, D.E. and Sharma M., “Factors Controlling the Stability of Colloid-Stabilized Emulsions: I. A Model for the Rheological Properties of Colloid-Laden Interfaces,” *J. Colloid Interface Sci*, **162**, 1-10 (1994).

Taylor, S.E., “Resolving Crude Oil Emulsions,” *Chem. Ind. London*, October 19, 770-773 (1992).

Taylor, S.D., Czarnecki, J. and Masliyah, J., “Disjoining Pressure Isotherms of Water-in-Bitumen Emulsion Films,” *J. Colloid Interface Sci.,* **252**, 149-160 (2002).

Vignati, E., Piazza, R. and Lockhart, T.P., “Pickering Emulsions: Interfacial Tension, Colloidal Layer Morphology, and Trapped-Particle Motion,” *Langmuir*, **19**, 6650-6656 (2003).

Watson, B.A. and Barteau, M.A., “Imaging of Petroleum Asphaltenes Using Scanning Tunneling Microscopy,” *Ind. Eng. Chem. Res*., **33**, 2358-2363 (1994).

Wu, X., “Investigating the Stability Mechanism of Water-in-Diluted Bitumen Emulsions through Isolation and Characterization of the Stabilizing Materials at the Interface,” *Energy Fuels*, **17**, 179-190 (2003).

Yaghi, B., Benayoune M. and Al-Bemani, A., “Viscosity of Water-Oil Emulsions with Added Nano-Sized Particles,” *Pet. Sci. Technol.*, **19** (3&4), 373-386 (2001).

Yan, N., Gray, M.R. and Masliyah, J.H., "On Water-in-Oil Emulsions Stabilized by Fine Solids," *Colloids Surfaces A: Physicochem. Eng. Aspects*, **193**, 97-107 (2001).

Yan, Z.; Elliot, J.A.W.; Masliyah, J.H. Roles of Various Bitumen Components in the Stability of Water-in-Diluted-Bitumen Emulsions. *J. Colloid & Int. Sci*., **220**, 329-337 (1999).

Yan, N. and Masliyah, J.H., "Characterization and Demulsification of Solids-Stabililzed Oil-in-Water Emulsions Part 2. Demulsification by the Addition of Fresh Oil," *Colloids Surfaces A: Physicochem. Eng. Aspects*, **96**, 243-252 (1995).

Yan, N. and Masliyah, J.H., **"**Characterization and demulsification of solids-stabilized oil-in-water emulsions part 1. Partitioning of clay particles and preparation of emulsions," *Colloids Surfaces A: Physicochem. Eng. Aspects*, **96**, 229-242 (1995b).

Yan, Y. and Masliyah, J.H., "Effect of Oil Viscosity on the Rheology of Oil-in-Water Emulsions with Added Solids," *Can. J. Chem. Eng.*, **71**, 852-858 (1993).

Yang, X., Hamza, H. and Czarnecki, J., "Investigation of Subfractions of Athabasca Asphaltenes and Their Role in Emulsion Stability," *Energy Fuels*, **18**, 770-777 (2004).

Yarranton, H.W., "Asphaltene Solubility and Asphaltene Stabilized Water-in-Oil Emulsions," Ph.D. Thesis, University of Alberta (1997).

Yarranton, H.W., Alboudwarej, H. and Jakher, R., "Investigation of Asphaltene Association with Vapor Pressure Osmometry and Interfacial Tension Measurements," *Industrial and Engineering Chemistry Research*, **39(8)**, 2916-2924 (2000b).

Yarranton, H.W., Hussein, H., and Masliyah, J.H. “Water-in-Hydrocarbon Emulsions Stabilized by Asphaltenes at Low Concentrations,” *J. Colloid Interface Sci.* **228**, 52-64 (2000a).

Yarranton, H., Beck, J., Alboudwarej, H., Svrcek, W.Y., “Symposium - Conversion Chemistry of Petroleum Residua - Asphaltene Self-Association and Precipitation Modeling,” *Preprints ACS Division of Petroleum Chemistry*, **47**(4), 336-337 (2002).

Yekeler, M., Ulusoy, U., and Hiçyilmaz, C., “Effect of Particle shape and roughness of talc mineral ground by different mills on the wettability and floatability,” *Powder Technol.*, **140**, 68 (2004).

Yen, T.F., “Multiple Structural Orders of Asphaltenes,” in Asphaltenes and Asphalts, 1., T.F. Yen and G.V. Chilingarian Eds., Elsevier Science, Amsterdam (1994).

Yen, T.F., “Structure of Petroleum Asphaltenes and its Significance,” *Energy Sources*, **1(4)**, 447-463 (1974).

Yeung, A., Dabros, T., Czarnecki, J. and Masliyah, J., “On the Interfacial Properties of Micrometre-Sized Water Droplets in Crdue Oil,” *Proc. R. Soc. Lond. A*, **455**, 3709-3723 (1999).

Yeung, A., University of Alberta, private communication, June 2004.

Zaki, N.N., Maysour, N.W.S. and Abdel-Azim, A., “Polyoxyalkylenated Amines for Breaking of Water-in-Oil Emulsions Stabilized by Asphaltenes and Clay,” *Pet. Sci. Technol.*, **18 (9&10)**, 1009-1025 (2000).

Zhang, L.Y., Lawrence, S., Xu, Z. and Masliyah, J.H., "Studies of Athabasca Asphaltene Langmuir films at Air-Water Interface," *J. Colloid and Interface Sci.*, **264(1)**, 128-140 (2003a).

Zhang, L.Y., Xu, Z. and Masliyah, J.H., "Langmuir and Langmuir-Blodgett Films of Mixed Asphaltene and a Demulsifier," *Langmuir*, **19**, 9730-9741 (2003b).

APPENDIX A
ERROR ANALYSIS

Sample error analyses for asphaltene and solids yields, asphaltene molar mass, interfacial tension measurements, elasticity measurements, drop size distribution measurements, mass surface coverage experiments, and emulsion stability measurements are presented in this appendix. For repeat measurements made at one experimental condition, confidence intervals are established based on the standard deviations of sets of repeated measurements. Otherwise, the confidence interval is established based on the standard deviations of experimental measurements from a line that "best fits" the data set. A 95% confidence interval was used for the assessment of error for all types of experiments.

A.1 THEORY

A.1.1 Error in Measurements Made at a Single Experimental Condition

The mean of several repeated measurements is given by:

$$\bar{x} = \frac{1}{n}\sum_{i=1}^{n} x_i \qquad \text{(A.1)}$$

where n is the number of repeat measurements and x_i is a measured value. The sample variance is given by:

$$s^2 = \frac{1}{n-1}\sum_{i=1}^{n}\left(x_i - \bar{x}\right)^2 \qquad \text{(A.2)}$$

The standard deviation, s, is the square root of the sample variance.

The statistical distribution used for determining the confidence interval is the t-distribution. The confidence interval is given by:

$$\bar{x} - t_{(\alpha/2,\nu)} \frac{s}{\sqrt{n}} \leq \mu \leq \bar{x} + t_{(\alpha/2,\nu)} \frac{s}{\sqrt{n}} \qquad \text{(A.3)}$$

where μ is the correct mean, $n = \nu$-1 and α = 1- (%conf/100). In the current work, a confidence interval of 95% is utilized in all error analyses. Therefore, α = 0.05.

A.1.2 Error in Experimental Measurements Falling on a Best Fit Line

Many of the experimental measurements performed in this thesis are very time-consuming and therefore remain unrepeated or are repeated only once. For such measurements, the error is assessed by examining the deviation of any experimental measurement away from a line that appears to best fit the data. Note that the best fit lines have no physical meaning and their forms (for example, quadratic or quartic) were chosen simply because the data appeared to follow those trends.

A dependent variable, *y*, is related to an independent variable, *x*, through some function *f* as follows:

$$y = f(x) \qquad \text{(A.4)}$$

Here, the function *f* contains constants *a*, *b*, *c*, etc. that relate *y* to *x*. For example, in the equation y = 4x + 5, a = 4 and b = 5. The objective is to find the values of the constants that "best fit" the line by performing least squares regression.

The equation for the population regression line can be estimated from the sample regression equation as follows:

$$\hat{y} = f(\hat{x}) \tag{A.5}$$

where $\hat{y}$ is the value of the dependent variable given by the function *f*. For a point *i* on the line given by the function *f*, the residual between the experimental measurement and the value given by the line is as follows:

$$\in_i = y_i - \hat{y} \tag{A.6}$$

The sum of the squares of the residuals is given by the function *P* as follows:

$$P = \sum_{i=1}^{n} \in_i^2 \tag{A.7}$$

where *n* is the number of measurements. To satisfy the condition that the sum of the squares of residuals is a minimum, *P* must be a minimum. This occurs when the partial derivative of the function *P* with respect to each constant is equal to zero. Hence,

$$\frac{\partial P}{\partial a} = \frac{\partial P}{\partial b} = \frac{\partial P}{\partial c} = \ldots = 0 \tag{A.8}$$

The variance is then given by:

$$s^2 = \frac{1}{n-2} \sum_{i=1}^{n} \in_i^2 \tag{A.9}$$

The standard deviation, *s*, is the square root of the variance. The statistical distribution used for determining the confidence interval is the t-distribution. The confidence interval for any dependent measurement, *y*, is given by:

$$\hat{y} - t_{(\alpha/2,\nu)} \frac{s}{\sqrt{n}} \leq y \leq \hat{y} + t_{(\alpha/2,\nu)} \frac{s}{\sqrt{n}} \qquad \text{(A.10)}$$

where $\nu = n - 2$ and α = 1- (%conf/100). In the current work, a confidence interval of 95% is utilized in all error analyses. Therefore, $\alpha = 0.05$.

A.1.3 Average Absolute Relative Deviation and Average Absolute Deviation

The Average Absolute Relative Deviation (AARD) and the Average Absolute Deviation (AAD) of fits of a curve to experimental data are assessed with the following equations:

$$\text{AARD} = \frac{\sum_{i=1}^{n} \left| \frac{\mu_{fit} - \mu_{exp}}{\mu_{exp}} \right|}{n} \qquad \text{(A.11)}$$

$$\text{AAD} = \frac{\sum_{i=1}^{n} \left| \mu_{fit} - \mu_{exp} \right|}{n} \qquad \text{(A.12)}$$

where μ_{exp} is the experimental measurement, μ_{fit} is the predicted model measurement, and n is the number of measurements.

A.2 ASPHALTENE AND SOLID YIELD

The error analyses for the yield of AS (Asphaltene-Solids), C_5 AS and Soxhlet-Washed AS extracted from Athabasca Bitumen 1 and the yield of AS extracted from Athabasca Bitumen 2 are summarized in Table A.1. On average, the yield of AS from Athabasca bitumen varies by ±0.7% for a confidence interval of 95%. For example, the yield of AS from Athabasca Bitumen 1 is 17.2% ±0.52%.

Table A.1: Error analyses of AS yield from Athabasca bitumen

Sample	$\bar{x}$ %	s %	n	t	$t_{(\alpha/2,\nu)}\frac{s}{\sqrt{n}}$, %
Bitumen 1					
AS	17.2	1.19	23	2.074	0.52
C_5 AS	23.1	0.67	5	2.776	0.83
SW AS	12.3	0.69	19	2.101	0.33
Bitumen 2					
AS	15.6	0.81	5	2.776	1.01

The error analyses for the fraction of solids in each AS sample are summarized in Table A.2. On average, the fraction of solids in any AS sample varies by ±0.3% for a confidence interval of 95%. For example, the fraction of solids in Athabasca Bitumen 1 AS is 4.7% ±0.28%. Although not shown here, the error in the yield of solids in the AEC wellhead emulsion and the rag layer and solids slurry of the IOL emulsion are similar.

Table A.2: Error analyses of solid fraction in Athabasca bitumen AS

Sample	$\bar{x}$ %	s %	n	t	$t_{(\alpha/2,\nu)}\frac{s}{\sqrt{n}}$, %
Bitumen 1					
AS	4.7	0.26	6	2.571	0.28
C_5 AS	3.0	0.13	4	3.182	0.20
SW AS	6.6	0.12	3	4.303	0.30
Bitumen 2					
AS	3.1	0.17	3	4.303	0.43

A.3 ASPHALTENE MOLAR MASS

The error analyses were performed for the molar mass of Athabasca Bitumen 1 Asphaltenes, C_5 Asphaltenes and Soxhlet-Washed Asphaltenes and for Athabasca Bitumen 2 Asphaltenes. The form of the equation relating the asphaltene molar mass, *M*, to the asphaltene concentration, c_A, is given by:

$$M = aC_A^3 + bC_A^2 + cC_A + d \qquad (A.13)$$

The parameters *a*, *b*, *c*, and *d* were found by applying Equation (A.8). The sum of the squares of the residuals, *P*, and the standard deviation, *s*, were calculated from Equations (A.7) and (A.9), respectively. The relevant statistical parameters are summarized in Table A.3 for all asphaltene samples. The largest deviation occurs for the Soxhlet-Washed asphaltenes.

Table A.3: Statistical parameters for error analyses of molar mass measurements about the best fit line

Sample	n	a	b	c	d	s g/mol	t	$t_{(\alpha/2,\nu)}\frac{s}{\sqrt{n}}$, g/mol
Bitumen 1								
Asphaltenes	15	0.02	-4.00	319	1965	397	2.160	221
C_5 Asphaltenes	13	0.01	-1.75	115	1467	220	2.201	134
SW Asphaltenes	14	0.08	-9.53	724	2849	894	2.179	520
Bitumen 2								
Asphaltenes	10	0.07	-6.43	260	1468	274	2.306	200

A.4 INTERFACIAL TENSION

The error analyses for the interfacial tension of solutions of Athabasca Bitumen 1 Asphaltenes dissolved in 25/75 heptol over water at several asphaltene concentrations are summarized in Table A.4. In this example, the measurements are the "unprocessed" measurements made directly with the Drop Volume Tensiometer. Table A.4 indicates that at any asphaltene concentration, the interfacial tension varies on average by ±0.12 mN/m for a 95% confidence interval.

Table A.4: Error analyses of interfacial tension of solutions of Athabasca bitumen 1 Asphaltenes dissolved in 25/75 heptol over water

Asphaltene Concentration (kg/m³)	$\bar{x}$ mN/m	s mN/m	n	t	$t_{(\alpha/2,\nu)}\frac{s}{\sqrt{n}}$, mN/m
0.5	33.38	0.20	18	2.110	0.10
1	32.48	0.13	12	2.201	0.09
2.5	30.55	0.10	12	2.201	0.06
5	29.20	0.15	12	2.201	0.10
10	28.50	0.15	18	2.110	0.07
25	27.32	0.23	24	2.069	0.09
50	28.34	0.32	6	2.571	0.33

The unprocessed mean values presented in Table A.4 are processed in order to account for the density of asphaltenes. The interfacial tension for any given asphaltene solution is given by:

$$\gamma = \gamma_{\mathrm{raw}}\left(\frac{\rho_{\mathrm{w}} - \rho_{\mathrm{c}}}{\rho_{\mathrm{w}} - \rho_{\mathrm{heptol}}}\right) \tag{A.14}$$

where γ_{raw} is the interfacial tension as measured with the Drop Volume Tensiometer, ρ_w the density of water, ρ_c the density of the continuous phase including asphaltenes, and ρ_{heptol} the density of a mixture of heptane and toluene at the required heptane volume fraction. As discussed in Chapter 4, the processed data was shown to exhibit linearity when plotted against the logarithm of asphaltene concentration. Therefore, the form of the equation relating the interfacial tension, γ, to the asphaltene concentration, c_A, is given by:

$$\gamma = \mathrm{a}\ln(\mathrm{c_A}) + \mathrm{b} \tag{A.15}$$

The parameters *a* and *b* were found by applying Equation (A.8). The sum of the squares of the residuals, *P*, and the standard deviation, *s*, were calculated from Equations (A.7) and (A.9), respectively. The relevant statistical parameters are summarized in Table A.5. According to Table A.5, the experimental data points deviate from the best fit line by ±0.40 mN/m at any asphaltene concentration. The analyses are similar for all other asphaltene solutions and are therefore not shown here.

Table A.5: Statistical parameters for error analyses of interfacial tension measurements about the best fit line

Parameter	Value
n	7
a (mN/m)	-1.71
b (mN/m)	32.09
P $(mN/m)^2$	0.84
s (mN/m)	0.41
t	2.571
$t_{(\alpha/2,\nu)} \frac{s}{\sqrt{n}}$ (mN/m)	0.40

A.5 ELASTICITY MEASUREMENTS

The error analyses for the total modulus and the phase angle measured after a 4 hour interface aging time and a 0.033 Hz oscillation frequency are shown in Table A.6 for Athabasca Bitumen 2 Asphaltenes dissolved in 0/100 heptol. The elastic modulus first increases and then decreases as a function of the logarithm of asphaltene concentration. The phase angle also increases approximately as a function of the logarithm of asphaltene concentration. Therefore, the form of the equation relating the total modulus, ε, to the asphaltene concentration, c_A, is given by:

$$\varepsilon = a \ln(c_A) + b \tag{A.16}$$

The equation relating the phase angle, ϕ, to the asphaltene concentration, c_A, is given by:

$$\phi = c\ln(c_A) + d \qquad (A.17)$$

The parameters *a, b, c* and *d* were found by applying Equation (A.8). The sum of the squares of the residuals, *P*, and the standard deviation, *s*, were calculated from Equations (A.7) and (A.9), respectively. The relevant statistical parameters are summarized in Table A.6. According to Table A.6, the experimental moduli deviate from the best fit line by ±0.34 mN/m for asphaltene concentrations less than 0.1 kg/m³, and ±0.22 mN/m for asphaltene concentrations greater than 0.1 kg/m³. The phase angle varies by ±0.56º over the entire concentration range.

Table A.6: Statistical parameters for error analyses of elasticity about the best fit line

Variable	n	a	b	c	d	s mN/m or º	t	$t_{(\alpha/2,\nu)}\frac{s}{\sqrt{n}}$ mN/m or º
ε (C_A<0.1 kg/m³)	15	3.25	22.54			0.61	2.160	0.34
ε (C_A>0.1 kg/m³)	12	-1.98	10.91			0.35	2.228	0.22
ϕ (C_A<0.1 kg/m³)	15			0.58	8.34	1.01	2.160	0.56
ϕ (C_A>0.1 kg/m³)	12			3.17	14.62	0.86	2.228	0.55

Curves of the form given by Equation 6.1 were fit to the experimentally measured total modulus, as discussed in Section 6.1.3. The Average Absolute Relative Deviation (AARD) and the Average Absolute Deviation (AAD) of these fits were assessed using equations (A.11) and (A.12), respectively. Table A.7 summarizes the AARD and the AAD for all the systems considered.

Table A.7: AARD and AAD of the fits of total modulus with time for model emulsions stabilized by Athabasca Bitumen 2 Asphaltenes

System (Conc., Solvent)	AARD (%)	AAD (mN/m)
20 kg/m³, 0/100 heptol	3.8	0.15
10 kg/m³, 0/100 heptol	0.8	0.04
5 kg/m³, 0/100 heptol	1.8	0.13
20 kg/m³, 25/75 heptol	6.3	0.28
10 kg/m³, 25/75 heptol	3.9	0.30
5 kg/m³, 25/75 heptol	2.3	0.20
20 kg/m³, 50/50 heptol	3.6	0.20
10 kg/m³, 50/50 heptol	4.0	0.29
5 kg/m³, 50/50 heptol	5.8	0.44

A.6 SAUTER MEAN DIAMETER

Figure 4.12 and 4.13 showed that for asphaltene equilibrium concentrations exceeding 10 kg/m³, the measured Sauter mean diameter was approximately constant. Therefore, an approximation of the error in the Sauter mean diameter can be performed if it is assumed that the Sauter mean diameter is independent of concentration. The example shown here is for the Sauter mean diameter of water droplets for an emulsion prepared with 40 vol% water and solutions of Athabasca bitumen 1 Asphaltenes dissolved in 25/75 heptol. Table A.8 summarizes the relevant statistical parameters and shows that for concentrations exceeding 10 kg/m³, the Sauter mean diameter is 8.02 microns ±0.29 microns for a confidence interval of 95%.

Table A.8: Statistical parameters for error analyses of the Sauter mean diameter

Parameter	Value
n	5
$\bar{x}$ (microns)	8.02
s (microns)	0.24
t	2.776
$t_{(\alpha/2,\nu)}\frac{s}{\sqrt{n}}$ (microns)	0.29

The analyses in Table A.8 are a good approximation if the error is required at higher asphaltene concentrations. However, it was found that for calculation purposes (i.e., in the gravimetric analyses), the Sauter mean diameter could be related to asphaltene equilibrium concentration through the following equation:

$$d_{32} = \frac{a}{\left(\left(C_A^{eq}\right)^e - b\right)^c} + d \qquad (A.18)$$

The parameters *a, b, c, d* and *e* were found by applying Equation (A.8). The sum of the squares of the residuals, *P*, and the standard deviation, *s*, were calculated from Equations (A.7) and (A.9), respectively. The relevant statistical parameters are summarized in Table A.8. According to Table A.8, the experimental data points deviate from the best fit line by ±0.34 microns at any asphaltene concentration between 0.7 and 35 kg/m³.

Table A.9: Statistical parameters for error analyses of Sauter mean diameter measurements about the best fit line

Parameter	Value
n	17
a	9.96
b	0.18
c	0.69
d	7.60
e	1.56
P (microns²)	6.60
s (microns)	0.66
t	2.131
$t_{(\alpha/2,\nu)}\frac{s}{\sqrt{n}}$ (microns)	0.34

In order to calculate the rate of change in the Sauter mean diameter with time, curves of the form given by Equation 6.1 were fit to the experimentally measured Sauter mean diameter, as discussed in Section 6.1.1. The Average Absolute Relative Deviation

(AARD) and the Average Absolute Deviation (AAD) of these fits were assessed using equations (A.11) and (A.12), respectively. Table A.10 summarizes the AARD and the AAD for all the systems considered.

Table A.10: AARD and AAD of the fits of Sauter mean diameter with time for model emulsions stabilized by Athabasca Bitumen 2 Asphaltenes

System (Conc., Solvent)	AARD (%)	AAD (μm)
20 kg/m³, 0/100 heptol	4.8	1.78
10 kg/m³, 0/100 heptol	1.1	0.26
5 kg/m³, 0/100 heptol	0.8	0.15
20 kg/m³, 25/75 heptol	4.9	0.94
10 kg/m³, 25/75 heptol	1.5	0.25
5 kg/m³, 25/75 heptol	3.6	0.61
20 kg/m³, 50/50 heptol	2.2	0.22
10 kg/m³, 50/50 heptol	1.1	0.09
5 kg/m³, 50/50 heptol	0.1	0.01

A.7 ASPHALTENE MASS SURFACE COVERAGE

The error analyses in the mass surface coverage are shown in Table A.11 for an emulsion prepared from 40 vol% water and solutions of Athabasca Bitumen 1 Asphaltenes dissolved in 25/75 heptol. The mass surface coverage, Γ, is related to the asphaltene equilibrium concentration, C_A^{eq}, as follows:

$$\Gamma = a\left(C_A^{eq}\right)^3 + b\left(C_A^{eq}\right)^2 + c\left(C_A^{eq}\right) + d \qquad (A.19)$$

The parameters *a*, *b*, *c*, and *d* were found by applying Equation (A.8). The sum of the squares of the residuals, *P*, and the standard deviation, *s*, were calculated from Equations (A.7) and (A.9), respectively. The relevant statistical parameters are summarized in Table A.11. According to Table A.11, the experimental mass surface coverage deviates from the best fit line by ± 0.0002 g/m².

Table A.11: Statistical parameters for error analyses of asphaltene mass surface coverage measurements about the best fit line

Parameter	Value
n	30
a	2.71×10^{-7}
b	-1.54×10^{-5}
c	2.89×10^{-4}
d	2.39×10^{-3}
P (g^2/m^4)	5.88×10^{-6}
s (g/m^2)	0.0005
t	2.048
$t_{(\alpha/2,\nu)} \frac{s}{\sqrt{n}}$ (g/m^2)	0.0002

A.8 FREE WATER RESOLUTION

The free water resolution is used to gauge relative emulsion stability. According to Figure 3.1, the free water appears to be constant for asphaltene equilibrium concentrations exceeding 20 kg/m^3. Therefore, an approximation of the error in the free water resolution can be performed if it is assumed that the free water is independent of concentration. The examples shown here are for the free water resolution after eight hours of treatment of emulsions prepared with 40 vol% water and solutions of either Athabasca bitumen 1 Asphaltenes or AS dissolved in 25/75 heptol. Table A.12 summarizes the relevant statistical parameters and shows that for concentrations exceeding 20 kg/m^3, the free water resolution of emulsions stabilized by Asphaltenes is 46.7% ±2.6% for a confidence interval of 95%. For emulsions stabilized by AS, the free water resolution is 14.1% ±4.5%.

Table A.12: Statistical parameters for error analyses of the free water resolution

Parameter	Value for Asphaltenes	Value for AS
n	8	8
$\bar{x}$ (%)	46.7	14.1
s (%)	3.08	5.41
t	2.365	2.365
$t_{(\alpha/2,\nu)}\frac{s}{\sqrt{n}}$ (%)	2.6	4.5